Geology and lithogeochemistry of the Powderhorn Lake VMS deposit, Newfoundland

Submitted to:
Department of Earth Sciences
Memorial University of Newfoundland
St. John's, Newfoundland
A1B 3X5

Submitted by:
Regan Jacobson, M.Sc. Candidate
4 Kimberly Row
St. John's, Newfoundland
A1C 4A5

Date:
September 11, 2023

Abstract

The Powderhorn Lake volcanogenic massive sulfide (VMS) deposit is hosted within the Ordovician Buchans-Roberts Arm (volcanic) belt (BRAB) in central Newfoundland. The deposit is hosted by coherent and clastic rhyolitic rocks that are interpreted to have formed within a rifted continental arc setting. The stratigraphy, alteration, and mineralization of the deposit is preserved within multiple, imbricated thrust panels that comprise a regional domal antiform. Mineralization occurs as multiple stacked lenses consisting of stringer to semi-massive and massive pyrrhotite, sphalerite, chalcopyrite, pyrite, and minor galena. Sulfide lenses typically contain relicts of host rocks and are interpreted to have formed by replacement-style processes at or below the seafloor. Hydrothermal alteration assemblages at Powderhorn Lake consist of weak to intense quartz-sericite and quartz-sericite-chlorite+/-pyrite. Lithogeochemical data, mass change calculations, and short-wave infrared spectroscopy identified key element associations and alteration assemblages that provide vectors towards mineralization. The lithogeochemical data have been used to create a 3D alteration model of the Powderhorn Lake deposit that highlights spatial relationships between key alteration characteristics and stratigraphy.

Acknowledgements

The completion of this thesis is largely attributed to the great support and guidance provided by my supervisor, Steve Piercey. I would like to personally thank him for his commitment of time and energy into furthering my thesis by providing comments, edits, and ideas. His aptitude to communicate science with great proficiency alongside humility and steady humor has changed the way I perceive academia and has played a large role in my development as a writer, geologist, and person. Above all, I am thankful for his kindness and patience throughout this entire process. I would also like to thank my MSc committee member Dr. Luke Beranek for his comments on this work.

A special thanks to the members of the Piercey research group: Nikola Denisova, Kei Quinn, Carly Mueller, Robert King, Matt Manor, Marko Szmihelsky, and Rosie Cobbett. The research discussions, office visits, dinners, and intermittent grumbling about thesis writing kept me in good spirits throughout. A personal thank you to my officemate and friend, Kei Quinn who was always there to answer my questions, collaborate, and offer plenty of advice.

I also want to thank Champion Iron Mines Ltd., Pearl Resources Inc., and their employees, namely, Vincent Blanchet, Hugues Longuepee, and Paul Delaney whose previous and current work greatly helped this project. I appreciate the lab assistance and support from both Wanda Aylward and Matthew Crocker of The Earth Resources Research Analysis (TERRA) facility at Memorial University of Newfoundland.

I am deeply thankful for the unwavering support given by my mom, Julie and my dad, Chad. They have supported my interest in geology since day one – from letting me dig up their backyard with the kitchen spoons to helping me pack-up my life and move to Canada for

graduate school. A large thank you to Abby, a friend beyond words, I would not have made it this far without her. Their encouragement, among many other family and friends helped push this project to the finish line.

Financial and logistical support for this project was provided by Champion Iron Mines Ltd., a Natural Sciences and Engineering Research Council of Canada (NSERC) Collaborative Research and Development Grant awarded to Steve Piercey, and Memorial University of Newfoundland.

Table of Contents

List of Tables

Chapter 2

List of Figures

Chapter 1

Chapter 2

Figure 2.19 Schematic tectonic model of the Powderhorn Lake deposit: A) Tectonic setting and evolution of the AAT, B) cross-section of basin development, C) cross-section of basin inversion and associated structural deformation.

List of Abbreviations

AAT	Annieopsquotch Accretionary Tract
AI	Hashimoto alteration index
AOB	Annieopsquotch Ophiolite Belt
Aq	Aqueous
Avg	Average
BLL	Beothuk Lake Line
BRAB	Buchans-Roberts Arm volcanic belt
BSE	Back scatter electron imaging
Bt	Biotite
BVOT	Baie Verte Oceanic Tract
Cal	Calcite
CCPI	Chlorite-carbonate-pyrite alteration index
Chl	Chlorite
Cm	Centimeter
Cpy	Chalcopyrite
CREAIT	Core Research Equipment and Instrument Training
D	Depth
EDX	Energy Dispersive X-Ray
Ep	Epidote
EPMA	Electron probe microanalysis
Eq	Equation
Feld	Feldspar
Fig(s)	Figure(s)
FW	Footwall
g/t	Grams per ton
Gt	Garnet
HFSE	High field strength elements
HREE	Heavy rare earth elements
HW	Hanging wall
ICP-MS	Inductively coupled emission-mass spectrometry
Km	Kilometer
K-feld	Potassium feldspar
Lap	Lapilli
LBOT	Lushs Bight Oceanic Tract
LDL	Lower detection limit
LFSE	Light field strength elements
LOI	Loss on ignition
LREE	Light rare earth elements
M	Meter
Mm	Millimeter

Max	Maximum
Min	Minimum
Mod	Moderate
MS	Mineralized sequence
Musc	Muscovite
N	Northing
Ppb	parts per billion
Ppm	parts per million
Py	Pyrite
QA/QC	Qaulity assurance/quality control
Qtz	Quartz
REE	Rare earth element
RIL	Red Indian Line
%RSD	Relative Standard Deviation
Ser	Sericite
Sp	Sphalerite
SWIR	Short-wave infrared
UTM	Universal Transverse Mercator
VMS	Volcanogenic massive sulfide
wt. %	Weight percent
Xtl	Crystal

List of Appendices

Chapter 1: Introduction to the Powderhorn Lake volcanogenic massive sulfide deposit, central Newfoundland, Canada

1.1 Introduction and Exploration History

The Notre Dame subzone of Newfoundland contains the remnants of Cambrian to Ordovician continental and oceanic arc-backarc and ophiolitic complexes that formed outboard of the Laurentian margin within the Iapetus Ocean (Williams, 1979, 1995; Williams et al., 1988). Accretion of the terranes onto the Laurentian margin occurred during the Taconic orogeny and are now preserved within the Annieopsquotch accretionary tract (AAT) (van Staal et al., 2007; van Staal and Barr, 2012; Zagorevski et al., 2015). The Buchans-Roberts Arm (volcanic) belt (BRAB) of the AAT is host to several notable volcanogenic massive sulfide (VMS) deposits including deposits in the Buchans, Gullbridge, and Pilley's Island districts (Fig 1.1). The polymetallic, felsic-siliciclastic Powderhorn Lake deposit is hosted within the BRAB and is located approximately 50 km south of the town of Springdale in central Newfoundland.

Sphalerite mineralization was discovered on the western shore of Powderhorn Lake by Kalliokoski (1955) during regional mapping. Follow-up exploration of the mineralization did not occur until 1997 when prospectors Jacob Kennedy and William Mercer brought hand samples into the Geological Survey of Newfoundland and Labrador (Kerr, 1999). Shortly thereafter, Canaco Resources Ltd. released information on the discovery of a second mineralized showing east of Powderhorn Lake consisting of Ni-Cu (Kerr, 1999). This discovery led to a limited drilling program near the eastern showing consisting of five holes that did not intersect significant mineralization; however, grab samples from the western shore contained semi-massive bands of sphalerite and lesser chalcopyrite (Jacobs et al., 1998;

Sparkes, 2018). Canaco gave up their option on the ground before further exploration was conducted. Copper Hill Resources Inc. optioned the property in 1999 and began drilling from the western shoreline of Powderhorn Lake, producing intersections of 7.4% Zn and 0.19% Cu over 1 m (Wilton and Akkerman, 2000). This mineralization highlighted the potential for Zn-Cu+/-Pb VMS-style mineralization (Wilton et al., 2001a) and procured interest for additional drilling. Significant drill core intersections in the following years include assays of 4.00% Zn, 0.14% Cu over 0.6 m (Wilton et al., 2001b) and the discovery of stringer-style mineralization that assayed up to 1.52% Zn over 5.7 m (Delaney et al., 2007). In 2008, Champion Iron Minerals (now Champion Iron Limited) and their contractors became joint-venture partners with Copper Hill Resources Inc., continuing the on-going exploration program at Powderhorn Lake. In the following years, multiple explorational surveys were conducted including ground gravity, petrography, airborne electromagnetic, and a deep-penetrating TITAN-24 direct current and induced polarization (DCIP) survey (Georghiou, 2011). These surveys outlined gravity and magnetic anomalies, structures, and possible alteration zones that provided the framework for additional diamond drilling.

In 2017 and 2018 Champion Iron Limited conducted a 4,000 m diamond drilling program that intersected several significant mineralized intervals: 1) PH18-01 intersected 3.31% Zn, 0.53% Cu, and 48 g/t Ag over 4.45 meters, and 2) 5.2% Zn, 0.48% Cu, and 22 g/t Ag over 4.46 m, and 3) PH18-06 intersected 6.94% Zn and 48 g/t Ag over 3.35 m (Champion Iron Limited, 2018). A preliminary geological model suggested the occurrence of three stacked lenses or layers of Zn-rich zones underlain by a Cu-rich zone (Champion Iron Limited, 2018). The promising results of the initial drilling program resulted in a second 12,000 m program in the Fall of 2018 to test the continuity between Zn-rich zones and distribution of Cu mineralization.

Significant mineralized intercepts from the program included: 1) PH18-12 intersected 6.90% Zn, 0.14% Cu, and 7.7 g/t Ag over 3.22 m; 2) PH18-34 intersected 14.54% Zn, 0.40% Cu, and 105.9 g/t Ag over 1.68 m; and 3) PH18-40 intersected 8.37% Zn, 0.62% Cu, and 21.6 g/t Ag over 2.57 m (Champion Iron Limited, 2019). Results from the 2017 and 2018 drilling programs indicated that the Zn-rich zones extend from surface to maximum vertical depths of ~630 m whereas the Cu-rich zone occurs at shallower depths from ~14 to ~75 m.

1.2 Tectonic Evolution and Regional Geology

The Newfoundland Appalachians are divided into four lithotectonic zones (from west to east): Humber, Dunnage, Gander, and Avalon, which are separated from one another by regional faults and suture zones (Fig. 1) (Williams, 1979; Williams et al., 1988, Williams, 1995). These lithotectonic zones record multiple orogenic events associated with the opening and closure of both the Iapetus and Rheic oceans during the formation of Pangea (Williams, 1979; Williams et al., 1988; Swinden, 1991; van Staal and Barr, 2012).

The Dunnage zone consists of Cambrian-Ordovician continental- and oceanic arc to back-arc assemblages and ophiolitic rocks that formed on opposite sides of the Iapetus Ocean (i.e., Laurentia and Gondwana) and related peri-continental seaways (Williams, 1995; Zagorevski et al., 2006; van Staal, 2007; van Staal and Barr, 2012). The Dunnage zone is subdivided into the peri-Laurentian Notre Dame and peri-Gondwanan Exploits subzones that accreted onto their respective margins during the second phase of the Taconic orogeny in the Lower to Middle Ordovician and the Early Ordovician Penobscot orogenies, respectively, and subsequently to each other during the final stages of the Taconic orogeny in the Late Ordovician along the Beothuk Lake Line (BLL; = Red Indian Line historically) suture zone (Williams, 1995; Zagorevski et al., 2006; Zagorevski et al., 2007; van Staal, 2007; van Staal and Barr, 2012).

The Notre Dame Subzone is comprised of Early Paleozoic terranes including the Lushs Bight and Baie Verte oceanic tracts (LBOT and BVOT), the Notre Dame arc, the Dashwoods microcontinent, and the Annieopsquotch accretionary tract (AAT) (Williams et al., 1988; van Staal et al., 2007; van Staal and Barr, 2012). The assemblage of these terranes and eventual accretion onto the Laurentian margin was associated with three phases of the Taconic orogeny (Fig. 1.2). The first phase occurred in the late Cambrian (500-493 Ma) as the LBOT (i.e., juvenile arc-crust) was obducted onto the Dashwoods microcontinent within the Taconic seaway (van Staal et al., 2007; van Staal and Barr, 2012). The formation of an eastward dipping subduction zone beneath the composite Dashwoods-LBOT terrane at ~490 Ma led to the formation and first magmatic pulse of the Notre Dame arc (489-477 Ma), initiation of a westward dipping oceanic suprasubduction zone and ophiolite belt (i.e., the Annieopsquotch ophiolite belt; AOB) outboard of Dashwoods, and eventual obduction of the BVOT onto the Laurentian margin (van Staal et al., 2007, van Staal and Barr, 2012). The prolonged subduction of the Laurentian margin associated with the second phase of the Taconic orogeny led to the Dashwoods-Laurentia collision, supported by the ~476-465 Ma magmatic gap of the Notre Dame arc (Waldron and van Staal, 2001; van Staal et al., 2007; van Staal and Barr, 2012). The collision marks the final stages of Taconic 2 that resulted in: 1) thickening of the Notre Dame arc; 2) break-off of the subducting Laurentian slab; 3) back-arc volcanism within the AOB (Zagorevski et al., 2006, 2008); 4) initiation of underplating-related accretion of the AAT to the Laurentian margin; and 5) the short, but voluminous, second phase of Notre Dame arc magmatism (464-459 Ma) (van Staal et al., 2007; van Staal and Barr, 2012). The presence of Ordovician plutonic rocks of the Notre Dame arc that display geochemical attributes of both mantle- and slab-derived sources throughout the Notre Dame Subzone further supports this

complex suprasubduction zone tectonic model (Whalen et al., 1997; van Staal and Barr, 2012). The final phase (~455-450 Ma) and end of the Taconic orogenic cycle involved the collision of the composite Laurentian margin (i.e., assembled peri-Laurentian terranes) with the leading, peri-Gondwanan Popelogan-Victoria arc (van Staal et al., 2007; Zagorevski et al., 2007a; van Staal and Barr, 2012).

The Penobscot orogeny (~515-478 Ma) coincided with the Taconic orogeny; however, there is no genetic link between the two orogenies (van Staal 1994; Zagorevski et al., 2010; van Staal and Barr, 2012). The orogenic cycle began with east-directed subduction beneath peri-Gondwana and resulted in the formation and eventual separation of the Penobscot arc from the Gondwanan margin (509-501 Ma) to create the Rheic Ocean (Neuman, 1967; Colman-Sadd et al., 1992; Zagorevski et al., 2010; van Staal and Barr, 2012). Continued subduction resulted in extension and the creation of the Penobscot back-arc (~500-485 Ma) until eventual closure (486-478 Ma) that coincided with the cessation of magmatic activity from the Penobscot arc (Colman-Sadd et al., 1992; Zagorevski et al., 2010; van Staal and Barr 2012).

The Salinic orogenic cycle began with initiation of a west-dipping subduction zone beneath the underplated AAT and resulted in the step-back of the composite Laurentian margin to create the Tetagouche-Exploits back-arc basin that was eventually subducted from 447-430 Ma (van Staal 1994; van Staal et al., 1998, 2003; Valverde-Vaquero et al., 2006; van Staal and Barr, 2012). This subduction event created regional-scale structural features such as mélanges, folds, and thrust faults that are found throughout northern and central Newfoundland (Williams et al., 1988; Elliot et al., 1991; Lafrance and Williams, 1992; Currie 1995; Lee and Williams, 1995; O'Brien, 2003; Zagorevski et al., 2007; van Staal et al., 2009). Lastly, the subduction of

back-arc lithosphere led to the final magmatic pulse of the Notre Dame arc between 445 and 435 Ma (van Staal, 1994; van Staal et al., 1998; Whalen et al., 2006).

The AAT juxtaposes the RIL, representing the easternmost unit of the Notre Dame Subzone and consists of multiple thrust-faulted, imbricated packages of suprasubduction ophiolitic rocks of the AOB and bimodal arc to back-arc rocks of the Buchans-Roberts Arm volcanic belt (BRAB) (Dunning and Krogh, 1985; Swinden et al., 1997; Lissenberg et al., 2005a; Lissenberg et al., 2005b; Zagorevski et al., 2006; O'Brien, 2007). The BRAB is host to many VMS deposits (e.g., Buchans, Gullbridge, Pilley's Island, etc.) and is comprised of the Early-Middle Ordovician Buchans, Roberts Arm, Cottrells Cove, Chanceport, and the Red Indian Lake groups (Kalliokoski, 1955; Swinden, 1991; Dickson, 2001; Rogers et al., 2005; O'Brien, 2007). The rocks of the Powderhorn Lake area are assigned to a younger metasedimentary unit and an older metavolcanic unit, both of which are intruded by metamorphosed late Ordovician to early Silurian intrusive rocks (Fig. 1.4). The rocks in this area are cut by and bounded by a series of faults that comprise a northwest plunging antiform (Dickson, 2000; O'Brien, 2007).

1.3 Geology of the Powderhorn Lake Deposit

The mineralization comprising the Powderhorn Lake deposit has been previously interpreted to be hosted within the Roberts Arm Group; a sequence of rocks that is host to past producing VMS deposits (e.g., Gullbridge and Buchans) (Akkerman, 2006). The deposit consists of multiple mineralized lenses that occur at different stratigraphic levels. The lithostratigraphy of the deposit has been divided into the hanging wall, mineralized sequence, and footwall.

Strata comprise interbedded felsic volcaniclastic rocks and rare sedimentary rocks that are intercalated with coherent, felsic volcanic rocks. The hanging wall consists of crystal-tuff, tuff, and lesser lapilli tuff that are typically underlain by aphyric to biotite +/- quartz-phyric massive to flow-banded rhyolite. The footwall strata are similar; however, the top of the sequence is dominated by crystal-tuffs and lapilli tuffs that are underlain by coherent rhyolite flow and lesser, discontinuous mudstone lenses. In the northern portion of the Powderhorn Lake area, volcanic hanging wall strata are overlain by a graphite- and pyrrhotite-rich volcanosedimentary (predominantly siltstone) cover sequence. All lithostratigraphic units are intruded by variably altered to unaltered, aphanitic to feldspar porphyritic intermediate dikes and rare quartz-feldspar-phyric rhyolite sills.

The mineralized sequence occurs at the hanging wall/footwall contact along interpreted synvolcanic faults and occurs as semi-conformable to conformable stacked lenses hosted within tuffaceous rocks. The sulfide lenses consist of semi-massive to massive, fine- to coarse-grained pyrrhotite, sphalerite, and chalcopyrite with variable pyrite and minor galena. Disseminated to stringer sphalerite and chalcopyrite with variable pyrite+/-pyrrhotite typically envelope semi-massive and massive sulfide lenses.

Hydrothermal alteration at the Powderhorn Lake deposit occurs in both the hanging wall and footwall strata of most lenses, with the most intense alteration occurring proximal to the mineralization. Alteration zones typically consist of widespread and pervasive sericite alteration that envelopes and laterally extends from proximal, discordant (pipe-like) chlorite alteration. Alteration mineralogy consists of variable amounts of quartz, sericite, and chlorite with lesser pyrite and rare carbonate. The main alteration assemblages consist of quartz-sericite and quartz-sericite-chlorite+/-pyrite.

Petrographic work and analyses demonstrate that original alteration minerals (i.e., sericite and chlorite) have been metamorphosed to K- and Al-rich assemblages composed of muscovite, biotite, sillimanite, lesser cordierite, and rare anthophyllite and spinel. Furthermore, there is mineralogical evidence supporting a late-stage calcic alteration that has manifested predominantly throughout volcaniclastic rocks in patches and veins consisting of epidote, garnet, calcite, and rare tremolite. These metamorphic overprints do affect, to some extent, the mobile element geochemistry as noted below; however, the complete extent or significance of these affects are not well understood.

1.4 Volcanogenic Massive Sulfide (VMS) Deposits

Volcanogenic massive sulfide (VMS) deposits typically occur as stratabound to stratiform lenses of Zn-Pb-Cu-(Ag-Au)-bearing sulfides that form from the exhalation of hot, metalliferous fluid onto, or just below, the seafloor and are associated with contemporaneous, submarine volcanism in subaqueous environments (Franklin et al., 1981, 2005; Lydon, 1984, 1988; Large, 1992; Barrie and Hannington, 1999; Galley et al., 2007; Hannington, 2014). The formation of these deposits occurs within extensional tectonic environments including mid-ocean ridges, intraoceanic and continental arcs, and back-arc basins, which provide the consistent high heat flow required for long lived, higher temperature hydrothermal convection (Franklin et al., 1981, 2005; Lydon, 1984, 1988; Large, 1992; Barrie and Hannington, 1999; Galley et al., 2007; Gibson et al., 2007; Piercey, 2011).

Volcanogenic massive sulfide deposits can be divided into six types based upon host lithostratigraphy: mafic, pelitic mafic, bimodal-mafic, bimodal-felsic, hybrid bimodal-felsic, and felsic-siliciclastic (Barrie and Hannington, 1999; Franklin et al., 2005; Galley et al., 2007). Each lithostratigraphic type provides information that broadly defines the tectonic regime and

processes that led to deposit formation along with general geologic and deposit characteristics (e.g., alteration assemblages, average deposit size and grade, etc.). The Powderhorn Lake deposit is characterized as felsic-siliciclastic, one of the first occurrences of this type defined as such within the Notre Dame subzone, whereas the Exploits subzone is host to two felsic-siliciclastic deposits (Tulks East and Boomerang; Piercey and Hinchey, 2012). This deposit type is associated with siliciclastic sedimentary rocks and volcanic rocks that are often volcaniclastic in nature (Barrie and Hannington 1999; Franklin et al., 2005; Galley et al., 2007; Piercey, 2009).

Volcanogenic massive sulfide deposits are typically associated with extensive, recharge-related semi-conformable alteration and more proximal, discharge-related discordant to pipe-like hydrothermal alteration (Riverin and Hodgson, 1980; Franklin et al., 1981, 2005; Gemmel and Large, 1992; Large, 1992; Galley 1993; Piercey, 2009). Semi-conformable alteration results from the fluid-rock interactions as seawater is drawn downward and heated within the semi-permeable volcanic sequences that are adjacent to, or overly, subvolcanic intrusions. Metals and mobile elements are stripped from the surrounding country rocks to produce stacked semi-conformable alteration zones (e.g. spilitization, silicification, etc.) that vary in mineralogy as a function of geothermal temperature gradients (Franklin et al., 1981, Lydon, 1988; Galley, 1993, 2003; Piercey, 2009). Discordant, pipe-like alteration zones are generally a function of the upward flow of hot, metal-enriched hydrothermal fluids through synvolcanic structures. Typically, the alteration mineralogy of the pipe can be distinguished by a chlorite-rich core enveloped by a chlorite-sericite zone that eventually grades into an outermost sericite-quartz zone; however, not all assemblages are found in every deposit

(Riverin and Hodgson, 1980; Franklin et al., 1981, 2005; Lydon, 1984; Lydon, 1988; Galley et al., 2007).

The classic genetic model for VMS deposit formation and emplacement of sulfides invokes exhalative processes whereby sulfide minerals are precipitated and deposited directly onto the seafloor as a result of mixing of hot, metal- and sulfide-bearing fluid with surrounding cold seawater; resulting in the oxidation and precipitation of sulfates (e.g., anhydrite) and sulfides (Hutchinson, 1973; Lydon, 1984, 1988; Ohmoto, 1996; Franklin et al., 1981, 2005). Continuous venting results in the growth of seafloor chimneys that eventually collapse, and the resulting breccia undergoes cementation and sequential replacement by sulfides (and anhydrite) (Lydon, 1984, 1988; Hannington et al., 1995; Ohmoto, 1996; Franklin et al., 2005; Galley et al., 2007). Subseafloor replacement deposits form as metalliferous hydrothermal fluids infiltrate and replace originally permeable clastic stratigraphy of the host country rock resulting in precipitation of sulfide minerals within open spaces (Doyle and Allen, 2003; Franklin et al., 2005; Piercey, 2015).

1.5 Thesis Objectives

Previous work at the Powderhorn Lake deposit was exploration focused with the main goal of defining the deposit and target area. This thesis represents the first academic project aimed at characterizing the strata, volcanic facies, hydrothermal alteration, and lithogeochemistry in order to reconstruct the lithostratigraphy and tectonic evolution of the deposit. Characterizing the tectonic framework and volcanic architecture of the deposit will aid in the delineation of the distribution of, and associated controls on, alteration and subsequent replacement-style mineralization in volcaniclastic-hosted VMS deposits. The main objectives are as follows:

1) construct a lithostratigraphic framework and document structures (e.g., faults, folding, etc.), mineralogy, and mineralization through graphic drill logs, cross-sections, petrography, and lithogeochemistry;
2) characterize hydrothermal alteration assemblages through petrography, mobile element lithogeochemistry, and short-wave infrared (SWIR) spectroscopy;
3) analyze lithofacies with respect to alteration to understand the main controls on hydrothermal alteration distribution;
4) utilize lithogeochemistry to develop a chemostratigraphic framework for the deposit. Determine a least-altered sample to conduct mass change calculations and quantify elemental gains and losses of alteration assemblages and zones;
5) combine above data to create a representative 3D geologic and alteration model of the deposit that will help to identify relationships between lithofacies and alteration to further understand formation of the sulfide deposit; and
6) interpret the above data to reconstruct the volcanic architecture and tectonic setting to understand the evolution and formation of the Powderhorn Lake deposit.

1.6 Methods

The Powderhorn Lake deposit model was defined using the following methods: 1) documentation of strata, synvolcanic structures, and alteration assemblages through graphic drill core logging; 2) representative sampling of lithologies and alteration to conduct thin section petrography, scanning electron microscope (SEM) analyses, major and trace element analyses (ICP-MS), and hyperspectral (TerraSpec) analysis; and 3) 3D reconstruction of geology, alteration, and lithogeochemistry of the Powderhorn Lake deposit.

1.6.1 Core logging

Approximately one and a half months of detailed core logging and geochemical sampling was completed in the Fall of 2019 and Summer of 2020 at the Powderhorn Lake core storage shed in Springdale, NL. Champion Iron Ltd. provided previous drill logs and simplified cross-sections. A total of 22 holes were re-logged from the area (Fig. 1.4). Entire holes were logged to document structure, lithology, mineralization, and alteration. Graphic core logs, rough cross-sections, supplementary notes, photos, and sample numbers were recorded in the field. Graphic logs and cross-sections were later digitized using Adobe Illustrator software (Appendix A). Lithologies and structures were extrapolated between re-logged holes and previously logged holes of the Powderhorn Lake area.

1.6.2 Lithogeochemistry

A total of 206 samples were collected (5 to 15 cm in length) from representative lithologies and alteration zones. Drill core that exhibited evidence of faulting (e.g., widespread quartz or carbonate veining) were avoided. Core samples collected from the Powderhorn core storage facility were cut in half, and the remaining material is archived at Memorial University of Newfoundland.

All samples were analyzed for major oxide elements (SiO_2, Al_2O_3, Fe_2O_3, MnO, MgO, CaO, Na_2O, K_2O, TiO_2, P_2O_5) and select trace elements (Ba, Sr, Y, Sc, Zr, Be, V, Hg), base metals (Zn, Cu, Pb, Sc, Ti, V, Cr, Mn, Co, Ni), and volatile elements (As, Bi, Cd, Sn, Sb, Tl) at ALS Minerals Ltd. in Sudbury, Ontario using the complete characterization package (CCP-PKG01) (Appendix B). At ALS Minerals, all samples were crushed using a standard jaw crusher and pulverized using mild steel. The major and trace elements were analyzed using lithium borate fusion pre-analysis with subsequent dissolution with an ICP-AES finish,

whereas HFSE (Zr, Hf, Nb, Ta, Y, Ga), LFSE (Ba, Th, U, Rb, Sr), and select transition metals (Cr, V, Sn) underwent identical pre-analysis procedures and analysis with an ICP-MS finish. Base metals (Cu, Zn, Pb), and Ag, Cd, Co, Li, Mo, Ni, and Sc were determined using four-acid dissolution with an ICP-MS finish. Quality assurance and quality control (QA/QC) protocols were followed by replicating analyses of internal ALS standards and an internal rhyolite standard (ORCA-1) and can be found in Appendix C.

1.6.3 Petrography and Scanning Electron Microscopy

Forty-one samples were cut into billets (2.5 cm x 4.5 cm) and sent to Vancouver Petrographics to be prepared into polished thin sections. Petrographic work was completed using a Nikon LV100POL polarizing microscope at Memorial University. Reflected and transmitted light were used to document basic petrography, mineral assemblages, and textures. SEM analyses were undertaken at Memorial University and were used to identify trace minerals and textural relationships within sulfide phases. Semi-quantitative composition analyses were collected using Energy Dispersive X-Ray (EDX) analysis mapping whereas mineral phases and textures were documented using backscatter electron (BSE) imaging.

1.6.4 Short-wave Infrared (SWIR) Spectroscopy

Hyperspectral analyses were undertaken at Memorial University using a Terraspec^{TM} mineral spectrometer with a Hi-Brite Muglight. Core samples were cleaned and dried prior to analysis. Terraspec^{TM} was optimized using a white reference disk every 20 samples or every 20 minutes to avoid instrument drift. Quality control was monitored using an internal pyrophyllite reference material and all analyses were conducted in a naturally sunlit room to avoid interference from artificial light. Hyperspectral data were collected using RS3 spectral acquisition software and processed using The Spectral Geologist Hotcore v. 7.1.55 software.

This software applies hull correction and quantifies diagnostic spectral absorption features (i.e., absorption wavelengths, depth of absorption hull) to identify specific minerals within the sample.

1.6.5 2D and 3D Modelling

The geology, structure, mineralization, and alteration zones were modelled in 3D using drill core and lithogeochemical (e.g., mass change, metallurgical assays, etc.) data. Geological models were produced using interval data from drill core logs whereas alteration zones and grade shells were produced using RBF interpolants.

1.7 Co-Authorship Statement

This research project was designed by Dr. Stephen J. Piercey. The primary research and data collection was conducted by the author including core logging and optical microscopy. Hyperspectral analysis and Leapfrog models were produced by the primary author with considerable help and teachings from Nikola Denisova. Scanning electron microscopy and electron microprobe analysis was conducted by the author with help and supervision of Wanda Aylward. The primary editor of this manuscript is Dr. Stephen J. Piercey with secondary editing from Dr. Luke Beranek.

1.8 Presentation

This thesis consists of three chapters and supplementary appendices. Chapter 1 provides the background information of the project, regional and local geology, and methodology. Chapter 2 is the main body of this thesis and contains detailed descriptions of the geology, alteration, and mineralization. This chapter provides evidence for the tectonic evolution and volcanic regime for the Powderhorn Lake VMS deposit based on data collected

from graphic core logging, optical microscopy, whole-rock analyses (ICP-MS), Leapfrog Geo, and short-wave infrared (SWIR) spectroscopy. This chapter is written with the intention of submission to a peer-reviewed journal. The third chapter provides a summary of the conclusions drawn from Chapter 2 and directions for future research. The appendices include digitized graphic drill logs, cross-sections, and geochemical data including whole rock lithogeochemistry, hyperspectral datasets, electron microprobe and scanning electron microscope results.

References

Akkerman, J.H., 2006, Report on geological assessment: Powderhorn VMS prospect, Buchans-Roberts Arm Belt, central Newfoundland, Canada, Unpublished Report for Copper Hill Resources Inc. (Assessment File 012H/01/2228 Newfoundland Department of Mines and Energy, Mineral Lands Division) St. John's, Newfoundland, 87 p.

Barrie, C.T., and Hannington, M.D., 1999, Introduction: classification of VMS deposits based on host rock composition, in volcanic-associated massive sulfide deposits: processes and examples in modern and ancient environments, (eds.) C.T. Barrie and M.D. Hannington; Society of Economic Geologists, Reviews in Economic Geology, v. 8, p. 2-10.

Champion Iron Mines Ltd., 2018, Champion Iron intersects several zinc-rich intervals at its Powderhorn project, Newfoundland: https://newsroom.championiron.com/index.php?s=2429&item=122491 (accessed February 2020).

Champion Iron Mines Ltd., 2019, Champion Iron reports exploration results at Powderhorn project, Newfoundland: https://newsroom.championiron.com/2019-03-20-Champion-Iron-Reports-Exploration-Results-at-Powderhorn-Project-Newfoundland (accessed February 2020).

Colman-Sadd, S.P., Dunning, G.R., and Dec, T., 1992, Dunnage-Gander relationships and Ordovician orogeny in central Newfoundland: a sediment provenance and U/Pb study; American Journal of Science, v. 292, p. 317-355.

Currie, K. L., 1995, The Northeastern End of the Dunnage Zone in Newfoundland; Atlantic Geology, v. 3 1, p. 25-38.

Delaney, P.W., Howard, A.E., and Renou, A.S., 2007, Second, tenth, eleventh and twelfth year assessment report on compilation and diamond drilling exploration for licenses 4643M, 5139M, 11073M, 11345M, 11346M, 11367M, and 12700M on claims in the Powderhorn Lake area, central Newfoundland, Newfoundland and Labrador Geological Survey, Assessment File 012H/01/1887, 261 p.

Dickson, W.L., 2000, Geology of the eastern portion of the Dawes Pond (NTS 12H/1) map area, central Newfoundland, *in* Current Research, Newfoundland Department of Mines and Energy, Geological Survey Branch, Report 2000-1, p. 127-145.

Dickson, W.L., 2001, Geology of the eastern portion of the Dawes Pond (NTS 12H/1) map area, central Newfoundland, Newfoundland Department of Mines and Energy, Geological Survey Map 2001-21, Open File 012H/01/1606.

Doyle, M.G., and Allen, R. L., 2003, Subsea-floor replacement in volcanic-hosted massive sulfide deposits; Ore Geology Reviews, v. 23, p. 183-222.

Dunning, G. R., and Krogh, T. E., 1985, Geochronology of ophiolites of the Newfoundland Appalachians; Canadian Journal of Earth Sciences, v. 22, p. 1659- 1670.

Elliott, C. G., Dunning, G. R., and Williams, P. F., 1991, New U/Pb zircon age constraints on the timing of deformation in north-central Newfoundland and implications for early Paleozoic Appalachian orogenesis; Geological Society of America Bulletin, v. 103, p. 125-135.

Franklin, J.M., Gibson, H.L., Jonasson, I.R., and Galley, A.G., 2005, Volcanogenic massive sulfide deposits; *in* Economic Geology 100th Anniversary Volume, p. 523– 560.

Franklin, J.M., Lydon, J.W., and Sangster, D.F., 1981, Volcanic-associated massive sulfide deposits; *in* Economic Geology 75th Anniversary Volume, p. 485-627.

Galley, A.G., 1993, Characteristics of semi-conformable alteration zones associated with volcanogenic massive sulphide districts; Journal of Geochemical Exploration, v. 48, p. 175-200.

Galley, A.G., 2003, Composite synvolcanic intrusions associated with precambrian VMS-related hydrothermal systems; Mineralium Deposita, v. 38, p. 2006-2017.

Galley, A.G., Hannington, M.D. and Jonasson, I.R., 2007, Volcanogenic massive sulfide deposits, *in* Contributions to Mineral Resources of Canada: A Synthesis of Major Deposit Types, District Metallogeny, the Evolution of Geological Provinces, and Exploration Methods, (eds.) W.D. Goodfellow and I.M. Kjarsgaard; Geological Association of Canada, Mineral Deposits Division, Special Publication No. 5, p. 141-161.

Gemmell, J. B., and Large, R. R., 1992, Stringer system and alteration zones underlying the Hellyer volcanic-hosted massive sulfide deposit, Tasmania, Australia; Economic Geology, v. 87, p. 620-649.

Georghiou, P.E., 2011, Supplementary assessment report on the compilation of the geophysical data acquired by Abitibi Geophysics, Quantec Geoscience, and Furgo Airborne Surveys Corp over the Gullbridge and Powderhorn Lake properties, Newfoundland and Labrador, Canada, Assessment File 012H/01/2183 Newfoundland Department of Mines and Energy, Mineral Lands Division, p. 20.

Gibson, H.L., Allen, R.L., Riverin, G., Lane, T.E., 2007, The VMS Model: Advances and application to exploration targeting, *in* Proceedings of Exploration 07: Fifth Decennial International Conference on Mineral Exploration; Toronto, ON, (ed.) B. Milkereit, p. 717-730.

Hannington, M.D., Honasson, I.R., Herzig, P.M., and Peterson, S., 1995, Physical and chemical processes of sea floor mineralization at mid-ocean ridges, *in* Seafloor Hydrothermal Systems: Physical, Chemical, Biological and Geological Interactions, (eds.) S.E. Humphris, R.A. Zierenberg, L.S. Mullineaux, and R.S. Thomson; American Geophysical Union, Monograph 91, p. 115-157.

Hannington, M. D., 2014, Volcanogenic massive sulphide deposits, *in* Treatise on Geochemistry (Second Edition), (ed.) Holland, H.D. and Turekian, K.K.; Elsevier, p. 463-488.

Hutchinson, R.W., 1973, Volcanogenic massive sulphide deposits and their metallogenic significance; Economic Geology, v. 68, p. 1223-1246.

Jacobs, W.J., Candy, C., Kerr, A., and Dickson, L., 1998, First second and third year assessment report on geological, geochemical, and geophysical, trenching and diamond drilling exploration for licence 4724 on claim block 8063 and licences 4559M, 4643M, 5138M, 5139M, 5144M,

5644M and 5854M on claims in the Powderhorn Lake area, central Newfoundland, 2 reports, Newfoundland and Labrador Geological Survey, Assessment File 12H/01/1552, 230 p.

Kalliokoski, J., 1955, Gull Pond, Newfoundland (NTS 12H/SE), Canada Department of Mines and Technical Services, Geological Survey of Canada, Preliminary Map 54-04, Open File 012H/01/0050.

Kerr, A., 1999, The Powderhorn Lake Ni-Cu showing and the potential for magmatic sulphide mineralization in central Newfoundland, *in* Current Research; Newfoundland and Department Mines and Energy, Geological Survey Branch, Report 99-1, p. 205-214.

Lafrance, B., and Williams, P. F., 1992, Silurian Deformation in Eastern Notre-Dame Bay, Newfoundland; Canadian Journal of Earth Sciences, v. 29, p. 1899-1914.

Large, R.R., 1992. Australian volcanic-hosted massive sulphide deposits: features, styles and genetic models; Economic Geology, v. 87, p. 471-510.

Lee, C.B. and Williams, H., 1995, The Teakettle and Carmanville melanges in the Exploits Subzone of northeast Newfoundland: recycling and diapiric emplacement in an accretionary prism, *in* New Perspectives in the Appalachian Orogen, (eds.) J. Hibbard, P. Cawood, S. Colman-Sadd, and C. van Staal; Geological Association of Canada, Special Paper 41, p. 147-160.

Lissenberg, C. J., van Staal, C. R., Bedard, J. H., and Zagorevski, A., 2005a, Geochemical constraints on the origin of the Annieopsquotch ophiolite belt, Newfoundland Appalachians; Geological Society of America Bulletin, v. 117, p. 1413-1426.

Lissenberg, C. J., Zagorevski, A., McNicoll, V. J., van Staal, C. R., and Whalen, J. B., 2005b, Assembly of the Annieopsquotch accretionary tract, Newfoundland Appalachians; age and geodynamic constraints from syn-kinematic intrusions; Journal of Geology, v. 113, p. 553-570

Lydon, J.W., 1984, Volcanogenic sulphide deposits, Part 1, A descriptive model; Geoscience Canada, v. 11, p. 195-202.

Lydon, J.W., 1988, Ore deposit models: Volcanogenic massive sulfide deposits, Part 2, Genetic models; Geoscience Canada, v. 15, p. 43–65.

Neuman, R.B., 1967, Bedrock geology of the Shin Pond and Stacyville quadrangles, Maine; U.S. Geological Survey, Professional Paper 524-1, 47 p.

O'Brien, B. H., 2003, Geology of the central Notre Dame Bay region (parts of NTS areas 2E/3,6, II), northeastern Newfoundland, Government of Newfoundland and Labrador, Department of Mines and Energy, Report 03-03, 134 p.

O'Brien, B.H., 2007, Geology of the Buchans-Roberts Arm Volcanic Belt, Near Great Gull Lake, *in* Current Research; Newfoundland and Labrador Department of Natural Resources, Geological Survey, Report 07-1, p. 85-102.

O'Brien, B.H., 2016, Geology of the Starkes Pond – Powderhorn Lake area (part of NTS 12H/01), central Newfoundland; Robert's Arm Volcanic Belt and Adjacent Rocks: Map 3 of 3. Scale 1:25,000; Government of Newfoundland and Labrador, Department of Natural Resources, Geological Survey, Map 2016-03, Open File NFLD/3268.

Ohmoto, H., 1996, Formation of volcanogenic massive sulfide deposits: The Kuroko perspective; Ore Geology Reviews, v. 10, p. 135-177.

Piercey, S.J., 2009, Lithogeochemistry of volcanic rocks associated with volcanogenic massive sulfide deposits and applications to exploration, *in* Submarine Volcanism and Mineralization: Modern through ancient, (eds.) B. Cousens and S.J. Piercey; Geological Association of Canada, Short Course, Quebec City, Canada, p. 15-40.

Piercey, S.J., 2011, The setting, style, and role of magmatism in the formation of volcanogenic massive sulfide deposits; Mineralium Deposita, v. 46, p. 449–471

Piercey, S. J., 2015, A semipermeable interface model for the genesis of subseafloor replacement-type volcanogenic massive sulfide (VMS) deposits; Economic Geology, v. 110, p. 1655-1660.

Piercey, S.J. and Hinchey, J., 2012, Volcanogenic Massive Sulphide (VMS) Deposits of the Central Mobile Belt, Newfoundland; Geologic Association of Canada-Mineral Association of Canada, Filed Trip Guidebook-B4, 56 p.

Riverin, G., and Hodgson, C.J., 1980, Wall-rock alteration at the Millenbach Cu-Zn mine, Noranda, Quebec; Economic Geology, v. 75, p. 424-444.

Rogers, N., van Staal, C.R., Pollock, J., and Zagorevski, A., 2005, Geology, Lake Ambrose and Part of Buchans, Newfoundland (NTS 12-A/10 and Part of 12-A/15); Geological Survey of Canada Open-File 4544, scale 1:50,000.

Sparkes, G.W., 2018, Preliminary investigations into the distribution of VMS-style mineralization within the central portion of the Buchans-Roberts Arm (Volcanic) Belt, central Newfoundland, *in* Current Research; Newfoundland and Labrador Department of Natural Resources, Geological Survey, Report 18-1, p. 167-184.

Swinden, H. S., 1991, Paleotectonic settings of volcanogenic massive sulphide deposits in the Dunnage Zone, Newfoundland Appalachians; Canadian Institute of Mining and Metallurgy Bulletin, v. 84, p. 59-89.

Swinden, H. S., Jenner, G. A., and Szybinski, Z. A., 1997, Magmatic and tectonic evolution of the Cambrian-Ordovician Laurentian margin of Iapetus: Geochemical and isotopic constraints from the Notre Dame subzone, Newfoundland, *in* The Nature of Magmatism in the Appalachian Orogen, (eds.) Sinha, A. K., Whalen, J. B., and Hogan, J.P.; Geological Society of America, Memoir 191, p. 337-365.

Valverde-Vaquero, P., van Staal, C. R., McNicoll, V., and Dunning, G. R., 2006, Mid-Late Ordovician magmatism and metamorphism along the Gander margin in central Newfoundland; Journal of the Geological Society of London, v. 163, p. 347-362.

van Staal, C.R., 1994, The Brunswick subduction complex in the Canadian Appalachians: record of the Late Ordovician to late Silurian collision between Laurentia and the Gander margin of Avalon; Tectonics, v. 13, p. 946-962.

van Staal, C.R., 2007, Pre-Carboniferous metallogeny of the Canadian Appalachians, *in* Mineral Deposits of Canada: A Synthesis of Major Deposit Types, District Metallogeny, the Evolution

of Geological Provinces, and Exploration Methods, (ed.) W.D. Goodfellow; Geological Association of Canada, Mineral Deposits Division, Special Publication No. 5, p. 793-818.

van Staal, C.R. and Barr, S.M., 2012, Lithospheric architecture and tectonic evolution of the Canadian Appalachians and associated Atlantic margin, Chapter 2, *in* Tectonic Styles in Canada: The LITHOPROBE Perspective, (eds.) J.A. Percival, F.A. Cook, and R.M. Clowes; Geological Association of Canada, Special Paper 49, p. 41-96.

van Staal, C.R., Dewey, J.F., MacNiocaill, C.M., and McKerrow, S, 1998, The Cambrian-Silurian tectonic evolution of the northern Appalachians: history of a complex, southwest Pacific-type segment of Iapetus, *in* Lyell: The Past is the Key to the Present, (eds.) Blundell, D.J. and Scott, A.C.; Geological Society, Special Publication 143, p. 199-242.

van Staal, C.R., Whalen, J. B., McNicoll, V. J., Pehrsson, S., Lissenberg, C. J., Zagorevski, A., van Breemen, O., and Jenner, G. A., 2007, The Notre Dame Arc and the Taconic Orogeny in Newfoundland; Memoir Geological Society of America, v. 200, p. 511-552.

van Staal, C.R., Whalen, J.B., Valverde-Vaquero, P., Zagorevski, A., and Rogers, N., 2009, Pre-Carboniferous, episodic accretion-related, orogenesis along the Laurentian margin of the northern Appalachians, *in* Ancient Orogens and Modern Analogues, (eds.) Murphy, J.B., Keppie, J.D., Hynes, A.J.; Geological Society London, Special Publication 327, p. 271-316.

van Staal, C.R., Wilson, R.A., Rogers, N., Fyffe, L.R., Langton, J.P., McCutcheon, S.R., McNicoll, V., and Ravenhurst, C.E., 2003, Geology and tectonic history of the Bathurst Supergroup and its relationships to coeval rocks in southwestern New Brunswick and adjacent Maine – a synthesis, *in* Massive Sulfide Deposits of the Bathurst Mining Camp, New Brunswick, and northern Maine, (eds.) Goodfellow, W.D., McCutcheon, S.R., and Peter, J.M.; Economic Geology, Monograph 11, p. 37-60.

Whalen, J.B., Jenner, G.A., Longstaffe, F.J., Gariepy, C., Fryer, B.J., 1997, Implications of granitoid geochemical and isotopic (Nd, O, Pb) data from the Cambrian-Ordovician Notre Dame arc for the evolution of the Central Mobile belt, Newfoundland Appalachians, *in* The Nature of Magmatism in the Appalachian Orogen, (eds.) Sinha, A.K., Whalen, J.B., Hogan, J.P.; Geological Society of America, Memoir 191, p. 367-395.

Waldron, J.W.F., and van Staal, C.R., 2001, Taconic Orogeny and the accretion of the Dashwoods block: a peri-Laurentian microcontinent in the Iapetus Ocean; Geology, v. 29, p. 811-814.

Whalen, J.B., McNicoll, V.J., van Staal, C.R., Lissenber, C.J., Longstaffe, F.J., Jenner, G.A., and van Breemen, O. 2006, Spatial, temporal and geochemical characteristics of Silurian collision-zone magmatism: an example of a rapidly evolving magmatic system related to slab break-off; Lithos, v. 89, p. 377–404.

Williams, H. 1979, Appalachian Orogen in Canada; Canadian Journal of Earth Sciences, v. 16: p. 792–807.

Williams, H., Colman-Sadd, S.P., and Swinden, H.S., 1988., Tectonostratigraphic subdivisions of central Newfoundland, *in* Current Research, Part B; Geological Survey of Canada, Paper 88-1B, p. 91–98.

Williams, H., 1995, Geology of the Appalachian-Caledonian Orogen in Canada and Greenland, (ed.) Williams, H.; Geological Survey of Canada, Temporal and Spatial Divisions; Chapter 2, v. 6, p. 21-44.

Wilton, D.H.C. and Akkerman, J.H., 2000, Second, third and fourth year assessment report on prospecting, geochemical exploration and diamond drilling for licence 4724 on claim block 8063 and licences 4559M, 4560M, 4643M, 5138M, 5139M, 5144M, 5400M, 5644M and 5854M on claims in Powderhorn Lake area, central Newfoundland; Newfoundland and Labrador Geological Survey, Assessment File 12H/01/1793, 114 p.

Wilton, D.H.C., Dwyer, B.L., and Wallis, R., 2001a, Third and fourth year, fourth supplementary, fifth year, fifth year supplementary, sixth year, and sixth year supplementary assessment report on geological, geochemical, geophysical and diamond drilling exploration for licence 4724 on claim block 8063 and licenses 4559M, 4560M, 4643M, 5138M, 5139M, 5144M, 5400M, 5644N and 5854M on claims in the Powderhorn Lake area, central Newfoundland, 3 reports; Newfoundland and Labrador Geological Survey, Assessment File 12H/01/1769, 222 p.

Zagorevski, A., McNicoll, V., van Staal, C.R., Kerr, A., Joyce, N., 2015, From large zones to small terranes to detailed reconstruction of an Early to Middle Ordovician arc-backarc system preserved along the Iapetus suture zone: A Legacy of Hank Williams; Geoscience Canada, v. 42, p. 125-150.

Zagorevski, A., Rogers, N., van Staal, C.R., McNicoll, V., Lissenberg, C.J., and Valverde-Vaquero, P., 2006, Lower to Middle Ordovician evolution of peri-Laurentian arc and back-arc complexes in the Iapetus: constraints from the Annieopsquotch Accretionary Tract, Central Newfoundland; Geological Society of America Bulletin, v. 118, p. 324–362.

Zagorevski, A., van Staal, C. R., McNicoll, V. J., and Rogers, N., 2007a, Upper Cambrian to Upper Ordovician peri-Gondwanan island arc activity in the Victoria Lake Supergroup, central Newfoundland; tectonic development of the northern Ganderian margin; American Journal of Science, v. 307, p. 339-370.

Zagorevski, A., van Staal, C.R., McNicoll V., Rogers, N., and Valverde-Vaquero, P., 2008, Tectonic architecture of an arc-arc collision zone, Newfoundland Appalachains, *in* Formation and Applications of the Sedimentary Record in Arc-Collision Zones, (eds.) Draut, A., Clift, P., and Scholl, D.; Geological Society of America, Special Paper 346, p. 309-334.

Zagorevski, A., van Staal, C.R., Rogers, N., McNicoll, V.J. and Pollock, J., 2010, Middle Cambrian to Ordovician arc-backarc development on the leading edge of Ganderia, Newfoundland Appalachians; Geological Society of America Memoirs, v. 206, p. 367-396.

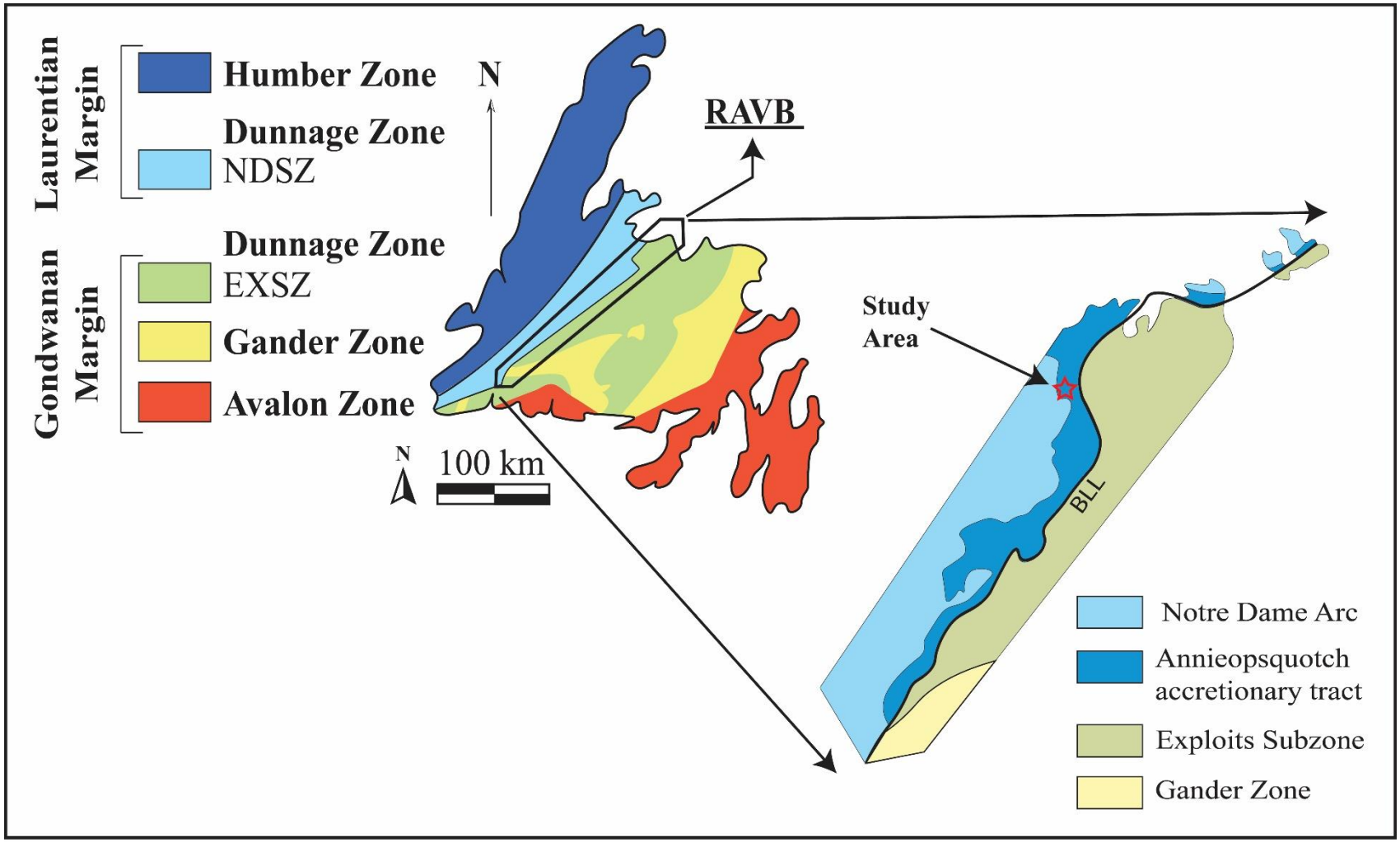

Figure 1.1. Geological map of Newfoundland Appalachians (modified after Williams et al., 1988) showing tectonostratigraphic zones with a subdivision showing a portion of the Notre Dame arc, Annieopsquotch accretionary tract (AAT), and Beothuk Lake Line (BLL; modified from van Staal et al.,1998). Study area indicated by red star. Figure is modified from Zagorevski et al., 2007.

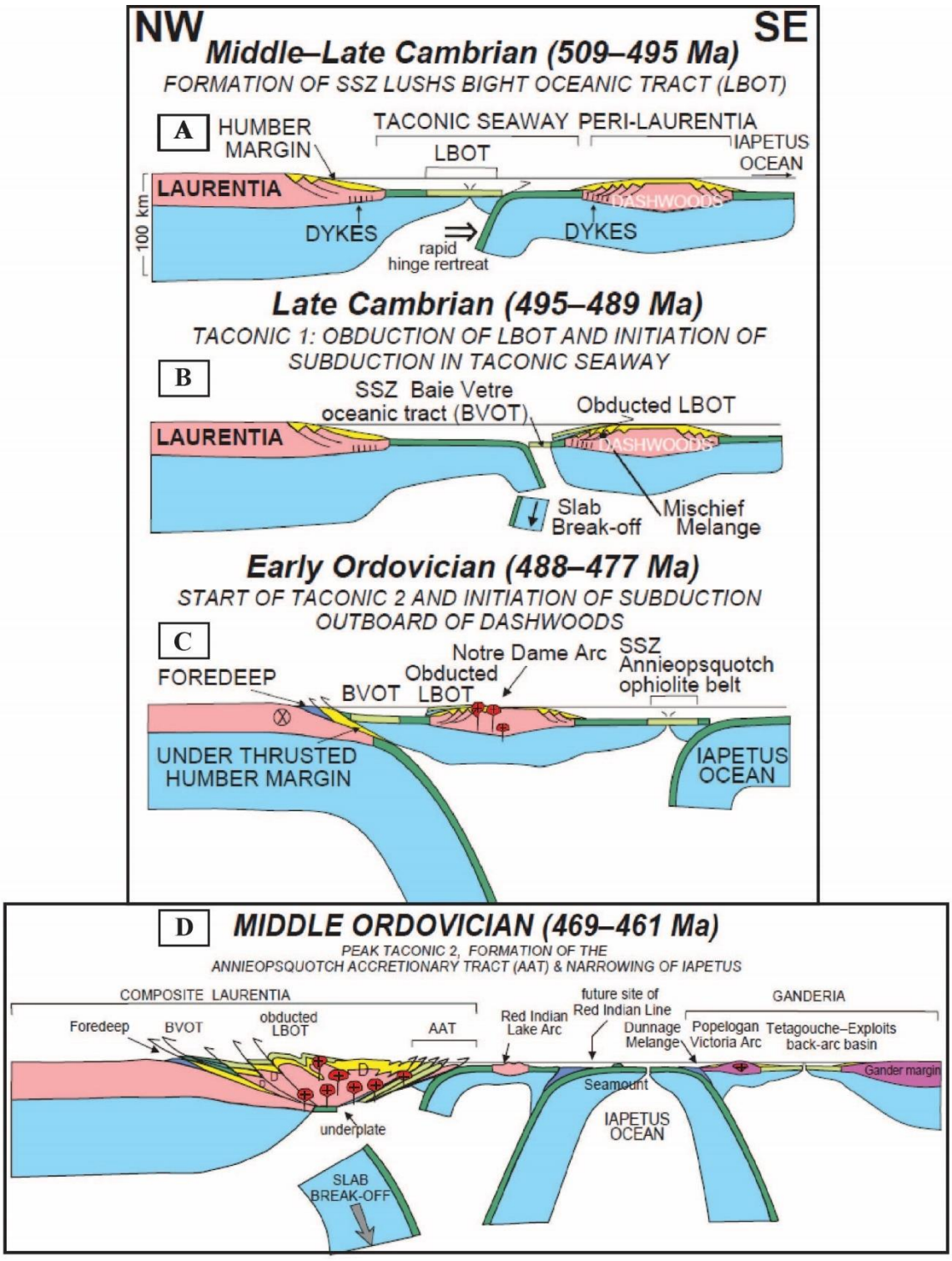

Figure 1.2. Tectonic evolution of the Laurentian margin. A) Rifting of Dashwoods off of Laurentia, opening of the Taconic seaway, subduction initiation, and formation of the LBOT. B) Obduction of LBOT. C) Initiation of a west-ward dipping subduction zone and formation of the AOB. D) Peak Taconic 2 resulting accretion of AAT and initiation of Salinic orogeny (from van Staal and Barr, 2012; modified from van Staal et al., 2007, 2009).

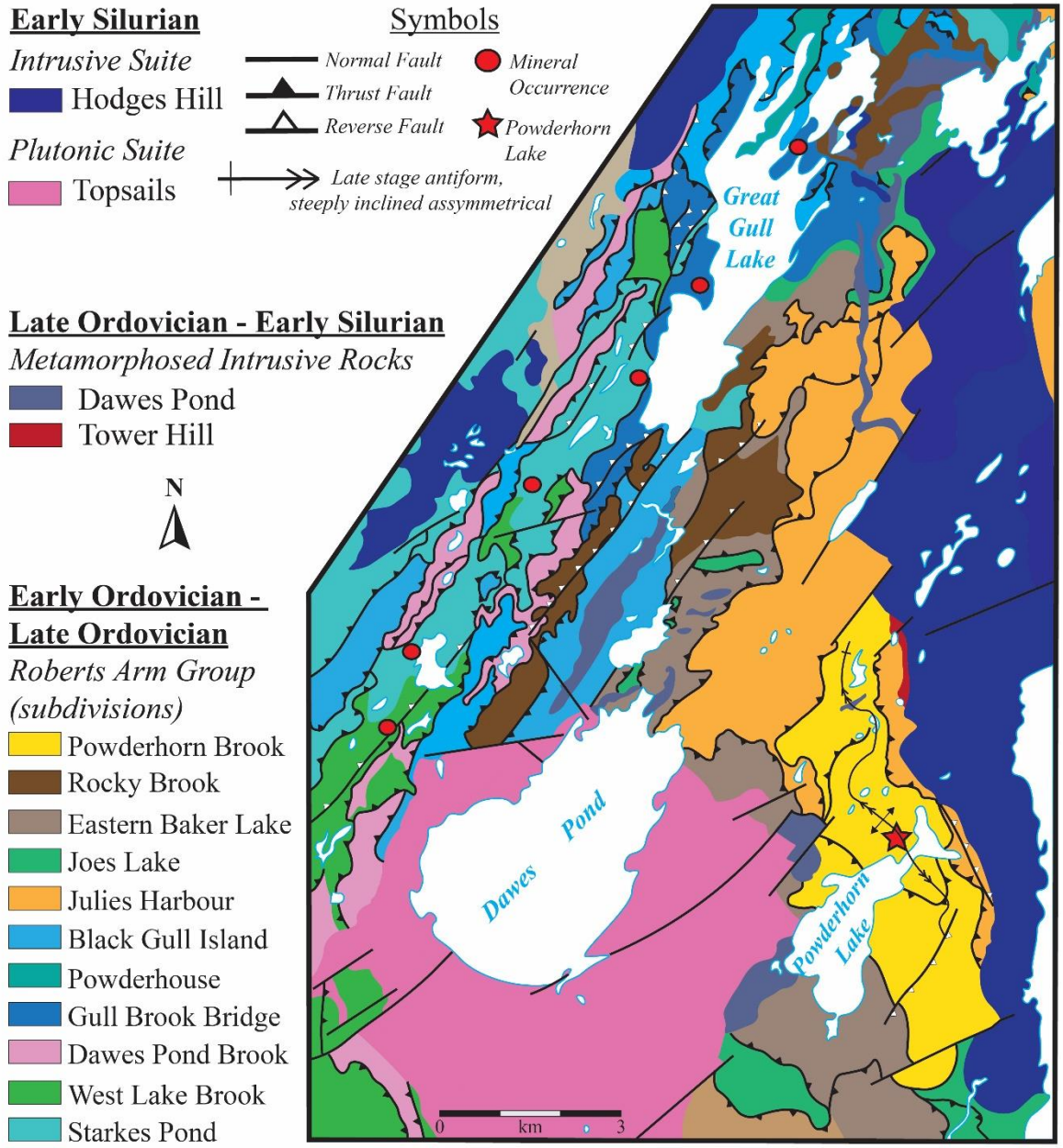

Figure 1.3. Simplified geological map of south-central portion of the Buchans-Roberts Arm belt showing select mineral occurrences and the study area. Modified from O'Brien (2016).

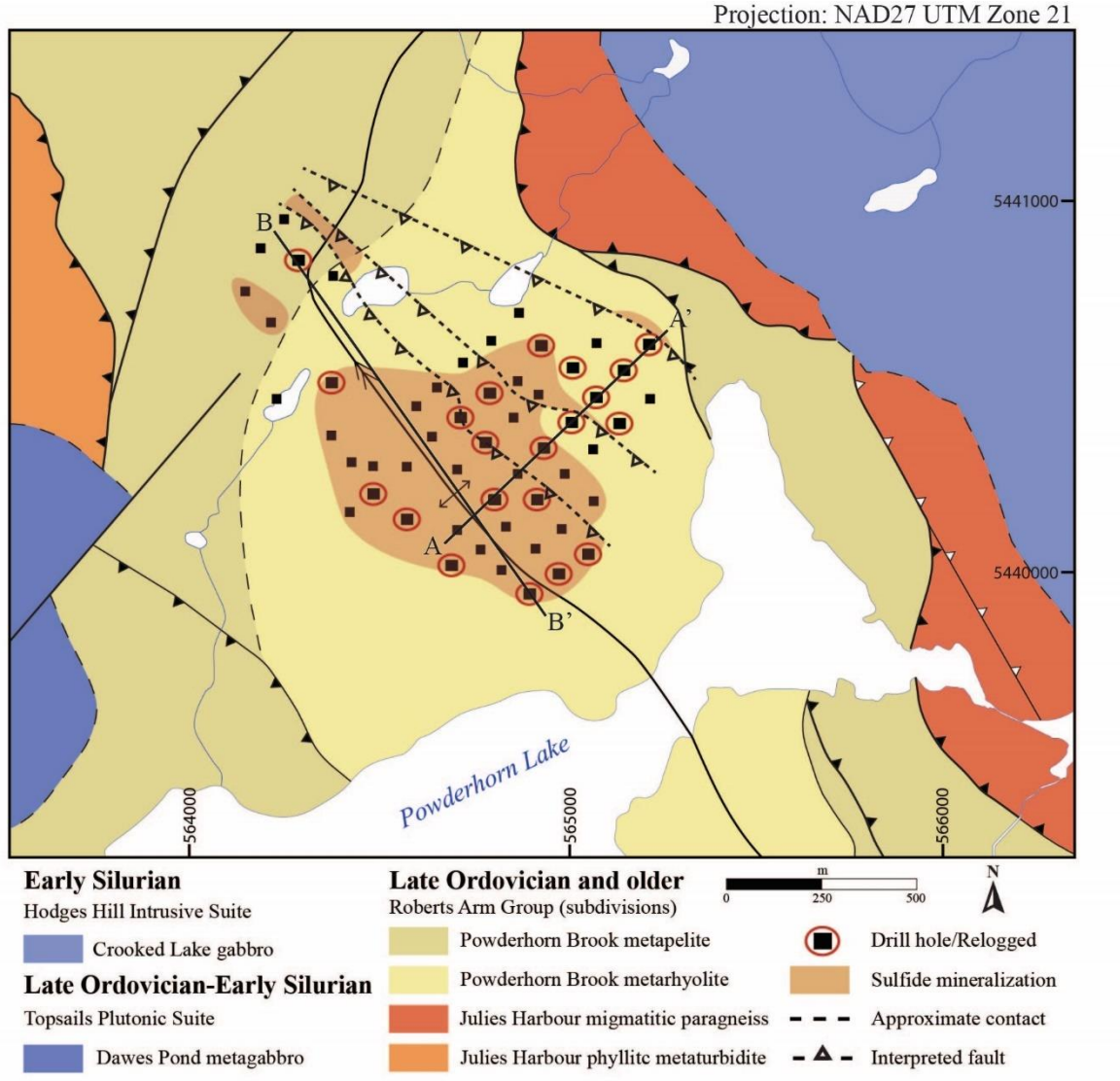

Figure 1.4. Geological map of the Powderhorn Lake area from surface mapping completed by O'Brien (2007, 2016). Mineralization projected to surface.

Chapter 2: Lithostratigraphic and Structural Reconstruction of the Powderhorn Lake Volcanogenic Massive Sulfide (VMS) deposit, central Newfoundland, Canada

2.1 Abstract

The Powderhorn Lake volcanogenic massive sulfide (VMS) deposit is located within the Ordovician Buchans-Roberts Arm (volcanic) belt (BRAB) of the Annieopsquotch accretionary tract (AAT) in central Newfoundland. The deposit is hosted within felsic volcaniclastic rocks and is an example of a felsic siliciclastic, replacement-style VMS deposit. The strata, alteration, and mineralization of the deposit is hosted within multiple, imbricated thrust panels that comprise a regional domal antiform. The footwall consists of interbedded crystal-tuffs, lapilli tuffs, and lesser mudstone that are overlain by massive rhyolite flows in the hanging wall. Intermediate to mafic dikes and rare felsic sills intrude the entire stratigraphic package.

Mineralization occurs at the hanging wall-footwall contact and consists of stringer to semi-massive pyrrhotite, sphalerite, chalcopyrite, variable pyrite, and minor galena that form multiple, stacked lenses. Sulfide lenses typically contain relict lapilli and quartz crystals of the host lithofacies, which is typical of replacement-type mineralization. Hydrothermally altered rocks at Powderhorn Lake consist of weak to intense quartz-sericite with lesser chlorite, pyrite, and local carbonate. Chlorite alteration occurs as proximal, discordant pipes interpreted to be hydrothermal upflow zones localized along synvolcanic structures, whereas quartz-sericite is pervasive, laterally extensive, conformable at the deposit scale, and extends into the hanging wall. The irregular alteration zones and the tree-branch like morphology of mineralized lenses likely result from the contrasting primary permeabilities between rock units during subseafloor replacement mechanisms. Both the hanging wall and footwall rocks have moderate to strong Na_2O depletions, K_2O-Fe_2O_3-MgO-Ba-Rb enrichments, and elevated alteration indices (e.g., chlorite-carbonate-pyrite index (CCPI) and Hashimoto alteration index (AI)), and enrichments in base metals (e.g., Cu and Zn). Short-wave infrared spectral analyses show that FeOH wavelengths and absorption depths of chlorite increase with proximity to Cu-rich mineralization.

Rhyolitic rocks are cogenetic and exhibit tholeiitic ($Zr/Y<2.8$) affinities, low Zr contents ($Zr<150$ ppm), La/Sm_{UCN} ratios <1 (upper-crust normalized), and primitive mantle normalized signatures with flat light rare earth element (LREE) and heavy rare earth element (HREE) patterns with large negative Nb-Ti anomalies. These immobile element characteristics, coupled with previous isotopic data and zircon inheritance patterns, suggest that felsic host rocks of the Powderhorn Lake deposit formed within a rifted continental arc environment. Geologically, this idea is further supported by: (1) the existence of bimodal volcanism throughout the BRAB; (2) the host lithofacies are consistent with formation within an extensional basin; and (3) the presence of preserved normal faults within the deposit-scale environment.

2.2 Introduction

The Powderhorn Lake deposit is located within the Newfoundland Appalachians and is an example of a felsic siliciclastic, replacement-style volcanogenic massive sulfide (VMS) deposit. Felsic siliciclastic deposit types are typically large, Zn-Cu-Pb rich stratiform bodies that form at, or just below, the seafloor within extensional tectonic regimes (Swinden, 1991; Barrie and Hannington, 1999; Franklin et al., 2005; Galley et al., 2007; Piercey, 2011; Hannington, 2014). This deposit type is dominated by felsic volcanic rocks, typically volcaniclastic in nature, and contain a primary sedimentary sequence that underlies and/or caps the volcanic facies (Barrie and Hannington, 1999; Franklin, et al., 2005; Galley et al., 2007; Piercey, 2011). These deposits are syngenetic and their geometry and emplacement style are often controlled by host lithofacies and primary synvolcanic structures; therefore, reconstruction of their ancient volcanic architecture is key to understanding the genesis and morphology of deformed, post-Archean VMS systems like the Powderhorn Lake deposit (e.g., Nelson, 1997).

The Ordovician (~473-462 Ma; Thurlow, 1981; Dunning et al., 1987; Kerr and Dunning, 2003; Zagorevski et al., 2007c) Buchans-Roberts Arm belt of central Newfoundland hosts several notable deposits including those in the Buchans, Gullbridge, and Pilley's Island districts (Swinden, 1991; Sparkes, 2018). Detailed studies of these deposits and regional mapping reveal multiple structural panels of thrusted and imbricated sequences of stratigraphy, mineralization, and hydrothermal alteration makes reconstruction of the host VMS environment challenging (Calon and Green, 1987; O'Brien, 2007, McKinley, 2013; O'Brien, 2016). Despite the region's metamorphic history, the Powderhorn Lake deposit remains relatively intact and provides an ideal opportunity to study a deformed, replacement-style VMS

deposit within the Newfoundland Appalachians. The goals of this paper are to: (1) characterize the lithofacies, major structures, and alteration of the deposit; (2) present new immobile element geochemical data to characterize and assess the tectonostratigraphic evolution of the deposit environment; (3) utilize petrography, mobile element geochemistry, mass change calculations, and short-wave infrared (SWIR) spectroscopy to characterize alteration assemblages in the deposit; and (4) provide a 3D geology and alteration model of the Powderhorn Lake deposit. The results of this study will reconstruct the ancient volcanic architecture of the deposit, identify key stratigraphic and structural controls of hydrothermal alteration, and provide new information on the tectonic evolution and metallogenic history of the Buchans-Roberts Arm belt. Furthermore, these results provide implications for exploration of felsic dominated, volcaniclastic-rich VMS deposits within arc basin architectures that can be utilized in analogous environments worldwide.

2.3 Geological Setting

The Newfoundland Appalachians are divided into four tectonostratigraphic zones: the Humber, Dunnage, Gander, and Avalon zones (Fig. 2.1) (William, 1979; Williams et al., 1988; Williams, 1995; van Staal, 2007; van Staal and Barr, 2012). The Dunnage Zone hosts the Powderhorn Lake deposit and is subdivided into the western Notre Dame and eastern Exploits subzones, which represent the deformed, Cambrian to Ordovician arc to back-arc complexes that formed proximal to the Laurentian (Notre Dame) and Gondwanan (Exploits) margins, respectively, within the Iapetus Ocean (Swinden et al., 1991; Kean et al., 1995; Evans and Kean; 2002; van Staal, 2007). The closure of the Iapetus Ocean resulted as peri-Laurentian and peri-Gondwanan terranes accreted onto the proximal margins during the roughly coincident Taconic (500-450 Ma) and Penobscot (486-478 Ma) orogenies, respectively (van Staal, 2007;

Zagorevski et al., 2007a, 2010; van Staal and Barr, 2012). The juxtaposition of these subzones occurred during the final stages of the Taconic orogeny and created the Beothuk Lake Line (BLL; = Red Indian Line historically) suture zone (van Staal, 2007; Zagorevski et al., 2007b, 2010; van Staal and Barr, 2012).

The Powderhorn Lake deposit is located in the Notre Dame Subzone that comprises four oceanic and volcanic terranes including: the Lushs Bight oceanic tract (LBOT, ~510 Ma), the Baie Verte oceanic tract (BVOT, ~489-477 Ma), Annieopsquotch accretionary tract (AAT, ~481-460 Ma), and the Notre Dame arc (~488-435 Ma) (Elliott et al., 1991 Williams, 1992; van Staal et al., 1998, 2007). The AAT consists of multiple, thrust-fault imbricated packages of suprasubduction ophiolitic rocks (Annieopsquotch ophiolite belt; AOB) and bimodal arc to back-arc rocks of the Early-Middle Ordovician Buchans-Roberts Arm volcanic belt (Dunning and Krogh, 1985; Swinden et al., 1997; Lissenberg et al., 2005a; Lissenberg et al., 2005b; Zagorevski et al., 2006; O'Brien, 2007).

This study focuses on the central portion of the Buchans-Roberts Arm belt that primarily consists of the Roberts Arm Group (c. 473-464 Ma: Dunning et al., 1987; Kerr and Dunning, 2003) and associated Late Ordovician to early Silurian intrusions (Fig. 2.2). Within this area, the Roberts Arm Group consists of imbricated successions of altered and mineralized bimodal flows and volcaniclastic rocks, epiclastic turbidites, and the variably metamorphosed volcanic and overlying sedimentary rocks that host the Powderhorn Lake deposit (Swinden, 1991; Dickson, 2000; O'Brien, 2007; Sparkes, 2018).

2.4 Deposit Geology

The Powderhorn Lake deposit is located approximately 40 km south of the town of Springdale and lies 10 km southeast of the past-producing Gullbridge mine. The deposit is hosted within a northwest plunging, domal antiform that is internally crosscut by three steeply dipping, northwest-southeast trending thrust faults (Fig. 2.3, 2.4A). The stratigraphy of the deposit has been divided into the hanging wall, mineralized sequence, and footwall.

Lithofacies in both the hanging wall and footwall are similar and consist of interlayered massive to flow banded rhyolite and quartz +/- feldspar crystal tuffs, lapilli tuffs, and rare mudstone. A graphite- and pyrrhotite-rich volcanosedimentary unit (predominantly siltstone) overlies the hanging wall strata in the northeastern portion of the deposit. The mineralized sequence is comprised of multiple, stratabound lenses that are composed of pyrrhotite, sphalerite, chalcopyrite, pyrite, and minor galena.

The northwestern-northern portion of the deposit area contains Zn-rich lenses downhole (>300m) that strike southwest-south and dip steeply (~45-60°) to the northwest, whereas Cu-rich lenses are found along strike in the southwestern-southern area, dip shallowly to the northwest, and are exposed at surface. Higher grade, semi-massive to massive, Cu and Zn sulfide lenses are often enveloped by lower grade stringer to semi-massive sulfides (Fig. 2.4B). The sulfide lenses occur at or near the hanging wall/footwall contacts of faults in permeable footwall crystal tuffs and lapilli tuffs that are typically capped and underlain by coherent, less permeable massive rhyolite and flows. Hydrothermal alteration is dominated by quartz and sericite with lesser amounts of fine-grained chlorite, pyrite, and local carbonate.

2.5 Lithostratigraphy and Lithofacies

The structures and lithofacies of the Powderhorn Lake deposit were identified and mapped across 22 re-logged diamond drill holes and were correlated with previous drill logs from Champion Iron Ltd. Faults were identified in drill core by sharp changes in lithology or lithofacies in combination with strong zones of alteration or bleaching, broken core, and fault gouge. Original volcanic and sedimentary rock names will be used as most primary textures are preserved. Volcaniclastic rocks have been classified using the nomenclature of Fisher (1966) and White and Houghton (2006). These classifications are non-genetic and are based on clast size and abundance that are readily visible at the macro-scale (i.e., drill core or surface samples).

2.5.1 General Lithostratigraphy

Faulting and regional deformation within the study area has resulted in multiple imbricated packages of stratigraphy and volcanic facies that is dissected into three thrust panels (O'Brien, 2007, O'Brien, 2016). Differences in rock units across juxtaposed panels are subtle and make reconstruction of a lithostratigraphy challenging. Therefore, the Powderhorn Lake lithostratigraphy has been simplified and divided into three packages: 1) the hanging wall; 2) mineralized sequence; and 3) footwall. These packages contain cogenetic volcanic facies that are described below.

2.5.2 Lithofacies

The Powderhorn Lake deposit consists of four main lithofacies which have been intruded by mafic to intermediate dikes and felsic sills. Representative photographs and photomicrographs of the lithofacies are displayed in Figures 2.5, 2.6, and 2.7 and their

relationships are illustrated in drill core logs (Appendix A) and stratigraphic sections in Figures 2.8A-C.

2.5.2.1 Volcaniclastic facies: tuff, crystal-tuff, lapilli tuff

Rocks of this lithofacies are predominantly rhyolitic/dacitic in composition and consist of interbedded tuffs, crystal-tuffs, and lapilli tuffs that interfinger with the coherent volcanic facies. This lithofacies locally hosts the massive sulfide mineralization, preferentially within lapilli tuffs and crystal-tuffs. Stratigraphically, this lithofacies is found at the top of both the hangingwall and footwall packages. These lithofacies can be up to 125m thick; contacts between the sub-facies are gradational. Opaque to gray chert lenses (<5 mm to 2 cm) and quartz veins (up to 20cm) occur throughout all units of this lithofacies (2.5B-E). Weak to strong foliations and local crenulations appear as micaceous layers (<5 mm-1 cm) of biotite, muscovite, sericite, and lesser chlorite; the latter minerals were at least partially formed during hydrothermal alteration and recrystallized during deformation and metamorphism (Fig. 2.6B, 2.6E).

Crystal-tuff and tuff are often light to dark gray, granular, and locally are thin-medium bedded (<2 mm-2 cm) beds (Fig. 2.5B-C). Both lithologies contain similar matrix material including poorly sorted, fine-grained quartz, sericite, biotite, muscovite, plagioclase, and K-feldspar (Fig. 2.6A-C). In crystal-rich tuffs, quartz crystals are rounded to sub-rounded, up to 3 mm in size, and vary in color from clear to milky and locally blue. K-feldspar crystals comprise <10% of the matrix and are lath-like, subhedral, and <2 mm in size (Fig. 2.5C).

Lapilli tuff consists of a poorly sorted, fine-coarse grained matrix that locally has fragmental or clast-like textures (Fig. 2.5D-E). This facies, and others, commonly contain

former volcanic glass that appears as dense, black, lenses that have wispy to flame-like textures in drill core samples and appears as condensed aggregates of recrystallized quartz and feldspar in thin section (Fig. 2.5D-E, 2.6B). Lapilli are felsic, opaque, subrounded to rounded, <1 cm to 4 cm in size, and are more quartz-rich than the matrix. The lapilli typically appear elongated or flattened, likely due to deformation (Fig. 2.5D). Alteration of lapilli fragments is similar to that observed in the matrix of the same unit.

This lithofacies also includes a volcanosedimentary cover sequence composed predominantly of pyrrhotite- and graphite-rich siltstones and lesser quartz-crystal tuffs. The siltstones are fine-grained with thin, irregular, wispy mud beds and are locally intercalated with quartz-crystal tuffs. This facies is only found in the north-northwestern portion of the deposit area and can be up to 90 m thick. These rocks have been excluded from lithogeochemical analyses due to their heterogenous and clastic nature. Contacts between the volcaniclastic and coherent volcanic lithofacies are sharp with rare, brecciated margins (Fig. 2.5C).

2.5.2.2 Coherent volcanic facies: massive flows

Rocks of this lithofacies are predominantly rhyolitic/dacitic in composition and consists of aphyric and biotite+/-quartz and massive to flow banded rhyolite (Fig. 2.5A). These lithofacies typically overlie and underlie the volcaniclastic facies in both hanging wall and footwall packages. The rocks are typically white to gray in color, but in some cases are mottled with red, pink, or green subhedral biotite than can comprise up to <15% of the matrix and imparts a spotted texture (Fig. 2.5C). The matrix is predominantly composed of quartz, former volcanic glass, plagioclase, biotite, muscovite, and rare relict K-feldspar crystals (Fig. 2.6D). Quartz crystals are identical to those found in the crystal-tuffs but are sparser in abundance.

Deformation within this lithofacies is represented by weak to moderate foliations of micaceous minerals. Contacts between coherent felsic volcanic rock endmembers are gradational.

2.5.2.3 Sedimentary facies: mudstone

Mudstone is rare, predominantly occurring as thin lenses (<1-3 m) within tuffaceous rocks of the footwall package and locally underlying mineralized units. This facies is dark gray to black, very fine-grained, thinly laminated to bedded, and locally intercalated with biotite-rich quartz-crystal tuff (Fig. 2.5F). Small (<2mm) pink garnet porphyroblasts, elongate clasts of tuff, and chert lenses occur locally within the mudstone unit. These rocks are often moderately to strongly foliated and crenulated.

2.5.2.4 Dikes and sills

Intrusive rocks are common and widespread throughout lithostratigraphic succession consisting of; 1) black, aphanitic, slightly magnetic mafic dikes; 2) light gray, non-magnetic, plagioclase porphyritic intermediate dikes; and 3) very rare, light gray, steel blue, or brick red quartz-feldspar porphyritic rhyolite sills (Fig. 2.7A-C). There are likely multiple generations of mafic and intermediate dikes as some exhibit minor pyrite-sericite-chlorite alteration and quartz-carbonate veins, whereas the majority of dikes are unaltered. Contacts of all intrusions are sharp with the surrounding lithofacies.

2.6 Mineralization and Alteration

2.6.1 Mineralization

Mineralization at the Powderhorn Lake deposit occurs as semi-conformable to conformable stacked sulfide lenses that are primarily composed of Cu-Zn sulfides (Fig. 2.8A-

C). Sulfide lenses are <1 to 6 m thick and consist of pyrrhotite, sphalerite, chalcopyrite, variable pyrite, and lesser galena. Semi-massive and massive mineralization have specific assemblages and textures, including: 1) blebby to banded pyrrhotite-chalcopyrite-sphalerite+/-pyrite; and 2) banded to massive sphalerite-pyrite with lesser, blebby chalcopyrite and local galena (Fig. 2.9A-C). Stringer sulfides consisting of chalcopyrite and/or sphalerite with variable pyrite+/-pyrrhotite typically underlie massive and semi-massive lenses but also locally extend into the hanging wall. The presence of relict quartz crystals, lapilli, gradational mineralized contacts, and a tree branch-like morphology of stacked sulfide lenses suggests the Powderhorn mineralization likely formed by subseafloor replacement (Doyle and Allen, 2003). The mineralization is interpreted to have been localized near faults at contacts between coherent and clastic lithofacies that likely reflected the permeability and porosity contrasts of originally porous and permeable footwall tuffs and impermeable hanging wall flows.

2.6.2 Alteration

Hydrothermal alteration at the Powderhorn Lake deposit is widespread in both hanging wall and footwall packages, becoming more intense proximal to mineralization, and exhibits irregular zonation and distribution. The predominant alteration assemblages consist of quartz-sericite and quartz-sericite-chlorite+/-pyrite (Fig 2.10A-D). Quartz-sericite alteration is pervasive throughout the deposit and occurs as fine- to coarse-grained bands, patches, and veinlets in varying shades of beige, apple green, or black. This assemblage is most intense within felsic volcaniclastic rocks and typically comprises up to 30% of the matrix within Zn-rich semi-massive and massive sulfides (Fig. 2.10A). The quartz-sericite-chlorite+/-pyrite assemblage typically envelopes intense quartz-sericite alteration and occurs within or just below the mineralized sequence. Most chlorite alteration is commonly fine-grained and

comprises <10-15% of the matrix occurring as blebby, spotted, and wispy textures in varying shades of light to dark green and black. Proximal, vertically extensive zones of more intense, coarse-grained, banded to clast-like massive chlorite alteration occurs near faults and can extend >20m into the hanging wall. Chlorite alteration is most intense within lapilli tuffs and is associated with local, milky white carbonate veinlets. Disseminated pyrite grades into the footwall of the deposit and can manifest as veinlets or subhedral to euhedral crystals within the sulfide lenses.

All alteration has been overprinted by regional metamorphic events, manifested as Al- and Mg-rich minerals such as muscovite, biotite, sillimanite, anthophyllite, and lesser cordierite that appear sporadically across lithofacies and are interpreted to be associated with metamorphism of original sericite and chlorite alteration (e.g., Hannington et al., 2003; Morrison, 2004). This metamorphic overprint is regionally extensive, and has been previously studied by Upadhyay (1970) and Upadhyay and Smitherngale (1972) who characterized similar cordierite-anthophyllite assemblages within the nearby Gullbridge deposit. The assemblages are interpreted to have been formed by contact metamorphism within the aureole of nearby Silurian granite and granodiorite plutons. Due to the proximity of the Powderhorn Lake deposit to two Silurian intrusive bodies (e.g., Topsails and Hodges Hill), it is plausible that the metamorphic overprint of original alteration assemblages were formed by the same process.

Additionally, Ca-rich minerals such as epidote, calcite, garnet, tremolite, and actinolite appear with quartz in veins, veinlets, and patches that are widespread, but preferentially affect permeable lithologies. This alteration event is interpreted to be part of a late-stage, post-ore formation process that occurred as the hydrothermal system waned and/or during later

deformation. The extent and significance of this alteration and its byproducts is not well understood.

2.7 Lithogeochemistry

2.7.1 Methods

A total of 206 drill core samples were selected for geochemical analysis from 22 representative drill holes from the Powderhorn Lake area during the 2019 and 2020 field seasons. Samples were taken every 15 to 20 m in representative holes or spot sampled wherever there was a significant change in stratigraphy or alteration.

All samples were analyzed for major oxide elements (SiO_2, Al_2O_3, Fe_2O_3, MnO, MgO, CaO, Na_2O, K_2O, TiO_2, P_2O_5), select trace elements (Ba, Sr, Y, Sc, Zr, Be, V, Hg), base and transition metals (Zn, Cu, Pb, Sc, Ti, V, Cr, Mn, Co, Ni), and volatile elements/metalloids (As, Bi, Cd, Sn, Sb, Tl) at ALS Minerals Ltd. in Sudbury, Ontario (Appendix B). At ALS Minerals, the samples were crushed using a standard jaw crusher and pulverized using mild steel. Major oxides were analyzed using lithium borate fusion pre-analysis with subsequent dissolution with an inductively coupled plasma emission spectrometry (ICP-ES) finish, whereas HFSE (Zr, Hf, Nb, Ta, Y, Ga), LFSE (Ba, Th, U, Rb, Sr), and select transition elements (Cr, V, Sn) underwent identical pre-analysis procedures and were analyzed with an inductively coupled plasma mass spectrometry (ICP-MS) finish. Base metals (Cu, Zn, and Pb), as well as Ag, Cd, Co, Li, Mo, Ni, and Sc, were determined using four-acid dissolution with an ICP-MS finish. Volatile elements (As, Bi, Hg, In, Re, Sb, Se, Te, and Tl) were determined using aqua regia digestion with an ICP-MS finish. Precision (% RSD) and accuracy (% RD) of major and trace element measurements were determined by replicate analyses of an internal rhyolite standard (ORCA-

1) in addition to ALS internal standards. Quality assurance and quality control (QA/QC) data are presented in Appendix C.

2.7.2 Results

Representative whole rock analyses of the Powderhorn Lake VMS deposit are contained in Table 2.1; however, only felsic rock lithogeochemistry will be discussed below as mafic and sedimentary rocks are a minor proportion of the stratigraphy and most had trace element results at or near detection limits. All samples from the Powderhorn Lake area have been affected by hydrothermal alteration and subsequent regional greenschist-facies metamorphism. All major elements (excluding Al_2O_3 and TiO_2), base metals, low field strength elements (LFSE; with the exception of Th-U) and volatile elements are considered to have been mobile during alteration and subsequent metamorphism (Spitz and Darling, 1978; Saeki and Date, 1980; Barrett and MacLean, 1994; Jenner, 1996; Large et al., 2001a). The rare earth elements (REE) (excluding Eu) and high field strength elements (HFSE) are often considered immobile but may become mobile under certain conditions during intense hydrothermal alteration (e.g., Maclean and Barrett, 1993). Plots utilizing petrogenetic ratios (e.g., Nb/Y, Zr/Y, Ti/V) versus the Spitz-Darling index (Al_2O_3/Na_2O) were used to test for obvious mobility (Appendix D); however, no significant correlations were found.

Overall, immobile elements are useful in determining the primary lithogeochemistry of the volcanic rocks to identify petrologic attributes such as magmatic affinity and tectonic environments, whereas mobile elements provide insight into the hydrothermal footprint of the deposit. The use of both immobile and mobile element geochemistry can further be used to undertake quantitative mass balance calculations to quantify element mobility (e.g., MacLean and Barrett, 1993). All approaches will be undertaken below.

2.7.3 Immobile Element Magmatic Affinity Monitors

The immobile trace elements such as Zr, Ti, La, Yb, and Nb have been utilized to determine primary magmatic affinities of the Powderhorn Lake host rocks (e.g., MacLean and Kranidiotis, 1987; MacLean and Barrett, 1993; Ross and Bedard, 2009). All felsic volcanic rocks of the Powderhorn Lake deposit are subalkaline (Nb/Y<0.7) and are rhyolitic/dacitic in composition (Fig. 2.11A) and exhibit tholeiitic magmatic affinities in both Zr/Y (<2.8, not pictured) and Th/Yb (<0.35; Fig. 2.11B) plots. All samples exhibit low Nb and Y contents on tectonic discrimination diagrams and plot near an M-type affinity that are common for rhyolites that have formed from the remelting of mafic crust (Fig. 2.11C). In addition, the low Zr contents (<150ppm), upper crust-normalized La/Sm ratios of <1, and low La/Yb (and Zr/Y - not pictured) ratios on felsic fertility plots support felsic rock formation from sources less evolved than upper continental crust in potentially a juvenile, extensional arc environment (Fig. 2.11D-F; Lentz, 1998; Piercey 2009, 2011).

Primitive mantle normalized multi-elements plots for felsic volcanic rocks are shown in Figure 2.12A-B and display flat LREE and HREE concentrations in addition to large negative Nb (relative to Th and La) and Ti anomalies indicative of arc signatures**.** Both immobile element ratios and multi-element plots suggest that all felsic volcanic rocks of the Powderhorn Lake area are cogenetic and have likely inherited elemental characteristics from the source which they melted from (i.e., unevolved arc crust).

2.8 Mobile Element Geochemistry

All rocks of the Powderhorn Lake deposit have undergone variable degrees of metasomatism and display broad trends of weak to strong hydrothermal alteration on the

alteration box plot (Fig. 2.13A; Large et al., 2001b). Most rocks plotting below the alteration field with low to moderate Ishikawa alteration index (AI) and chlorite-carbonate-pyrite (CCPI) values contain CaO values >1.20 wt. % and reflect the late-stage, VMS-related calcic alteration event that was described previously. The majority of volcaniclastic footwall samples with quartz-sericite-chlorite+/-pyrite alteration plot near the chlorite-pyrite node and have Spitz-Darling index (Al_2O_3/Na_2O) values >10 and up to ~80 (Fig. 2.13B). Hanging wall rocks with quartz-sericite+/-chlorite+/-pyrite alteration display a weak but positive trend towards both the chlorite-pyrite and sericite nodes and have Spitz-Darling index values up to 20. Stratigraphic distribution of alteration assemblages is more clearly displayed in bivariate plots (e.g., MgO vs Al_2O_3 and K_2O vs Al_2O_3; Fig. 2.13C-D). In both bivariate plots, footwall rocks primarily display chlorite-sericite and intense chlorite assemblages whereas hangingwall rocks are dominated by quartz-sericite and K-feldspar assemblages. Select trace element plots, including Hg/Na_2O vs. Ba/Sr and Tl vs Sb, are used to display sample proximity to ore; however, the majority of samples at Powderhorn Lake contain low Hg, Tl, and Sb contents and do not show significant trends on these plots (Fig. 2.13E-F; Large et al., 2001a, b). Copper and Zn mineralization are generally associated with increased CCPI and AI values, respectively; however, AI values are highly variable across the deposit (Fig. 2.14A-B).

2.8.1 Mass Change Calculations

Mass change calculations are used to quantify absolute elemental gains and losses of mobile major (e.g., Na_2O, K_2O, CaO, MgO, etc.) and select trace (e.g., Th, Ba, Rb, S, Y, etc.) elements, while accounting for the effects of mass and volume changes during hydrothermal alteration (Gresens, 1967; Grant, 1986; MacLean, 1990; MacLean and Barrett, 1993). The Powderhorn Lake deposit samples plot along a single trend line in Th-Yb, Zr-Nb, and La-Sm

discrimination plots indicating formation from a similar source; therefore, a single precursor method can be used to quantify mass changes (e.g., MacLean and Kranidiotis, 1987; MacLean, 1990; Barrett and MacLean, 1991; MacLean and Barrett, 1993).

A least-altered rhyolite sample was selected based on minimal Na_2O loss (2-5 wt.%), low loss of ignition (LOI; <3%), low total base metal values (Cu+Zn+Pb = <100 ppm), and overall lack of alteration minerals seen in hand specimen and via optical microscopy. Despite careful selection of least-altered precursor, all rocks in the Powderhorn Lake area have experienced some degree of alteration; therefore, only the most altered samples show significant elemental gains and losses.

The single precursor method by MacLean (1990) was used to calculate an enrichment factor (EF) = i_p/i_a, wherein i_p = concentration of immobile element (i) in the least-altered precursor (PC) and i_a = immobile element (i) in the altered sample; in this case the immobile element (i) is Al_2O_3. The EF is used to determine the reconstructed composition of the altered rock by multiplying and determining the reconstructed elemental concentrations (RC) in the altered sample by RC = EF*Za, where Za = the concentration of element (a) in the altered sample. Final mass change (MC) results are calculated by the difference between the concentration of elements between the precursor and reconstituted altered sample: MC = RC – PC. The calculated mass change results are discussed below and shown in Appendix E.

2.8.2 Mass Change Calculation Results

Rocks of the Powderhorn Lake deposit show variable mass gains and losses of major oxide elements (e.g., SiO_2, Fe_2O_3, MgO, CaO, K_2O, and Na_2O) and select trace elements (e.g., Ba, Rb, Sr, Y) due to hydrothermal alteration. Generally, it is best practice to calculate mass

balance on coherent volcanic rocks due to their homogenous nature; however, these calculations will also include volcaniclastic rocks as their primary immobile element characteristics exhibit the same signatures as coherent rocks. Volcanosedimentary, basalt, and dike samples are excluded from these calculations due to limited sample availability and heterogeneity. Additionally, results discussed below exclude samples that were noted to have high abundances of metamorphic minerals (e.g., cordierite and sillimanite) and produced abnormal values. The calculated major element oxide mass changes and a 3D alteration model for the Powderhorn Lake deposit are displayed in Figures 2.15A-C and 2.16 and are discussed below, whereas calculations for transition metals, base metals, LFSE, and HFSE are found in Appendix E.

SiO_2*:* The gains and losses of SiO_2 account for the largest mass and volume changes throughout the deposit but are generally quite variable regardless of assemblage, lithology, or stratigraphy. However, a notable trend of the quartz-sericite assemblage shows that both footwall and hanging wall rocks exhibit similar, moderate gains and losses. The greatest gains (~30%) and losses (~55%) of SiO_2 occur in the footwall rocks of the quartz-sericite-chlorite+/-pyrite assemblage.

Na_2O and CaO*:* Sodium and CaO depletion occurs in most samples (up to 4.5% and 6.5%, respectively). The greatest Na_2O loss is associated with the quartz-sericite-chlorite+/-pyrite assemblage within tuff samples proximal to mineralization. Gains in Na_2O and CaO are associated with local albite and carbonate, respectively.

K_2O*:* Almost all samples of the Powderhorn Lake deposit exhibit gains of K_2O except for minor losses (<0.25%) likely due to chlorite formation. The majority of hanging wall tuff with quartz-sericite alteration exhibit the greatest K_2O gains (up to ~4.5%). The quartz-sericite-

chlorite+/-pyrite altered footwall rocks exhibit lesser gains (0.05% to ~1.5%) likely due to the formation of chlorite.

MgO and Fe_2O_3: Most samples show both MgO and Fe_2O_3 gains that likely reflect chlorite formation; however, Fe_2O_3 gains are also be attributed to pyrite formation and Fe-rich biotite. The greatest gains of MgO (up to ~8%) and Fe_2O_3 (~10%) are associated with the quartz-sericite-chlorite-pyrite alteration within footwall tuff and lapilli tuff. Quartz-sericite altered hanging wall rocks exhibit <2% MgO gain to minor losses (<1%).

Transition Metals (Sc, V, Ni): Transition metals display variable mass changes across the deposit. In both the hanging wall and footwall, Sc exhibits minor gains (<10 ppm) in tuff, whereas losses are associated with rhyolite, regardless of alteration assemblage. Nickel is primarily lost throughout the deposit but shows minor enrichment (up to ~9.5 ppm) associated with the quartz-sericite-chlorite-pyrite assemblage. Significant gains in V (up to ~41 ppm) are associated with chlorite altered tuffs of the footwall with moderate losses occurring in more sericite-rich rocks.

Base Metals (Cu, Zn, Pb): Significant gains in Cu, Zn, and Pb are primarily associated with the quartz-sericite-chlorite+/-pyrite assemblages within the footwall. Both Cu and Zn display moderate enrichments in the hanging wall, primarily in tuff and lapilli tuff, but also in several rhyolite samples, as well.

LFSE (Th, Sr, Ba, Rb): Thorium does not display significant mass change throughout the deposit. Most samples show Ba and Rb enrichment with the largest gains being 527 ppm and ~28 ppm, respectively, primarily appearing in intensely sericite altered footwall rocks. Strontium losses are common except for select tuff samples exhibiting significant enrichment (up to ~110 ppm) likely associated with local carbonate alteration.

HFSE (Y, Nb, Hf, Ta): Throughout the deposit, Y displays the most significant mass changes whereas Nb, Hf, and Ta display little to no change. Quartz-sericite altered hanging wall rocks exhibit ~10 ppm Y gain and quartz-sericite-chlorite+/-pyrite altered footwall rocks exhibit 12-20 ppm gain associated with local carbonate alteration.

2.9 Shortwave Infrared (SWIR) Spectroscopy

A total of 325 analyses were obtained from samples of the Powderhorn Lake deposit using the Terraspec^{TM} mineral spectrometer with a Hi-Brite Muglight at Memorial University. Analyses were performed on dry, cleaned samples within a naturally sunlit room to avoid interference from artificial lighting. Optimization and white references were taken every 20 analyses, or roughly every 20 minutes to avoid instrument drift, and quality control was monitored using an internal pyrophyllite reference material. Spectral data were collected using RS3 spectral acquisition software and processed using The Spectral Geologist Hotcore v 7.1.55 software. This software applies hull correction and quantifies diagnostic spectral absorption features (i.e., absorption wavelengths, depth of absorption hull) to identify specific minerals within the sample. The complete SWIR absorption data is reported in Appendix B and key characteristics are displayed in Figures 2.17A-B and 2.18A-D.

Short wave infrared spectroscopy (SWIR) data have been an effective tool for characterizing alteration in VMS deposits (e.g., Herrmann et al., 2001). SWIR spectroscopy utilizes a light source to measure the wavelengths that are absorbed by certain bonds within minerals. Diagnostic hulls are generated by molecular bonds of OH, H_2O, CO_3, NH_4, AlOH, FeOH, and MgOH (Thompson et al., 1999; AusSpec International, 2008). The most commonly used absorption features for exploration are the AlOH and FeOH bonds which correspond to

white mica (sericite) and chlorite, respectively. A defined, deep absorption feature for white mica occurs in the AlOH band between 2,180-2,228 nm (Herrmann et al., 2001). Variance in wavelength is related to the proportion of Al within the octahedral site which produces differences in absorption features. Shorter wavelengths (2,180-2,195 nm) of the AlOH bond correspond to sodium-rich mica (paragonite), whereas longer wavelengths (2,210-2,228 nm) are diagnostic of Fe-Mg mica (phengite) (Herrmann et al., 2001; Yang et al, 2003). Potassic mica (muscovite) typically produces absorption features between 2200 and 2204 nm (Herrmann et al., 2001). Wavelength variations between 2,235-2,260 nm and 2,320-2,360 nm correspond to FeOH and MgOH bonds in chlorite spectra (Herrmann et al., 2001). Additionally, the wavelengths of both bonds have shown to increase with iron content (McLeod and Stanton, 1984; Pontual et al., 1997).

2.9.1 Results

The SWIR data from the Powderhorn Lake deposit show AlOH and FeOH wavelengths that range from 2,196-2,202 nm and 2,248-2,252 nm, respectively (Fig. 2.17A-B). White mica is generally potassic (muscovite) in composition, typically indicative of mixed micas or micas of intermediate composition (Herrmann et al., 2001). Potassic mica is pervasive throughout both the footwall and hanging wall of the deposit and does not show any spatial or systematic variation relative to mineralization (Fig. 2.18A).

FeOH wavelengths show that chlorite is generally transitional in composition with variation and absorption features showing trends proximal to mineralization. Longer FeOH wavelengths are associated with Fe-rich chlorite and is typically associated with Cu-rich, higher-grade mineralization, whereas intermediate and shorter wavelengths of FeMg- and Mg-rich chlorite is associated with Zn-rich, lower-grade mineralization (Fig. 2.18B). FeOH

absorption depths broadly increase with proximity to mineralization apart from Zn-rich massive sulfide (Fig. 2.18C). The ratio of the AlOH to FeOH absorption depth (AlOH/FeOH) reflects the decrease of white mica with respect to increasing chlorite content closer to mineralization (Fig. 2.18D).

2.10 Discussion

2.10.1 Tectonic setting and implications for VMS formation

The tectonic setting and petrogenesis of the Buchans-Roberts Arm belt (BRAB) has been previously interpreted using stratigraphic, geochemical, and isotopic data (e.g., Swinden and Thorpe, 1984; Swinden et al., 1997; Zagorevski et al., 2006). Early studies of the belt suggested that tholeiitic rocks likely formed within an intra-oceanic island arc setting, whereas bimodal sequences of the belt were produced by arc magmatism atop continental crust (Swinden and Thorpe, 1984; Swinden et al., 1997). Continued work revealed that the BRAB (within the AAT) likely represents peri-Laurentian continental arc magmatism within a series of geochemically juvenile and evolved crustal blocks that were later juxtaposed into multiple, structural panels through strike-slip translations and thrust faulting (O'Brien, 2007, 2016; Zagorevski et al., 2006). New lithogeochemical data obtained from felsic rocks of the Powderhorn Lake deposit broadly agree with this environment but suggest several inconsistencies with respect to felsic magma generation.

The felsic rocks of the Powderhorn Lake area display very low Zr (<100 ppm) contents with significant negative Nb-Ti anomalies on primitive mantle normalized plots (Fig. 2.12A-B). These geochemical patterns are consistent with a continental arc environment; however, the tholeiitic to M-type Zr-Y and Nb-Y systematics and upper crust normalized La/Sm ratios <1

are consistent with formation from a weakly juvenile crustal substrate rather than via solely continental crust contamination, or fractionation of Nb- and Ti-rich phases (Fig. 2.11B-E; e.g., Piercey, 2011, and references therein). Isotopic data of VMS-related mineralization within the BRAB show nonradiogenic Pb isotopic signatures indicating that the source that was leached was more juvenile than evolved, upper continental crust (e.g., Bell and Blenkinsop, 1981; Swinden and Thorpe, 1984). Furthermore, the BRAB predominantly consists of bimodal packages more akin to arc rift environments, wherein felsic rocks are produced by partial melting of overlying crust by basaltic underplating (Barrie et al., 1993; Wright et al., 1996; Smith et al., 2003; Hart et al., 2004) rather than the sequential volcanism of basalt, andesite, dacite, and rhyolite that is typically found within continental arcs (Arculus, 1994; Lentz 1998; Hart et al., 2004). Lastly, the abundance of volcaniclastic rocks with interlayered cogenetic coherent rocks that abruptly change unit thickness provides evidence for synvolcanic faulting during subsidence and emplacement within an extensional basin (Gibson et al., 1999; Gibson, 2005). Thus, the incorporation of geochemical, isotopic, and lithological evidence suggests that the Powderhorn Lake deposit likely formed within a rifted continental arc setting that involved juvenile arc crust and a potentially heterogeneous basement (Fig. 2.19A).

An extensional, rift-related tectonic environment is conducive to VMS formation as extension would have resulted in rifting and crustal thinning and asthenospheric mantle upwelling that would result in basaltic underplating of the overlying arc crust, crustal melting, bimodal volcanism, increased heat flow, and allow for emplacement of shallow crustal heat sources (e.g., magma chambers, intrusions, etc.) required to drive convection of modified seawater within a high-temperature subseafloor hydrothermal system (e.g., Lesher et al., 1986; Swinden, 1991; Lentz, 1998; Galley, 2003; Hart et al., 2004; Piercey, 2009, 2011). Normal

faults that accommodated rifting could also have acted as fluid conduits that localized hydrothermal fluid discharge and recharge needed for VMS formation (e.g., Franklin et al., 1981, 2005; Lydon, 1984, 1988; Large, 1992; Lentz, 1998; Barrie and Hannington, 1999; Galley et al., 2007; Piercey, 2009, 2011).

Research conducted in ancient, deformed VMS terranes has demonstrated that synvolcanic normal faults can be reactivated and structurally inverted during deformation to give sense of thrust or transform fault movement during post-VMS formation deformation (e.g., Fig. 2.19B; Nelson, 1997, Lafrance et al., 2020). Typically, sulfide mineralization accumulates within a subbasin above or near graben-bounding normal faults that act as hydrothermal fluid conduits. Subsequent compression and deformation during accretionary tectonics can lead to that reverse fault motion, creating thrust or reverse faults that invert the basin into a structural high. Depending on the degree of deformation, an eastward dipping graben-bounding normal fault may be completely overturned to become a westward dipping out-of-graben thrust fault (Nelson, 1997). Additionally, antiformal pop-up structures may develop depending on original basin geometries and structures (Fig. 2.19C).

The Powderhorn Lake deposit is hosted within an imbricated domal antiform that is cut by three steeply dipping, northwest-southeast trending faults. Evidence for synvolcanic faulting includes fault breccia, fault gouge, and lithostratigraphic reconstruction of the deposit area which indicates significant abrupt changes in the thickness or termination of volcaniclastic rocks and lesser coherent rocks. All above features are common to synvolcanic faults within extensional basins (Gibson et al., 1999). Furthermore, the occurrence of these steeply dipping northwest-southeast trending faults is not exclusive to the Powderhorn Lake area but is rather a regional feature in the BRAB and has also been reported in other districts like Pilley's Island

(e.g., McKinley, 2013) and Buchans (e.g., Thurlow, 2010). Thus, the thrust faults at the Powderhorn Lake deposit are interpreted to have been the original structures that formed and localized ascending VMS fluid flow and mineralization emplacement during rift-basin development.

The structural, lithostratigraphic, and geochemical characteristics presented above suggests that the Powderhorn Lake deposit is an example of a deformed, syngenetic VMS deposit that formed within a rifted continental arc basin that was subsequently inverted during later, regional accretionary tectonics during the Taconic and/or Salinic/Acadian orogenic activity.

2.10.2 Characteristics of hydrothermal alteration

Hydrothermal alteration at the Powderhorn Lake area was largely controlled by hydrothermal fluid discharge from synvolcanic faults into unconsolidated volcaniclastic rocks that produced both: 1) proximal, vertically extensive discordant alteration; and 2) diffuse, pervasive zones of laterally extensive alteration (Fig. 2.8A, Fig. 2.16). The widespread, lateral distribution of alteration is interpreted to be a function of laterally directed hydrothermal fluid upflow accommodated by permeable volcaniclastic units and not from hydrothermal recharge during VMS formation, particularly given that it is dominated by feldspar destructive sericite-(chlorite) alteration and K-Mg-Fe-metasomatism, which is not common during hydrothermal recharge (e.g., Gibso and Watkinson, 1990, Galley, 1993; Gibson, 2005; Franklin et al., 2005). The geometry of alteration zonation is likely due to the original porosity and permeability of the host rocks. For example, the discharge of hydrothermal fluid into the originally highly porous and permeable volcaniclastic rocks would have allowed fluid to flow both vertically along synvolcanic faults and also laterally until they met more impermeable, flow-dominant

facies (e.g., Gibson and Watkinson, 1990; Doyle and Allen, 2003; Gibson, 2005; Franklin et al., 2005).

The hydrothermal alteration at Powderhorn Lake is dominated by white mica that is predominantly muscovitic in composition and reflects the white mica alteration throughout the deposit. White mica forms through the destruction of existing feldspars (e.g., albite) and volcanic glass due to hydrothermal fluids and is likely the result of one or more of the following reactions (Riverin and Hodgson, 1980; Barrett and MacLean, 1994b):

(1) $3NaAlSi_3O_8 + 2K^+_{(aq)} + 2H^+_{(aq)} = KAl_3Si_3O_{10}(OH)_2 + 6SiO_{2\,(aq)} + 3Na^+_{(aq)}$

Albite Muscovite Quartz

(2) $2Ca_{0.5}Na_{0.5}Al_{1.5}Si_{2.5}O_8 + 4.48Al(OH)_{4\,(aq)} + 1.16K^+_{(aq)} + 2.23H^+_{(aq)}$

Andesine

$= 1.16KAl_3Si_3O_{10}(OH)_2 + 1.5SiO_{2\,(aq)} + Na^+_{(aq)} + Ca^{2+}_{(aq)}$

Muscovite Quartz

(3) $Ca_2Al_2Si_3O_{12}(OH) + K^+_{(aq)} = KAl_3Si_3O_{10}(OH)_2 + 6SiO_{2\,(aq)} + 3Na^+_{(aq)} + 2Ca^{2+}_{(aq)}$

Ziosite Muscovite Quartz

The above reactions 1-3 generally result in the gain of K_2O with losses of Na_2O and CaO, which is reflected in the mass change results for quartz-sericite+/-chlorite assemblages (Table C.1.1). All assemblages also show gains of Ba and Rb coincident with losses of Sr, further reflecting feldspar destruction and white mica formation, as Ba and Rb readily substitute into white mica, whereas Sr behaves like CaO and is lost during feldspar and zoisite destruction (e.g., Riverin and Hodgeson, 1980). Some samples exhibit CaO and SrO gains; however, this can be attributed to either graphite-rich samples and/or the addition of calcite from minor carbonate alteration.

Chlorite in samples from the Powderhorn Lake deposit vary in chemical composition from Mg- to Fe- to FeMg-chlorite and is typically fine-grained and much less prevalent than white mica. Chlorite alteration of felsic rocks was most likely a product of chloritization of previously formed white micas (e.g., Riverin and Hodgson, 1980):

(4) $2KAl_3Si_3O_{10}(OH)_2 + 3H_4SiO_4 + 9Fe^{2+}_{(aq)} + 6Mg^{2+}_{(aq)} + 18H_2O =$

Muscovite

$3Mg_2Fe_3Al_2Si_3O_{10}(OH)_8 + 2K^+_{(aq)} + 28H^+_{(aq)}$

Chlorite

(5) $K_2(Fe^{2+}, Mg)Al_3Si_7AlO_{20}(OH)_4 + 9FeCl_{2(aq)} + 16H_2O =$

Phengite

$(Fe^{2+}, Mg)_{10}Al_2Si_6Al_2O_{20}(OH)_{16} + H_4SiO_{4\,(aq)} + 2KCl_{(aq)} + 16HCl_{(aq)}$

Chlorite

The reactions above result in net gains of MgO and Fe_2O_3 and loss of K_2O (+/-SiO_2 and Na_2O), which is observed in the quartz-sericite-chlorite+/-pyrite assemblage. However, gains of K_2O and SiO_2 within this assemblage vary depending on the abundance of sericite and quartz relative to chlorite within the sample. The greatest mass gains of MgO and Fe_2O_3 are associated with chlorite alteration and the presence of pyrite stringers and other sulfides.

Cross-sections and three-dimensional models illustrate similar alteration characteristics and assemblages throughout strata hosting the deposit (e.g., mass change and SWIR results) illustrating the broadly diffuse nature of hydrothermal alteration at Powderhorn Lake (Fig., 2.8B., Fig. 2.16, Fig. 2.18A-D). The 3D models show three faults, mineralized lenses, and alteration features (Figs., 2.14A-B, 2.16, 2.18A-D). The mineralization occurs as stacked lenses that are bounded, at their upper and lower contacts, by massive rhyolite (Fig. 2.8A-C).

Lenses are stratabound and are typically localized along hanging wall/footwall contacts of synvolcanic faults enveloped by broad zones of K_2O, Fe_2O_3, and MgO gains with variable SiO_2 gains and losses. Typically, Cu-rich mineralization is found at the top of these zones and is characterized by high CCPI values (Fig. 2.14A), long FeOH wavelengths (i.e., Fe-chlorite), and relatively increased FeOH and AlOH/FeOH SWIR absorption depth values (Fig 2.18B-D). Increased AlOH absorption depth values broadly correlate to Zn-rich mineralization; however, AlOH wavelengths do not exhibit any significant variance with respect to stratigraphy or mineralization (Fig. 2.18A).

2.10.3 Controls on hydrothermal fluid flow and distribution of alteration

The distribution of alteration in the Powderhorn Lake VMS deposit was likely controlled by primary porosity and permeability of the host sequence (e.g., faulting and lithofacies), fluid:rock ratio, and fluid characteristics. The development of vertically extensive discordant alteration zones proximal to interpreted synvolcanic faults suggests that they acted as conduits for upwelling hydrothermal fluids, whereas the broad, laterally extensive alteration is interpreted to be the result of fluids diffusing into juxtaposed permeable strata.

Strata hosting the Powderhorn Lake deposit consists of lithofacies interpreted to be impermeable (e.g., massive to flow-banded rhyolite) interlayered with originally more porous and permeable lithofacies (e.g., crystal-tuff and lapilli tuff). The alteration is most intense within the interpreted glassy tuffaceous units rather than the coherent, siliceous flows (e.g., McPhie et al., 1993; Large et al., 2001a). The interpreted impermeable nature of flows relative to the tuff units likely created an aquifer/aquitard-like geometry that allowed fluid to migrate along multiple paths but focused along flow-tuff boundaries resulting in increased fluid-rock

interaction in the tuffs and the widespread alteration observed in the footwall and hanging wall rocks.

While the alteration distribution reflect permeability/porosity controls of the host sequence (e.g., Riverin and Hodgson, 1980; Lydon, 1984, 1988; Gemmell and Large, 1992; Large et al., 2001a; Schardt et al., 2001; Franklin et al., 2005; Gibson, 2005; Galley et al., 2007), the alteration mineral assemblages reflect the physicochemical conditions and evolution of VMS mineralizing fluids. Chlorite typically forms at moderate to higher temperatures (200-350°C) with moderate pH values (4.5-5.5), whereas white mica preferentially forms at lower temperatures (<250°C) and pH (<5) (Schardt et al., 2001). Although fine-grained chlorite is documented near the interpreted synvolcanic faults, its overall abundance near these faults and throughout the deposit is much lower than white mica and quartz. This dominance of white mica in the deposit suggests that the initial hydrothermal fluids had a pH of <5 and they were of relatively low temperature (~250°C maximum) only allowing minor amounts of Mg fixation and chlorite formation. It is suggested that the progressive cooling of the fluid and increase in acidity resulted from increased fluid-rock interactions (e.g., Schardt et al., 2001) and resulted in the widespread distribution of quartz-sericite alteration throughout the footwall and hanging wall packages. Furthermore, the dominance of Zn in the mineralization throughout this assemblage suggests that throughout the evolution of the Powderhorn mineralization (as is presently observed), it was dominated by primarily low temperature (<250^{o}C) fluids hydrothermal (e.g., Large, 1992; Lydon, 1986; Hannington, 2014).

2.10.4 Implications for replacement-style mineralization

Many ancient and modern VMS deposits formed on the sea floor by precipitation and accumulation of sulfides from exhalative hydrothermal fluids (e.g., Ohmoto, 1996; Franklin et

al., 2005; Galley et al., 2007). However, a subset of deposits in the ancient record are interpreted to have formed within the subsea-floor environment by precipitation of sulfide minerals within pre-existing space (e.g., pore spaces and fractures) and/or by replacement of original constituents of permeable volcanic or sedimentary host strata (Doyle and Allen, 2003, and references therein). Replacement-style VMS deposits are often larger and exhibit higher grades than seafloor-formed deposits due to the efficiency of precipitation and the processes of zone refining (e.g., Doyle and Allen, 2003; Piercey, 2015). The Powderhorn Lake deposit is well preserved and displays several textures and features indicative of subseafloor replacement processes. Doyle and Allen (2003) outlined 5 criteria for distinguishing subseafloor replacement-style deposits: 1) relicts of host rock are preserved within the mineralized sequence, 2) enclosure of massive sulfides within rapidly emplaced facies, 3) evidence of replacement fronts between the host rock and mineralization, 4) presence of strong hanging wall alteration with similar intensity to the footwall, and 5) discordance between the deposit and enclosing lithofacies. Criteria 1-3 are diagnostic of subseafloor replacement, whereas criteria 4 and 5 are supportive, but not diagnostic.

The first 4 criteria are observed within the Powderhorn Lake deposit. The clastic host lithofacies exhibit evidence of deposition by debris flows (e.g., laminated nature and rounded lapilli) that were subsequently enclosed and overlain by coherent flows that suggests rapid emplacement (e.g., McPhie et al., 1993; Fig., 2.5C-D, criteria 2). Both sharp and gradational replacement fronts are observed at Powderhorn Lake (Fig. 2.9B, criteria 3). Sharp contacts are locally between volcaniclastic rocks and local, less permeable sedimentary rock or chert lenses, whereas the progressive appearance of disseminated to spotty and blebby massive sulfides throughout tuff units indicate gradational contacts with mineralization. Massive sulfide lenses

occur at multiple stratigraphic levels (Fig. 2.8A-B, criteria 3) and contain relict lapilli and quartz crystals (Fig. 2.9A-C, criteria 1) providing stratigraphic and textural evidence indicative of subseafloor replacement. Additionally, pervasive quartz-sericite extends into the hanging wall of mineralized lenses and is accompanied by base metal enrichment (Appendix E), high alteration index values (Figs. 2.13A, 2.14A-B) and exhibits similar elemental gains and losses relative to footwall alteration (Figs. 2.15A-C, 2.16, and Appendix E). Additional evidence of replacement-style mineralization can be found in Appendix F.

The style of mineralization and formation of the Powderhorn Lake deposit was likely a function of the primary permeability of host rocks and facies architecture of the deposit. It is interpreted that hot, metalliferous hydrothermal fluid ascended along synvolcanic faults, resulting in local discordant alteration, until meeting impermeable rhyolites and was diverted laterally into permeable, unconsolidated volcaniclastic rocks along their mutual contacts, resulting in cooling, and mixing of VMS fluid and ambient seawater/porewater within the unconsolidated volcaniclastic rocks, which resulted in sulfide precipitation in the subseafloor environment. The tree branch-like morphology of mineralized horizons and their location along contacts between coherent lavas and incoherent volcaniclastic rocks supports the interpretation that contrasting permeability between lithofacies assisted with the formation of multiple, stacked mineralized lenses, also leading to the distinctive hydrothermal alteration characteristics and patterns now present in the deposit. Although not diagnostic of replacement, the broad stratabound hanging wall alteration at Powderhorn Lake is likely a function of a caprock, or rapid covering of the deposit syn-VMS formation, under which replacement of host facies occurred and further reflects replacement-style processes.

The above observations from field, geochemistry, and mineralogy strongly suggest that deposition and distribution of sulfides and hydrothermal alteration at the Powderhorn Lake deposit was dominantly produced by subseafloor replacement-style processes.

2.10.5 Conclusions

The main conclusions of this manuscript include:

1) The Powderhorn Lake deposit formed on the leading edge of Laurentia within a rifted continental arc basin consisting of rhyolite flows and felsic volcaniclastic rocks. This is supported by structural and lithostratigraphic relationships in addition to immobile element lithogeochemistry.
2) Hydrothermal alteration at the Powderhorn Lake deposit is widespread throughout both hanging wall and footwall strata and consists of three alteration assemblages: quartz-sericite, quartz-sericite-chlorite, and quartz-sericite-chlorite-pyrite. Quartz-sericite alteration occurs as stacked, laterally extensive stratabound zones, whereas quartz-sericite-chlorite+/-pyrite assemblages are vertically extensive and discordant to stratigraphy. The distribution and geometries of the alteration zones are largely controlled by synvolcanic structures and the primary porosity and permeability of host rocks.
3) The diffuse nature of hydrothermal alteration throughout strata produced broad trends in mass change results. Extensive white mica alteration shows evidence for moderate gains and losses of SiO_2 with coincident gains in K_2O and MgO (>2%). Chlorite alteration is much less abundant and associated with greatest SiO_2 losses, moderate Fe_2O_3 gains, and significant gains of MgO (>2%) relative to white mica

alteration. Greatest Fe_2O_3 gains are associated with Fe-rich chlorite and biotite, pyrite alteration, and other sulfide mineralization. Most samples exhibit gains in Ba and Rb, regardless of alteration assemblage, and further reflects pervasive sericite alteration and feldspar destruction. Select HFSE and REE remain relatively immobile throughout the deposit, regardless of alteration type.

4) Hyperspectral data reveals that white mica in both the hanging wall and footwall strata is K-rich in composition and does not show any significant compositional variation. Most chlorite samples at Powderhorn Lake exhibit transitional (FeMg-) compositions. However, longer FeOH wavelengths (Fe-rich chlorite) and higher absorption depth values occur proximal to Cu-rich mineralization, whereas shorter wavelengths (Mg- and FeMg-rich) are associated with Zn-rich mineralization.
5) Useful vectors towards Cu-rich mineralization include increased CCPI and elemental gains of Cu, Fe_2O_3, MgO (>2%), and loss of SiO_2, whereas Zn-mineralization is associated with increased AI and elemental gains of Zn, Pb, K_2O(+/-SiO_2), Fe_2O_3, and MgO (<2%).
6) The Powderhorn Lake deposit formed via subseafloor replacement mechanisms. Evidence for replacement style mineralization include: a) sulfides are hosted within rapidly emplaced facies (e.g., tuff, lapilli tuff, and flows); b) relicts of host facies occur within the deposit (e.g., quartz-crystals, lapilli fragments, and flow bands); c) replacement fronts between the host facies and mineralization; and d) pervasive hanging wall alteration.

References

Arculus, R. J., 1994, Aspects of magma genesis in arcs: Lithos, v. 33, p. 189-208.

AusSpec International, 2008, Spectral Interpretation Field Manual; GMEX, Edition 3, Volumes 1-10.

Barrie, C.T., and Hannington, M.D., 1999, Introduction: classification of VMS deposits based on host rock composition, in volcanic-associated massive sulfide deposits; Reviews in Economic Geology, v. 8, p. 2-10.

Barrie, C.T., Ludden, J.N., and Green, T.H., 1993, Geochemistry of volcanic rocks associated with Cu-Zn and Ni-Cu deposits in the Abitibi Subprovince; Economic Geology, v. 88, p. 1341-1358.

Barrett, T. J., and MacLean, W. H., 1991, Chemical, mass, and oxygen isotope changes during extreme hydrothermal alteration of an Archean rhyolite, Noranda, Quebec; Economic Geology, v. 86, p. 406-414.

Barrett, T.J., and MacLean, W.H., 1994, Chemostratigraphy and hydrothermal alteration in exploration for VHMS deposits in greenstones and younger rocks, *in* Alteration and Alteration Processes Associated with Ore-Forming Systems, (ed.) Lentz, D. R.; Geological Association of Canada, Short Course Notes, v. 11, p. 433-467.

Barrett, T. J., and MacLean, W. H., 1994b, Mass changes in hydrothermal alteration zones associated with VMS deposits of the Noranda area; Exploration and Mining Geology, v. 3, p. 131-160.

Bell, K. and Blenkinsop, J., 1981, A Geochronological study of the Buchans area, Newfoundland, *in* The Buchans Orebodies, (eds.) Swanson, E.A., Strong, D.F., and Thurlow, J.G.; Geological Association of Canada, Special Paper 22, p. 91-111.

Buschette, M., 2016, Hydrothermal Alteration and Lithogeochemistry of the Boundary Volcanogenic Massive Sulfide (VMS) Deposit, Central Newfoundland, Canada [MSc thesis]: St. John's, Memorial University of Newfoundland, 286 p.

Calon, T. J., and Green, F. K., 1987, Preliminary results of a detailed structural analysis at Buchans, *in* Buchans Geology, Newfoundland, (ed.) Kirkham, R.V.; Geological Survey of Canada, Paper 86-24, Report 17, p. 273-288.

Collins, C.J., 1989, Report on lithogeochemical study of the Tally Pond Volcanics and associated alteration and mineralization: Unpublished Report for Noranda Exploration Company Limited, Assessment File 012A/1033, Newfoundland Department of Mines and Energy, Mineral Lands Division: St. John's, Newfoundland, 87 p.

Dickson, W.L., 2000, Geology of the eastern portion of the Dawes Pond (NTS 12H/1) map area, central Newfoundland, *in* Current Research, Newfoundland Department of Mines and Energy, Geological Survey Branch, Report 2000-1, p. 127-145.

Doyle, M.G., and Allen, R. L., 2003, Subsea-floor replacement in volcanic-hosted massive sulfide deposits; Ore Geology Reviews, v. 23, p. 183-222.

Dunning, G. R., and Krogh, T. E., 1985, Geochronology of ophiolites of the Newfoundland Appalachians; Canadian Journal of Earth Sciences, v. 22, p. 1659- 1670.

Dunning, G.R., Kean, B.F., Thurlow, J.G. and Swinden, H.S., 1987, Geochronology of the Buchans, Roberts Arm, and Victoria Lake groups and Mansfield Cove Complex, Newfoundland; Canadian Journal of Earth Sciences, v. 24, p. 1175-1184.

Elliott, C. G., Dunning, G. R., and Williams, P. F., 1991, New U/Pb zircon age constraints on the timing of deformation in north-central Newfoundland and implications for early Paleozoic Appalachian orogenesis; Geological Society of America Bulletin, v. 103, p. 125-135.

Evans, D.T.W., and Kean, B.F., 2002, The Victoria Lake Supergroup, central Newfoundland - its definition, setting and volcanogenic massive sulphide mineralization; Newfoundland and Labrador Department of Mines and Energy, Geological Survey, Open File NFLD/2790, p. 68.

Fisher, R. V., 1966, Rocks composed of volcanic fragments and their classification; Earth Science Reviews, v. 1, p. 287-298.

Franklin, J.M., Gibson, H.L., Jonasson, I.R., and Galley, A.G., 2005, Volcanogenic massive sulfide deposits; *in* Economic Geology 100th Anniversary Volume, p. 523– 560.

Franklin, J.M., Lydon, J.W., and Sangster, D.F., 1981, Volcanic-associated massive sulfide deposits; *in* Economic Geology 75th Anniversary Volume, p. 485-627.

Galley, A.G., 1993, Characteristics of semi-conformable alteration zones associated with volcanogenic massive sulphide districts; Journal of Geochemical Exploration, v. 48, p. 175-200.

Galley, A.G., 2003, Composite synvolcanic intrusions associated with precambrian VMS-related hydrothermal systems; Mineralium Deposita, v. 38, p. 2006-2017.

Galley, A.G., Hannington, M.D. and Jonasson, I.R., 2007, Volcanogenic massive sulfide deposits, *in* Contributions to Mineral Resources of Canada: A Synthesis of Major Deposit Types, District Metallogeny, the Evolution of Geological Provinces, and Exploration Methods, (eds.) W.D. Goodfellow and I.M. Kjarsgaard; Geological Association of Canada, Mineral Deposits Division, Special Publication No. 5, p. 141-161.

Gemmell, J. B., and Large, R. R., 1992, Stringer system and alteration zones underlying the Hellyer volcanic-hosted massive sulfide deposit, Tasmania, Australia; Economic Geology, v. 87, p. 620-649.

Gibson, H.L., 2005, Volcanic-hosted ore deposits, *in* Volcanoes in the environment, Chapter 12, (eds.) Marti, J. and Ernst, G.G.J.; Cambridge University Press, p. 333-386.

Gibson, H. L., Morton, R. L., and Hudak, G. J., 1999, Submarine volcanic processes, deposits, and environments favorable for the location of volcanic-associated massive sulfide deposits; Reviews in Economic Geology v.8, p. 13-51.

Gibson, H.L., and D.H. Watkinson, 1990, Volcanogenic massive sulphide deposits of the Noranda cauldron and shield volcano, Quebec, *in* The Northwestern Quebec Polymetallic Belt: A Summary of 60 Years of Minin Exploration, (eds.) M. Rive, P. Verpaelst, Y. Gagnon, J.-M. Lulin, G. Riverin, A. Simard; Canadian Institute of Mining and Metallurgy, Special Volume 43, p. 119-132.

Grant, J. A., 1986, The isocon diagram: A simple solution to Gresens' equation for metasomatic alteration; Economic Geology, v. 81, p. 1976-1982.

Gresens, R. L., 1967, Composition-volume relationships of metasomatism; Chemical Geology, v. 2, p. 47-65.

Hannington, M.D., Kjarsgaard, I.M., Galley, A.G., Taylor, B., 2003, Mineral-chemical studies of metamorphosed hydrothermal alteration in the Kristineberg volcanogenic massive sulfide district, Sweden; Mineral Deposita, p. 423-442.

Hannington, M. D., 2014, Volcanogenic massive sulphide deposits, *in* Treatise on Geochemistry (Second Edition), (ed.) Holland, H.D. and Turekian, K.K.; Elsevier, p. 463-488.

Hart, T. R., Gibson, H. L., and Lesher, C. M., 2004, Trace element geochemistry and petrogenesis of felsic volcanic rocks associated with volcanogenic massive Cu- Zn-Pb sulfide deposits; Economic Geology, v. 99, p. 1003-1013.

Herrmann, W., Blake, M., Doyle, M., Huston, D., Kamprad, J., Merry, N., and Pontual, S., 2001, Short wavelength infrared (SWIR) spectral analysis of hydrothermal alteration zones associated with base metal sulfide deposits at Rosebery and Western Tharsis, Tasmania, and Highway-Reward, Queensland; Economic Geology, v. 96, p. 939-955.

Ishikawa, Y., Sawaguchi, T., Ywaya, S., and Horiuchi, M., 1976, Delineation of prospecting targets for Kuroko deposits based on modes of volcanism of underlying dacite and alteration haloes; Mining Geology, v. 26, p. 105-117

Jenner, G.A., 1996, Trace element geochemistry of igneous rocks: geochemical nomenclature and analytical geochemistry, *in* Trace Element Geochemistry of Volcanic Rocks: Applications for Massive Sulphide Exploration, (ed.) Wyman, D.A.; Geological Association of Canada, Short Course Notes, v. 12, p. 51–77.

Kean, B. F., Evans, D. T. W., and Jenner, G. A., 1995, Geology and mineralization of the Lushs Bight Group: St. John's, Newfoundland; Geological Survey of Newfoundland and Labrador, Mineral Development Division, Report 95-02, 204 p.

Kerr, A., Dunning, G.R., 2003, A note on the U-Pb zircon age of the Woodford's Arm granite, and its relationship to the Roberts Arm Group, central Newfoundland (NTS 2E/12), *In* Current Research; Newfoundland Department of Mines and Energy, Geological Survey, Report 03-1, p. 47-50.

Lafrance, B., Gibson, H.L., and Stewart, M.S., 2020, Internal and external deformation and modification of volcanogenic massive sulfide deposits hydrothermal escaped precipitation site discharge heat source; Reviews in Economic Geology, v. 21, p. 147-171.

Large, R.R., 1992. Australian volcanic-hosted massive sulphide deposits: features, styles and genetic models; Economic Geology, v. 87, p. 471-510.

Large, R. R., McPhie, J., Gemmell, J.B., Herrmann, W., and Davidson, G.J, 2001a, The spectrum of ore deposit types, volcanic environments, alteration halos, and related exploration vectors in submarine volcanic successions: some examples from Australia; Economic Geology, v. 96, p. 913-938.

Large, R. R., Allen, R. L., Blake, M. D., and Herrmann, W., 2001b, Hydrothermal alteration and volatile element halos for the Rosebery K lens volcanic-hosted massive sulfide deposit, western Tasmania; Economic Geology, v. 96, p. 1055-1072.

Lentz, D.R., 1998, Petrogenetic evolution of felsic volcanic sequences associated with Phanerozoic volcanic-hosted massive sulphide systems: the role of extensional geodynamics; Ore Geology Reviews, v. 12, p. 289–327.

Lesher, C.M., Goodwin, A.M., Campbell, I.H., and Gorton, M.P., 1986, Trace-element geochemistry of ore-associated and barren, felsic metavolcanics rocks in the Superior province, Canada; Canadian Journal of Earth Sciences, v. 23, p. 222–237.

Lissenberg, C. J., van Staal, C. R., Bedard, J. H., and Zagorevski, A., 2005a, Geochemical constraints on the origin of the Annieopsquotch ophiolite belt, Newfoundland Appalachians; Geological Society of America Bulletin, v. 117, p. 1413-1426.

Lissenberg, C. J., Zagorevski, A., McNicoll, V. J., van Staal, C. R., and Whalen, J. B., 2005b, Assembly of the Annieopsquotch accretionary tract, Newfoundland Appalachians: age and geodynamic constraints from syn-kinematic intrusions; Journal of Geology, v. 11 3, p. 553-570

Lydon, J.W., 1984, Volcanogenic sulphide deposits, Part 1, A descriptive model; Geoscience Canada, v. 11, p. 195-202.

Lydon, J.W., 1988, Ore deposit models: Volcanogenic massive sulfide deposits, Part 2, Genetic models; Geoscience Canada, v. 15, p. 43–65.

MacLean, W, H., 1990, Mass change calculations in altered rock series; Mineralium Deposita, v. 25, p. 44-49.

MacLean, W. H., and Barrett, T. J., 1993, Lithogeochemical techniques using immobile elements; Journal of Geochemical Exploration, v. 48, p. 109-133.

MacLean, W.H., and Kranidiotis, P., 1987, Immobile elements as monitors of mass transfer in hydrothermal alteration: Phelps Dodge massive sulfide deposit, Matagami, Quebec; Economic Geology, v. 82, p. 951-962.

McDonough, W.F., and Sun, S., 1995, Composition of the earth; Chemical Geology, v. 120, p. 223-253.

McKinley, C., 2013, Volcanic and hydrothermal reconstruction of the Pilley's Island volcanogenic massive sulfide district, central Newfoundland [MSc thesis]: St. John's, Memorial University of Newfoundland, 269 p.

McLeod, R.L., and Stranton, R.L., 1984, Phyllosilicates and associated minerals in some Paleozoic stratiform sulfide deposits of southeastern Australia: Economic Geology, v. 79, p. 1-21.

McPhie, J., Doyle, M., and Allen, R.L., 1993, Volcanic textures: A guide to the interpretation of textures in volcanic rocks; Hobart, Australia, University of Tasmania, p. 198.

Morrison, I., 2004, Geology of the Izok Massive Sulfide Deposit, Nunavut Territory, Canada; Exploration and Mining Geology, v. 13, p. 25-36.

Nelson, J., 1997, The quiet counter-revolution: structural control of syngenetic deposits; Geoscience Canada, v. 24, p. 91–98.

O'Brien, B.H., 2007, Geology of the Buchans-Roberts Arm Volcanic Belt, Near Great Gull Lake, *In* Current Research; Newfoundland and Labrador Department of Natural Resources, Geological Survey, Report 07-1, p. 85-102.

O'Brien, B.H., 2016, Geology of the Starkes Pond – Powderhorn Lake area (part of NTS 12H/01), central Newfoundland; Robert's Arm Volcanic Belt and Adjacent Rocks: Map 3 of 3. Scale 1:25,000; Government of Newfoundland and Labrador, Department of Natural Resources, Geological Survey, Map 2016-03, Open File NFLD/3268.

Ohmoto, H., 1996, Formation of volcanogenic massive sulfide deposits: The Kuroko perspective; Ore Geology Reviews, v. 10, p. 135-177.

Pearce, J., 1996, A users guide to basalt discrimination diagrams, *in* Trace element geochemistry of volcanic rocks: application for massive sulphide exploration, (ed.); Geological Association of Canada, Short Course Notes: v. 12, p. 79-113.

Pearce, J.A., Harris, N.B. and Tindle, A.G., 1984, Trace element discrimination diagrams for the tectonic interpretation of granitic rocks; Journal of Petrology, v. 25 p. 956-983.

Piercey, S.J., 2009, Lithogeochemistry of volcanic rocks associated with volcanogenic massive sulfide deposits and applications to exploration, *in* Submarine Volcanism and Mineralization: Modern through ancient, (eds.) B. Cousens and S.J. Piercey: Geological Association of Canada, Short Course 29-30 May 2008, Quebec City, Canada, p. 15-40.

Piercey, S., 2011, The setting, style, and role of magmatism in the formation of volcanogenic massive sulfide deposits; Mineralium Deposita, v. 46, p. 449–471

Piercey, S. J., 2015, A semipermeable interface model for the genesis of subseafloor replacement-type volcanogenic massive sulfide (VMS) deposits; Economic Geology, v. 110, p. 1655-1660.

Piercey, S.J. and Colpron, 2009, Composition and provenance of the Snowcap assemblage, basement to the Yukon-Tanana terrane, northern Cordillera: Implications for Cordilleran crustal growth; Geosphere, v. 5, p. 439-464.

Pontual, S., Merry, N., and Gamson, P., 1997, G-Mex Vol. 1, Spectral interpretation field manual: Kew, Victoria 3101, Australia; AusSpec International Pty. Ltd., p. 169.

Riverin, G., and Hodgson, C.J., 1980, Wall-rock alteration at the Millenbach Cu-Zn mine, Noranda, Quebec; Economic Geology, v. 75, p. 424-444.

Ross, P.-S., and Bedard, J. H., 2009, Magmatic affinity of modern and ancient subalkaline volcanic rocks determined from trace-element discriminant diagrams; Canadian Journal of Earth Sciences, v. 46, p. 823-839.

Ruks, T.W., Piercey, S.J., Ryan, J.J., Villeneuve, M.E. and Creaser, R.A., 2006, Mid-to late Paleozoic K- feldspar augen granitoids of the Yukon-Tanana terrane, Yukon, Canada: Implications for crustal growth and tectonic evolution of the northern Cordillera; Geological Society of America Bulletin, v. 118, p. 1212-1231.

Saeki, Y., and Date, J., 1980, Computer application to the alteration data of the footwall dacite lava at the Ezuri Kuroko deposits, Akito Prefecture; Mining Geology, v. 30, p. 24 1-250.

Schardt, C., Cooke, D., Gemmell, B., Large, R., 2001, Geochemical Modeling of the Zone Footwall Alteration Pipe, Hellyer Volcanic-Hosted Massive Sulfide Deposit, Western Tasmania, Australia; Economic Geology, v. 96, p. 1037-1054.

Smith, I., Worthington, T.J., Stewart, R.B., Price, R.C., and Gamble, J.A., 2003, Felsic volcanism in the Kermadec Arc, SW Pacific: Crustal recycling in an oceanic setting; Geological Society of London, Special Publications, v. 219, p. 99–118.

Sparkes, G.W., 2018, Preliminary investigations into the distribution of VMS-style mineralization within the central portion of the Buchans-Roberts Arm (Volcanic) Belt, central Newfoundland, *In* Current Research; Newfoundland and Labrador Department of Natural Resources, Geological Survey, Report 18-1, p. 167-184.

Spitz, G., and Darling, R., 1978, Major and minor element lithogeochemical anomalies surrounding the Louvem copper deposit, Val d'Or, Quebec; Canadian Journal of Earth Sciences, v. 15, p. 1161– 1169.

Sun, S.S, and McDonough, W.F., 1989, Chemical and isotopic systematics of oceanic basalts: implications for mantle composition and processes, *in* Magmatism in the Ocean Basins, (eds.) Saunders, A.D., and Norry, M.J.; Geological Society Special Publication 42, p. 313-345.

Swinden, H. S., 1991, Paleotectonic settings of volcanogenic massive sulphide deposits in the Dunnage Zone, Newfoundland Appalachians; Canadian Institute of Mining and Metallurgy Bulletin, v. 84, p. 59-89.

Swinden, H. S., and Dunsworth, S.M., 1995, The Appalachian/Caledonian Orogen: Canada and Greenland, (eds.) Wheeler, J.O., Williams, H.; Geological Survey of Canada, Geology of Canada, No.6, p. 681-814.

Swinden, H. S., Jenner, G. A., and Szybinski, Z. A., 1997, Magmatic and tectonic evolution of the Cambrian-Ordovician Laurentian margin of Iapetus: Geochemical and isotopic constraints from the Notre Dame subzone, Newfoundland, *in* The Nature of Magmatism in the Appalachian Orogen, (eds.) Sinha, A. K., Whalen, J. B., and Hogan, J.P.; Geological Society of America, Memoir 191, p. 337-365.

Swinden, H. S., and Thorpe, R. 1., 1984, Variations in style of volcanism and massive sulfide deposition in Early to Middle Ordovician island-arc sequences of the Newfoundland Central Mobile Belt; Economic Geology, v. 79, p. 1596-1619.

Taylor, S. R., and McLennan, S. M., 1995, The geochemical evolution of the continental crust; Reviews of Geophysics, v. 33, p. 241-265.

Thompson, A. J., Hauff, B., and Robitaille, P. L., 1999, Alteration mapping in exploration: Application of short-wave infrared (SWIR) spectroscopy; Society of Economic Geologists Newsletter, v. 39, p. 16-27.

Thurlow, J.G., 1981, Geology, ore deposits and applied rock geochemistry of the Buchans Group, Newfoundland, [PhD thesis]: St. John's, Memorial University of Newfoundland, 305 p.

Upadhyay, H.D., 1970, Geology of the Gullbridge copper deposit, central Newfoundland, [Msc Thesis]: St. John's, Memorial University of Newfoundland, 134 p.

Upadhyay, H.D. and Smitheringale, W.G., 1972, Geology of the Gullbridge copper deposit, Newfoundland: volcanogenic sulfides in cordierite-anthophyllite rocks; Canadian Journal of Earth Sciences; v. 9, p. 1061-1073.

van Staal, C.R., 2007, Pre-Carboniferous metallogeny of the Canadian Appalachians, *in* Mineral Deposits of Canada: A Synthesis of Major Deposit Types, District Metallogeny, the Evolution of Geological Provinces, and Exploration Methods, (ed.) W.D. Goodfellow; Geological Association of Canada, Mineral Deposits Division, Special Publication No. 5, p. 793-818.

van Staal, C.R., Dewey, J.F., MacNiocaill, C.M., and McKerrow, S, 1998, The Cambrian-Silurian tectonic evolution of the northern Appalachians: history of a complex, southwest Pacific-type segment of Iapetus, *in* Lyell: the Past is the Key to the Present, (eds.) Blundell, D.J. and Scott, A.C.; Geological Society, Special Publication, v. 143, p. 199-242.

van Staal, C. R., Whalen, J. B., McNicoll, V. J., Pehrsson, S., Lissenberg, C. J., Zagorevski, A., van Breemen, O., and Jenner, G. A., 2007, The Notre Dame Arc and the Taconic Orogeny in Newfoundland: Memoir Geological Society of America, v. 200, p. 5 11-552.

van Staal, C.R., Whalen, J.B., Valverde-Vaquero, P., Zagorevski, A., and Rogers, N., 2009, Pre-Carboniferous, episodic accretion-related, orogenesis along the Laurentian margin of the northern Appalachians, *in* Ancient Orogens and Modern Analogues, (eds.) Murphy, J.B., Keppie, J.D., Hynes, A.J.; Geological Society London, Special Publication 327, p. 271-316.

van Staal, C.R. and Barr, S.M., 2012, Lithospheric architecture and tectonic evolution of the Canadian Appalachians and associated Atlantic margin, Chapter 2, *in* Tectonic Styles in Canada: The LITHOPROBE Perspective, (eds.) J.A. Percival, F.A. Cook, and R.M. Clowes; Geological Association of Canada, Special Paper 49, p. 41-96.

White, J. D. L. and Houghton, B. F., 2006, Primary volcaniclastic rocks; Geology, v. 34, p. 677-680.

Williams, H. 1979, Appalachian Orogen in Canada; Canadian Journal of Earth Sciences, v. 16: p. 792–807.

Williams, H., Colman-Sadd, S.P., and Swinden, H.S., 1988., Tectonostratigraphic subdivisions of central Newfoundland, *in* Current Research, Part B; Geological Survey of Canada, Paper 88-1B, p. 91–98.

Williams, H., 1992, Lower Ordovician (Arenig-Llanvirn) graptolites from the Notre Dame subzone, central Newfoundland; Canadian Journal of Earth Sciences, v. 29, p. 1717-1733

Williams, H., 1995, Geology of the Appalachian-Caledonian Orogen in Canada and Greenland, (ed.) Williams, H.; Geological Survey of Canada, Temporal and Spatial Divisions; Chapter 2, v. 6, p. 21-44.

Winchester, J.A. and Floyd, P.A., 1977, Geochemical magma type discrimination: application to altered and metamorphosed basic igneous rocks; Earth and Planetary Science Letters, v. 28, p. 459-469.

Wright, I., Parson, L.M., and Gamble, J.A., 1996, Evolution and interaction of migrating cross-arc volcanism and backarc rifting: An example from the Southern Havre Trough (35°20′–37°S); Journal of Geophysical Research, v. 101, p. 22071–22086.

Yang, K., Scott, S.D., and Goodfellow, W. D., 2003, Footwall alteration associated with some massive sulfide deposits in the Bathurst mining camp, New Brunswick; implication for sea-floor hydrothermal mining processes; Economic Geology Monographs, v. 11, p. 435-456.

Zagorevski, A., Rogers, N., van Staal, C.R., McNicoll, V., Lissenberg, C.J., and Valverde-Vaquero, P., 2006, Lower to Middle Ordovician evolution of peri-Laurentian arc and back-arc complexes in the Iapetus: constraints from the Annieopsquotch Accretionary Tract, Central Newfoundland; Geological Society of America Bulletin, v. 118, p. 324–362.

Zagorevski, A., van Staal, C.R., McNicoll, V.C., and Rogers, N., 2007a, Upper Cambrian to Upper Ordovician peri-Gondwanan island arc activity in the Victoria Lake Supergroup, Central Newfoundland: tectonic development of the Ganderian margin; American Journal of Science, v. 307, p. 339-370.

Zagorevski, A., van Staal, C. R., and McNicoll, V. J., 2007b, Distinct Taconic, Salinic, and Acadian deformation along the Iapetus suture zone, Newfoundland Appalachians: Canadian Journal of Earth Sciences, v. 44, p. 1567-1585.

Zagorevski, A., van Staal, C.R., Rogers, N., McNicoll, V.J. and Pollock, J., 2010, Middle Cambrian to Ordovician arc-backarc development on the leading edge of Ganderia, Newfoundland Appalachians; Geological Society of America Memoirs, v. 206, p. 367-396.

Table 2.1 Representative whole rock analyses for Powderhorn Lake samples

Sample ID	62609	62584	62634	62692	62758	62693	62707
Hole ID	PH-18-34	PH-18-34	PH-18-40	PH-18-44	PH-19-11	PH-18-44	PH-18-13
Depth (m)	422.16	160.75	212.87	22	124.43	54.05	97.66
Lithology	Rhyolite	Rhyolite	Rhyolite	Xtl-Tuff	Xtl-Tuff	Lap. Tuff	Lap. Tuff
Stratigraphy	FW	HW	FW	HW	FW	HW	FW
Alteration	Least-altered	QS+/-C	QSC	QS	QSC+/-Py	QSC	QSC+/-Py+Sil
SiO_2 (wt. %)	74.33	73.55	78.42	74.78	72.07	79.80	70.38
Al_2O_3	11.49	13.50	12.17	12.87	12.91	10.71	16.57
Fe_2O_3	1.16	2.45	2.17	1.74	5.55	1.77	7.08
FeO	1.04	2.20	1.96	1.56	4.99	1.60	6.37
CaO	6.63	2.20	0.16	1.62	1.21	0.84	0.41
MgO	0.70	0.23	1.84	0.08	2.87	2.23	2.70
Na_2O	4.85	4.17	3.99	3.32	3.67	4.04	1.59
K_2O	0.52	3.41	1.02	5.12	1.04	0.40	0.95
Cr_2O_3	0.00	0.00	<.002	0.00	0.00	0.00	0.00
TiO_2	0.13	0.36	0.14	0.35	0.37	0.12	0.13
MnO	0.15	0.02	0.05	0.02	0.22	0.06	0.12
P_2O_5	0.01	0.08	0.03	0.08	0.07	0.02	0.01
SrO	0.01	0.01	<0.01	0.05	0.01	0.05	0.01
BaO	0.01	0.02	0.01	0.02	0.01	0.01	0.05
LOI	0.80	0.60	1.57	0.19	1.88	1.06	2.93
Total	99.14	100.26	101.42	99.28	100.25	101.44	100.97
C	0.17	0.07	0.01	0.04	0.03	0.02	0.03
S	0.26	0.9	0.58	0.42	1.96	0.24	3.02
Ba (ppm)	72.8	175.5	132.0	193.5	99.1	76.7	442.0
Ce	14.0	13.5	20.6	13.0	13.7	14.5	24.8
Cr	20	20	20	20	10	10	10
Cs	0.08	0.35	0.88	0.20	0.59	0.62	0.97
Dy	8.93	6.51	8.07	6.35	6.23	8.99	17.5
Er	5.98	4.30	5.46	4.56	4.59	6.31	11.35
Eu	0.90	1.24	0.76	1.06	0.88	1.14	1.66
Ga	12.90	14.7	10.4	12.6	13.1	11.0	23.5
Gd	6.36	5.25	6.31	4.82	4.58	6.39	12.2
Ge	<5	<5	<5	<5	<5	<5	<5
Hf	3.3	2.6	3.8	2.5	2.6	3.4	7.2
Ho	1.95	1.51	1.96	1.42	1.40	1.98	3.65
La	5.6	5.4	8.5	5.2	5.2	5.8	9.1
Lu	1.08	0.75	1.09	0.59	0.75	1.07	1.96
Nb	1.1	1.3	1.3	1.3	1.0	1.1	2.1
Nd	11.6	10.6	16.6	9.9	10.8	12.0	21.8
Pr	2.21	1.82	3.23	2.01	2.10	2.26	3.96
Rb	3.70	21.9	10.2	24.9	7.2	4.8	6.0
Sm	4.11	3.54	5.15	3.94	3.38	4.48	8.75
Sn	1	1	1	1	1	1	5

Sample ID	62609	62584	62634	62692	62758	62693	62707
Hole ID	PH-18-34	PH-18-34	PH-18-40	PH-18-44	PH-19-11	PH-18-44	PH-18-13
Depth (m)	422.16	160.75	212.87	22	124.43	54.05	97.66
Lithology	Rhyolite	Rhyolite	Rhyolite	Xtl-Tuff	Xtl-Tuff	Lap. Tuff	Lap. Tuff
Stratigraphy	FW	HW	FW	HW	FW	HW	FW
Alteration	Least-altered	QS+/-C	QSC	QS	QSC+/-Py	QSC	QSC+/-Py+Sil
Sr	104.5	67.6	66.5	75	40.2	44.8	79.9
Ta	<0.1	<0.1	<0.1	0.2	0.1	0.1	0.3
Tb	1.16	0.94	1.37	0.83	0.82	1.17	2.34
Th	1.16	1.12	1.52	1.15	0.94	1.21	1.57
Tm	0.93	0.64	0.91	0.67	0.68	0.93	1.79
U	1.32	3.06	0.58	0.50	0.34	0.51	0.66
V	10	15	<5	<5	57	14	5
W	1	1	1	<1	2	<1	1
Y	55.9	39.5	49.7	37.5	38.5	52.4	99.5
Yb	7.22	4.57	6.22	4.68	4.70	6.70	13.05
Zr	90	83	98	75	71	90	190
As	2.7	3.1	3.1	3.2	0.6	1.5	1.9
Bi	0.07	0.1	0.69	0.14	0.44	0.08	1.28
Hg	0.01	<0.005	<0.005	<0.005	0.008	0.006	0.056
In	0.03	0.04	0.13	0.06	0.07	0.04	0.95
Re	0.001	0.001	0.002	0.001	0.001	0.001	<0.001
Sb	0.11	0.18	0.07	<0.05	<0.05	0.10	0.05
Se	<0.2	0.4	0.2	<0.2	0.9	<0.2	0.4
Te	0.01	0.10	0.22	0.15	0.25	0.05	0.47
Tl	0.04	<0.02	0.02	<0.02	0.02	0.03	0.13
Ag	<0.5	<0.5	<0.5	<0.5	<0.5	<0.5	2.2
Cd	<0.5	<0.5	<0.5	0.8	<0.5	1.5	3.6
Co	1	<1	2	<1	4	<1	<1
Cu	4	5	36	7	116	29	1120
Li	<10	<10	20	<10	10	10	50
Mo	1	2	3	3	3	2	2
Ni	2	4	3	<1	2	<1	1
Pb	12	2	2	<2	10	5	18
Sc	15	14	12	11	16	12	20
Zn	73	68	67	332	112	340	895

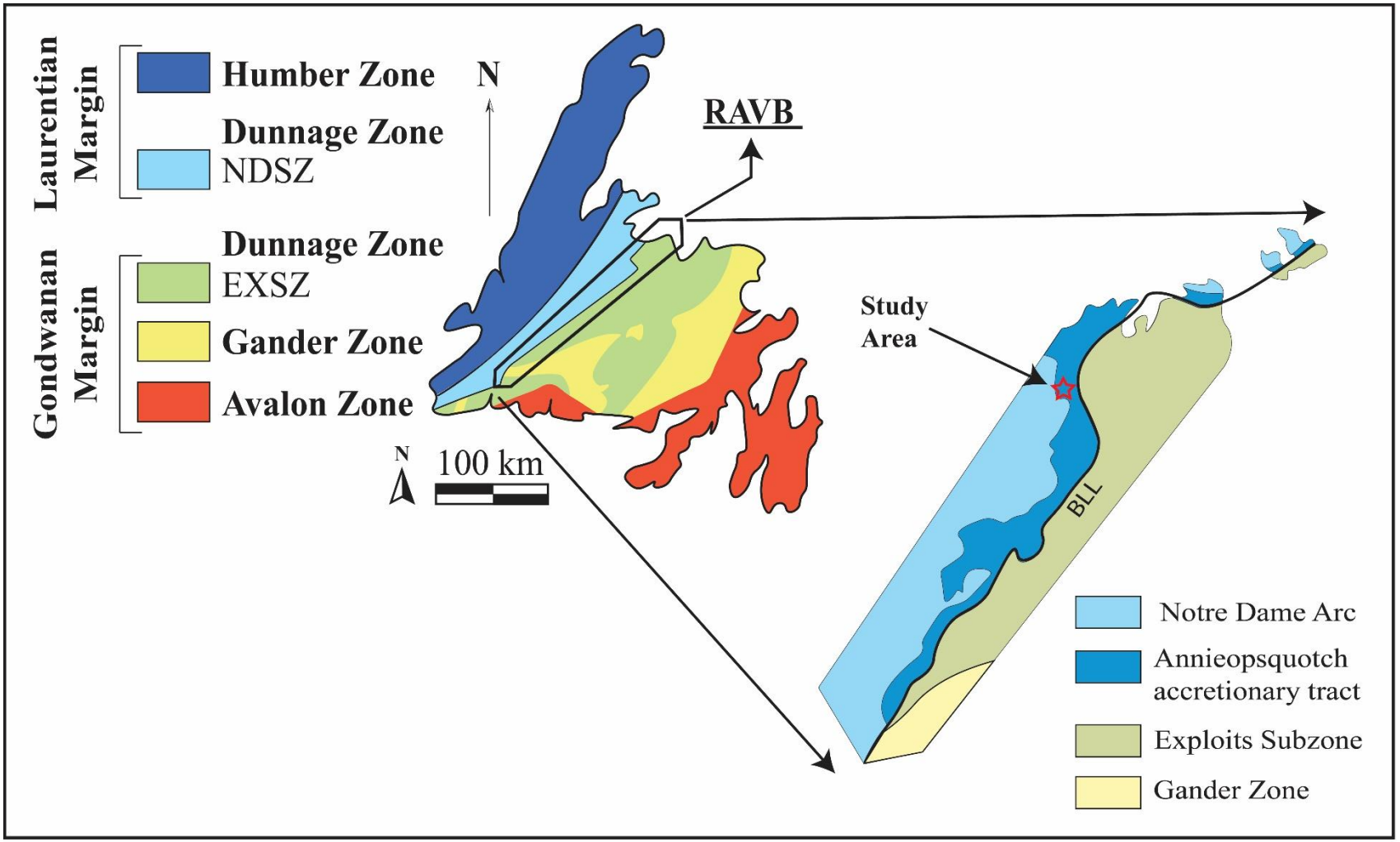

Figure 2.1. Geological map of Newfoundland Appalachians (modified after Williams et al., 1988) showing tectonostratigraphic zones with a subdivision showing a portion of the Notre Dame arc, Annieopsquotch accretionary tract (AAT), and Beothuk Lake Line (BLL; modified from van Staal et al.,1998). Study area indicated by red star. Figure is modified from Zagorevski et al., 2007.

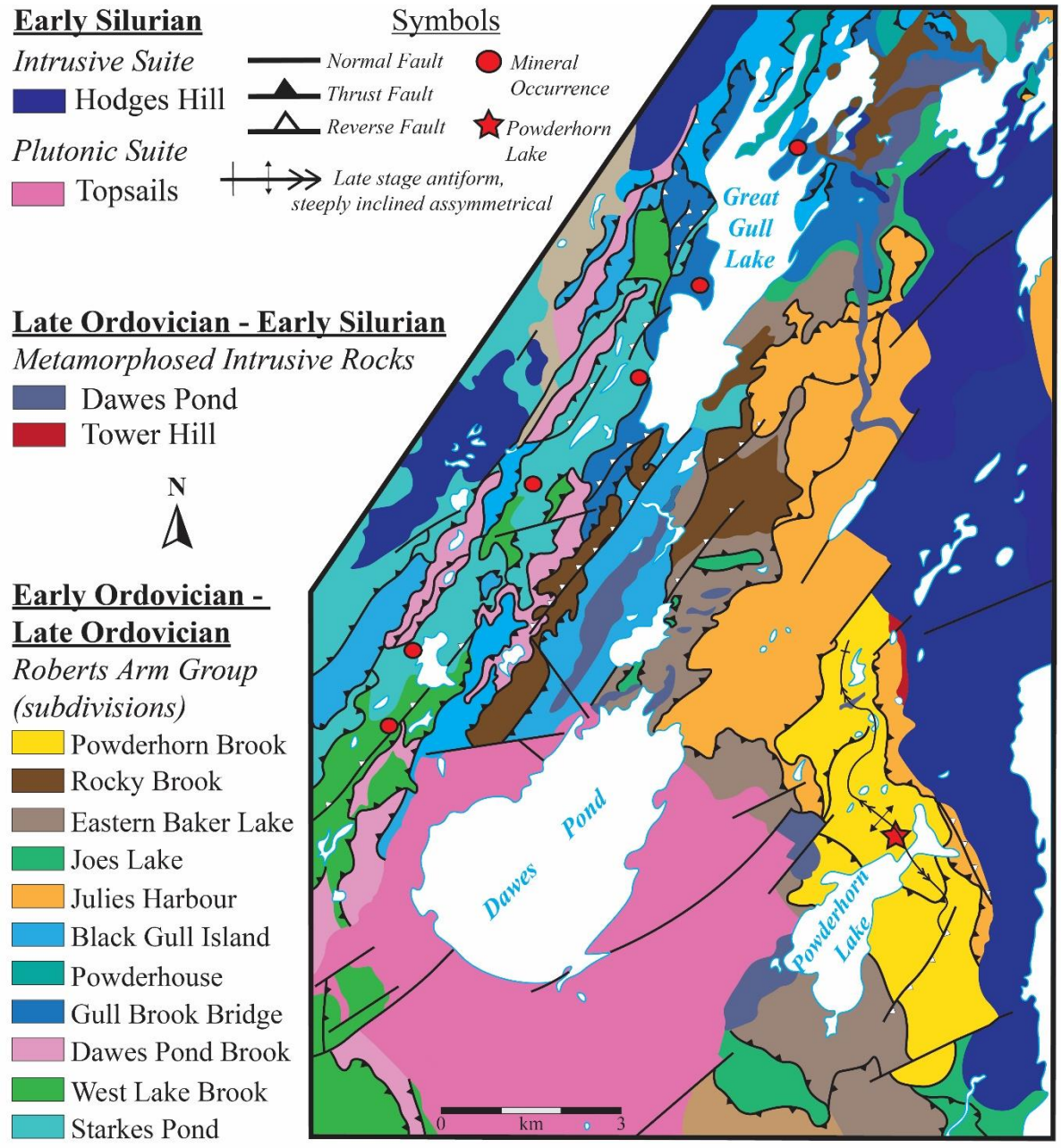

Figure 2.2. Simplified geological map of south-central portion of the Buchans-Roberts Arm belt showing select mineral occurrences and the study area. Modified from O'Brien (2016).

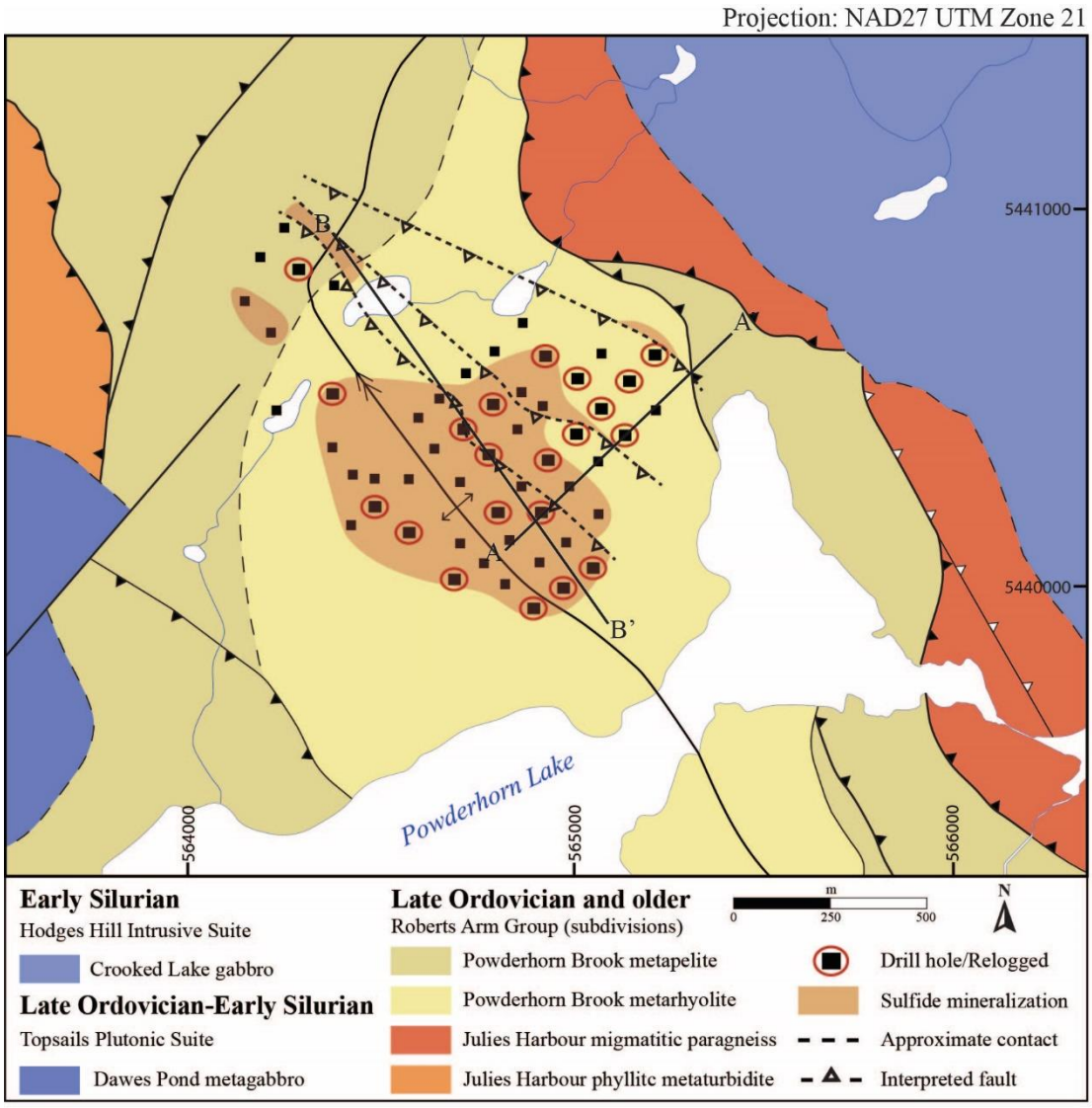

Figure 2.3. Geological map of the Powderhorn Lake area from surface mapping completed by O'Brien (2007, 2016). Mineralization projected to surface.

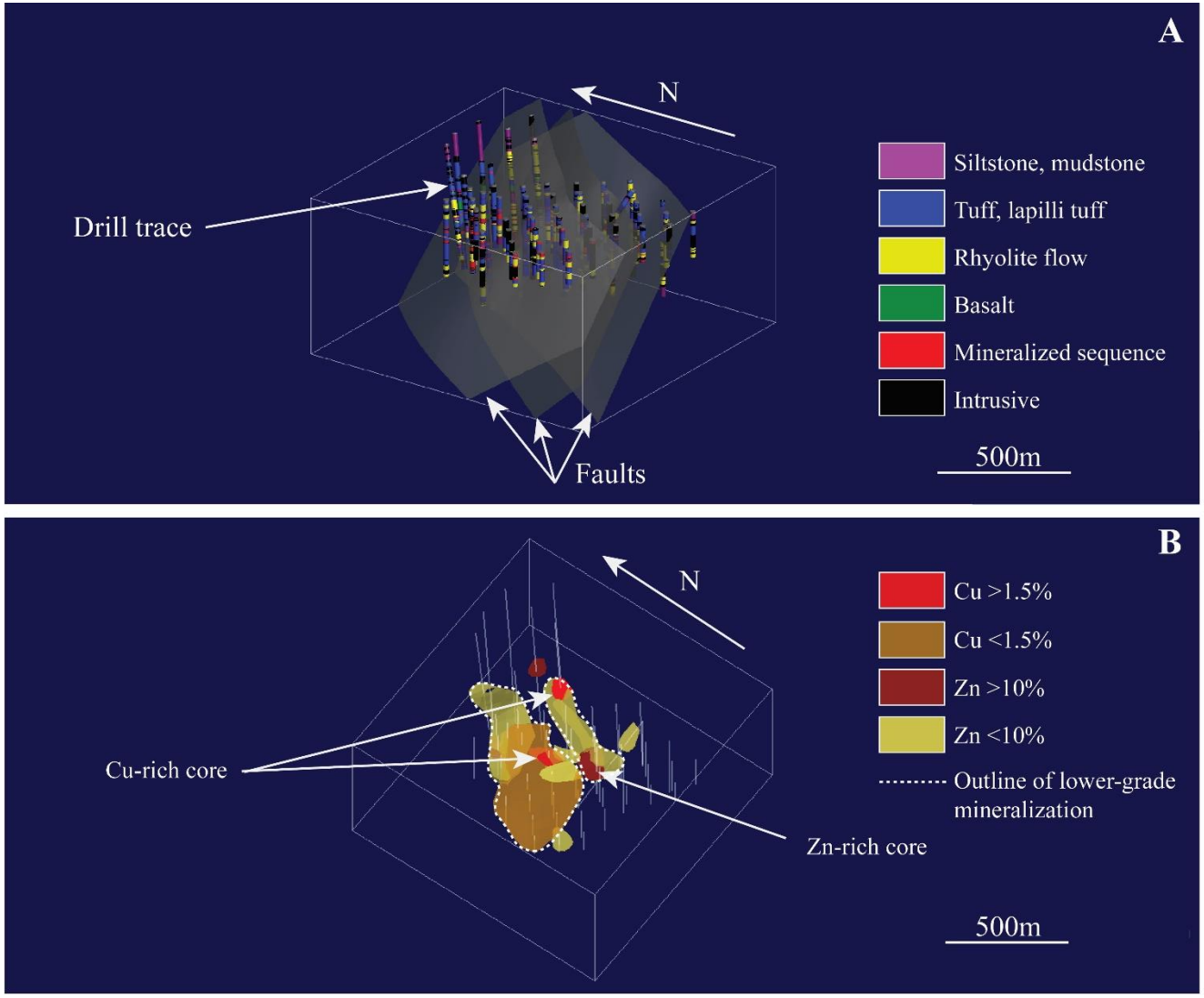

Figure 2.4. 3D models of the Powderhorn Lake deposit. A) Base LeapFrog model displaying main structures and lithologies. B) Cu and Zn lenses with respective grades displaying higher-grade Cu and Zn semi-massive to massive sulfides enveloped by lower-grade semi-massive to stringer sulfides outlined in white dashed lines.

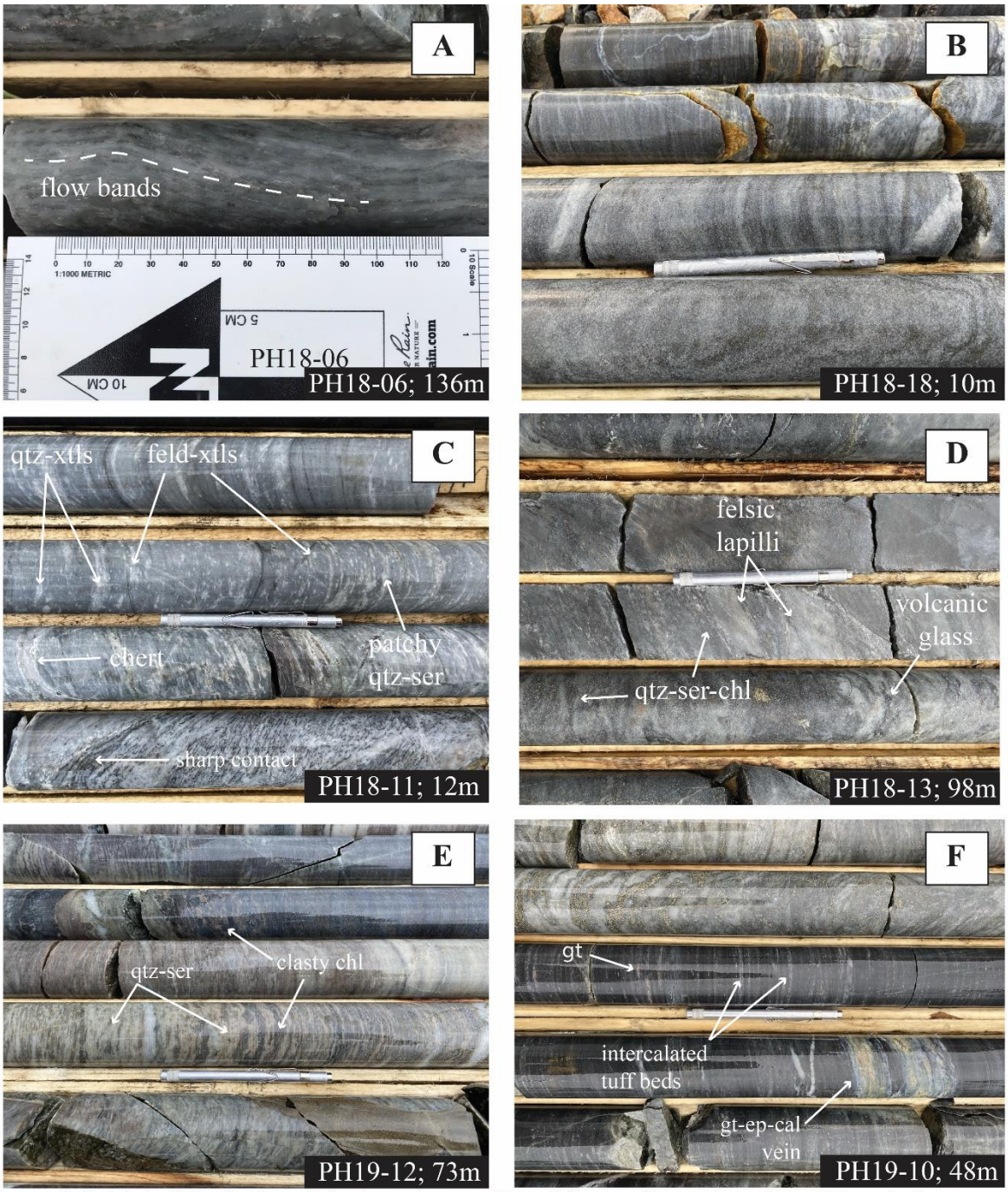

Figure 2.5. Main lithofacies of the hanging wall and footwall stratigraphy of Powderhorn Lake. A) Relatively unaltered flow banded rhyolite of the hanging wall. B) Weak quartz-sericite altered tuff of the hanging wall. C) Moderately quartz-sericite altered hanging wall quartz-feldspar-crystal tuff with garnet-epidote-calcite vein overprints in sharp contact with biotite-rich massive rhyolite. D) Moderately quartz-sericite-chlorite+/-pyrite altered lapilli tuff of the footwall. E) Intensely quartz-sericite-chlorite-silica altered lapilli tuff of the footwall. F) Mudstone with intercalated tuff beds locally beneath stringer sulfides in the footwall. Abbreviations: cal-calcite, chl-chlorite, ep-epidote, feld-feldspar, gt-garnet, qtz-quartz, ser-sericite, xtl-crystal.

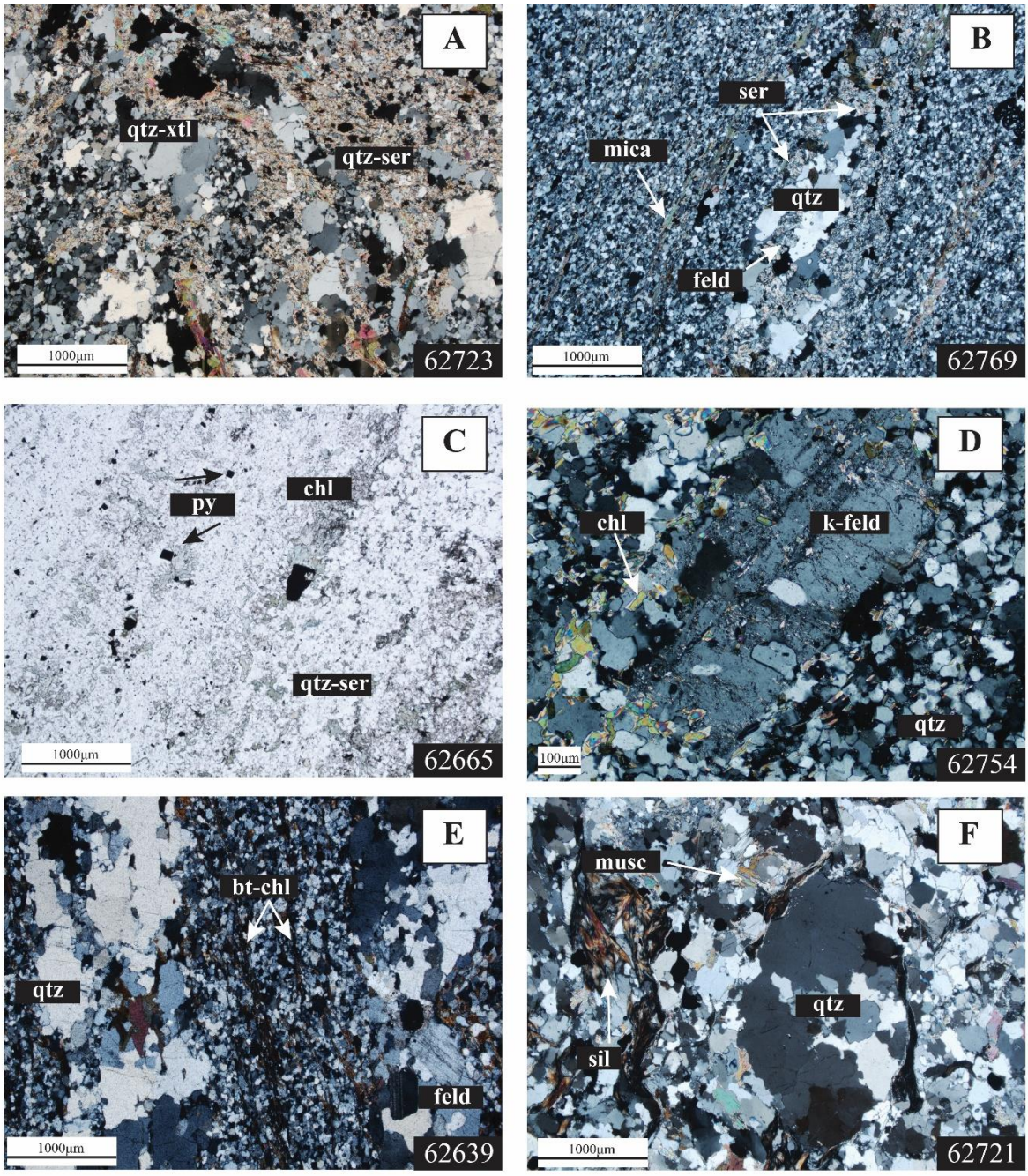

Figure 2.6. Photomicrographs of main lithofacies and asociated alteration at Powderhorn Lake. A) Patchy quartz-sericite altered crystal-tuff. B) Weakly foliated and quartz-sericite altered lapilli tuff with varying quartz grain sizes and volcanic glass consisting of feldspar and quartz. C) Quartz-sericite-chlorite altered tuff exhibiting fine, veinlets to bands of chlorite and trace pyrite surrounded by quartz-sericite groundmass. D) Relict k-feldspar crystal in rhyolite flow being altered by chlorite and sericite. E) Weakly sericite altered crystal-tuff with veinlet micaceous minerals and quartz veins. F) Lapilli tuff with overprinted sillimanite and muscovite alteration. Abbreviations: bt-biotite, chl-chlorite, feld-feldspar, musc-muscovite, py-pyrite, qtz-quartz, ser-sericite, sil-silimanite, xtl-crystal.

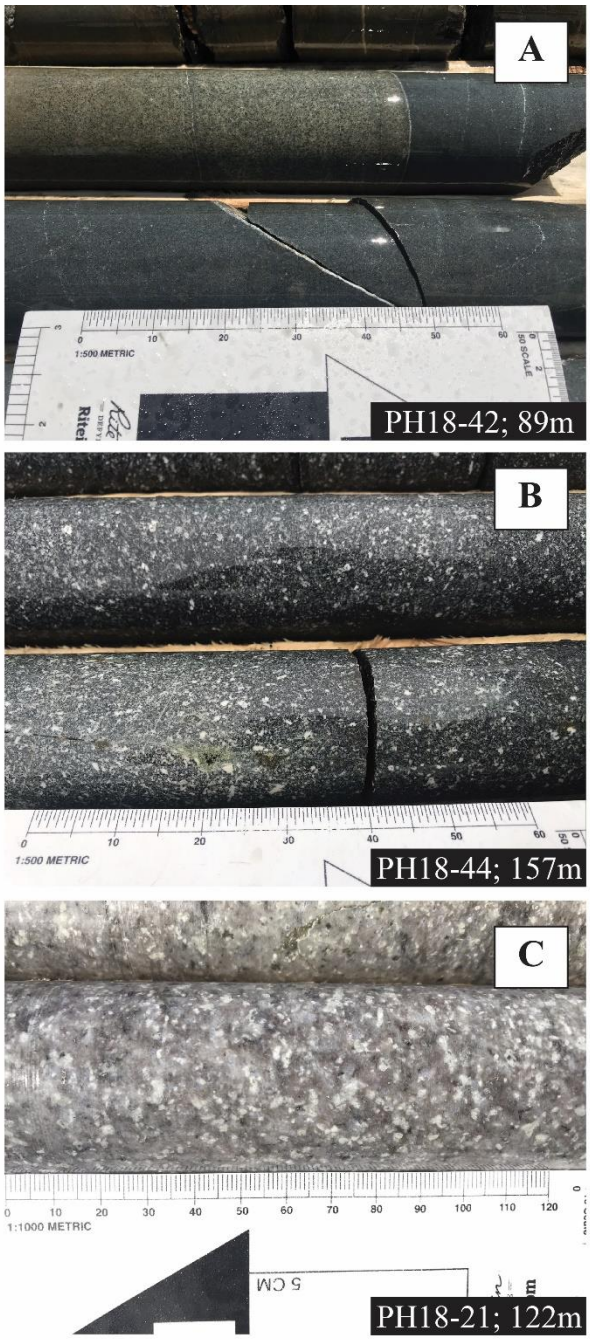

Figure 2.7. Intrusive rocks of the Powderhorn Lake deposit. A) Aphanitic mafic dike. B) Feldspar porphyritic intermediate dike. C) Quartz-feldspar rhyolite sill.

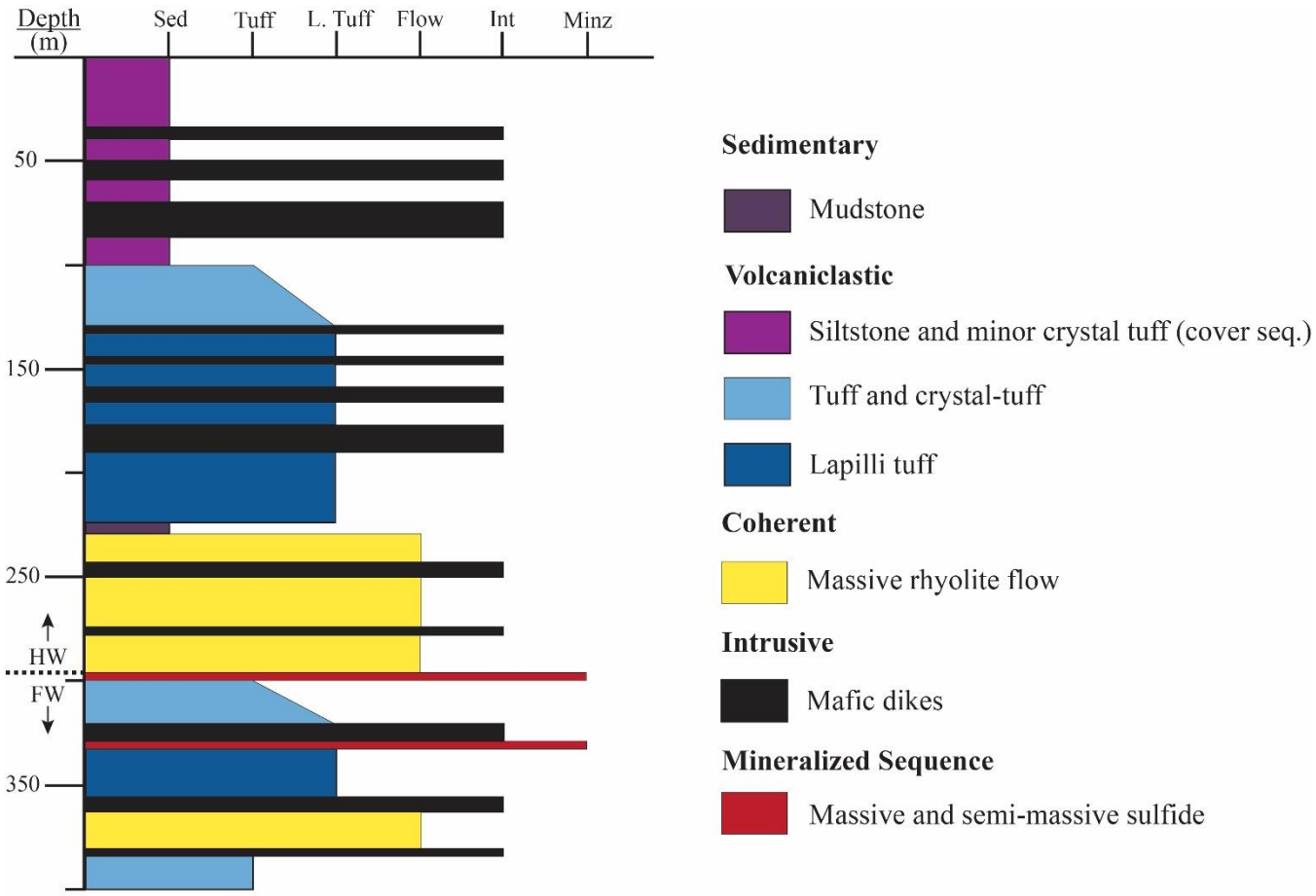

Figure 2.8A. A portion of drillhole PH-18-34 used as a simplified stratigraphic column to show relationships between the lithofacies and mineralized sequence in the Powderhorn Lake deposit. Abbreviations: FW-footwall, HW-hanging wall, Int-instrusive, L. Tuff-lapilli tuff, Minz-mineralization, Sed-sediment, seq.-sequence.

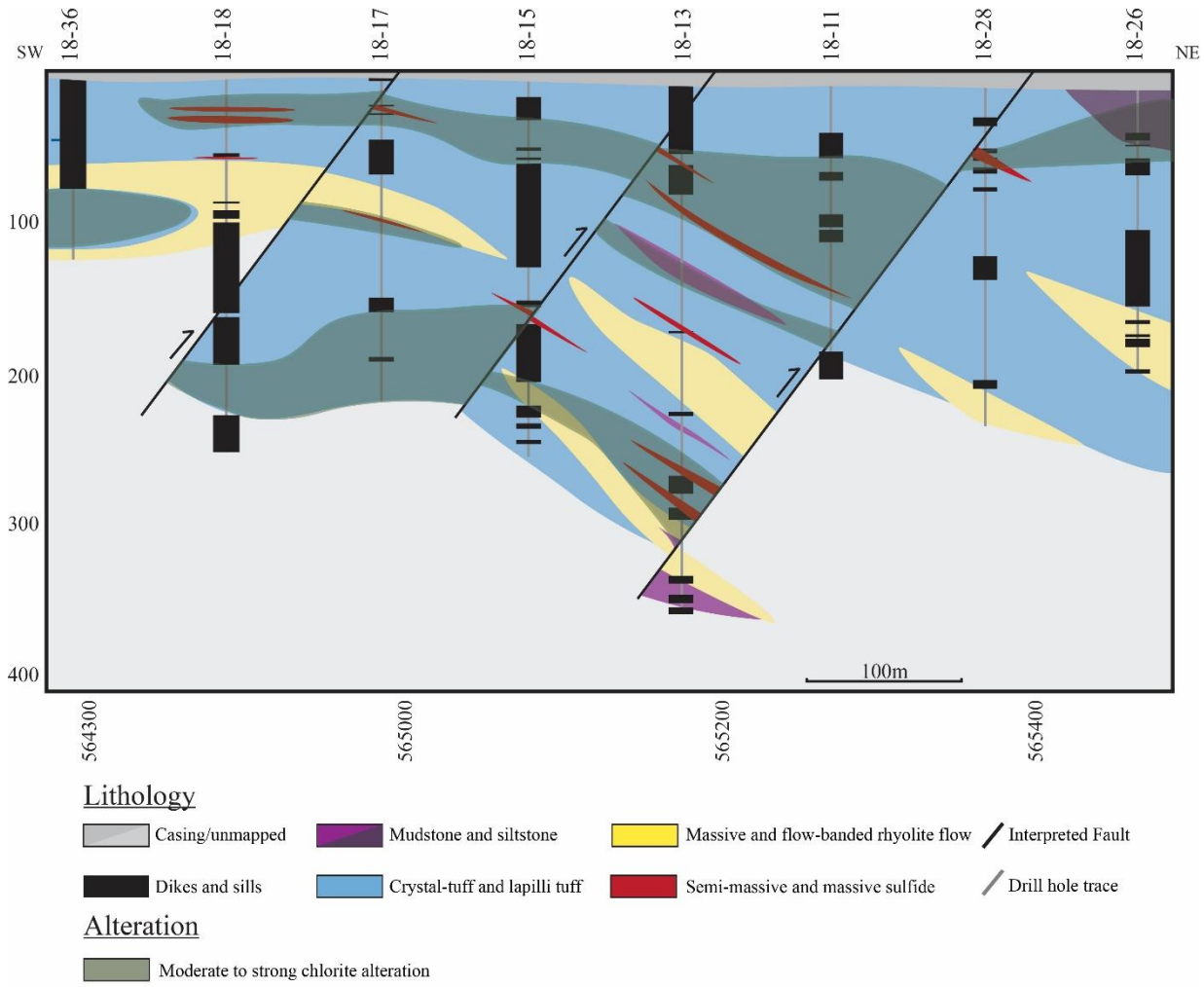

Figure 2.8B. A-A'. Cross-section of the Powderhorn Lake deposit illustrating relationships between lithofacies, structures, mineralization, and alteration. All lithologies have quartz-sericite alteration unless depicted otherwise. Alteration of dikes and sills not pictured.

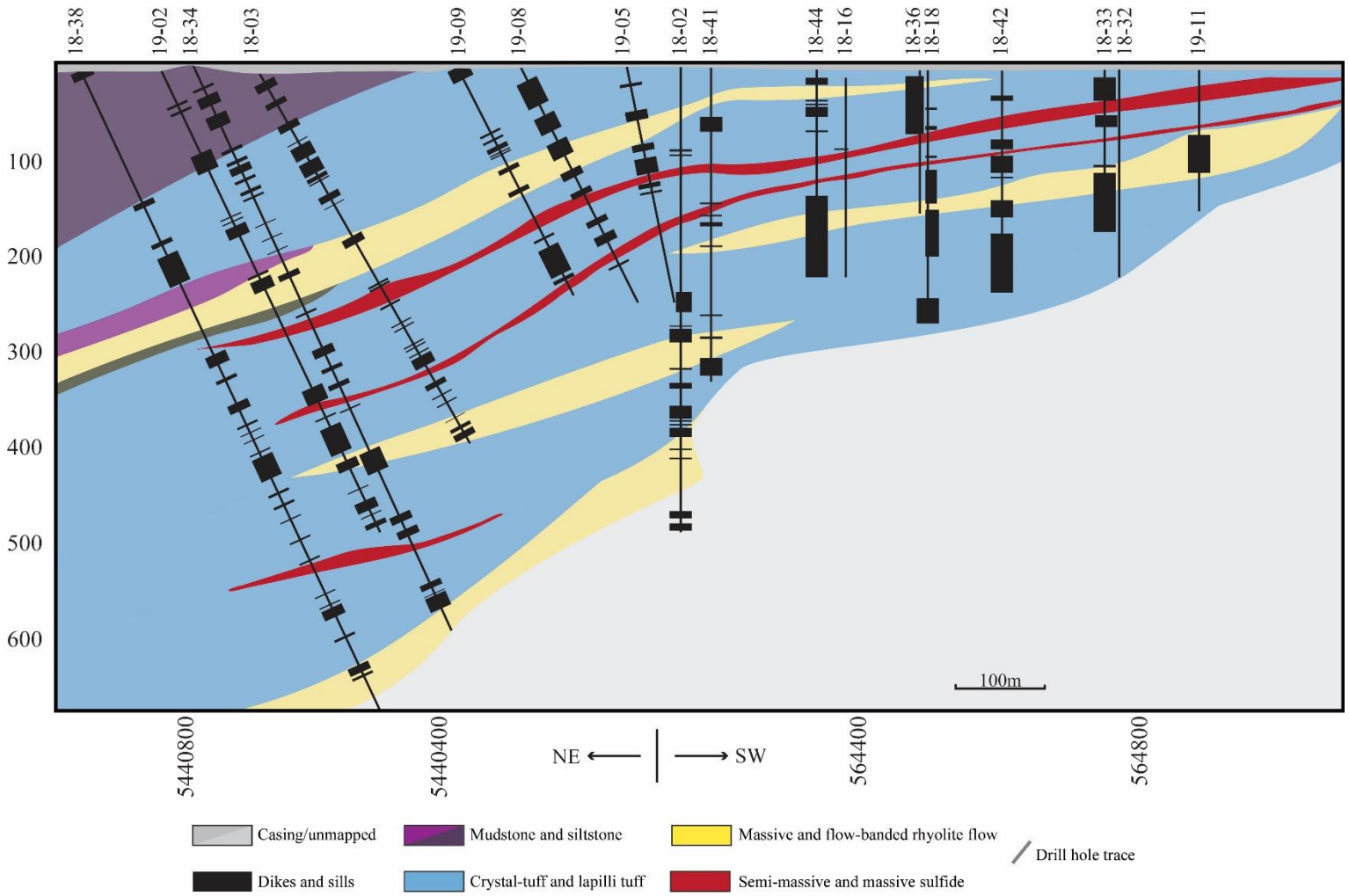

Figure 2.8C. B-B'. Long section of Powderhorn Lake deposit illustrating relationships between lithofacies and mineralization.

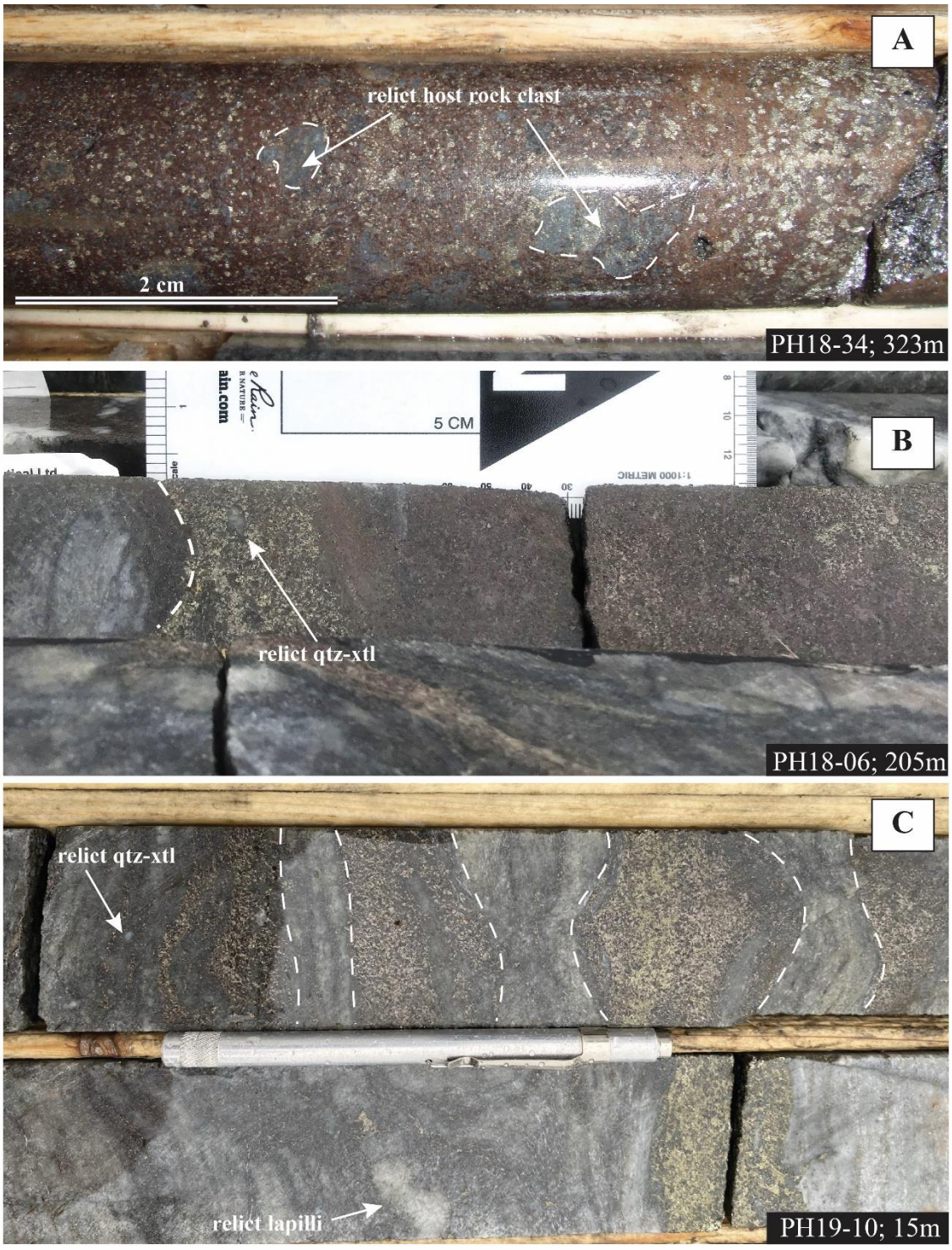

Figure 2.9. Mineralization textures present at Powderhorn Lake. A) Massive buck-shot textured sphalerite-pyrite with relict host rock clasts outlined in white. B) Sharp replacement front contact between tuff and massive sphalerite-pyrite. C) Banded pyrrhotite-chalcopyrite in lapilli tuff with relict quartz crystals and lapilli. Preferential replacement of less siliceous beds outlined in white. Abbreviations: chl-chlorite, qtz-quartz, xtl-crystal.

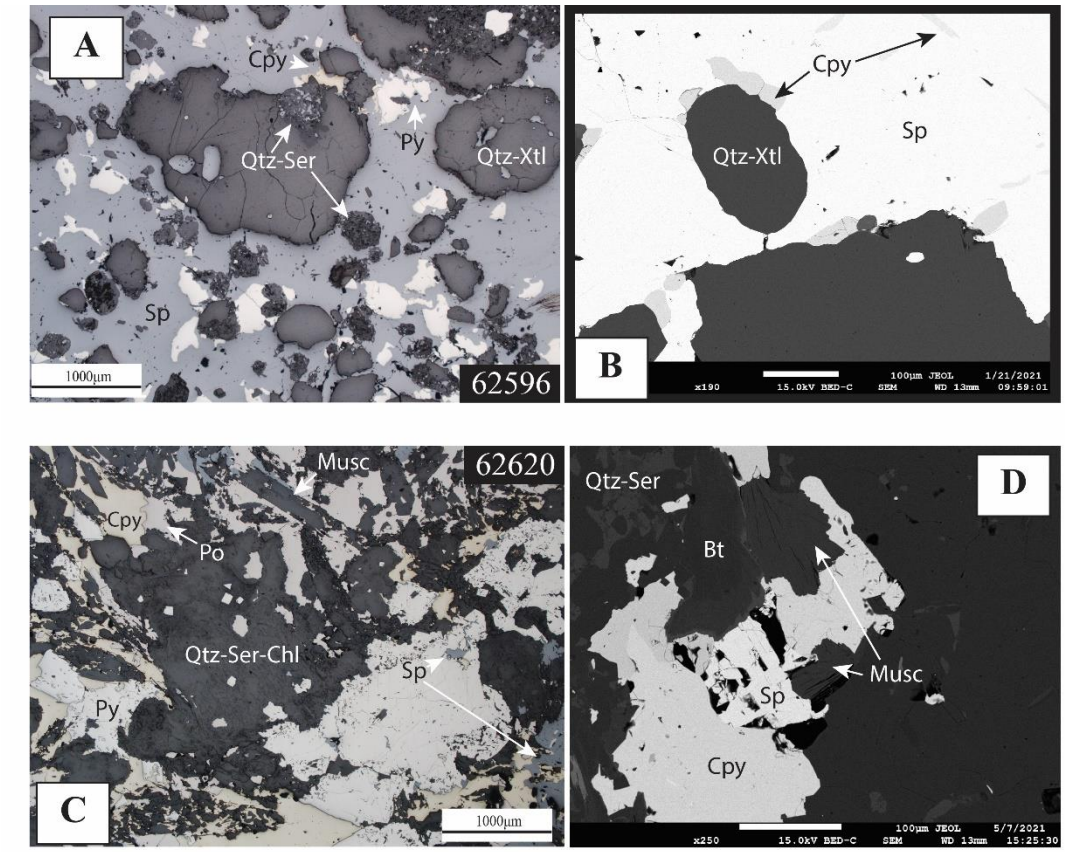

Figure 2.10. Photomicrographs of mineralization and associated alteration. A) Massive sphalerite with trace chalcopyrite and pyrite within strongly quartz-sericite altered quartz-crystal tuff. B) SEM image of previous sample in different location showing chalcopyrite blebs on the margin of a quartz-crystal and as inclusions within sphalerite. C) Pyrite with blebby sphalerite and chalcopyrite inclusions within quartz-ser-chl altered rhyolite with large muscovite crystals. D) SEM image of previous sample in different location showing chalcopyrite-pyrite surrounded by muscovite and biotite. Abbreviations: Bt-biotite, Chl-chlorite, Cpy-chalcopyrite, Musc-muscovite, Po-pyrrhotite, Py-pyrite, Ser-sericite, Sp-sphalerite, Xtl-crystal.

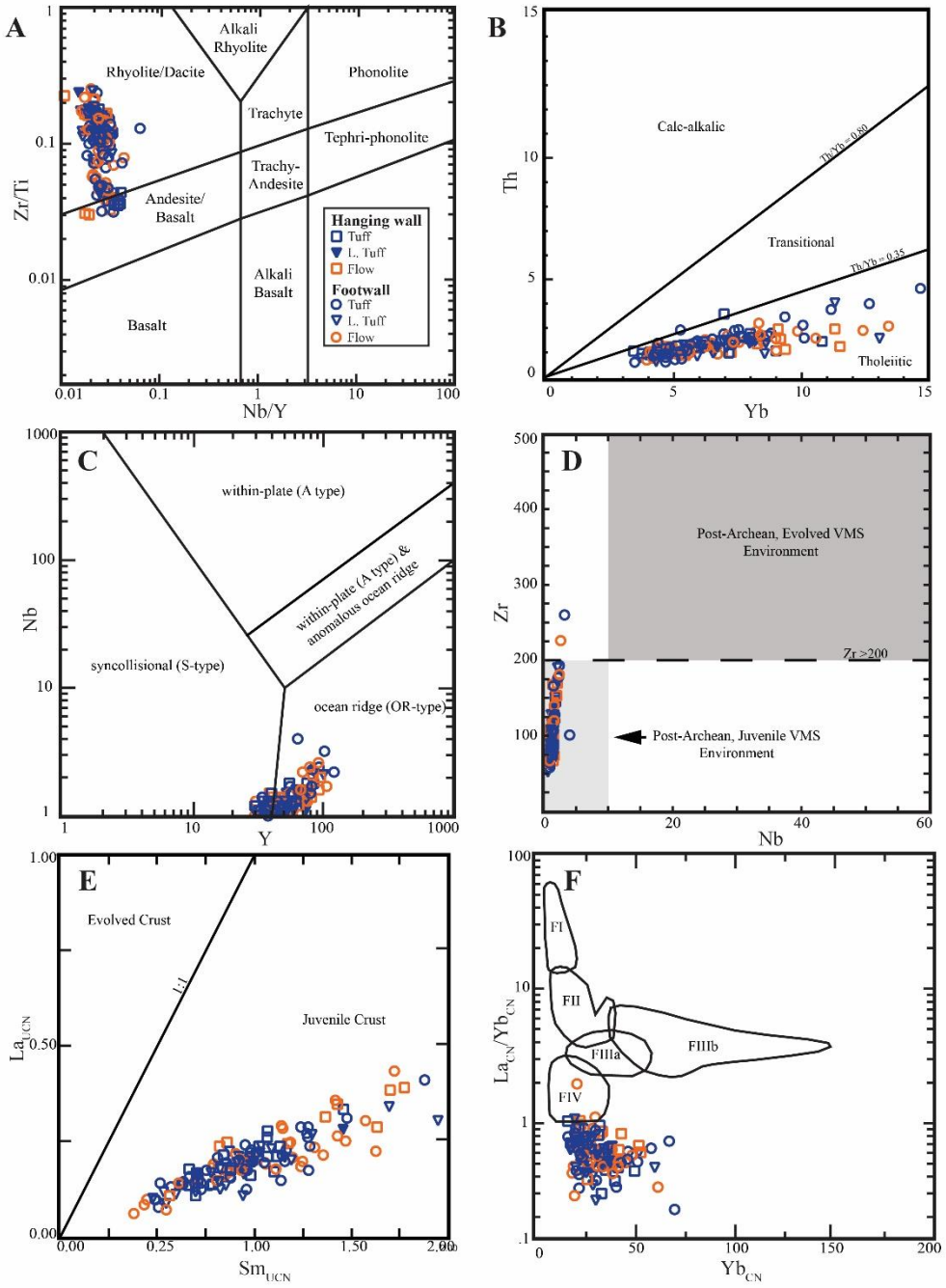

Figure 2.11. Immobile element discrimination diagrms of rhyolitic rocks of Powderhorn Lake. (A) Modified Winchester and Floyd (1977) $ZrTiO_2$-Nb/Y discrimination diagram rock classification (from Pearce, 1996). B) Th-Yb discrimination diagram for magmatic affinity (modified from Ross and Bedard, 2009). C) Nb-Y tectonic discrimination diagram (from Pearce et al., 1984). D) Zr-Nb diagram discriminating juvenile vs. evolved environments (modified from Piercey, 2009). E) Upper-crust normalized (UCN) La-Sm diagram (Taylor and McLennan, 1985; from Piercey and Colpron, 2009). F) La/Yb-Yb(cn) FI-FIV rhyolite discrimination diagram (chondrite normalized values (CN) from McDonough and Sun, 1995; from Lesher et al., 1986; Hart et al., 2004).

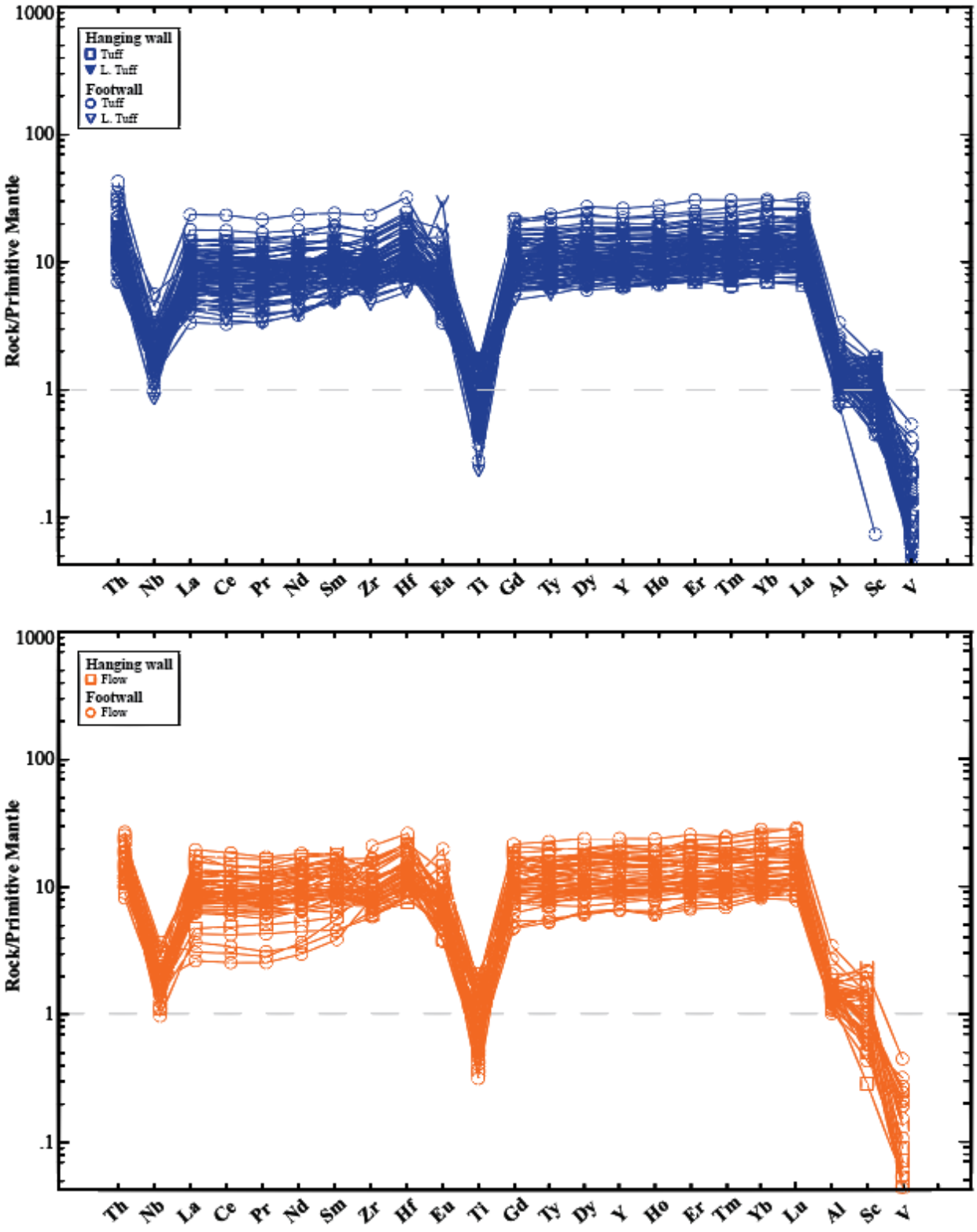

Figure 2.12. Primitive mantle normalized multi-element plots for felsic volcanic rocks of Powderhorn Lake (primitive mantle-normalized values of McDonough and Sun, 1995). A) Volcaniclastic lithofacies. B) Coherent volcanic lithofacies.

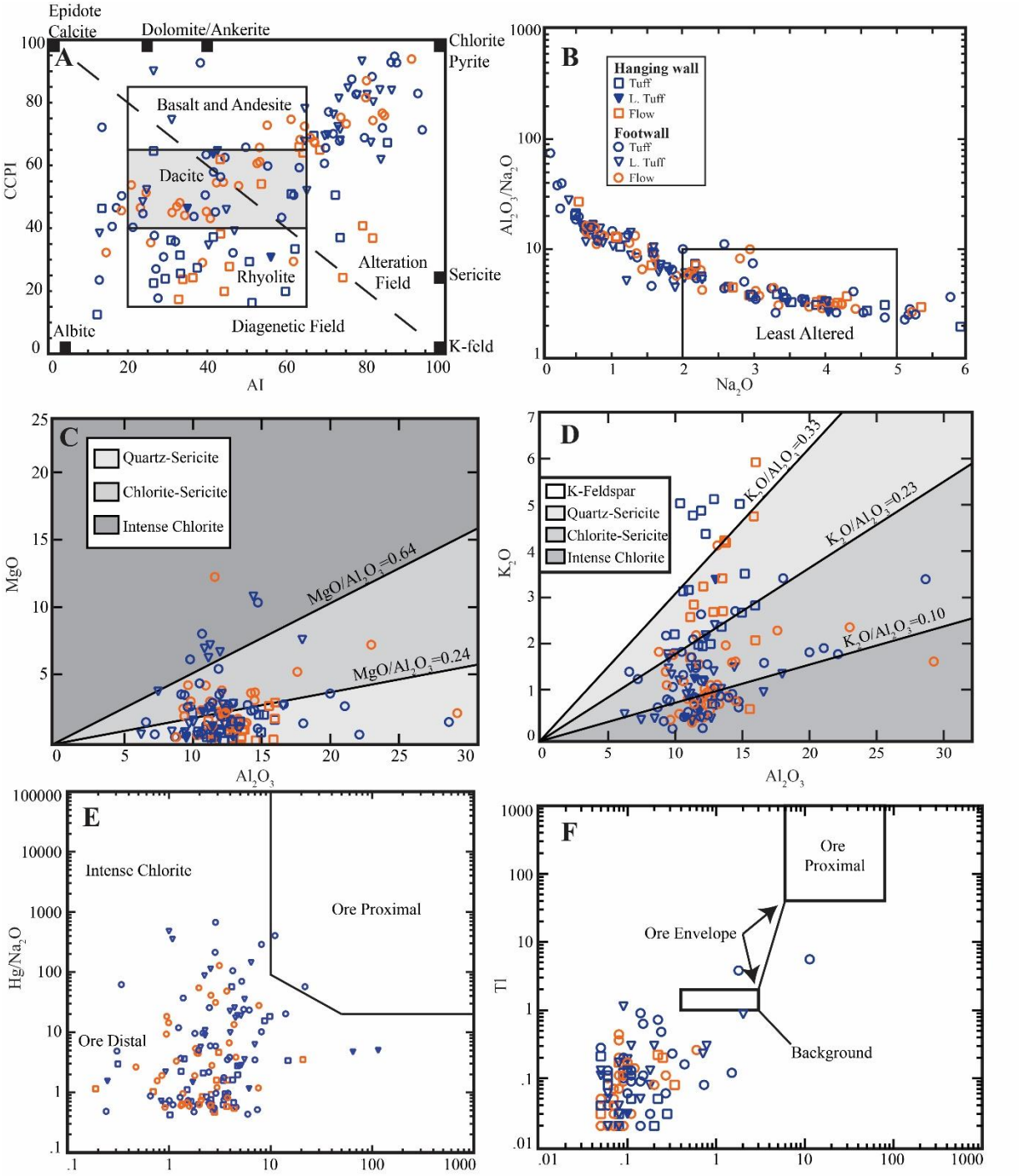

Figure 2.13. Mobile element plots for hanging wall and footwall rocks of Powderhorn Lake. A) Alteration box plot (from Large et al., 2001a). B) Spitz-Darling (1978) index vs. Na_2O (modified from Ruks et al., 2006). C&D) Diagram of MgO vs. Al_2O_3 and K_2O vs. Al_2O_3 defining alteration assemblages (from Buschette et al., 2016). E) Hg/Na_2O-Ba/Sr showing "Duck Pond index" (modified from Collins, 1989). F) Tl-Sb (from Large et al., 2001a).

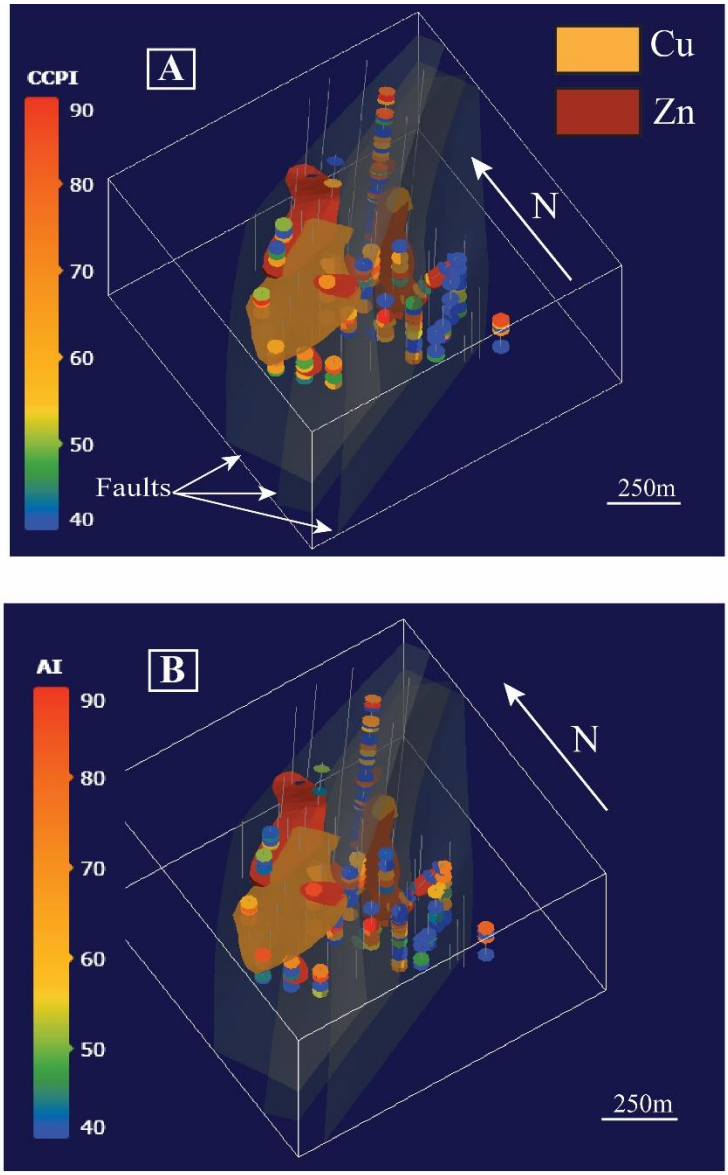

Figure 2.14. 3D models of the Powderhorn Lake deposit showing mobile element characteristics in relation to Cu and Zn mineralization. A) Model showing CCPI values. B) Model showing AI values.

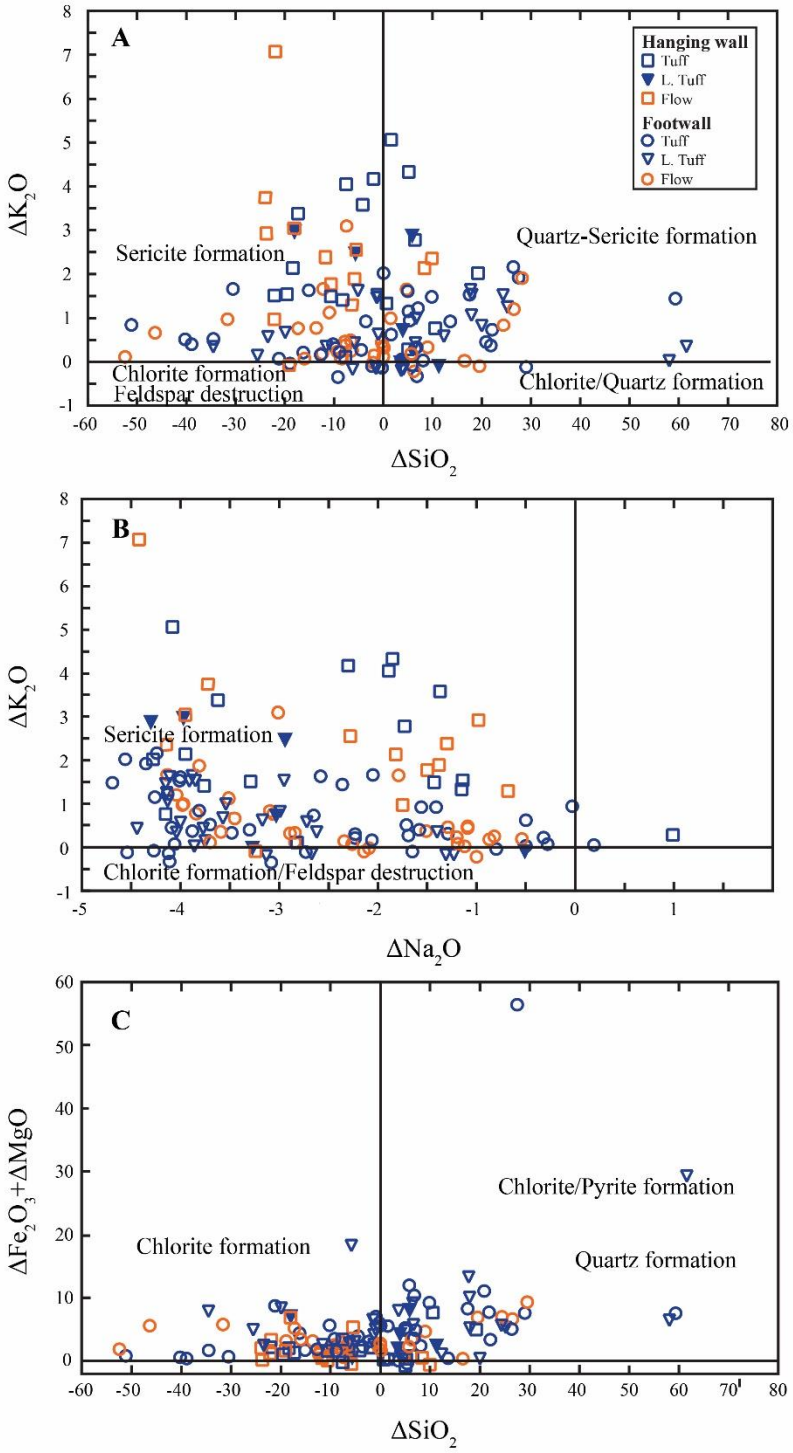

Figure 2.15. Mass balance plots showing elemental gains and losses. A) K_2O vs. Na_2O showing the formation of sericite and chlorite. B) K_2O vs. SiO_2 showing formation of sericite, quartz-sericite, and chlorite-quartz. C) Fe_2O3+MgO vs. SiO_2 showing formation of chlorite, pyrite, and quartz.

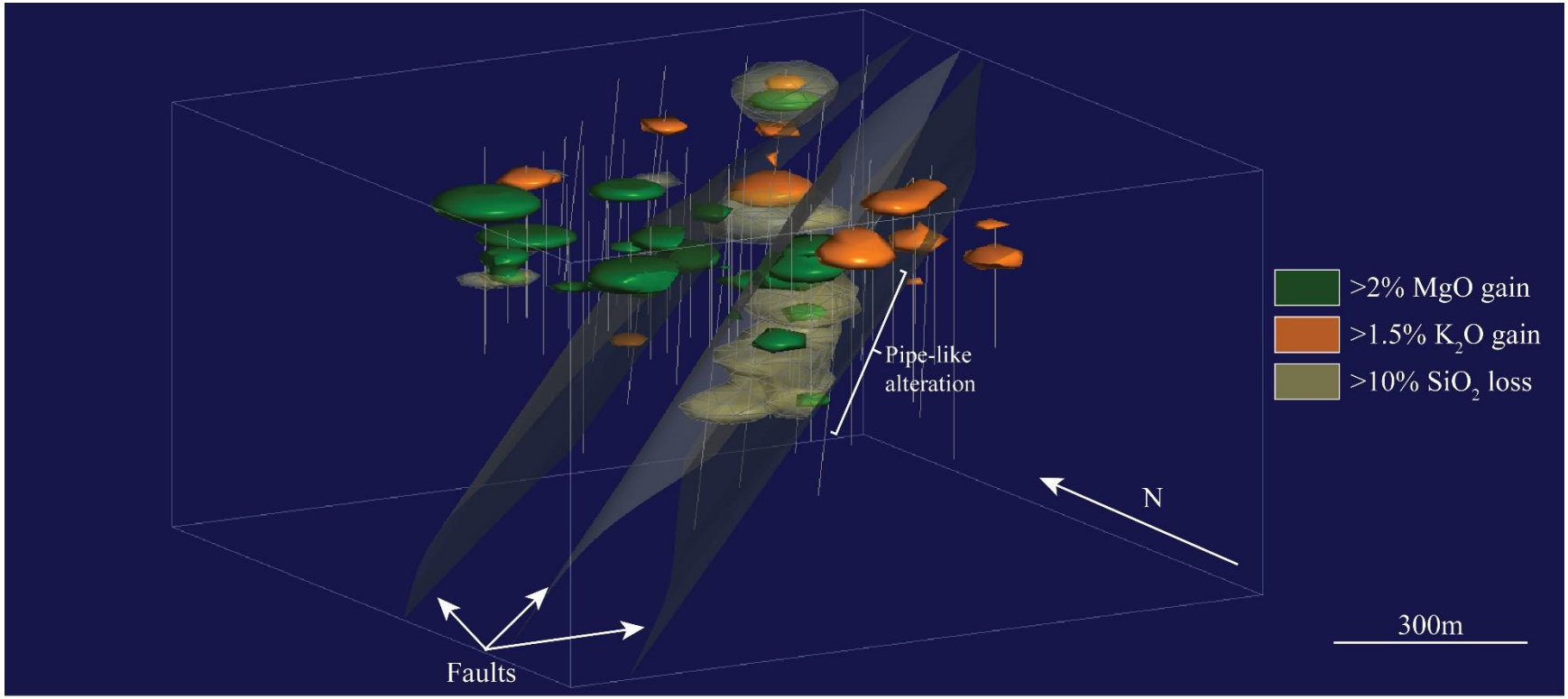

Figure 2.16. 3D alteration model of the Powderhorn Lake deposit created using mass change calculations and interpolated using a radial basis function (RBF) to produce spheroidical projections of alteration distribution. MgO gain with coincident SiO_2 losses is associated with moderate to strong chlorite alteration whereas >1.5% K_2O gain is associated with strong white mica alteration. Vertically extensive pipe-like alteration can be seen along the middle and easternmost fault. Rounded nature of gains and losses is a function of the RBF projection; additionally, the lateral extent of alteration distribution cannot be fully depicted due to software and sampling limitations (e.g., data connectivity).

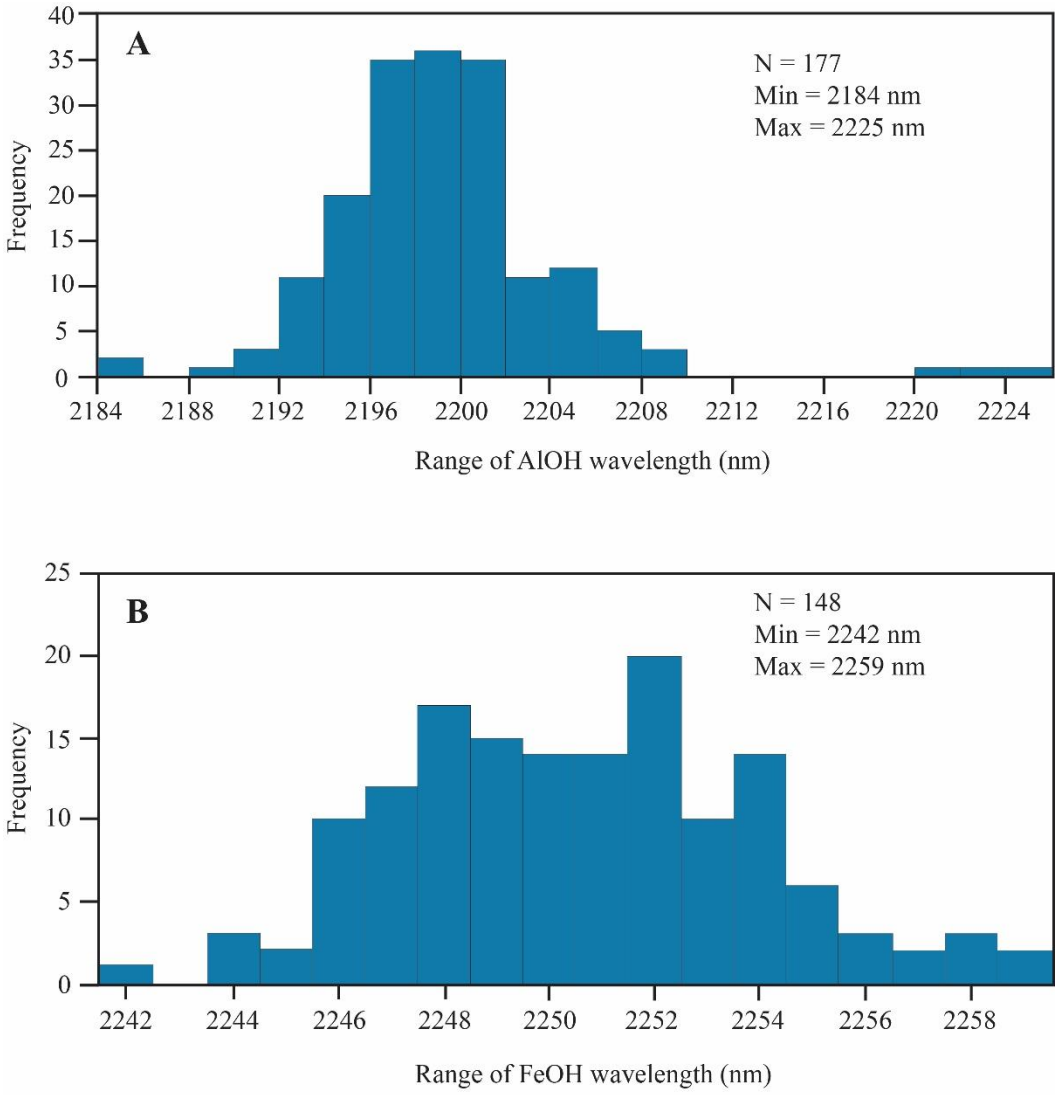

Figure 2.17. SWIR results. A) Histogram of AlOH wavelengths present at the Powderhorn Lake deposit. B) Histogram of FeOH wavelengths.

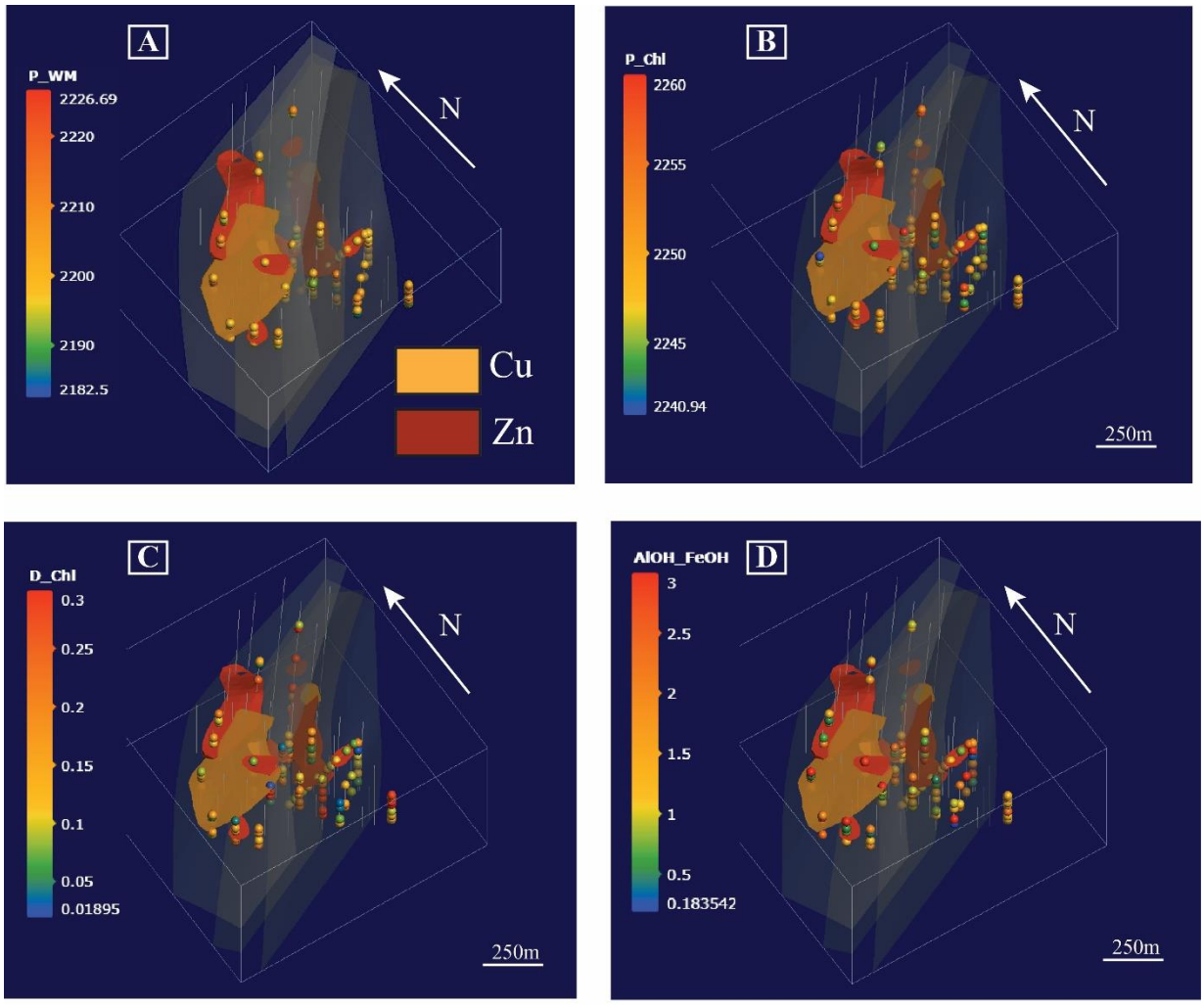

Figure 2.18. 3D models showing SWIR charactersitics of the Powderhorn Lake deposit in relation to Cu and Zn mineralization. A) Model showing AlOH wavelengths. B) Model showing FeOH wavelengths. C) Model showing FeOH absorption depth. D) Model showing AlOH/FeOH depth.

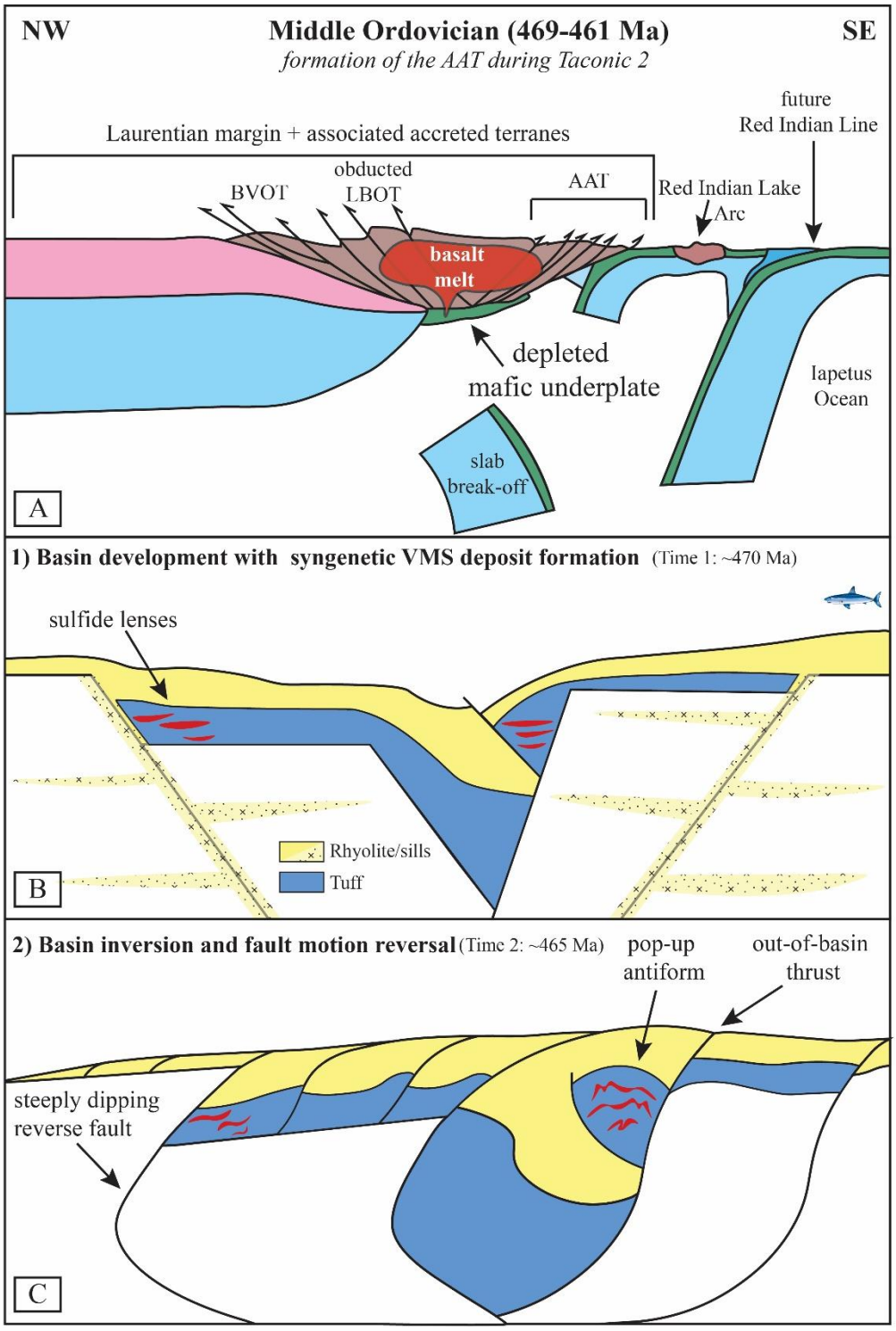

Figure 2.19. Schematic models showing the tectonic evolution of the Powderhorn Lake deposit, felsic rock formation, and present-day structural setting. A) Middle Ordovician tectonic evolution of the Laurentian margin displaying underplating and subsequent partial melting of juvenile, trace element depleted (mafic) arc crust (modified from van Staal et al., 2009; van Staal and Barr, 2012). B) Cross-section showing basin development and sill emplacement. C) Cross section showing crustal shortening and basin inversion during thin-skinned tectonics. Abbreviations: AAT-Annieopsquotch accretionary tract, BVOT-Baie Verte oceanic tract, LBOT-Lusch Bight oceanic tract.

Chapter 3: Summary and Future Research

3.1 Summary

The felsic-siliciclastic Powderhorn Lake VMS deposit hosted within the Buchans-Roberts Arm belt (BRAB) represents a deformed, subseafloor replacement-style VMS deposit in the Newfoundland Appalachians, Canada. The deposit is interpreted to have formed within a rifted arc basin that is now a sequence of imbricated thrust panels that formed as a result of basin inversion during thin-skinned accretionary orogenesis. The preservation of primary structural features and lithologic textures make it an ideal site to reconstruct an arc basin environment and study the lithostratigraphic and tectonic framework controls on the distribution of alteration and mineralization of replacement-type VMS deposits. Primary and mobile element geochemistry provide insight into the genesis of the Powderhorn Lake deposit and evolution of the hydrothermal alteration system, respectively. The major conclusions of this study are:

1. The Powderhorn Lake deposit is hosted by felsic volcanic rocks of the BRAB that were formed and deposited within a peri-Laurentian arc rift basin. Subsequent accretionary orogenic events and basin inversion resulted in: 1) a reversal of fault motion (i.e., normal sense succeeded by reverse displacement); 2) imbrication of stratigraphic packages, hydrothermal alteration, and mineralization; and 3) development of a domal antiform. This is supported by structural and lithostratigraphic relationships and immobile element signatures, in addition to previous geochemical and isotopic studies of the BRAB.

2. Alteration assemblages of the Powderhorn Lake deposit include quartz-sericite, quartz-sericite-chlorite, and quartz-sericite-chlorite-pyrite. These assemblages exhibit broad geochemical trends and hyperspectral signatures. Distribution and geometries of alteration zones are largely controlled by synvolcanic structures and primary porosity and permeability of host rocks.
3. Useful vectors towards Cu-rich mineralization include increased CCPI and elemental gains of Cu, Fe_2O_3, MgO (>2%), and loss of SiO_2, whereas Zn-mineralization is associated with increased AI and elemental gains of Zn, Pb, K_2O(+/-SiO_2), Fe_2O_3 and MgO (<2%).
4. The diffuse nature of hydrothermal alteration throughout hanging wall and footwall strata produced broad trends in mass change results. Extensive sericite alteration is characterized by moderate gains and losses of SiO_2 with coincident gains in K_2O and MgO (<2%). Chlorite alteration is much less abundant and associated with greatest SiO_2 losses, moderate Fe_2O_3 gains, and greater gains of MgO (>2%) relative to sericite alteration. Greatest Fe_2O_3 gains are associated with Fe-rich chlorite and biotite, pyrite alteration, and sulfide formation. Most samples exhibit gains in Ba and Rb regardless of alteration assemblage and further reflects pervasive sericite alteration and feldspar destruction. Select HFSE and REE were relatively immobile throughout the deposit, regardless of alteration.
5. Hyperspectral data reveals that white mica in the hanging wall and footwall strata is K-rich in composition and does not show any significant compositional variation. Most chlorite samples at Powderhorn Lake exhibit transitional (FeMg-rich) compositions. However, longer FeOH wavelengths (Fe-rich chlorite) and higher absorption depth

values occur proximal to Cu-rich mineralization whereas shorter wavelengths (Mg- and FeMg-rich) are associated with Zn-rich mineralization.

6. The original basin architecture of the Powderhorn Lake deposit resulted in the formation of a hydrothermal system that produced subseafloor replacement-style VMS mineralization. Active rifting and basin development resulted in the formation of large, steeply dipping graben-bounding normal faults that acted as primary hydrothermal fluid conduits. Upward and vertical flow of hydrothermal fluids were impeded by impermeable rhyolite flows that resulted in diffuse, laterally extensive fluid flow into originally highly porous and permeable volcaniclastic rocks. The capping of hydrothermal circulation led to downward and lateral focused fluid flow that resulted in replacement of volcaniclastic host facies with sulfide mineralization. Contrasting permeability between lithofacies led to the development of multiple, stacked mineralized lenses that are concordant to stratigraphy and exhibit a tree-branch like morphology. Widespread alteration within the hanging wall suggests that the hanging wall rocks were emplaced either prior to, or synchronously with, the development of the hydrothermal system.

3.2 Future Research

This thesis has built the initial framework for understanding the genesis and evolution of the Powderhorn Lake deposit, but there are still several knowledge gaps. Acquiring U-Pb ages from felsic rocks in the BRAB has proved to be difficult due to the undersaturation of zircon; however, obtaining ages from other minerals (e.g., titanite and rutile) may constrain the timing of tectonostratigraphic events in the belt. A detailed study of the sulfide mineralogy (e.g., microscopy, SEM, EMPA), in addition to S and Pb isotopes, could determine sulfide

paragenesis, the source of metals, and the physiochemical composition of the hydrothermal fluids responsible for the formation of the Powderhorn deposit. Additional Terraspec and EMPA of sericite and chlorite compositions on remaining drill holes may reveal more distinct trends between wavelengths and mica compositions. Overall, the Powderhorn Lake deposit would greatly benefit from additional drilling, preferably oriented, to better characterize the extent of structural features (e.g., faulting and folding) with respect to lithostratigraphy and mineralization.

Appendix A: Graphic Logs

Fieldwork at the Powderhorn Lake deposit was conducted from September to October 2019 and from July to August 2020 and consisted of detailed logging and representative sampling of the hanging wall, mineralized sequence, and footwall in diamond drill core. The focus of core logging was to characterize lithology, alteration assemblages, and mineralization. A total of 22 drill holes were logged and 206 samples were collected with 163 of those samples analyzed for representative whole-rock lithogeochemistry. A total of 41 thin sections were made from these samples.

The Abbreviation Key and Legend (Appendix A.1, A.2) for the 22 drill holes logs (Appendix A.3) is below. Drill holes were labeled following the nomenclature: PH-YY-XX, where PH stands for Powderhorn Lake deposit, YY stands for the last two numbers in the year that the whole was drilled, and XX is the hole number that was completed in that year's drilling program (e.g., PH-18-01 was drilled at the Powderhorn Lake deposit in 2018 and is the first hole drilled that year).

Contacts between subfacies (e.g., tuff and lapilli tuff) should be interpreted as gradational unless noted otherwise. Most contacts between coherent and volcaniclastic facies (e.g., flow and tuff) are sharp; however, some contacts are depicted as gradational due to the contact being obscured by subsequent deformation or alteration. Units and subfacies with gradational contacts will be colored to whichever unit is downhole (i.e. on the bottom).

Appendix A.1 Abbreviation Key for Graphic Logs

General	
E	Easting
m	Meter
N	Northing
UTM	Universal Transverse Mercator
Alteration Types	
Gt	Garnet
Sil	Sillimanite
Qtz	Quartz
Ser	Sericite
Chl	Chlorite
Sulf	Sulfide
Lithology	
Sed	Sediments
L. Tuff	Lapilli Tuff
Flow	Volcanic Flow
Int	Intrusion
Minz	Mineralized
Other (in description)	
Alt	Alteration
Aph	Aphanitic
Bt	Biotite
Cpy	Chalcopyrite
Dissem	Disseminated
EOH	End of hole
FBR	Flow banded rhyolite
Gn	Galena
Inter	Intermediate
Mod	Moderate
Po	Pyrrhotite
Porph	Porphyritic
Py	Pyrite
Rhy	Rhyolite
Semi-mass	Semi-massive
Sp	Sphalerite
Xtl	Crystal

Legend

Volcaniclastic Rocks

Mudstone and siltstone

Rhyolitic bt-tuff and quartz-phyric +/-feldspar crystal tuffs

Rhyolitic lapilli tuff

Coherent Rocks

Aphyric and flow-banded to qtz-phyric +/-bt-rhyolite

Aphyric and fine-coarse grained basaltic flows

Intrusion

Aphanitic basaltic and porphyritic andesitic dikes, qtz-phyric rhyolitic sills

Mineralized Sequence

Massive to semi-massive and stringer Cu-Zn sulfides

Alteration Intensity

Weak

Moderate

Strong

Other symbols

Fault

(S) Lithogeochemical sample

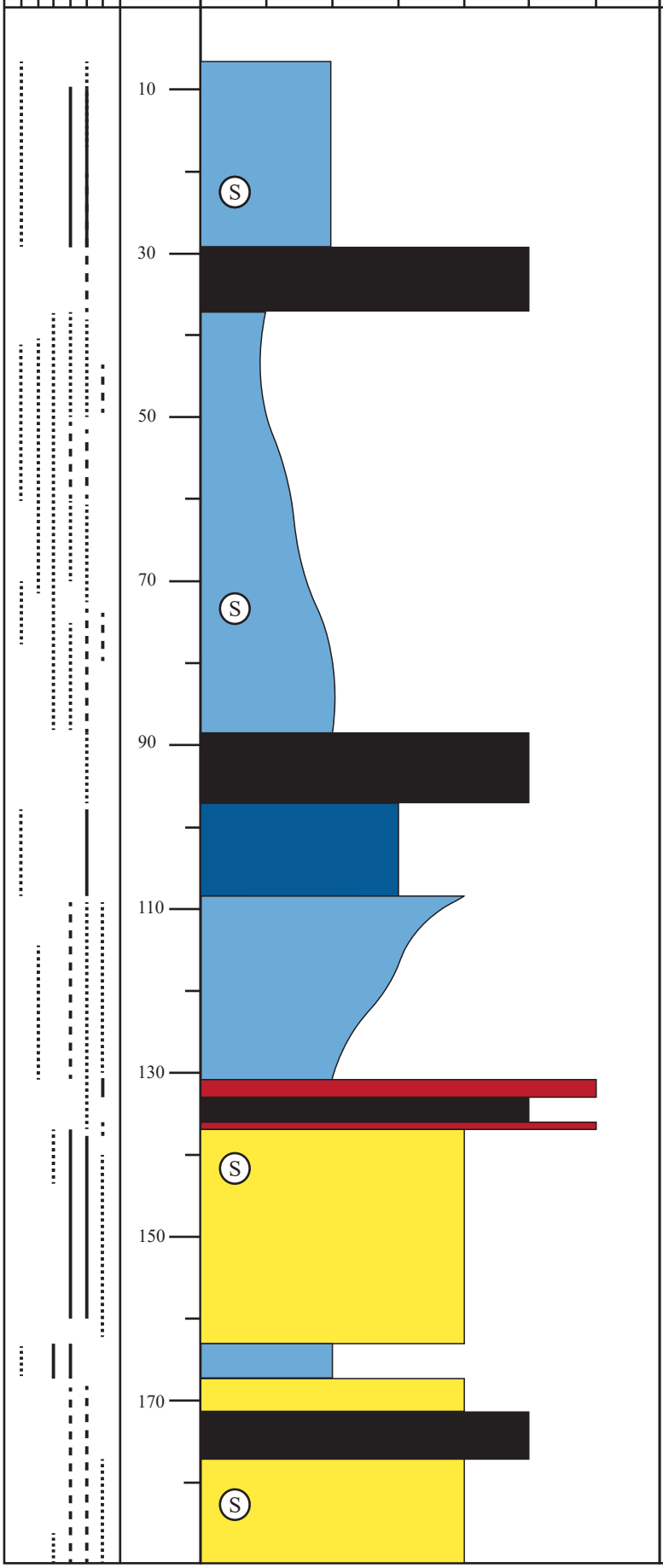

Project: Powderhorn Lake
Drill Hole: PH-18-01
Date: July 30, 2020

UTM: 565E 544N (NAD83)
Azimuth, Dip: 200, -50
Length: 499m

7m beginning of unit is drab gray - very opaque, fine-grained tuff with fine bt crystals (<1mm), weakly alt by chl, small dikelets of dioritic composition cutting through
~11m becomes mod-strongly chl+ser alt, mod qtz alt, can see zoned ser-gt-ep+/-sil veins
@16.4m small 30cm aph mafic dike and transition into reddish green tuffaceous sediments
22m mottled green and reddish brown tuff seds with irregular whispy beds, mod-strongly alt by chl, barren in sulfides, crenulations in part, end of unit becomes "clasty" with black chl clots/clasts
Sample 62667

29.04m chloritized dike with white 2-3mm chunky, irregular plag phenocrysts

37.4m light-medium gray volcanicalstic seds with reddish whispy beds with green (chl?) foliations, some bt, becomes darker in color with thinner beds that are prominantly reddish/brown, presence of zoned veins towards end of unit, white plag phenocrysts visible

45m localized sp (<15%) and py (<5%) - (50m) gradual change to more plag-qtz crystal tuff, lighter in color overall with bt following foliation, mod chl and weak ser alt, zoned veins and weak albite (?) alt - (55m) the tuff shows gts that are oblong - somewhat stretched, ser+chl increases from ~54m to ~58m - (60m) Sparse qtz eyes (clear), barren sulfides, chalky pink alt

70m darker thin beds, weakly foliated, can still see bt-spts @71m 30cm aph dike - (75m) zoned vuggy veins, small plag crystals (<1mm), very grainy when dry, beds fade back and transition into tuff, larger milky qtz eyes, mod chl and weak ser alt, sharp contact to dike
Sample 62668

88.32m porphyritic QFP dark-colored dike - 1m dark aphanitic dike ~93m

97.72m dark gray to black unit with irregular clasty, elongate lapilli - some sandy/silty red layers mod-strong chl+ser alt, presence of zoned vein, end of unit is crenulated/deformed

108.14m light gray, fine-coarse grained bt-spotted rhyolite, mod alt by ser+chl, becomes mod foliated, split core until ~110m with vein-foliation hosted po (10%) and sp (<10%) generally dissem with local matrix-fill, sparse bluish qtz eyes ~115m white whispy sil and trace dissem brown sp-po (<10%), mod alt by apple green ser, weakly foliated, some milky plag phenocrysts ~126.5m increase in tannish green ser cast, crenulations visible in part, black chl "clasts/clots" (2-4mm), more tuffaceous influence

131.62m localized semi-massive with sp (60%) ~8cm long matrix-fill, reddish-brown, trace cpy (<5%) - aph mafic dike - 133.66m local semi-massive sp (15-50%<) predominantly vein-foliation and matrix-fill, small local splotches of cpy (<10%) hosted in heavily alt massive rhy, very dark in color, presence of minor qtz phenocrysts - more irregular than eyes
Sample 62669
138m grades into relatively barren massive rhy with characteristic red+green mottling, mod-strong chl+ser alt, bt follows foliation (overall weak), qtz alt and veining increases 144m, crenulations become more obvious ~147m, trace po-sp (<5%)
160.2-160.94m plag phenocryst interm dike with large qtz veins
Red+green, split core with trace sp-py-po (<10%)
163m sharp contact to dark tuffaceous unit, heavily alt, zoned veins, strongly
foliated, apple green ser, pinkish albite, reddish beds
167.13m light-medium gray massive, half core, weakly foliated, trace sp (5-10%) and py (5%)
171.25m dark, fine-medium grained plagioclase phenocryst dike

177.12m beginning massive rhy grading into tuff/lapilli tuff
Sample 62670

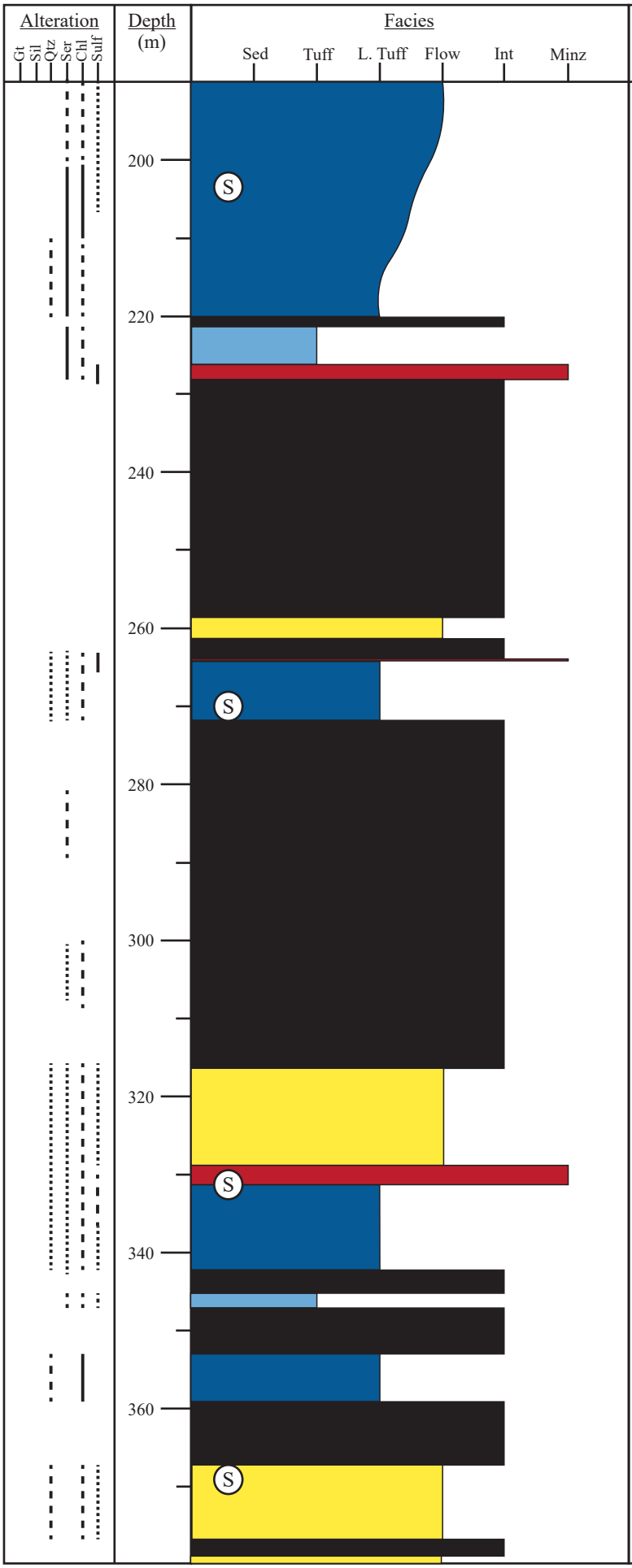

Project: Powderhorn Lake
Drill Hole: PH-18-01
Date:

UTM:
Azimuth, Dip:
Length:

grayish green massive rhy (halved core), mod alt by chl with reddish/brown alt flow banding, realtively fine-grained, trace dissem sp (<10%) , qtz increase ~187m, large qtz vein at 190.10m for 70cm

Ser alt increase to mod and chl increases to strong ~199m, as color becomes darker - flow textures are lost, trace py (<5%) - 205m very green and whispy sil with some type of flow or quench texture

Sample 62671

Light-med gray, fine-med grained lapilli tuff mod-strongly alt by ser, mod by chl, local plag phenocrysts, trace sp (<5%), weakly foliated, black chl clasts ~213m grading into lighter qtz-crystal tuff with greenish whispy chl bands, texture is lost

220.5m aph mafic dike

221.55m heavily altered tuff unit like above

226m semi-massive sp (<25%), cpy (<10%), and py (<10%) hosted in qtz-eye tuff, matrix vein-foliation hosted, strongly alt by ser+chl+qtz, sp can be seen in 3 colors (honey, reddish brown, orange)

228m plag and bt porphyritic dike until 238.20m - Dark, aph dike with spidery/glomerocrystic (?) plag phenocrysts (mag) until 244.10m - Back into light gray colored plag phenocryst dike (slight mag) - 252.80m into mag aph dike (70cm) - White spidery plag (slight mag)

259.2m mottled red/brown with spotty black chl, no distinguishable textures, trace dissem py (<5%), qtz eyes are sparse and milky blue

261.33m dark aph mafic dike slightly mag

264m semi-massive sp (15-25%) reddish brown, dark qtz eyes within minz, deformed/crenulated

264.96m mod foliated with mod chl+ser alt, spotty chl clasts, crenulated in part, milky qtz eyes, trace dissem sp (<5%)

Sample 62673

272.22m aph magnetic dike with rhy or tuff rafts ~277m oblong clasts very rich in chl, weakly ser ~285m mod sericitic, slightly mag ~292 slightly mag with plag phenocrysts ~300m phenocrysts become larger and becomes less magnetic - more chl than ser alt ~303m aph dark, grades into spidery plag, mag ~314m loss of plag, completely aph

316.32m medium gray heavily altered qtz-eye tuff, no distinguishable beds, mod alt by chl, weakly foliated, can see crenulations

Sample 62674

~329m localized sp (15-30%) minz, qtz eyes milky, py (10%)

331m tuff is darker in color, grainy texture, loss of qtz eyes, matrix-fill py (<10%), increase in chl alt, dissem sp (<5%) throughout

340m red/green volc sediments-tuff more qtz alt, grainy, loss of qtz eyes

342.68m aph mafic dike

345.6m green and tan mottled colors, trace sp (<10%) with black chl clasts - interbedded and deformed bt-tuff

347.79m aph mafic dike

353.95m light gray lapilli tuff strongly alt by ser and mod by qtz, crenulations visible, milky qtz veins grades into darker grainier tuff

Dark aph mafic dike, mag

Ssample 62675

367.45m red+green mottled, varibaly alt aphyric rhy, mod-strong chl, mod ser+qtz alt, weakly folaited, texture is gone, no distinct beds, trace py+sp (<10%), local whispy/clasty red beds (?)

376.42m medium gray, 4-6mm, glassy, euhedral plag porphyritic dike

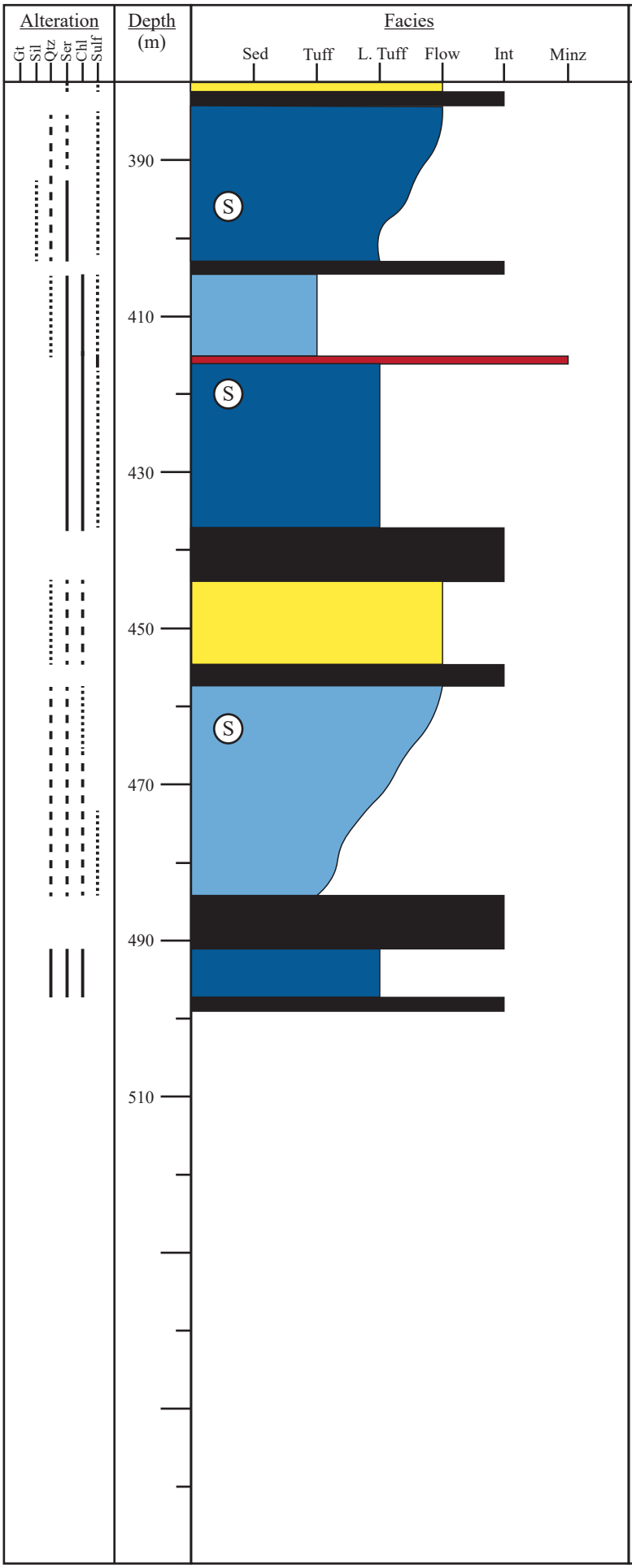

Project: Powderhorn Lake
Drill Hole: PH-18-01
Date:

UTM:
Azimuth, Dip:
Length:

378.97m red/green mottled bt-spotted rhy, minor qtz eyes, dissem dark brown sp (<10%)
381.86m aph mafic dike
383.4m light-medium gray, red/green mottled alt rhy, weakly foliated with long oblong chl clasts (maybe lapilli), trace po and sp (<5%)
387m grading into darker, grainier, bedded tuff strongly alt by ser, mod by qtz, red silty/sandy interbeds, presence of sil, sparse qtz-eyes, very alt and clasty, trace po (<5%) but relatively barren
Sample 62676
403.7m aph mafic dike
404.36m mottled red/green, grainy tuff mod-strongly alt by chl+ser, dark black chl or bt crystals can be seen, minor bluish qtz eyes, trace sp+py (<5%)

415m honey and orange colored semi-mass-dissem matrix-fill sp (10-15%) and cpy (<5-8%)
Sample 62677
416m loses bedded texture, presence of dark oblong clasts (lapilli) that fill with trace py+sp (<5%), minor qtz eyes - (421m) small 1m aph mafic dike - Grades into granier tuff, strongly alt by ser+chl, minor qtz eyes with large bt crystals, end of unit looks brecciated with heavy ser alt

437m plag porphyritic dike, slightly mag

444.2m light-medium gray faintly bt-spotted rhy, mod ser+chl alt ~446m localized bt and sil matrix-fill patchy alteration ~449.5. increase in ser+ch+sil, possible quench texture (?), minor presence of qtz eyes

454.16m plag porphyritic dike

457m light gray, green/red/brown mottled, fine-coarse grained, mod alt by chl+qtz, weak by ser, weakly foliated, somewhat grainy texture ~459.5m, trace py (<5%) dissem throught, increase in ser alt ~465m and clasty bt+chl - grading into unit darker in color, presence of reddish/brown thin grainy beds, bt and chl spots are visible, mod chl+ser alt ~475.5 strong ser+cl+qtz alt, some pinkish alt, back into grainy sed beds, large qtz veins, trace py and sp (<5%)
Sample 62678

484.68m aph mafic dike, mag - 1m section of plag porphyritic at end of unit

491.4m light gray, bt-spotted, no real beds, mod-strong ser+chl+qtz alt, trace py (<5%), heavily altered towards dike contact

497m fine-grained plag porphyritic dike

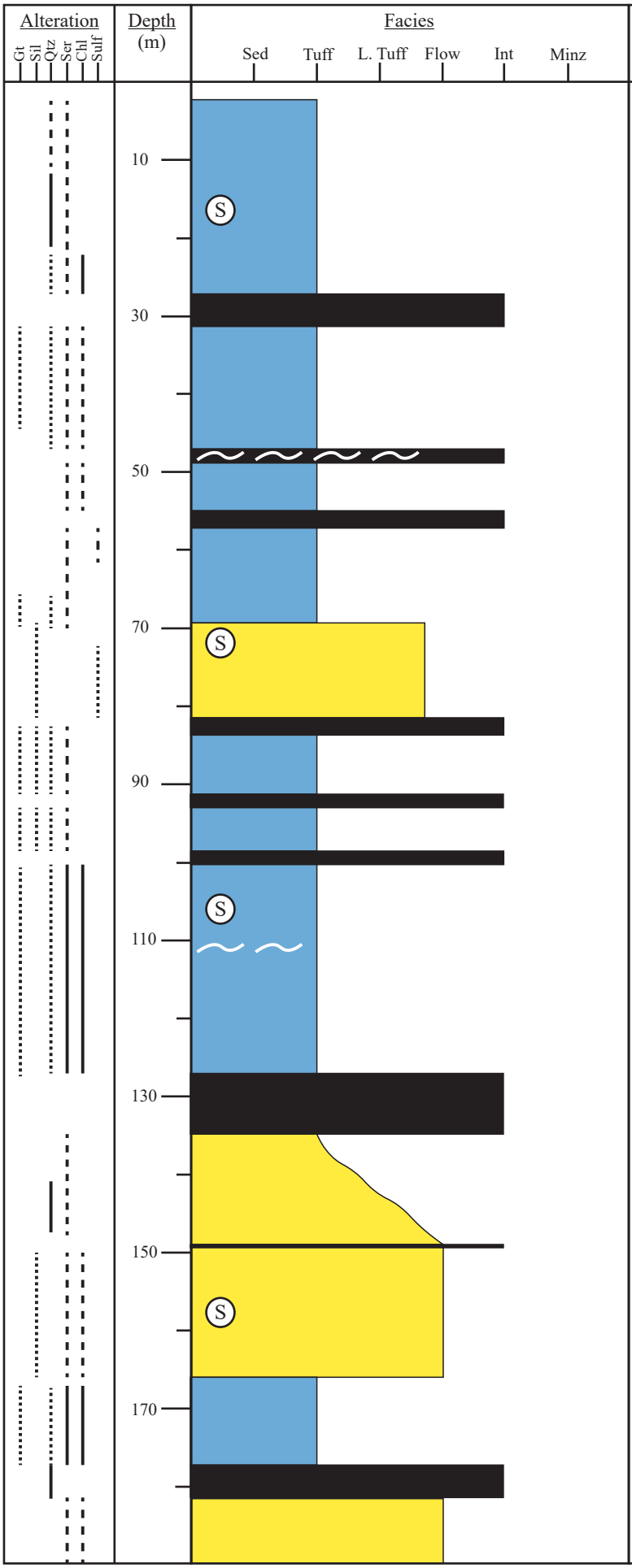

Project: Powderhorn Lake
Drill Hole: PH-18-04
Date: September 27, 2019

UTM: 565020E 5440848N (NAD83)
Azimuth, Dip: 360, -90
Length: 360 m

2.25m beginning of unit is rusty crumbly, grades into medium gray-green siliceous qtz-crystal tuff, mod alt by ser, sparse bt
12.32m highly alt aphyric felsic volcanic - possible deformed/alt FBR or heavily qtz alt tuff, red/green mottling, crenulated in part, pervasive qtz veining throughout unit, minor qtz eyes
Sample 62745
22.35m grades into dark colored, fine-grained, alternating brown/red bands (or beds?), with siliceous white and green mottling, dark green chl is clasty/clotty, minor qtz eyes

27.89m black aph mafic dike, slightly mag

31.11m mottled red/green, highly siliceous, aphyric alt felsic volcanic, fine glass, very clasty/crenulated/deformed ~44m very dark fine-grained ash (?) seems to be small-thin beds of above unit with zoned qtz-gt-ep veins (possibly heavily alt tuff)
47.17m black aph mafic dike, slightly mag - very crumbly and faulted
48.68m crumbly beginning of unit, same as above - variably alt felsic volcanic, end of unit seems to be more tuffaceous - dark, fine-grained, loses texture
55m black aph, slightly mag
57.15m light-medium gray aphyric tuff, mod alt by ser - 61.7m small net-textured sp-cpy (<10%; <3%) stringers until 62 ~66m increase in ser alt, presence of zoned veins

69.88m light gray, aphyric, highly siliceous, variably alt massive rhy with mottled pink patches and white whispy sil (<5-8%), mod ser alt, vuggy qtz sockets, bt increases down unit, begin to see local po-spy (<5%) patches, and crenulations, original dark black glass can be seen
Sample 62749
82.62m aph mafic dike, non-mag
83.80m light gray-pale green siliceous, aphyric tuff with zoned qtz-gt veins with why whispy qtz phenocrysts, minor sil and pink mottling

91.17m aph mafic dike, non-mag
93.08m (same as above) light gray-pale green siliceous, aphyric tuff with zoned qtz-gt veins with why whispy qtz phenocrysts, minor sil and pink mottling
98.54m aph mafic dike, non-mag
Sample 62746
100.1m dark reddish brown, faintly bt-spotted tuff, mod-strongly ser+chl alt, no obvious bedding, mod-strongly foliated, zoned gt-qtz-ep veins with network-like alteration veining (stockwork), sparse qtz-eyes, trace dissem po-py blebs (<5%), some beds seem to be unaltered bt-tuff 110.90-113m crumbly possibly fault zone 114m fine-grained dark, possible seds interbed, heavily green/dark brown/red alt and grades into patchy bt-tuff, clasty/clotty chl+/-bt throughout, crenulations in part, heavily alt end of unit, local qtz-eyes and trace dissem po blebs (<5%)

127.08m aph mafic dike, non-mag

134.40m same unit as above - dark, fine-grained, bt-spotted tuff, mod ser, grades into highly siliceous aphyric mass rhy - gray-opq white, aphyric, highly siliceous-cherty alt massive rhy, crenulations in part, end of unit seems more tuffaceous again
149m aph black mafic dike, non-mag
149.5m light gray, siliceous bt-spotted massive rhy-alt FBR, red/green mottled with crenulated/deformed clasty chl bands and fine-grained altered glasses (?) - the clasty spotted bt may also be brown ser (?), minor whispy sil and qtz-crystals
Sample 62747
166m dark, fine-grained to aph, strongly ser+chl alt tuff or very alt rhyolite, zoned gt-ep-qtz veins, no real bedding, mod foliated
Sample 62748
177.5m large qtz vein or completely wiped silica alt. tuff/rhy - some clasty rafts of unit above/below
181.43m light-med gray, aphyric, bt-spotted massive rhy with red mottling, mod ser+chl alt, minor whispy white sil, crenulations in part ~186.5m grainier appearance

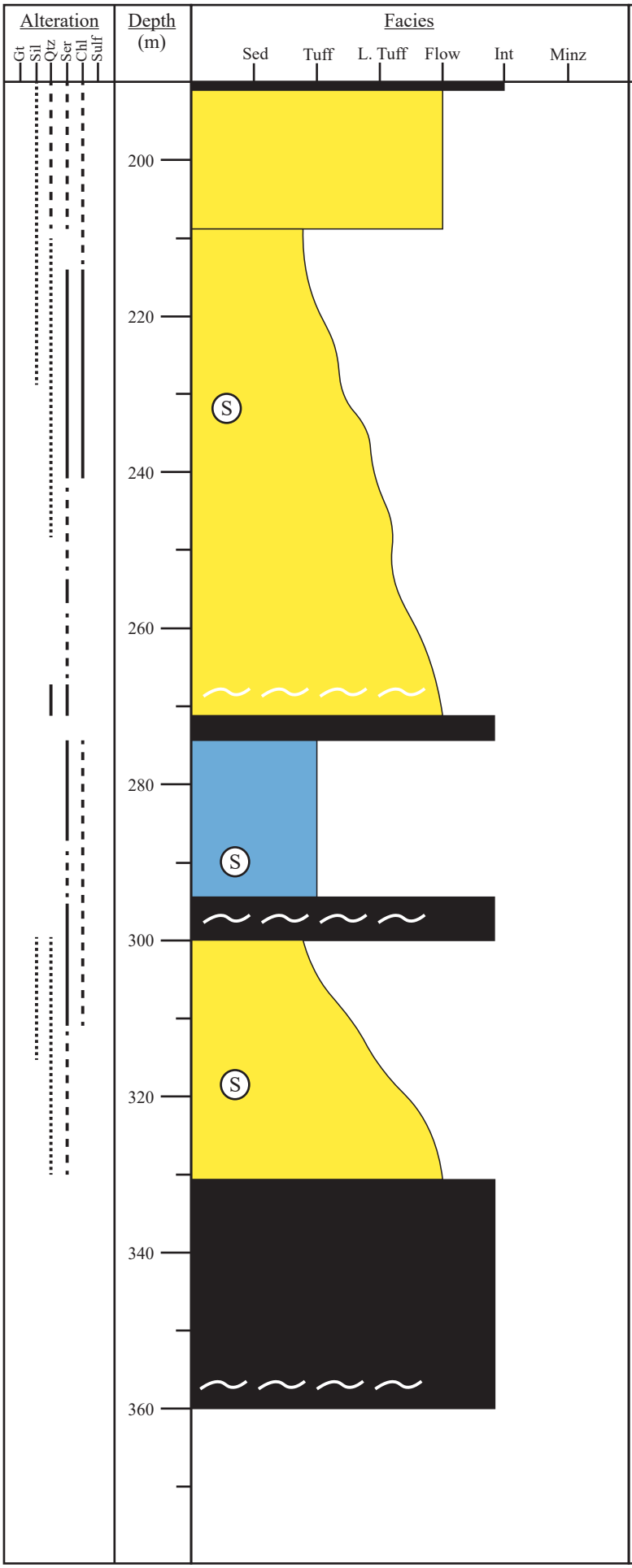

Project: Powderhorn Lake
Drill Hole: PH-
Date:

UTM:
Azimuth, Dip:
Length:

190.19m aph black mafic dike, non-mag

191.33m light-med gray, red mottled, highly siliceous variably alt bt-chl-spotted massive rhy, same unit as 150-166m

209.56m dark, fine-grained alt tuff unit, no bedding, can see faint qtz-eyes, grades into light gray, grainy siliceous alt rhy
215m alteration very intense - struggling to identify units! - primarily seems to be heavily qtz+chl+ser alt massive rhy with possible <.5m tuffaceous beds (?) bt-chl-spotted in part with white whispy sil, zoned tz veins appear in grainier textured rock
Sample 62750
234m dark, qtz-phryic, highly alt mass rhy or tuff, stockwork-like ser alt, some localized tannish-white/clay-like patches of alt, weak-mod foliation - qtz phenocrysts fade by 249m along with major alt veining - mostly homogenous medium gray/green rock

254m 1m of strongly sericitic and siliceous unit grading back to medium gray, fine-grained tuff-alt. rhy, has opq white (<1mm) qtz phenocrysts - 269m-270.5m crumbly highly clay/ser alt possible fault zone

271.17m highly ser+qtz cherty alt zone

274.09m white/cream, strongly ser tuff (mafic tuff?/basalt?), alt wipes all texture, mod foliated - grades into fine-grained to aph very alt tuff with green (olive drab) stockwork ser veins ~287m begins to resemble thin red/brown bedded sed/tuff with sparse qtz-eyes, lots of bt, grainy appearance overall
Sample 62751

294.32m aph green dike until 296.43m then into brecciated/faulted, crumbly and clayey fault zone

300m dark, aph strongly alt tuff (mafic tuff?/basalt?) with patchy green ser and large alt gts, whispy white sil veins in part, qtz veining throught ~322m lighter in color, can see partial bt-spots - grading into massive rhy, pink mottling, local patches are so altered that it looks brecciated ~321m framboidal (?) qtz-crystals
Sample 62752

330.68m greenish black aph mafic dike, non-mag ~357-360 crumbly fault zone

360m EOH

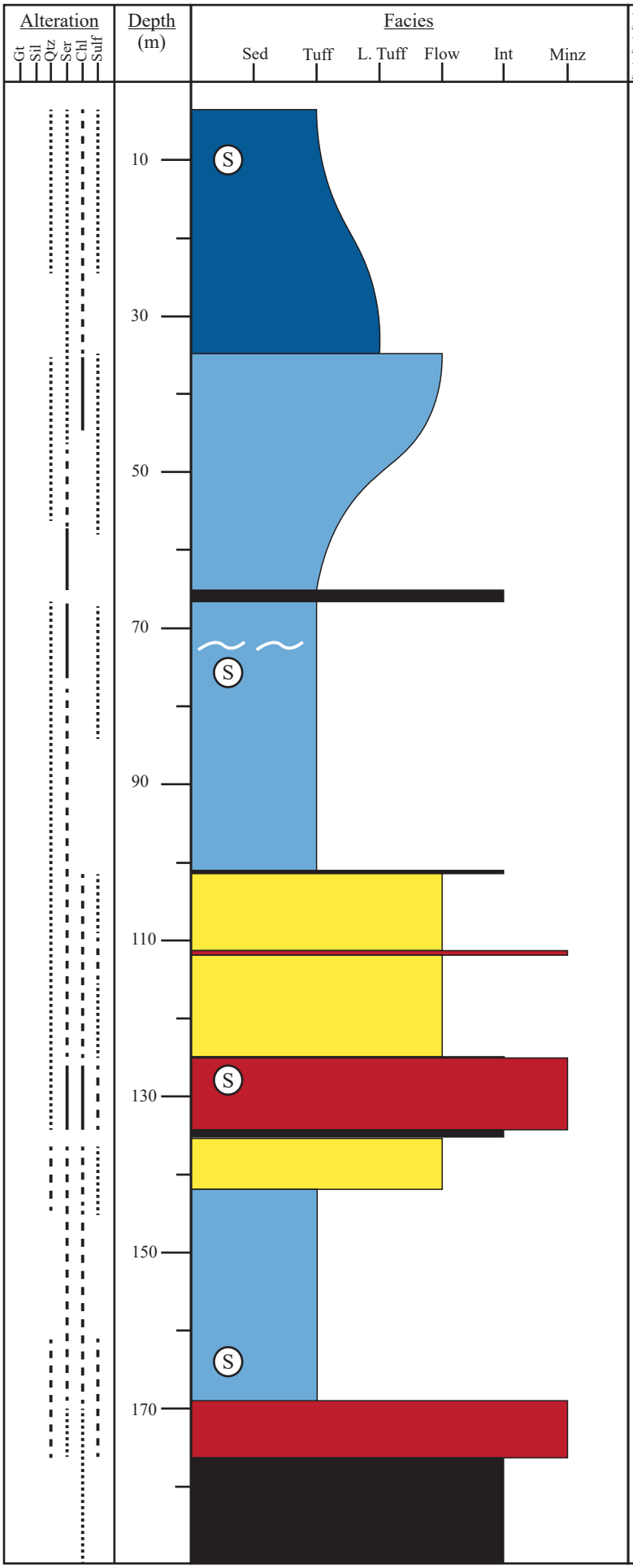

Project: Powderhorn Lake
Drill Hole: PH-18-06
Date: July 29, 2020

UTM: 564872E 5440711N (NAD83)
Azimuth, Dip: 360, -90
Length: 340m

3.8m light-medium gray, fine-medium grained, bt-spotted tuff, weakly-moderately foliated, moderately altered by chlorite and weakly by apple green sericite, presence of bluish qtz eyes (1-2mm), trace py and po (<5%) - towards end of unit, distinct reddish brown layering
13m red and green mottling, variably altered by ser+chl, minor crenulations, qtz eyes and altered garnets, trace po and orangey-brown sp (<5%)
Sample 62656
27.3m dark gray tuffaceous sediments, almost aphanitic but slightly grainy with dark elongate clasts (lapilli?), bt-spots, weakly foliated

Mixed section - hard to break out units

35.08m sharp contact to heavily altered camo-patterned rhyolite with pink and green mottled blotches of albite (?) and sericite, minor qtz eyes, trace py and po (<5%) - down unit, light, qtz-altered bt-spotted massive rhyolite, weakly sericite altered and foliated, loss of qtz eyes, trace orangey-red sp (<5%) - down unit gradational into more tuffaceous unit with reddish cast, weak-moderate sericite alteration, moderately foliated, bt-spots are still seen (not prominent), trace dissem py (<5%)

~59m heavy sericite alteration and broken core - large quartz veins (fault?)

65.72m medium gray, plag porphyritic dike

66.5m greenish gray, heavily sericite altered tuff - extremely crumbly until ~71m (fault) - grades into darker gray with reddish bands, minor milky qtz eys, bt still present, trace py (<5%)
Sample 62657
~79m moderately foliated, less red possible bt-spotted rhyolite/tuff, green sericite cast, bluish quatz eyes, trace disseminated vein to crenulation-hosted py and po (<5%) - end of unit is very dark and fine grained, large qtz veins, extremely grainy when dry

101m black aphanitic mafic dike
101.39m split core - medium gray, fine-medium grained massive bt-spotted rhyolite, moderate ser+chl alteration, moderately foliated with trace disseminated py and po throughout (5%) - ~107m qtz eyes appear
111m localized semi-massive mineralized rhyolite with red sp (~7-10%), py and po (<10%)
112m becomes pink and green camo-patterned/mottled, moderate chl+ser alteration, heavily crenulated, presence of qtz eyes
125.03m black aphanitic mafic dike

125.53m light gray, fine-grained, heavily chl+ser altered tuff, moderately silicified, bt along crenulation and foliations, presence of bluish qtz eyes, trace disseminated vein-hosted sp (5-8% to locally 15%), py (5-8%)
Sample 62658
134.26m black aph mafic dike with trace disseminated py (<5%)
135.38m light gray, fine-medium grained massive rhyolite, local flow bands - loss of camo texture from previous unit, weak-moderately altered by chl+ser+qtz, trace dissem py (<10%) and red-brown sp (<5%) obscured contact to -

142.48m medium gray, cd-spotted thinly bedded meta-tuff/seds, quite grainy in appearance, moderately altered by ser +/- ksp or albite, grades into altered rhyolite? with blue qtz eyes, darker moderate chl alteration

Sample 62659
~169m core becomes lighter in color, less chl alteration?, increase of qtz eyes - overall less altered than above, core is halved, reddish brown sp appears disseminated in foliations and veins (10%)

176.27m chloritized mafic/andesitic dike with white irregular plag phenocrysts

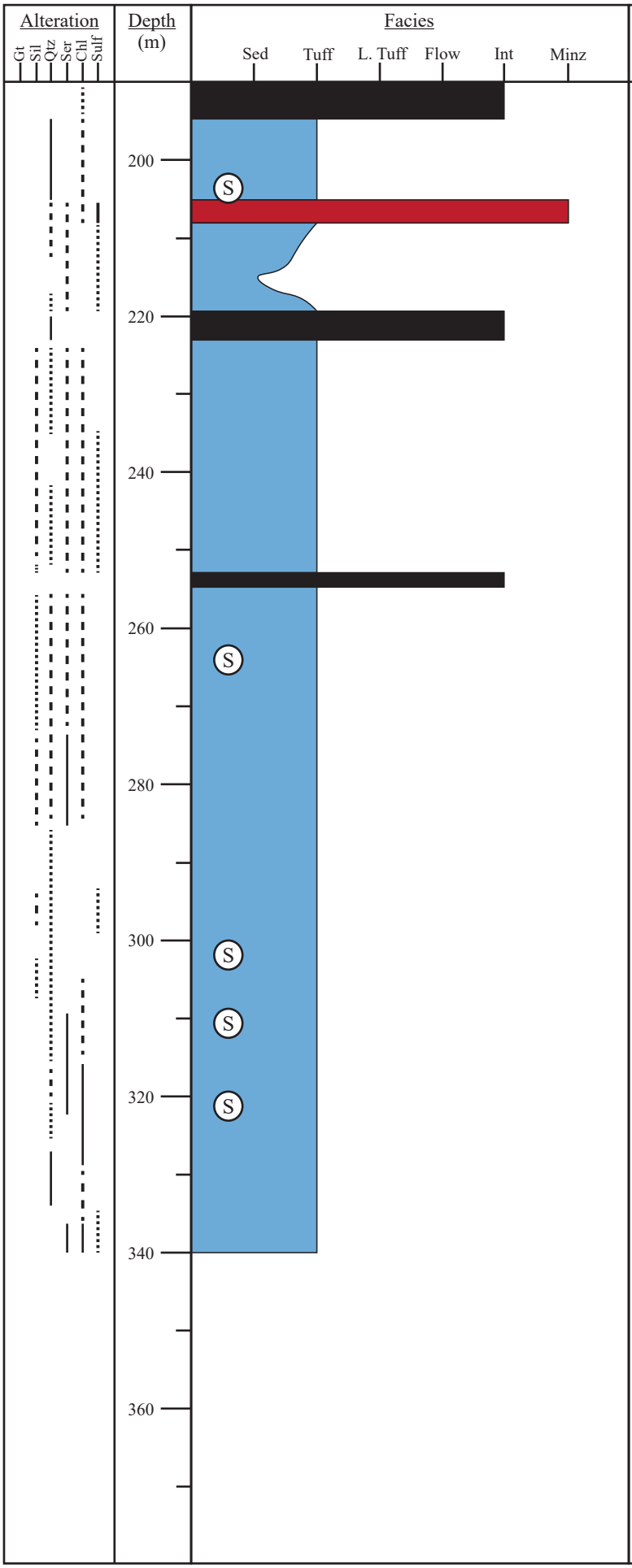

Project: Powderhorn Lake
Drill Hole: PH-18-06
Date:

UTM:
Azimuth, Dip:
Length:

~192.30m large xenolith of below unit, possibly cross-cutting and re-entering, sharp contact to heavily altered tuff
194.6m beginning of unit is extremely qtz-rich/siliceous, light gray altered bt-spotted tuff with bt and black chl following moderate foliation, clearish-pink albite, small presence of qtz eyes
Sample 62661
205.26m semi-massive qtz-eye tuff with orange, red/brown sp (10-20%, up to 80% locally), py (10-15%), cpy (<5%)
208m medium gray, reddish brown altered tuff, moderately foliated with bluish qtz eyes, trace py and cpy (<5%)
213.34m splotchy, mottled thin bedded tuff or seds, loss of qtz eyes
216.38m qtz eyes reapear, large qtz "bed", trace py (<5%)
219.26m qtz bed or heavily siliceous dike, opaque, small patches of bt

223.69m whispy white sillimanite altered tuff to sediment, no bedding, highly altered and cd-spotted in part, moderate ser+chl alteration, minor bluish qtz eyes, lots of massive qtz veining - ~235m trace py (<5%), greenish cast increases, large greeny phenocrysts (andalusite?)
~243m halved core, minz increased until ~251m presence of disseminated sp (all colors; honey, red/brown, cream), minz follow crenulations, less-no silimanite, milky qtz eyes/crystals (2-4mm)

253.5m black aph mafic dike

254.1m mottled pink/green light gray, highly siliceous felsic volcaniclastic seds or tuff moderately altered by chl+ser+qtz with long, wavy crenulations, faint presence of sillimanite, large qtz clasts and veins - ~261m foliation increases, reddish-pink banding along foliation is more prominent - increase in sillimanite until 271m
Sample 62663
~273m strong increase in ser alteration, very clay-like and tannish green, spotted overprint (white/clear) - increase in ser until ~285m and foliation decreases after 285m, very barren in sulfides - ~289m more qtz veining, crenulations still present, very sparse qtz eyes

~294m sillimanite (white, whispy) returns, but disappears after 1.5m ~301m sillimanite returns and foliation seems to increase, minor sp (10%) - dark brown along foliation/crenulation, milky qtz eyes
Sample 62664
~305m reddish brown layers are very crenulated , black chl clasts?

Sample 62665
~316m strong ser+qtz alterations, large reddish fine-grained patches

~320m very chl altered, green spotted volcanic (?) with pink albit alteration, sparse blue qtz eyes, barren sulfides
Sample 62666
~326m vuggy qtz and hgihly crenulated beds, strong qtz alteration until

~333m - returns to spotted green trace dissem py (<5%), skarn-like white vein with large chunky white/opaque plag or calcite crystals

~336m-EOH primarily dark-reddish brown and green strongly foliated seds or tuff, bt is seen crystallizing in qtz beds, strongly ser+chl altered

340m EOH

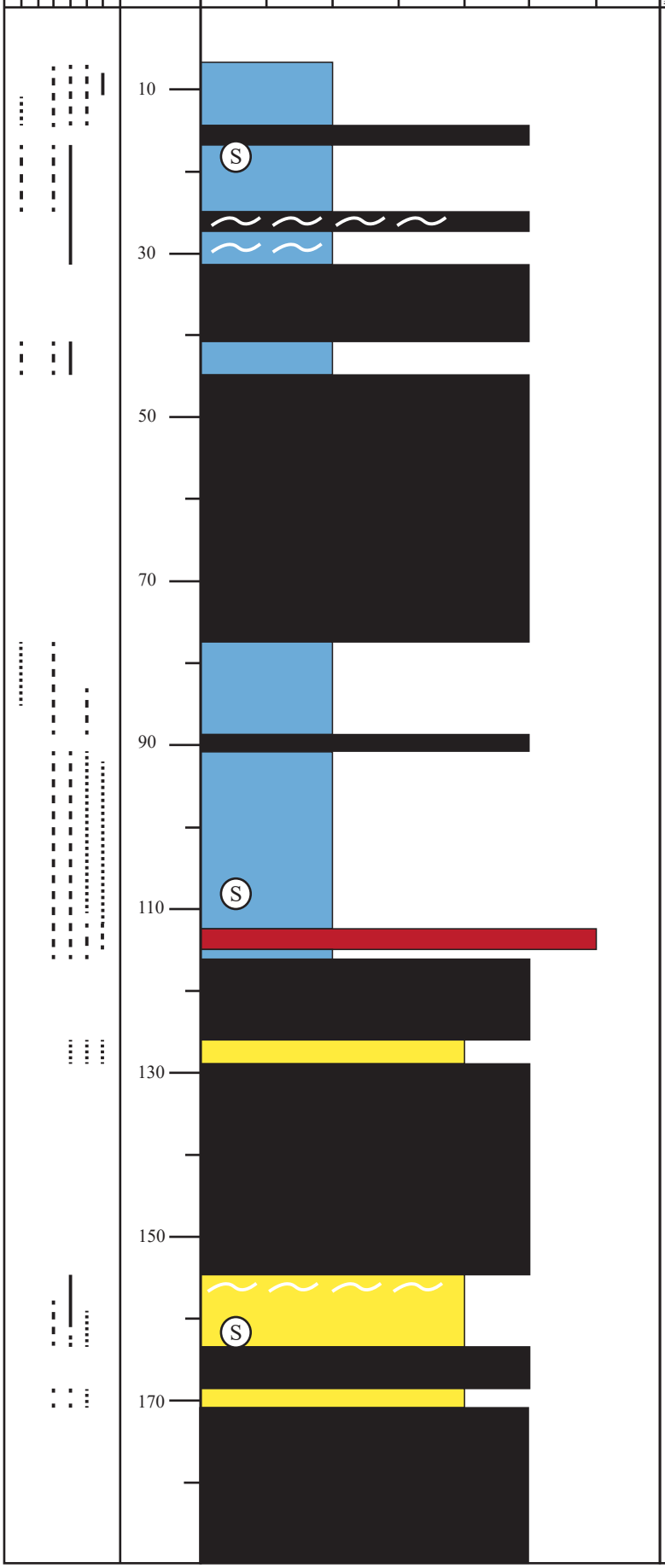

Project: Powderhorn Lake
Drill Hole: PH-18-08
Date: September 30, 2019

UTM: 565089E 5440771N (NAD83)
Azimuth, Dip: 360, -90
Length: 275.90m

6.45m light gray, red/green mottled and rusty tuff moderately altered by chl+ser with minor qtz eyes ~9.48-9.53m net textured semi-massive sp-py (40-50%) +/-cpy (<2%) grades into siliceous light gray qtz-crystal tuff with zoned veins, strongly ser altered at 11m
14.05m black aph mafic dike, non-mag
16.21m light gray-pale green tuff, highly ser altered with lots of network gt-qtz-veins (big gts 4-8mm)
Sample 62760
25.86m faulted aph mafic dike
27.66m same as above, presence of clayey fault gouge, crumbly

31.21m dark aph mafic dike, non-mag

40.66m same as above with rusty fractures

44.75m dark aph dike, non-mag ~59m lighter in color w/small lathy plag crystals but minor

77.49m light-dark gray, highly altered qtz-crystal tuff with dark and olive green patchy aphanitic gt-ep-qtz zoned veins into lighter qtz phyric bt-spotted, weak-moderately foliated with dark green chl clasts (lapilli?)

88.62m dark aph dike with thin/spidery lathy plag crystals
90.9m light gray siliceous qtz-crystal tuff with white (opq) qtz crystals, moderately altered by ser with disseminated blebs-whispy bands of po (<5%)
92.5m possibly dark, fine-grained heavily altered tuff or metasediments ? with dark gray to dark olive green bads with zone gt-ep-ser-qtz-veins - grades into and out of tuff above and below
95m same as above ~107m becomes highly siliceous, increase in foliations that host bt and minor po (<5%) ~112.70-114.31 minor sp stringers in qtz phyric tuff, these qtz phenocrysts look broken/conchoidal glass (spheuro-litic?), sp-py (locally up to 20-25%, 5% py) ~114.89-115.82m another minor sp stringer zone (<10%), more chl altered
Sample 62762
116.07m black aph mafic dike, non-mag
126m light gray and red mottled, dark banded and deformed FBR with spotty clasty bt - the bands are quite irregular, minor ser+chl alteration, trace blebs and veinlets of sp (<2-5%), crenulations in part

128.42m dark gray aph dike, mafic

152.4m 152.40-154.87 faulted zone- rusted, crumbly, fault gouge, strongly ser altered and oxidized, rest of unit is mixed sections of mafic aph dikes (<.5m) and irregular banded FBR (whispy, dark) with bt-spots, moderate ser and minor chl alteration, qtz phyric with whispy ghost-white qtz phenocrysts
Sample 62761
163.75m black aph dike

168.73m rhyolite same as above

170.8m dark gray, spidery small plag porphyritic, slightly mag

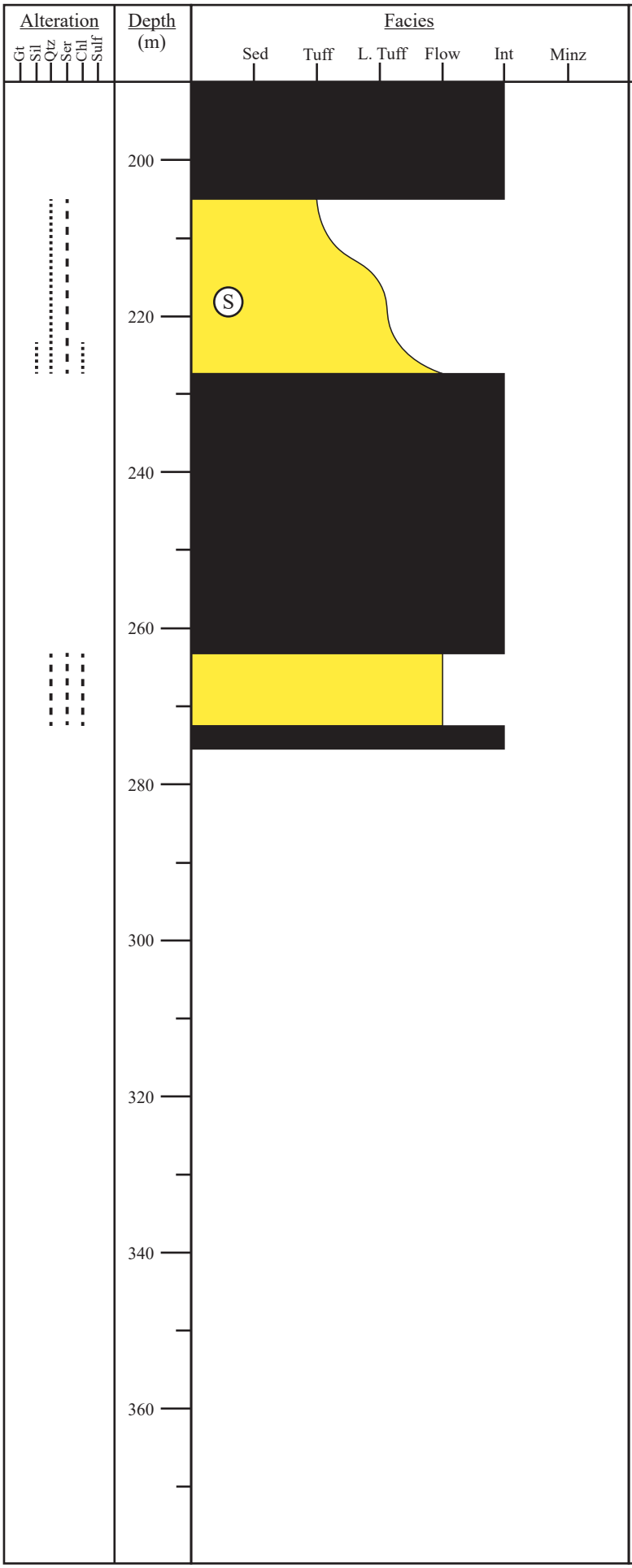

Project: Powderhorn Lake
Drill Hole: PH-18-08
Date:

UTM:
Azimuth, Dip:
Length:

207.16m mixed tuffs and flows - light gray siliceous bt-spotted tuff, grades into darker fine-grained (possible intense chl alteration), qtz phyric rhy, weak-moderate ser alteration, minor/not prominent qtz eyes
~216m along with red mottling, slight oxidation
Sample 62763
~220.62m small 15cm possible red/brown tuff interbed with disseminated po (<3%) - end of unit has more bt and chl with whispy white sillimanite (<8%)

277.58m black aph mafic dike, slightly mag

263.22m light gray, highly siliceous qtz phyric bt-ser-spotted rhy with red mottling, minor-moderate ser and chl alteration (clasty), minor qtz eyes

271.25m black aph dike, slightly mag

275.90m EOH

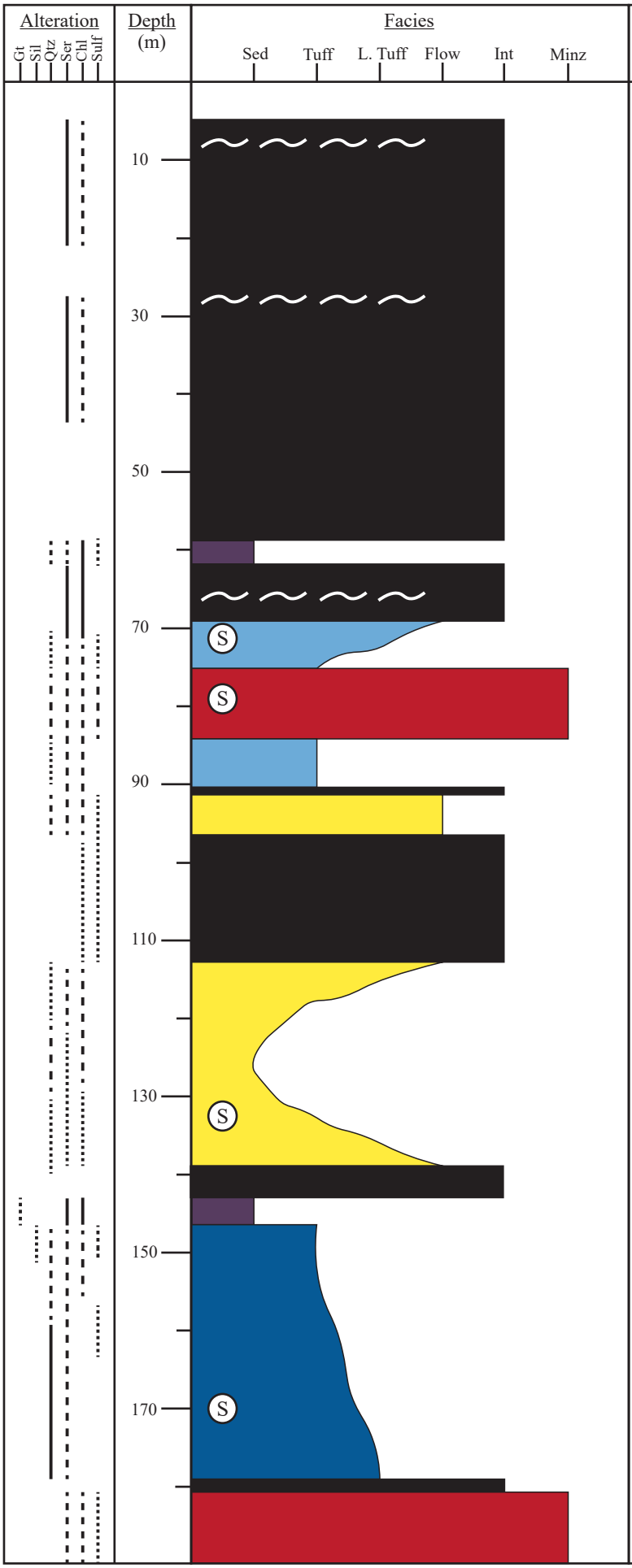

Project: Powderhorn Lake
Drill Hole: PH-18-10
Date: August 1, 2020

UTM: 564798E 5440644N (NAD83)
Azimuth, Dip: 360, -90
Length: 294.71m

4.5m light gray, bleached (tan when wet) porphyritic dike with anhedral-subhedral palg (white/opaque, <2mm) and bt (brown, <2mm) phenocrysts, end of unit orangey oxidized crumbled pieces and fault gouge - non-mag

~22.59m post-fault non-bleached mafic black aphanitic dike, magnetic
~27.36m orangey/pink porphyritic dike with anhedral pinky white <2mm plag phenocrysts, bleach/oxidizing from fault including crumbly, gouge sections, reddish color is non-mag but grades into dark gray mag. plag phenocryst dike (original/non-altered)

58.72m dark gray, thin dark bedded, highly altered volcaniclastic seds, moderately altered by ser, strongly by chl, with matrix and vein-fill py, po, and sp (<10%), clear/milky colored qtz phenocrysts/clasts (4mm)
61.9m light sandy tan, bleached dike with plag phenocrysts - heavily altered muddy fault gouge
69.25m medium gray, fine-coarse grained, weakly foliated, strongly altered by chl+ser ~71m greenish cast and trace disseminated cpy and po (<5%), increases down unit and is vein-filling ~72.5m qtz-eyes are dark/milky not prominent
Sample 62679, 62680
75m disseminated sp and py (10%) in qtz-phyric qtz-crystal tuff and increasing down unit with prominent blue qtz eyes
84.1m same as above
90.43m black aph mafic dike
91.34m light gray, mottle pink-orangey/green altered rhyolite, moderately to strongly altered by chl+ser, prominent qtz eyes, trace matrix-fill cpy (<5%) and orange/red vein-filling sp (<5%)

96.59m brownish green, QFP, trace py (<5%) on fractures, non-mag

113.32m light gray, green mottled rhyolite moderately altered by ser+chl, weakly foliated, sparse qtz eyes, trace brown vein-hosted brown/red sp (<5%), somewhat grainy as it grades into next unit
121m dark gray, thinly bedded sedimdents moderately altered by chl+qtz, weakly by ser, weakly foliated, trace disseminated matrix-fill py+sp (<5-10%), unit grades to next

129m lighter gray bt-spotted rhyolite, bt somewhat patchy and forming along fractures, sparse milky qtz eyes, trace dissem py+sp (<5%)
Sample 62681
139m black aph mafic dike, non-mag

143.17m dark gray, thin bedded bt-gt volcaniclsatic seds, strong chl+ser alteration, zoned veins, barren in sulfides
146.13m medium-dark gray, varibaly altered tuff - moderate chl+ser+qtz alteration, weakly foliated, trace disseminated vein-foliation hosted py+po (<10-15%), dark localized lapilli or chlorite clasts
~149m localized sillimanite and increase of sp (<15%) until 150.5m, localized leucogranite dikes, crenulations and mineralization decreases, and appearance of white whispy lapilli
~155.5m increase in qtz veining until 158m, moderate apple-dark green ser, trace matrix-fill sp (<5%) - more concentrated in folds, strong qtz alteration until end of unit
Sample 62683
179m black aph mafic dike
180.41m light gray, grainy fine-grained rhyolite with dark bt +/- chl, moderately altered by chl+ser, no qtz eyes, disseminated brown/red matrix-fill sp (<5-10%)

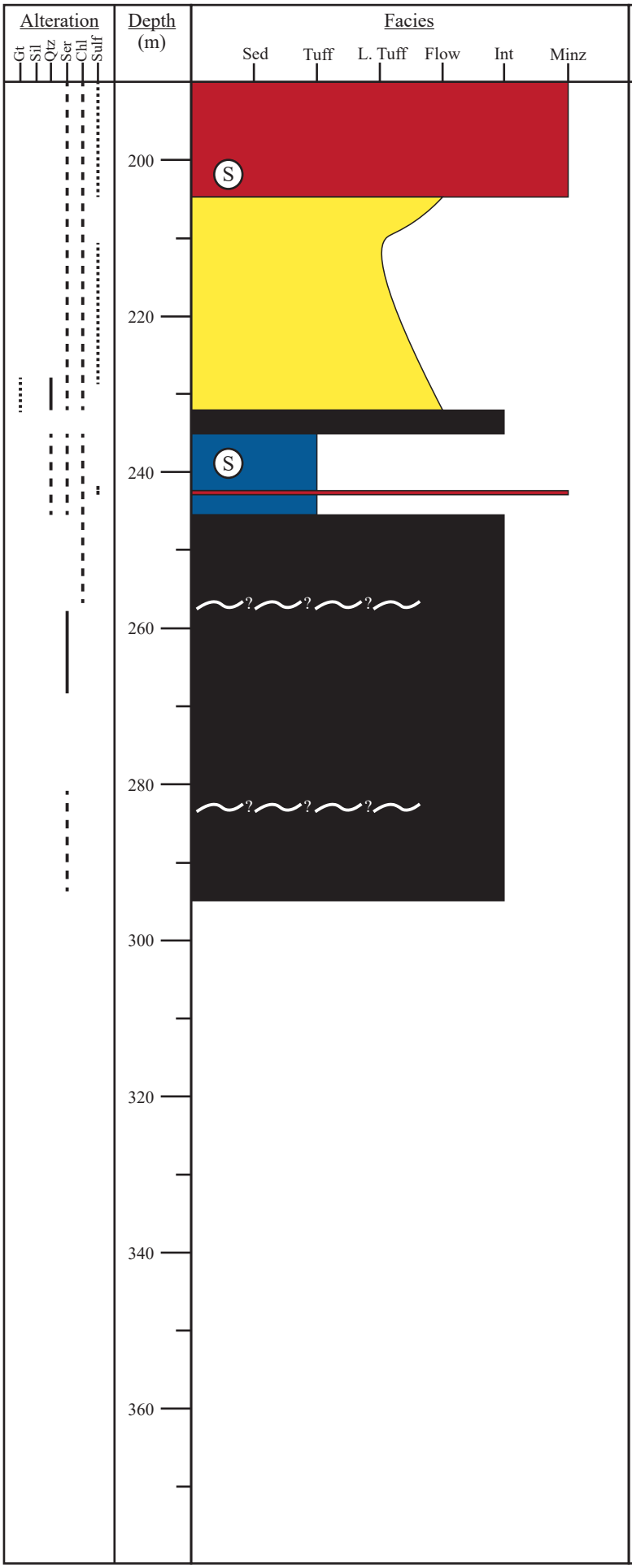

Project: Powderhorn Lake
Drill Hole: PH-18-10
Date:

UTM:
Azimuth, Dip:
Length:

Sample 62682

205m mixed flows and tuffs - rocks are moderately altered by chl with chl-greenish cast, fine-grained/aphyric
209m grades into reddish grainy bt-sediment/tuff moderately altered by chl+ser, dark oblong lapilli
216m grainy, aphyric fine-grained bt-rhyolite (possibly tuff) with trace disseminated vein-foliation hosted sp+py (<5-8%) ~229m crenulations, folding bt-spotted rhyolite with strong qtz alteration, possible very altered gts

232m leucogranite dike into black aph mafic dike, mag
Sample 62684
235.16m medium gray, green mottled bt-banded rhyolite, moderate chl+ser alteration, quite siliceous with dark chl or lapilli clasts
242.15m localized disseminated matrix-fill to banded sp+py (<5-10%)
242.45m medium gray, green mottled bt-tuff/lapilli tuff, moderate chl+ser alteration, quite siliceous with dark chl or lapilli clasts

245.54m black, plag and bt porphyritic chloritized dike, slightly magnetic ~256.5m reddish oxidized color ~258m bleached heavily sericitic until 268m into black aphanitic mafic mag dike until 270.96m ~270.96-272.26m weakly foliated, aphyric green/pinkish mottled altered rhyolite ~272.26m plag-bt porphyritic dike ~278.87 black aph mafic dike, mag ~281.73m plag-bt porphyritic, bleached dike, moderately sericitic ~292.5-EOH grainy altered barren sediments

294.71m EOH

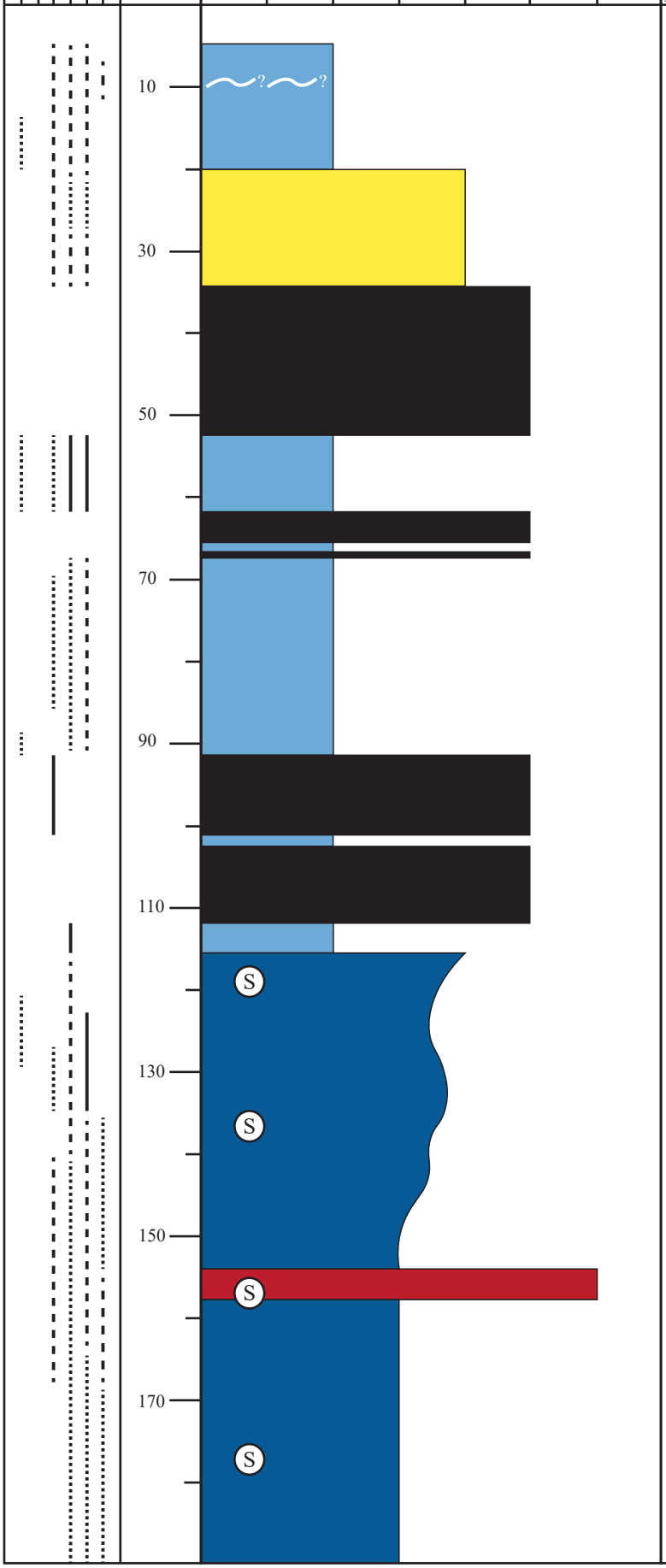

Project: Powderhorn Lake
Drill Hole: PH-18-11
Date: September 24, 2020

UTM: 565157E 5440695N (NAD83)
Azimuth, Dip: 360, -90
Length: 209m

4.57m beginning of unit dark gray qtz-phyric ser+chl altered tuff to rhyolite, very rusty - possible fault 8.90m-11m, disseminated to banded sp at ~9m with local semi-massive net textured py and po 9.05-9.20m + 9.50-9.69m (65-80%) ~15m unit becomes barren - light gray, highly siliceous tuff to rhyolite flow with zoned ep-ser-gt-qtz veins with fine bt flecks, becomes more ser+chl altered towards dike

34.11m medium gray plag porphyritic non-mag dike

52.42m pale light green, mottled reddish brown highly altered aphyric tuff, presence of zoned veins
61.95m medium gray plag porphyritic non-mag dike
65.85m light-medium gray, finely banded tuff (same as below)
66.35m medium gray plag porphyritic non-mag dike

67.22m light-medium gray, finely banded aphyric tuff moderately altered by chl and weak ser (apple green) with red/brown rusty fractures, presence of zoned veins - small sections of highly altered dark units, extremely fine-grained and thin bedded po sediments, contacts are gradational ~90.5m spotted altered gts

91.68m heavily silicified portion of above unit

101.2m same unit as above
102.44m rhyolite dike
107m aphanitic mafic dike

112m light gray tuff, highly altered by ser with small leucogranite dikes cutting through
Sample 62627
115.77m light gray, red mottled, banded and crenulated FBR moderately altered by ser ~123m grading into tuff, dark gray - black highly altered by dark chl, presence of altered gt and zoned veins, alteration weakens by 129m

129m light gray aphyric lapilli tuff with local felsic lapilli, sparse qtz eyes, small localized patches of py and po, moderate ser alteration with pale green color - half core beginning
~136m beginning to see sp +/- cpy stringers that increase down unit
Sample 62728

~146m darker in color, leading into massive highly altered po-py +/- cpy stringers, crenulations visible

~154m begins main po-sp net-textured to banded stringers until 159m
Sample 62729

~167m increase in bt and disseminated bands and veins of sp-py +/- cpy, mineralization fades to end of unit

Sample 62730

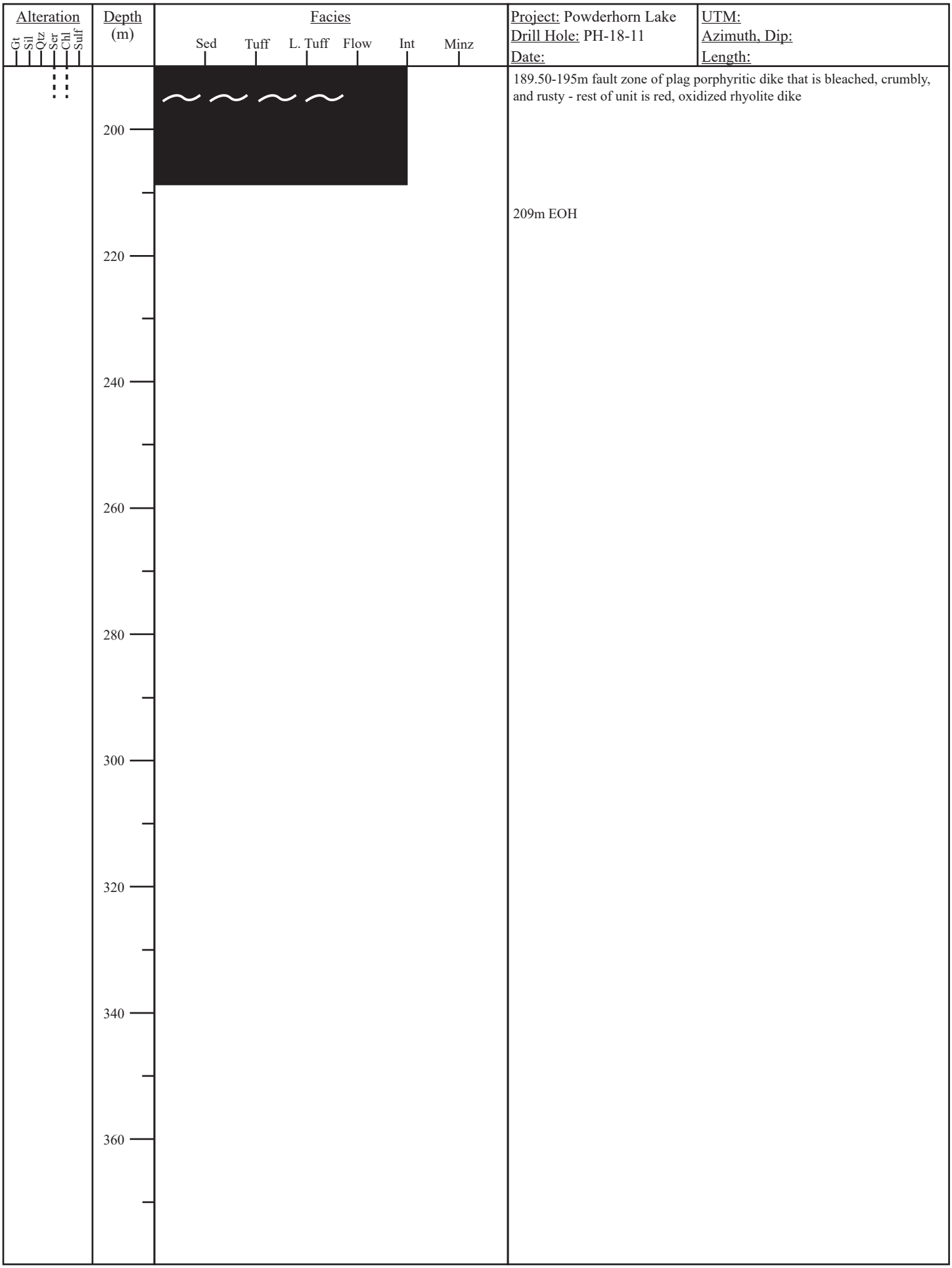
Alteration
Gt
Sil
Qtz
Ser
Chl
Sulf
Depth
(m)
Facies
Sed
Tuff
L. Tuff
Flow
Int
Minz
Project: Powderhorn Lake
Drill Hole: PH-18-11
Date:
UTM:
Azimuth, Dip:
Length:
189.50-195m fault zone of plag porphyritic dike that is bleached, crumbly, and rusty - rest of unit is red, oxidized rhyolite dike
209m EOH
200
220
240
260
280
300
320
340
360

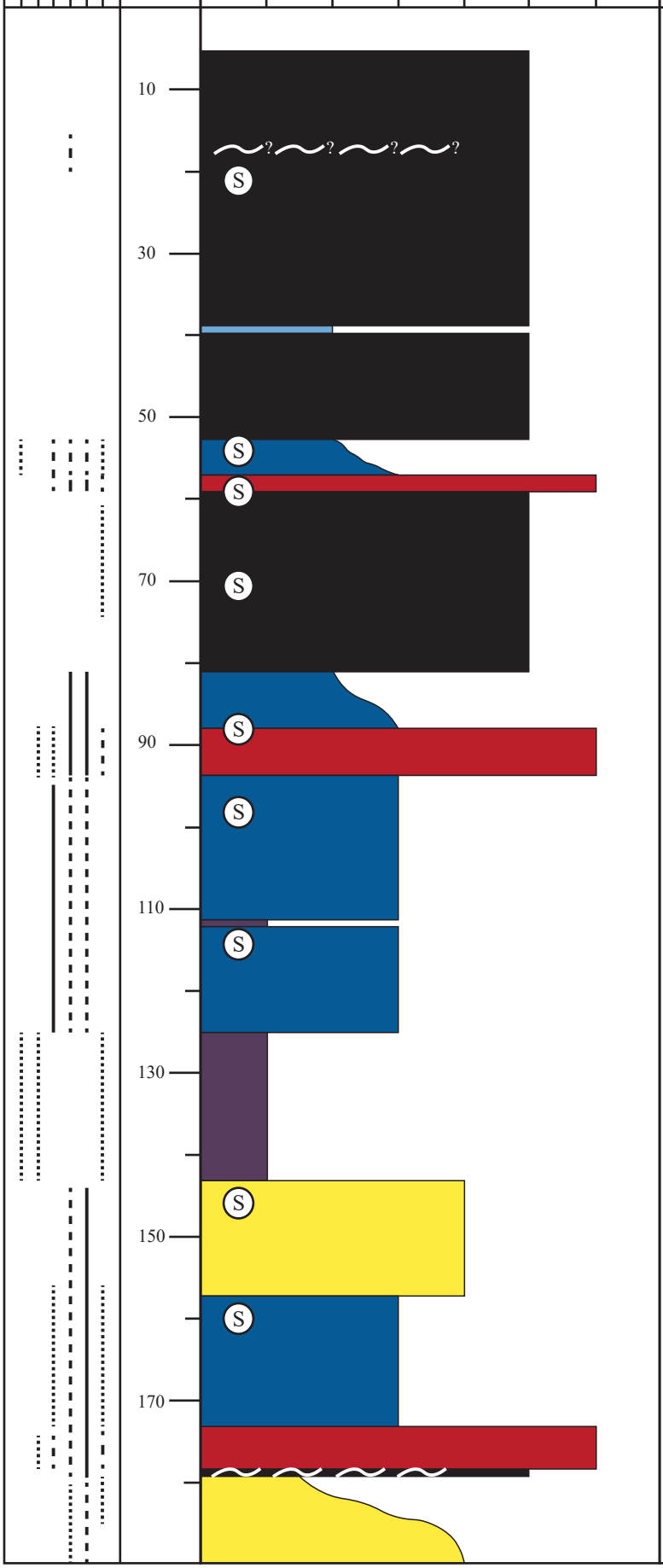

Project: Powderhorn Lake
Drill Hole: PH-18-13
Date:

UTM: 565082E 5440628N (NAD83)
Azimuth, Dip: 360, -90
Length: 382m

5.79m gray-green mafic dike with porphyritic bt (<2mm), non-magnetic - 18-20m crumbly and rusty (possible fault)
Sample 62702

38.75m white, aphyric fine-grained tuff with brown-green bt following foliation
39.7m beginning of unit- dark gray, euhedral plag porphyritic dike that grades into aphyric lathy plag, slightly magnetic
52.55m light-medium gray, fine-grained tuff with altered gt porphyroblasts,- moderate to strong chl and weak ser alteration, weakly-moderately foliated, euhedral py in fractures, trace disseminated veins of sp (<2%) grading into lapilli tuff with "fibrous" textured chl+ser alteration
Sample 62703, 62704
57.35m mineralized lapilli tuff moderate-strongly altered by ser+chl alteration with orange sp stringers (<10%) grading into much darker qtz-phyric tuff with net-textured whispy-banded replacement po-sp (5-10%), py-cpy (2-8%)
59.25m dark gray slightly mag mafic dike with large anhedral-subhedral plag phenocrysts with lesser lathy plag - small section 61.26-61.32m tuff with disseminated-foliation hosted po-py (<10%) and 74.40-74.90 banded felsic volcanic
Sample 62705
80.68m light gray, ashy, fine-grained tuff moderate-strongly chl+ser altered, minor milky qtz eyes, no real textures, disseminated po-py (<2%), grading into more foliated-banded tuff with local oblong lapilli
Sample 62706
88m lapilli tuff, appearance of qtz eyes along with whisy bands to veins of sp (5-8%) with small fleck of VG ~90m grading into strong chl alteration with increase in sulfide veinlest po-py (2-5%), cpy (<2%) ~91m local bands sp-po-py+/-cpy (<5%) and whispy sillimanite
Sample 62707
94m light gray, ashy, fine-grained tuff moderately altered by chl+ser, strongly by qtz, becomes bt-rich with local green opaque lapilli
Sample 62708
111.38m light pale green/gray highly ser altered tuffaceous sediments

112m light gray, ashy, fine-grained tuff moderately altered by chl+ser, strongly by qtz, becomes bt-rich with local green opaque lapilli

125.05m dark, fine-grained gt-bt-qtz metasediments with small pink gt porphyroblasts, thinly laminated ~143m reddish beds, easily see red sediment/qtz beds folding, crenulating, grainy bt-prominent patches, trace disseminated po-py (<5%)

143.13m light gray massive rhy moderately altered by chl+ser, presence of deformed fold closures and felsic domes
Sample 62709
156.95m light greenish gray, ashy, bt-spotted lapilli tuff, felsic lapilli, moderate-strongly altered by chl, minor qtz-eyes, dissem vein-hosted or foliation hosted network textured brown and orange sp (5-7%) replacing bt
Sample 62710

~169-172.5m patchy bt with associated sp (<5%)
173m py-po-sp+/-cpy in blebs (dark chl vein associated, <3%)
~174.5m whispy sillimanite and qtz phyric, disseminated py (<2%)

178.3m faulted aph mafic dike
179.15m light gray/green, red mottled qtz phyric tuff-rhyolite moderately altered by chl and weakly by ser, highly siliceous and moderately foliated, few bt-spots along fractures +/-foliation = more bt w/sp replacement - mostly barren except for few localized patches at beginning of unit

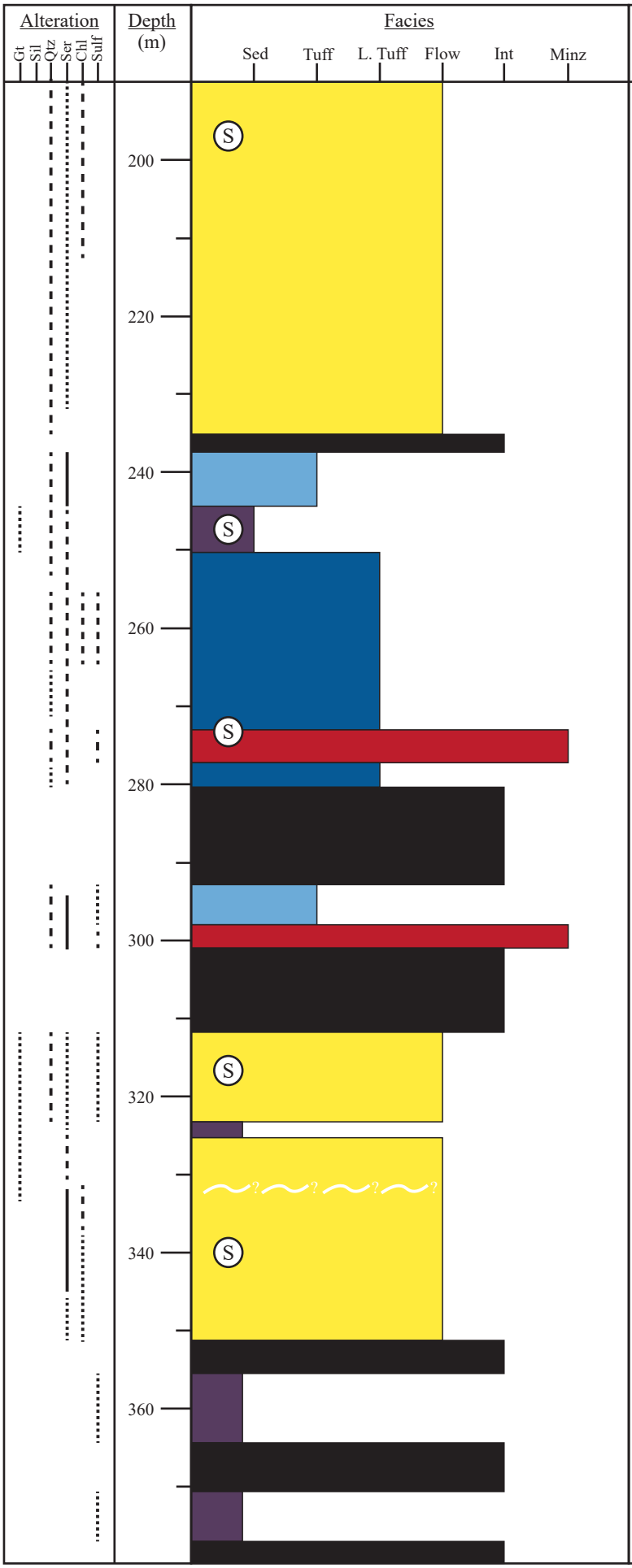

Project: Powderhorn Lake
Drill Hole: PH-18-13
Date:

UTM:
Azimuth, Dip:
Length:

Sample 62711

~229m reddish qtz-phyric, possible unaltered/less-altered version of above unit, presence of small-scale faulting

234.96m aph mafic dike
237.47m pale green/gray with red/brown mottling, qtz phyric rhyolite tuff strongly ser altered, moderately foliated with oblong qtz eyes near end of unit, disseminated py (<5%)

244.19m dark , fine-grained sediments with small pink gt porphyroblasts, zoned gt-ep-ser veins, magnetic
Sample 62712
250.17m light gray, fine-grained qtz-phyric tuff highly siliceous, moderate ser alteration, blebs of brown sp in foliation w/bt (<5%) ~253-254m localized patch of frothy textured epidote ? ~259.20m nice whispy bands of sp (8%) with local increase in black chl, qtz eyes become blue, sillimanite appears, felsic lapilli (264m), crenulations present

273m increase in sp (5-8%) along w/bt-patches and veins with disseminated trace blebs of cpy (<2%)
Sample 62713
277m same unit as above

280.15m aph mafic dike, non-mag

292.67m light gray, aphyric-fine-grained, minor bt-spotted, silicified tuff or altered massive rhyolite, veiny-foliation po-py (<5%)
298-301.9m half core, fine-grained/grainy, highly ser altered with sp-py+/-cpy in bands and veins (<5-8%)
301.9m aph mafic dike

311.91m light gray - mottled red/purple variably altered qtz phyric, bt-spotted massive rhyolite moderate ser alteration, presence of qtz-ep-gt zoned veins, and local bands of disseminated network textured orange/red sp-po (<5%)
Sample 62714
323.5m dark gray, bt-rich sediments
325m increase in ser alteration, presence of crenulations, local trace disseminated veinlets to net textured bands of py-sp (<5%) with recystalliz-ing py
~331m crumbly core - possible fault ~335m darker, more chloritic, very fine-grained zoned ep-gt-qtz veins
Sample 62715
~343-346m bleached and strongly sericitic, possible fault/fracture

~348.88-351.25m red/green mottled altered bt-spotted massive rhyolite
351.25m mixed section of aph mafic dike, mag and plag-bt porphyritic dike

355.84m barren thinly laminated-thin bedded, crenulated metasediments, bt-rich, disseminated po throughout (<10%)

364.15m porphyritic plag mafic-intermediate dike, non-mag
370.27m same as above, grainy, po-rich
376.9 aph mafic dike, mag

382m EOH

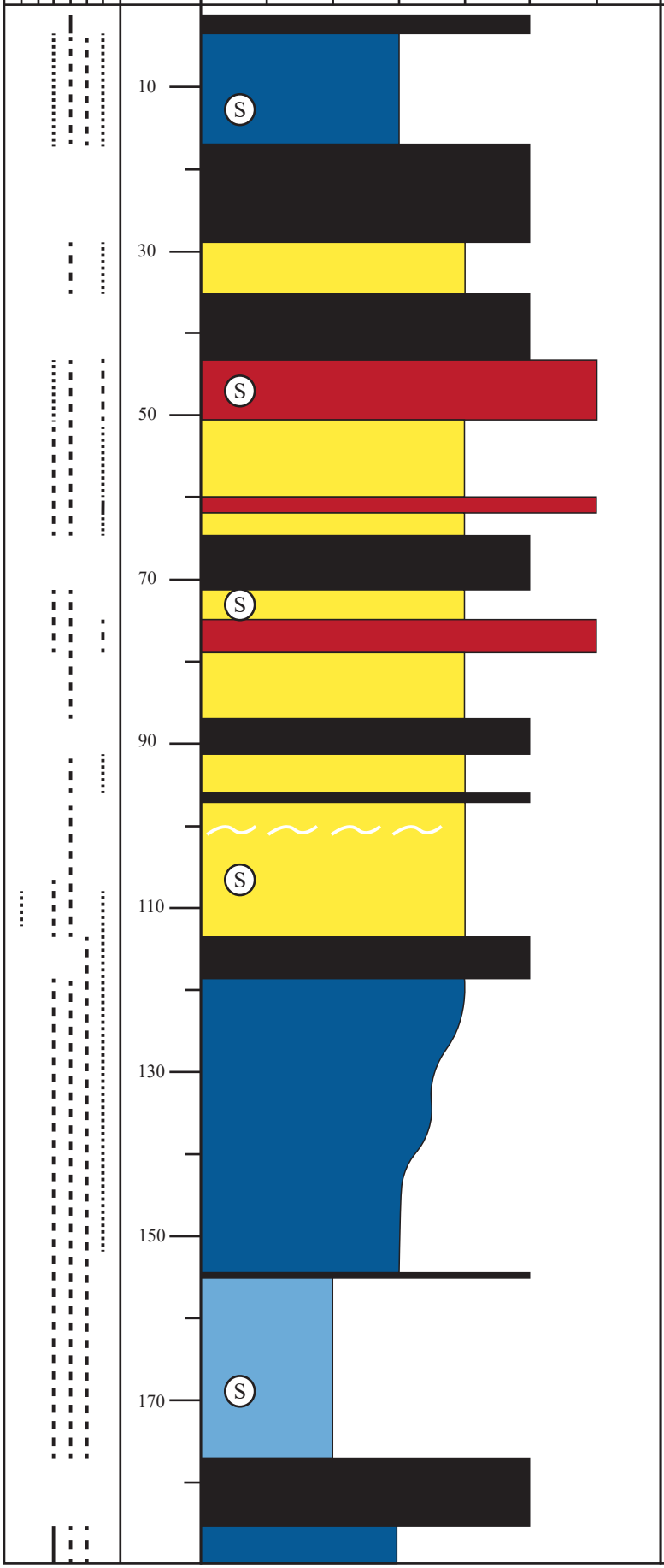

Project: Powderhorn Lake
Drill Hole: PH-18-14
Date: October 14, 2019

UTM: 564865E 5440569N (NAD83)
Azimuth, Dip: 360, -90
Length: 266.19m

1.5m dark gray aph mafic dike, trace dissem py (<5%) - faulted unit with mud/sand/gouge, red mottled and jasperized
3.5m light-med gray, fine-med grained lapilli tuff with alternating gray and light gray layers, mod chl+ser alt, weakly-mod foliated, trace pyrite (<5%)
~9.5m dissem sp in qtz phyric tuff, qtz eyes, ~11m dissem-bands and blebs sp, mod ser+chl
Sample 62552

17m plag porphyritic (small <1mm crystals) dike

28.8m light-med gray, fine-med grained FBR spotted with bt, mod apple green ser alt, mottled with pink alt, minor deformation structures in part, trace dissem py (<5%)

35.5m white, elongate plag porphyritic dike

43m medium-dark gray, fine-coarse grained, bt-spotted rhy or tuff, mod alt by apple green ser, with bluish qtz eyes, dissem-semi-mass po-cpy-py (10-15%) (Cu-zone)
Sample 62555
50.5m light-med gray, mottle pink, fine-med grained FBR with banded ser alt, mod qtz alt, presence of qtz eyes, trace dissem py (<5%)
60m semi-massive minz with brown po (~10%) and reddish brown sp (5-10%) with replacement/buckshot textures, somewhat vein-hosted
62m highly siliceous, aphyric FBR, mod ser alt, blue qtz eyes, trace py-po (<5%)
64.5m dark gray aph dike with xenoliths of above/below unit
71.2m same as above
Sample 62559
75.08m medium gray, red-pink mottled bands of fine-coarse grained semi-massive sp-po+/-py (10-15%; 5-10%; <5%), somewhat vein-hosted, bluish qtz eyes, mod alt by ser
78.6m medium gray, red mottling, moderately ser altered felsic volcanic

87m dark gray aph dike with minor py growth on ends of core
91.5m light gray FBR, mod alt by ser and mottled pink alt, trace vein-hosted sub-euhedral dissem py (<5%)
96m aph mafic dike
97m light gray FBR, mod alt by ser, weak-mod foliated, visible pearlitic textures, dissem py (<5%) throughout, fault zone ~99-103m
Sample 62563
108m very dark gray unit, banding only seen when dry - altered glassy/fractured textures, fine-medium grained, mod ser alt, small pink gt porphyroblasts, veins with euhedral qtz crystals, trace py (<5%)
113.9m green cast intermediate dike with fine plag crystals, 12cm raft/xenolith of below unit, trace py (<5%)

118.4m tan-green gray FBR with siliceous qtz veins throughout, mod ser+chl alt, crenulated in part, dissem py-sp (<5-10%)

154.38m graded into grainy lapilli tuff with small felsic lapilli, very green and ser alt, bt+chl forming clasts/clots

158.33m mafic dike with fine, subhedral plag crystals

158.88m medium gray, fine-med grained tuff with dark bt+chl, mod alt by qtz+ser, minor crenulation and deformation found closer to dike
Sample 62566

177.08m black mafic dike with minor local plag crystals

185.4m mixed section of lapilli tuffs and flows

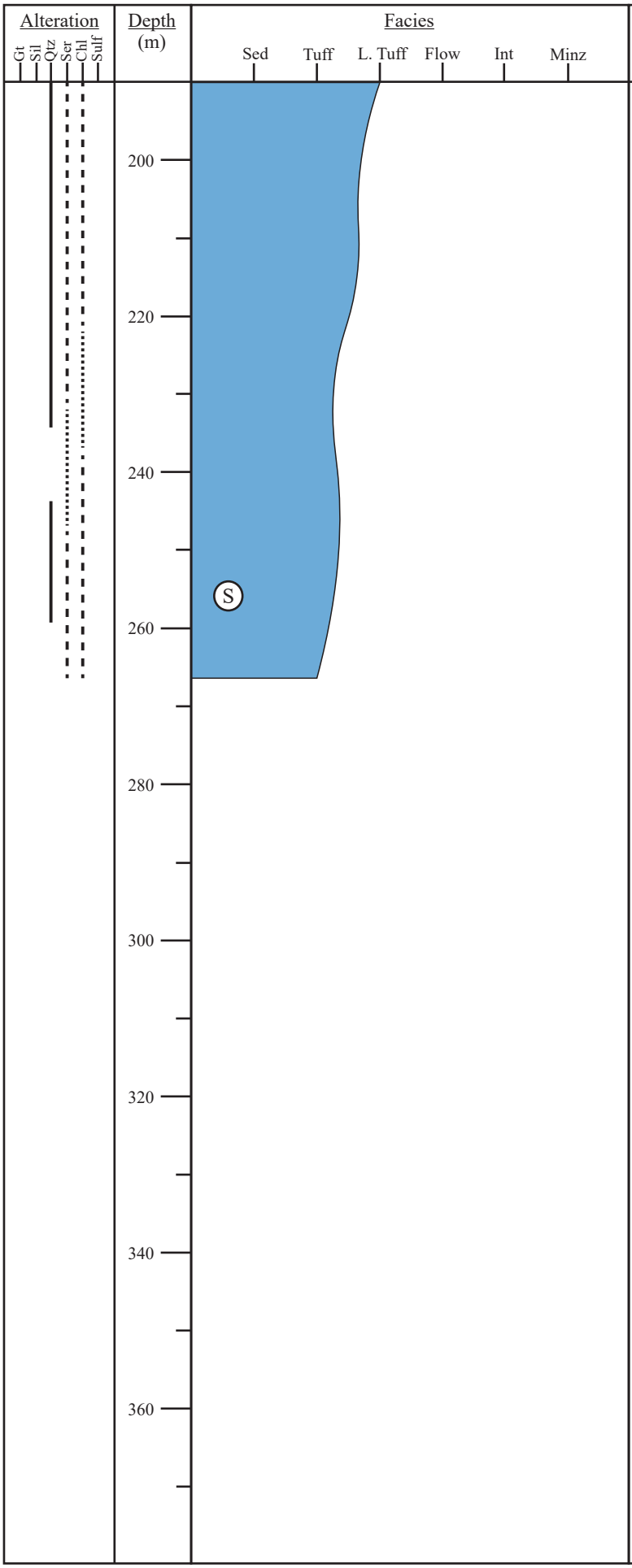

Project: Powderhorn Lake
Drill Hole: PH-18-14
Date:

UTM:
Azimuth, Dip:
Length:

185.4m light-medium gray, heavily silicified bt-tuff, mod ser+chl and strong qtz alt, trace py (<5%), minor crenulation

216m grading to light-medium gray, heavily silicified bt-tuff, mod ser+chl alt, mod-strongly foliated - pushing into bt-schist, crenulations in part,

230-233m heavy qtz veining

~233m darker gray, mod-strong black chl alt, weak ser, texture is lost

~238m slight more green and pink mottling with trace dissem py (<5%), mod foliated with bt following foliation

~245m increase in black chl and py (5-10%) - heavily silicified downhole with pink mottling, weak-mod chl+ser alt
Sample 62569

266.19m EOH

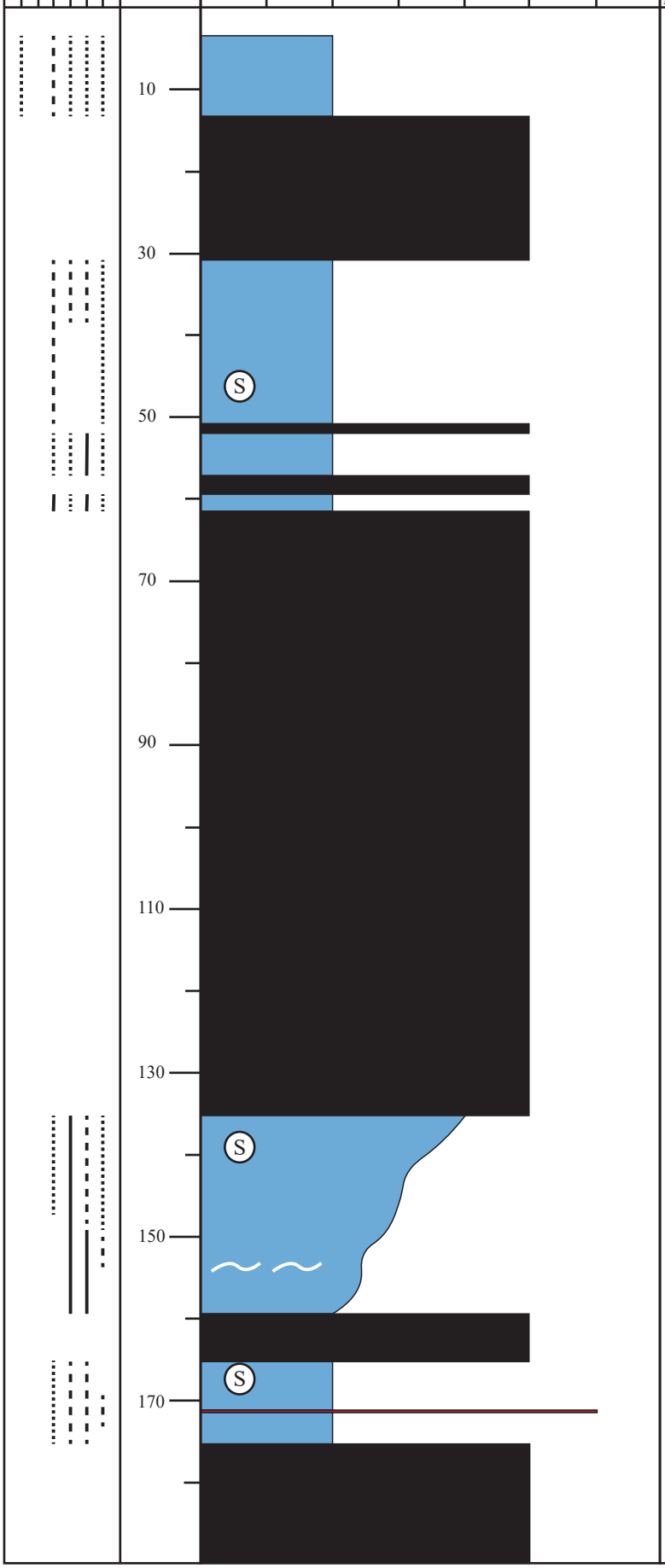

Project: Powderhorn Lake
Drill Hole: PH-18-15
Date: September 25, 2020

UTM: 565008E 5440562N (NAD83)
Azimuth, Dip: 360, -90
Length: 281m

3.82m light gray and spotted mottled rusty orange, highly siliceous qtz-crystal tuff with fine, thin dark beds of lithics and/or bt, weak ser+chl alt, presence of altered gt-ep-qtz zoned veins, trace disseminated cpy (<1%)

13.51m gray/green plag porphyritic dike, slightly mag, lots of small iron oxide spots on fractured ends, rusty

30.62m medium-dark gray, irregular banded qtz phyric tuff with qtz eyes, whispy deformed glass following weak-moderate foliation, moderate chl+ser alteration (loss of texture 39-44m), localized patches and blebs of cpy at 38.64-38.70m (<2%) - end of unit crenulated, deformed banding with trace disseminated py-cpy (<2-3%)
Sample 62731
50.56m gray/green plag porphyritic dike, slightly mag, lots of small iron oxide spots on fractured ends, rusty
52m medium gray, irregular banded qtz-eye tuff with pale green cast, moderate-strong chl alteration, local disseminated bands and veinlets of py-po (<8%), localized disseminated blebs of cpy (<5%)
57.54m same as above dike
59.27m silicified unit of above

61.86m mixed dike section of green plag porphyritic, non-mag and black aph dike, slightly mag (aph black till 64m)

Sample 62733

135.57m pale gray/green, aphyric, crenulated/folded rhyolite-tuff dark bands of vitric glass, sparse milky qtz eyes, mod-strong ser and mod chl alteration - 140m localized patch of po-sp-cpy in folded band with coarse bt - few disseminated blebs down unit (<5-8%) of po (<5%) sp and cpy (<2%)
~149m banding becomes less obvious, rocks become red/brown mottled, local sp (10%) and sparse cpy blebs (<5%)
154-163m fault zone with aphyric felsic volcanic moderately-strongly altered by ser+chl, crumbly

159.5m crumbly rusty, clay-like green plag porphyritic dike
Sample 62734
165.58m green/gray grainy qtz phyric tuff, bands/beds are quite altered and only visible in part, moderate chl+ser alteration, qtz veining throughout unit
171.23m good local cpy bands (10%)
171.71m same as above

175.47m mixed dike section

Alteration (Gt, Sil, Qtz, Ser, Chl, Sulf)	Depth (m)	Facies (Sed, Tuff, L. Tuff, Flow, Int, Minz)	Project: Powderhorn Lake Drill Hole: PH-18-15 Date:	UTM: Azimuth, Dip: Length:

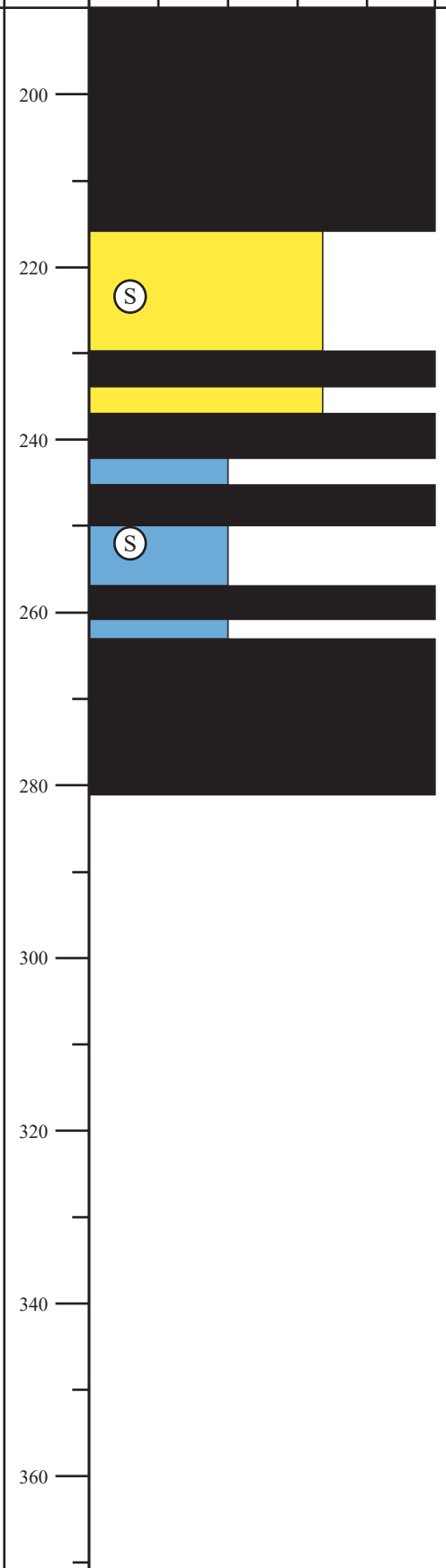

black aphanitic slightly mag (end 185m, begins 201m), and gray/green plag porphyritic slightly mag (begins 185m, ends 201m)

216.02m pale green/gray siliceous rhyolite, crenulations visible in part, moderately altered by ser, barren in sulfides
Sample 62735

229.95m balck aph mafic, slightly mag

233.96m same unit as above, somewhat red mottled and with an increase in bt in local patchy coarse flecks
236.87m black aph mafic, slightly mag
242.05m red/brown mottled and swirly fine-coarse grained qtz-phryic tuff to tuffaceous sediments, moderately ser altered, clasty dark bt/chl in foliations, qtz clasts (possible lapilli)
245.45m black aph mafic, slightly mag
250m same as above - qtz phyric, increase in bt and grainier texture
Sample 62736
256.73m black aph mafic, slightly mag

260.5m same as above, qtz-phyric, bleached, trace po-py

263.3m dark, plag porphyritic, non-mage but grades to finer plag crystals and becomes slightly mag at 275m

281m EOH

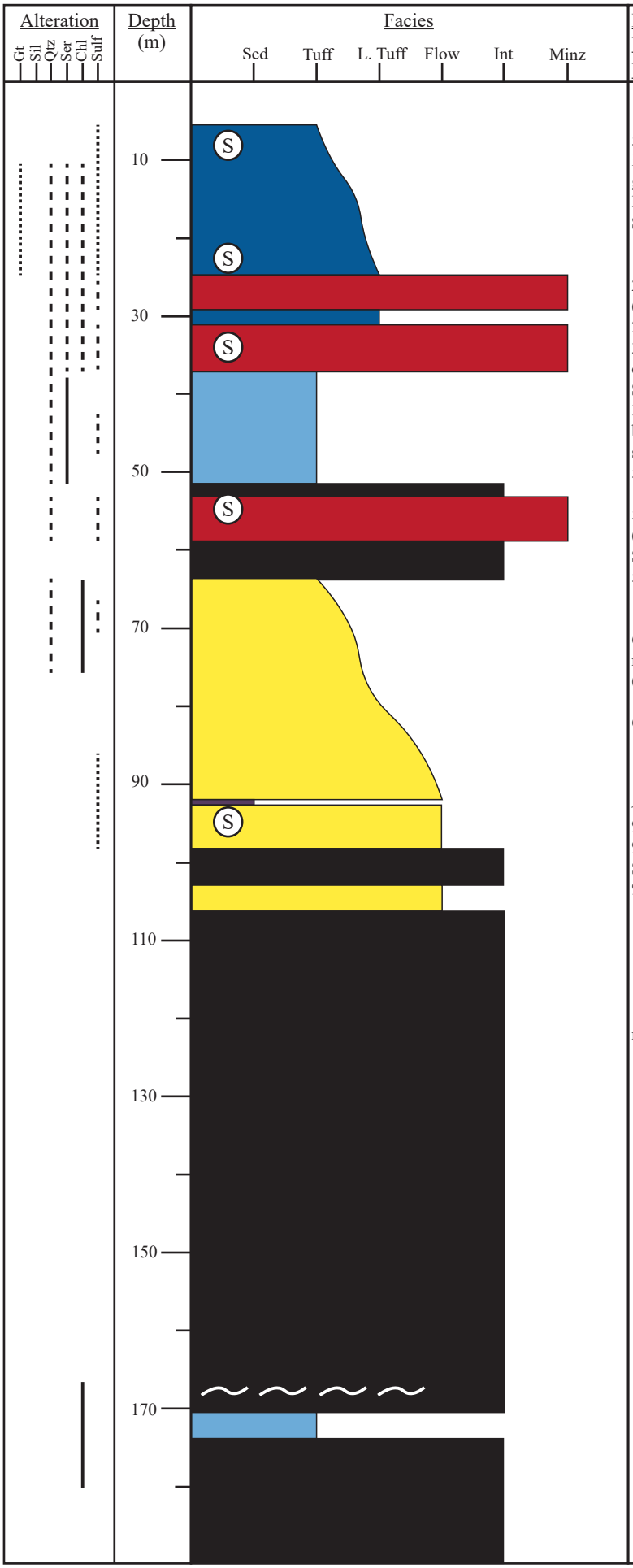

Project: Powderhorn Lake
Drill Hole: PH-18-18
Date: September 23, 2020

UTM: 564858E 5440427N (NAD83)
Azimuth, Dip: 360, -90
Length: 269m

5.86m light-medium gray, poorly banded tuff, sparse qtz eyes, crenulations in part, dissem po (<10-15%) ~10.90 darker red/brown beds or bands, zoned gt-ep-qtz veins, mod ser+chl alt - graded into lapilli tuff unit with felsic lapilli, beginning to see sulfides in bands and veinlets
Sample 62716, 62717

24.56m coarse, net-textured po (up to 30% locally), disseminated sp-cpy (<10%; <2%) stringers, qtz-eyes visible
29m as above
31m po-py-sp+/-cpy (<10-15%) stringers with light-med gray, pink mottled, qtz-phyric bt-tuff unit, mod alt by chl+ser, bt forming patches
Sample 62718
37.2m medium gray, red/pink mottled, variably alt qtz-phyric tuff with bluish qtz-eyes, moderate-strongly ser altered, 45.45.5m po-py-cpy+/-sp stringers and 46.5-47m net-textured po-py (10-20%) and cpy (2-5%)
51.89m aph mafic dike, slightly mag

52.92m medium-dark gray variably alt, qtz-phyric bt-tuff-rhyolite with sp (15%) stringers (Zn-zone)
Sample 62719
58.5m medium gray, lathy subhedral plag porphyritic dike, slightly mag

63.94m medium-dark gray banded, variably alt qtz-phyric tuff-rhy, mod-strong chl alt with blue qtz eyes ~68-70m heaviest minz po-py-cpy (10-15%) stringers associated with black chlorite/coarse-grained bt

68m original flow banding starts to return

~86m, sparse po-stringers continue down unit
92m <1m unit of dark, fine-graind gt porphyroblastic sediments
92.5m back into relatively unaltered rhyolite
Sample 62720
98.26m dark-med gray QFP bt-rhyolite dike
102.95m same as above

106.06m dark-med gray QFP bt-rhyolite dike

110.74 begins plag porphyritic intermediate dike for rest of unit, slightly mag

168.30-172.45m fault zone begins near end of unit

170.5m light-med gray qtz-plag-crystal tuff heavily alt by ser

173.19m slightly bleached plag porphyritic dike of above

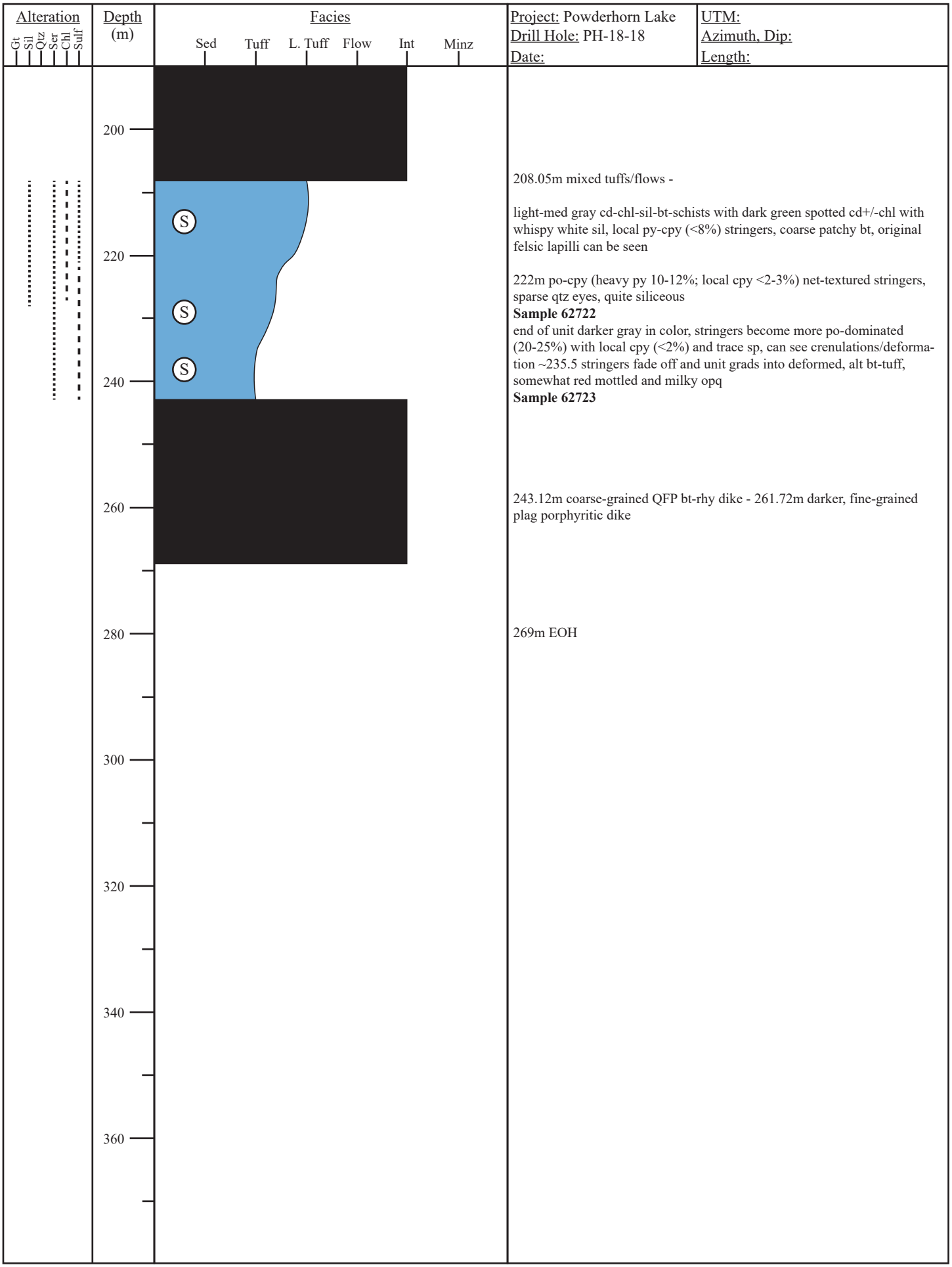

Project: Powderhorn Lake
Drill Hole: PH-18-18
Date:

UTM:
Azimuth, Dip:
Length:

208.05m mixed tuffs/flows -

light-med gray cd-chl-sil-bt-schists with dark green spotted cd+/-chl with whispy white sil, local py-cpy (<8%) stringers, coarse patchy bt, original felsic lapilli can be seen

222m po-cpy (heavy py 10-12%; local cpy <2-3%) net-textured stringers, sparse qtz eyes, quite siliceous
Sample 62722
end of unit darker gray in color, stringers become more po-dominated (20-25%) with local cpy (<2%) and trace sp, can see crenulations/deformation ~235.5 stringers fade off and unit grads into deformed, alt bt-tuff, somewhat red mottled and milky opq
Sample 62723

243.12m coarse-grained QFP bt-rhy dike - 261.72m darker, fine-grained plag porphyritic dike

269m EOH

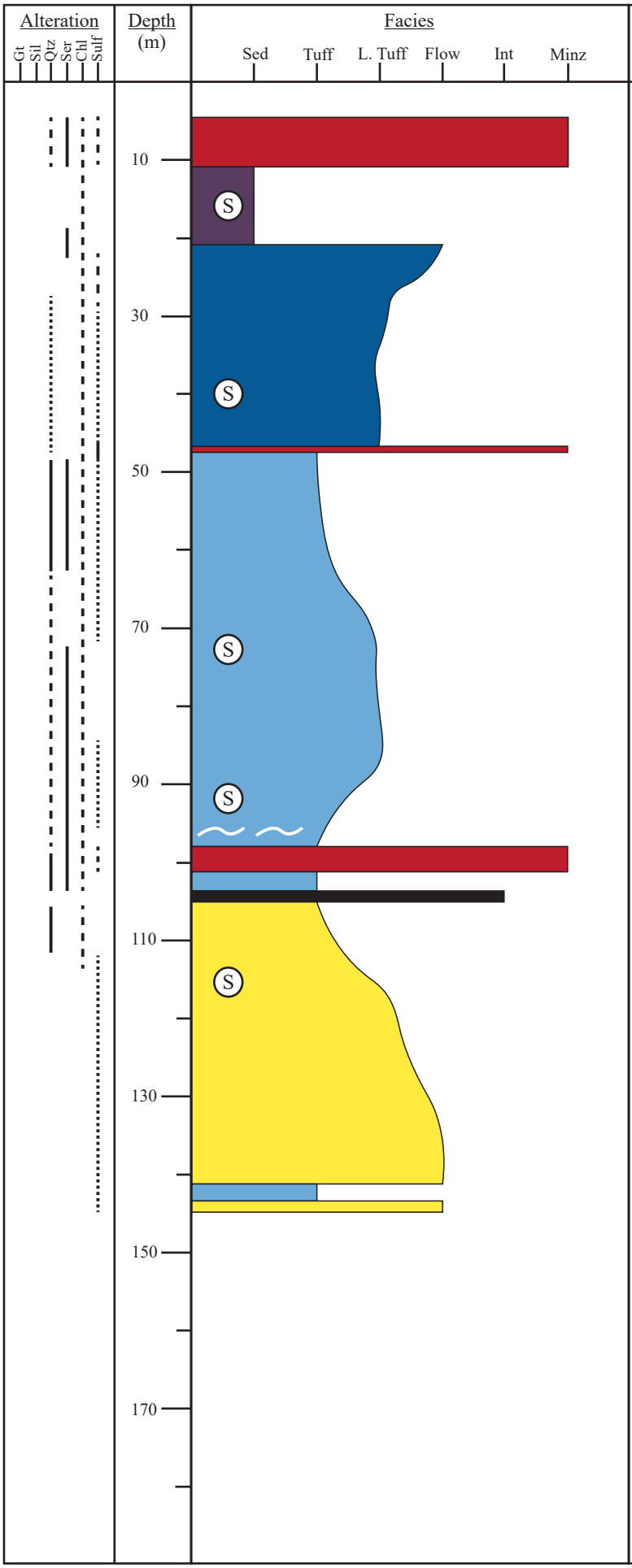

Project: Powderhorn Lake
Drill Hole: PH-18-21
Date: August 2, 2020

UTM: 565000E 5440420N (NAD83)
Azimuth, Dip: 360, -90
Length: 144.60m

4.3m rusty brown-sandy beige semi-massive to massive sulfide containing matrix-fill orange/red/brown/honey sp (10-<50%), vein-hosted cpy (<20%), py+/-po (10-20%), strong ser and mod chl (black banded) alteration, lots of qtz eyes
10.7m medium gray, tan-green cast, qtz eye tuff/volcanic sediment with thin beds of fine-grained sandy/silt, chl envelopes qtz eyes, crumbly end of unit
Sample 62685

20.5m beginning of unit strongly ser and crumbly ~22m bt-spotted rhyolite with bt+chl black veinlets, milky qtz eyes ~22.80m veinlet-hosted orange oxidized po (10-15%), pyrite (<5-8%), and cpy (<5%) and black chl bands+veins
26m grades into lapilli tuff - lapilli are dark and oblong, presence of thin beds with grainy/silty texture, bluish qtz eyes present, trace vein and foliation-hosted disseminated po-py (<10%), local cpy (<5%)
Sample 62686
46.7m local semi-massive po-py+/-cpy (15-30%)

47.3m same textures as above, no lapilli
50.92m light greenish gray, bt-gt-sediments with thin, grainy reddish-brown-brown chl-bt beds, strong ser and qtz alteration, sparse milky qtz eyes, trace vein-foliation-hosted disseminated py-po-cpy (<5%) - end of unit has increase in qtz alteration, more siliceous
64.36m medium gray and red/green mottling, heavily altered tuff with black chl bands and veins, local large qtz veining, sparse milky qtz eyes, trace veinlet hosted py-po+/-sp (<5%),
~72m lapilli, very ser altered, clay-like/opq appearance, gradational contact to next unit 76m appearance of reddish-brown beds, highly siliceous
Sample 62688
84.3m light tan-gray and red/green mottled, variably altered bt-spotted tuff mod-strongly altered by ser and moderately by qtz, weak-moderate chl, clasty black bt and minor qtz eyes, local altered chalky-looking gts, disseminated veinlet-hosted orange sp (<5%) and py (<5%)
Sample 62690
~96m crumbly and brecciated probable fault zone, strong ser alteration

98m halved core with red/brown matrix fill sp (<20%) - spotty and blebby - in large quartz vein ? or heavily silicified tuff, coarse py and minor cpy
101m same as above
103.75m mixed section of large qtz vein and leucogranite dike
105.11m light gray, fine-coarse grained bt-tuff/sediment, very clasty/de-formed appearance, strongly qtz and moderately chl altered, localized qtz eyes, grades into rhyolite

112.6m variably altered and deformed bt-rhyolite possibly tuffaceous with trace disseminated po (<5%) - gradational into light-medium gray porphyritic QFP-bt-rhyolite, aphanitic matrix, sub-euhedral 1-2mm clear/yellow plag, anhedral 1-2mm bt, subhedral blue qtz eyes <1-2mm, trace po (2-3%) disseminated throughout but associated/replacing bt, locally disseminated red/brown sp (<5%)
Sample 62691
141.3m light gray, grainy bt-spotted qtz phyric qtz-crystal tuff with disseminated mica-associated po-py (<5%)

143.53m same as rhyolite above, slightly darker in color

144.60m EOH

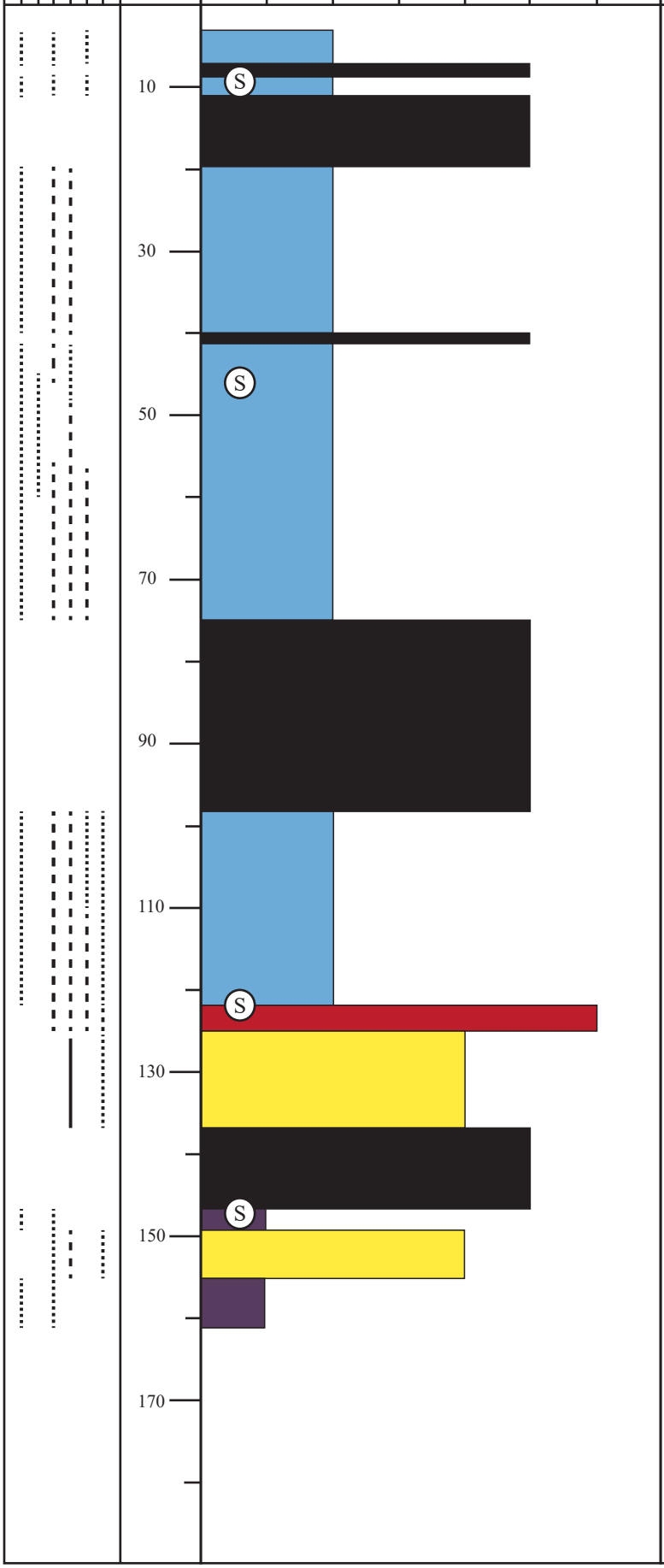

Project: Powderhorn Lake
Drill Hole: PH-18-25
Date: September 24, 2020

UTM: 565225E 5440622N (NAD83)
Azimuth, Dip: 360, -90
Length: 161m

3.64m light gray, siliceous qtz-crystal tuff weakly altered by chl, presence of zoned gt-ep-qtz veins, rusty fractures
7.34m black, subhedral plag porphyritic, non-mag
8.65m light gray, siliceous qtz-crystal tuff weakly altered by chl, presence of zoned gt-ep-qtz veins, rusty fractures
Sample 62737
10.67m black, subhedral plag porphyritic, non-mag

19.92m light gray, qtz phyric qtz-crystal tuff with altered gt porphyroblasts, moderately altered by ser - yellow green veins throughout, presence of zoned gt-ep-qtz veins, possible dark, fine-grained ash beds (?) ~20-30cm localized leucogranite veins

40.02m black, subhedral plag porphyritic, non-mag
41.22m light-medium gray, highly siliceous qtz-crystal tuff with sparse gt porphyroblasts and thin foliated bt
~45m pale green color, ser increases, alteration has fibrous texture, qtz-crystals disappear
Sample 62738
~58m rocks become seafoam green, bt is altered out, zoned gt-ep-ser-qtz veins, texture is wiped by strong dark chl alteration, fine-grained but no evidence of beds - continued green/dark gray-black bands of alteration, large irregular patchy/altered gts - rest of the unit fades in and out of this heavy alteration

75.6m black aph mafic, non-mag

98.13m light gray, aphyric, highly siliceous qtz phyric tuff with minor bt, apple green ser veins, large qtz veins - grades into distinctive gray qtz-crystal tuff with an increase of bt, zoned gt-ser-ep-qtz veins with trace disseminated py (<2%) throughout ~110m slightly darker, increase in chl

~117m grades into aphyric, silicified ? tuff - sparse patchy bt and blue qtz eyes

122m disseminated to locally semi-massive, net-textured and banded sp-py+/-cpy stringers (10-15% sp and locally up to 50%; <8% py; <2-5% cpy) in lapilli tuff?
Sample 62739
125m mottled red/green bt-spotted massive rhyolite, moderate-strong ser alteration, sparse stringers down unit

136.77m black plag porphyritic, slightly mag ~143.5m plag fades and the dike becomes more mag once aph
Sample 62740

146.36m dark gray, fine-grained gt porphyroblast metasediments, thinly laminated, bt-rich layers in part (inter beds?), minor sparse qtz eyes
149.39m light gray-pale green aphyric massive rhyolite with irregular banding of bt, moderate ser alteration, disseminated sp+/-cpy stringers (<8-10% sp; <2% cpy)
155.39m gt-metaseds, thinly laminated, slight green case with bt-rich patches and inter beds

EOH 161m

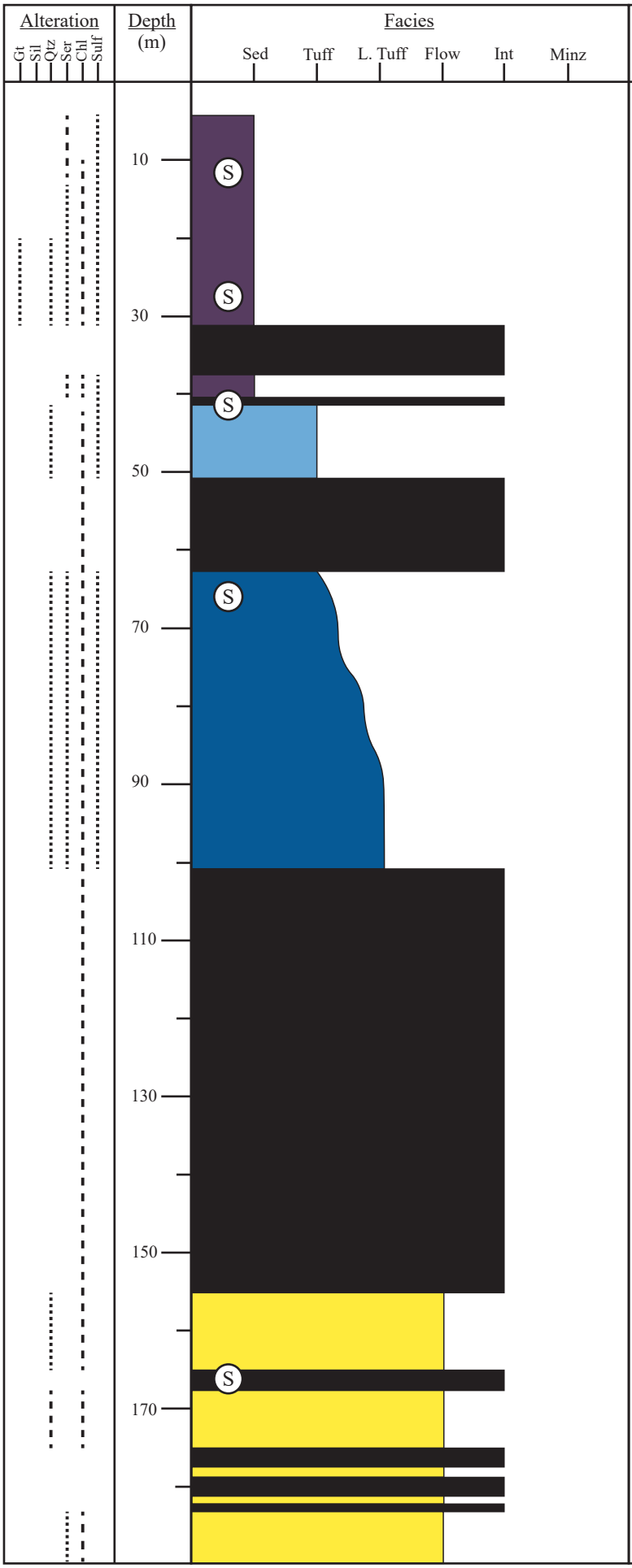

Project: Powderhorn Lake
Drill Hole: PH-18-26
Date:

UTM: 565306E 5440831N (NAD83)
Azimuth, Dip: 360, -90
Length: 203m

3.47m light gray, weathered and oxidized weakly welded to re-worked volcaniclastic sediments, looks quite grainy and has elongate white whispy clasts and spotted cd (possible tuff?) - grades into darker, heavily chl alt po-rich sediments ~20m the unit has reddish brown thin beds with zoned qtz veins and alt gt porphyroblasts

Sample 62641

Sample 62642

31.67m black aph mafic dike

37.5m same as above - moderately foliated, bt-qtz present, mod ser+chl alt, trace dissem po (<5%)

40.2m medium gray, fine-med grained plag porphyritic dike

Sample 62649

41.6m light gray, grainy bt-qtz tuff with irregular banding, weakly-mod foliated, local qtz veins, mod chl alt, trace dissem po (<5%)

50.44m light gray-green chloritized fine-coarse grained lathy plag porphyritic dike

Sample 62644

62.49m light gray and red/brown mottled, highly siliceous bt-spotted lapilli tuff with light-dark green mod chl alt, qtz veins and felsic lapilli tuff throughout, minor trace dissem py-po (<5%)

100.69m light gray-green chloritized fine-coarse grained lathy plag porphyritic dike (diabase texture?)

155.43m light gray and mottled red/brown, highly siliceous bt-spotted rhy, heavily folded, mod chl, milky qtz and plag crystals

165.25m medium gray dike with oxidized plag phenocrysts

Sample 62653

167.9m highly siliceous, folded bt-spotted rhy, strongly foliated

175.1m medium gray dike with plag phenocrysts

177.42m light gray and red mottled, strongly foliated bt-spotted rhy

178.45m aph mafic dike

181.05 same as above

182.07m medium gray dike with plag phenocrysts

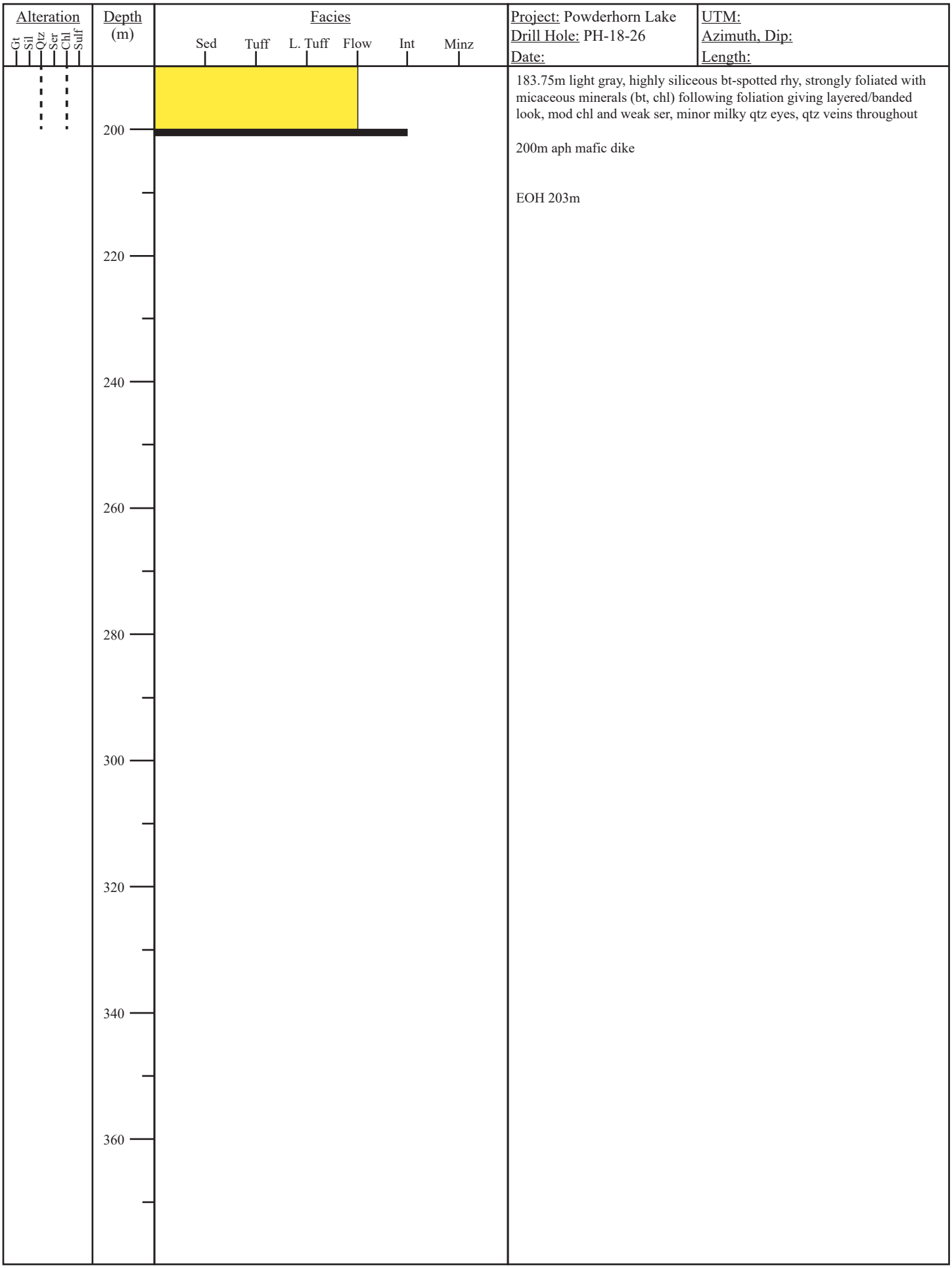
Alteration
Gt
Sil
Qtz
Ser
Chl
Sulf
Depth
(m)
Facies
Sed
Tuff
L. Tuff
Flow
Int
Minz
200
220
240
260
280
300
320
340
360
Project: Powderhorn Lake
Drill Hole: PH-18-26
Date:
UTM:
Azimuth, Dip:
Length:
183.75m light gray, highly siliceous bt-spotted rhy, strongly foliated with micaceous minerals (bt, chl) following foliation giving layered/banded look, mod chl and weak ser, minor milky qtz eyes, qtz veins throughout
200m aph mafic dike
EOH 203m

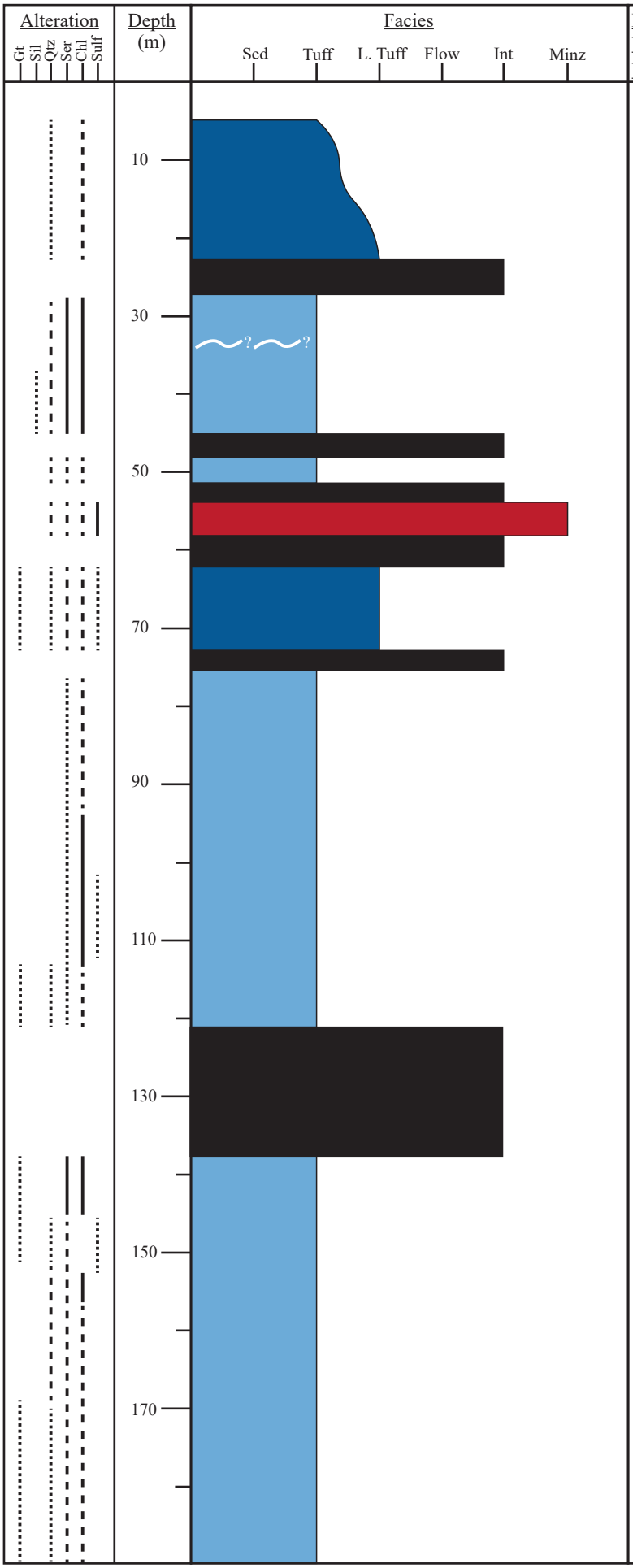

Project: Powderhorn Lake
Drill Hole: PH-18-28
Date: October 21, 2019

UTM: 565231E 5440764N (NAD83)
Azimuth, Dip: 360, -90
Length: 239m

5m light gray, highly siliceous bt-spotted variably alt tuff, weakly-mod foliated, dark bands of bt +/- chl grades into lapilli tuff with local felsic lapilli, becomes lighter in color with reddish/brown mottlings, sparse calcite veins, minor milky qtz eyes

22.87m black aph mafic dike

27.43m light gray, highly siliceous bt-spotted lapilli tuff-tuff, intensely alt by chl+ser, mod foliated, reddish-brown thin layers-mottling, darker chl clasts
~39m heavy green banding and oxidized veins, bt-spotting returns, local feldspar crystals, minor white whispy sil alt

45.48m dark gray dike with minor plag+bt crystals
48.20m darker med gray bt-spotted rhy tuff with minor pink mottling, moderately alt by chl+ser, very siliceous
51.55m aph mafic dike
53.83m bt-spotted tuff primarily alt by mod chl+ser ~55m localized minz po-py and sp-cpy (locally >50%, overall ~20%) net-textured bands to stringers, felsic lapilli and qtz eyes visible
58.14m aph mafic dike
62.17m light gray with greenish cast and reddish brown mottling, siliceous bt-spotted lapilli tuff with local felsic lapilli, mod chl+ser alt, milky qtz eyes, possible alt gts, trace dissem po (<5%)
72.87m dark gray dike with small milky plag crystals

75.62m light gray with greenish cast and pink mottling, highly siliceous tuff-lapilli tuff, localized bands and patches of ser alt, dark green-black chl clots/clasts

~93m gradational color change to med-dark gray, more alt by chl (?), heavy dark green to black bands, minor dissem po (<5%)

~113m dark reddish brown mottling, presence of zoned gt-ep-qtz veins, grainy tuffaceous textures

121.58m bt-plag porphyry dike

137.87m beginning of unit is dark, heavily alt by dark green-black chl in bands to elongate clots/clasts (altered lapilli?), presence of zoned qtz veins, can still see spotted bt, mod foliation, heavy alt until
~145m trace dissem py (<5%)
~145m gradational to highly siliceous chl alt tuff unit like above, mod foliated, can see bt-spots, small milky qtz veins+eyes, minor presence of alt pink gts or Fe-carb spots, splotchy pink mottling
~151.5m gradational into strongly chl alt unit, mod foliated, bt-spotted, qtz eyes are a bit more prevelant, gradational to less alt siliceous possible rhy by
~155m highly siliceous unit, mod-strongly foliated, bt-chl following foliation, reddish brown mottling and milky qtz eyes - could be more of a tuffaceous unit
~169m back into strong chl alt unit with zoned qtz veins, slight crenulations, alt gts

Alteration: Gt, Sil, Qtz, Ser, Chl, Sulf

Depth (m)

Facies: Sed, Tuff, L. Tuff, Flow, Int, Minz

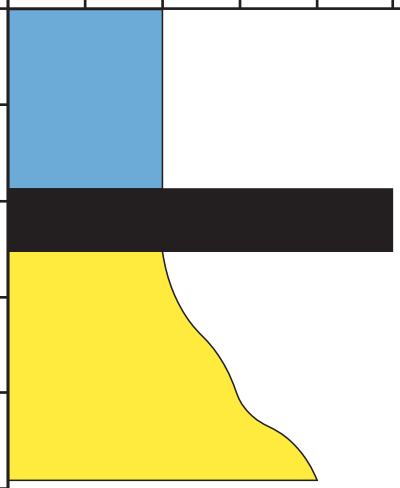

200
220
240
260
280
300
320
340
360

Project: Powderhorn Lake
Drill Hole: PH-18-28
Date:

UTM:
Azimuth, Dip:
Length:

~188m extremely green chl altered tuffaceous unit

208.79m aph mafic dike

215.3m medium gray, heavily chl alt bt-tuff with bands of dark green/black chl, minor gts or Fe-carb spots
~224m gradational to regular siliceous bt-spotted rhy with red/brown mottling, minor blue and milky qtz eyes, minor chl clots/clasts

EOH 239m

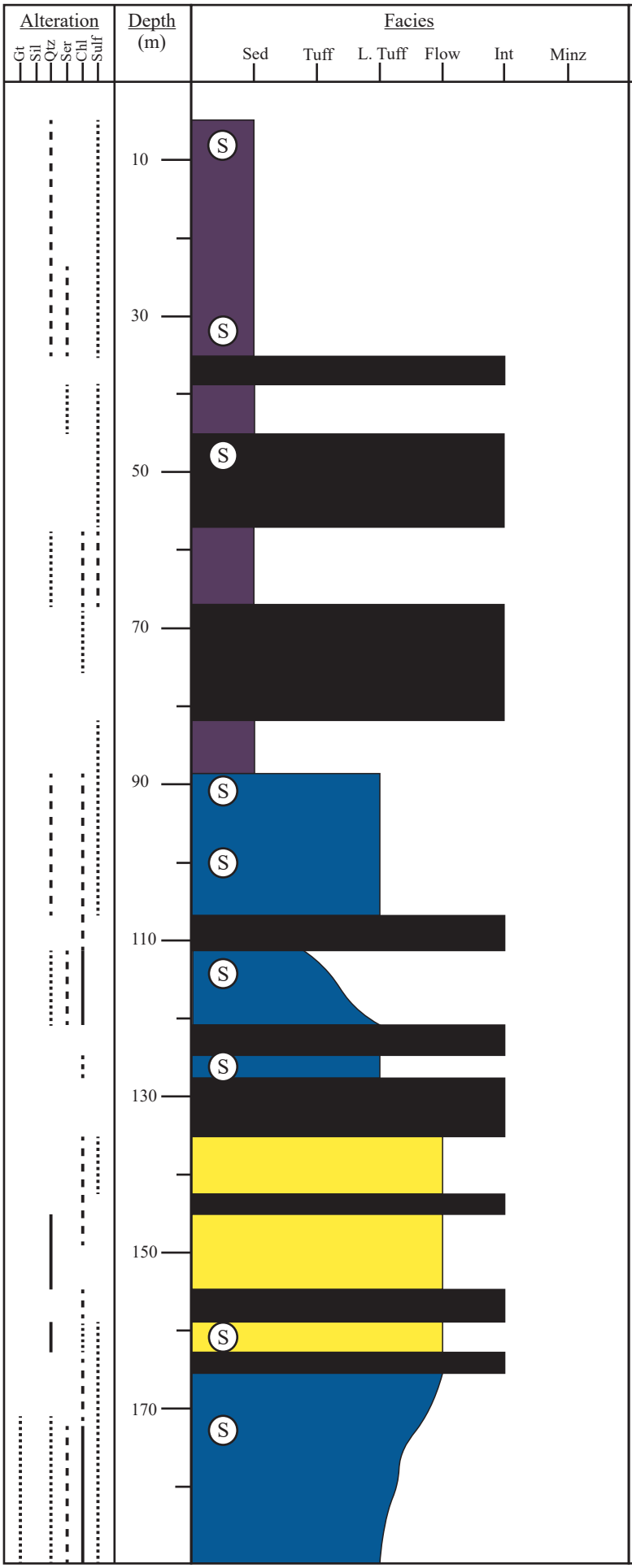

Project: Powderhorn Lake
Drill Hole: PH-18-34
Date: October 17, 2019

UTM: 564319E 5441023N (NAD83)
Azimuth, Dip: 135, -65
Length: 671m

Sample 62571
6.36m mod welded volcaniclastic sediments with whispy elongate clasts, thin reddish brown interbeds, wavy lenticular clasts (2-3 cm), coarse grained bt within whispy clasts, trace dissem interbeds of po and py throughout (<5%), somewhat spotted appearance when dry (cordierite ?), localized crenulation and qtzite layers (~50 cm), downhole becomes mod alt by light green-white chalky, soapy ser, minor presence of qtz eyes
Sample 62573

35.44m mafic dike with brecciated contacts

38.42m medium gray weakly-mod welded volcaniclastic sediments with lenses of po (<5%) minor to weak ser alteration and minor cd spots

45.21m aph mafic dike, core breaks alng contact, minor localized po (<5%) lenses
Sample 62575
57.25m medium to dark gray, mod welded volcaniclastic sediments with dissem to semi-massive sulfides whispy lenses of po (up to 15-20%), minor cpy (<5%), mod alt by black chl forming “clasts”, presence of qtz eyes and veins
67.30m light gray intermediate dike gradationally contacts sediments above and below, fine-coarse grained plag, bt, and hornblende - looks like chloritized diorite/tonalite and grades into dark aph
82m medium gray, weakly to mod welded sediments with thin whispy reddish brown interbeds, trace dissem po lenses, minor localized cordierite spots, 45cm siliceous xenolith
89.11-89.90m local bands of massive to semi-massive po (10-15%)
Sample 62579
92.7m mixed section of tuffs, lapilli tuffs, thin flows
light gray, aphyric flows, weak to mod chl alt - 95m with trace dissem vein-hosted po and py throughout (<5%), highly siliceous, some coarse grained bt, fine felsic white lapilli, highly siliceous containing dissem to semi-massive lenses and veins of po
Sample 62580
94.14m light to medium gray, fine-grained, qtz-phyric tuffs, low to mod ser+chl, possible felsic lapilli
~103m back into aphyric flows
107.88m aph mafic dike mod alt by chl
111.12m medium to dark gray, tuff to lapilli tuff, alternating light and dark bands, pretty aphyric with minor speckled bt, strong chl and mod ser alt, local qtz veins
Sample 62581, 62582
120.9m dark gray aph dike, trace dissem po and py
124.3m lapilli tuff with localized rounded black-green chl clasts, felsic lapilli, and mod alt chl veins
127.97m dark gray intermediate-mafic dike with spotted plag crystals (up to 2mm), crystals fade gradually, sharp contacts
135.79m massive rhyolite with coarse-grained bt “spotted”, mod chl alteration, minor oxidation, trace dissem po and py (<5%)
142.36m aph mafic dike mod alt by chl, local brecciation, trace dissem py (<5%)
144.92m light gray massive rhyolite, mod chl alt near top of unit and gradually fades out to primarily heavily silicified bt spotted black veins throughout, localized pinkish/oxidation alteration
154.59m mafic dike with lathy white plag crystals phenocrysts mod alt by chl
159.07m light gray bt spotted, highly siliceous massive rhyolite weakly alt by chl, trace vein-hosted py (<5%)
Sample 62584
163.8m aph mafic dike mod chl alt trace dissem po (<5%)
165.81m dark-medium gray massive rhyolite grading from mod chl alteration (dark) to opaque tan ser or more tuffaceous (?)
~167.2-171m still spotted bt and chl with brownish/black veins throughout, slight pink - possible oxidation, trace dissem po (<5%)
~171m rhyolite-tuff has fragmental texture being heavily alt by chl and mod by ser, lapilli, localized zoned qtz veins by apple green ser, trace dissem py (<5%)
Sample 62585

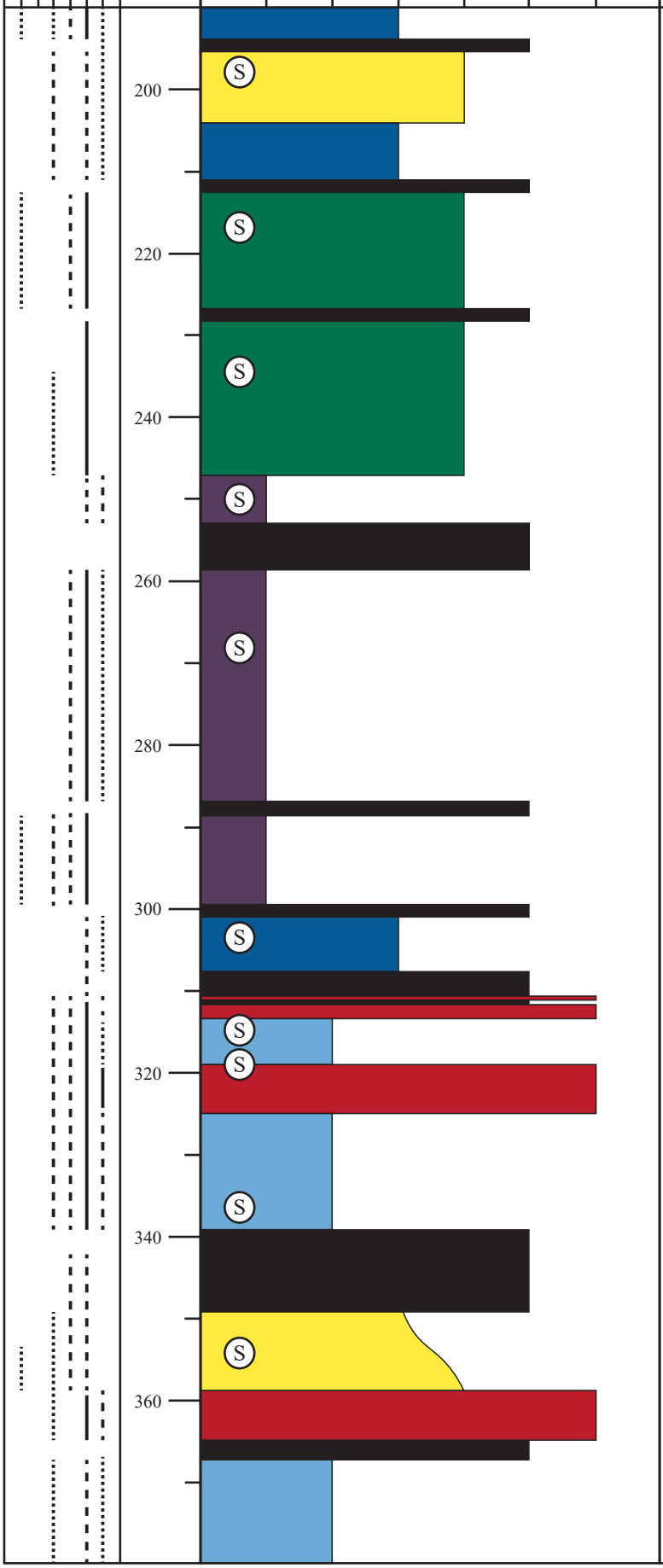

Project: Powderhorn Lake
Drill Hole: PH-18-34
Date:

UTM:
Azimuth, Dip:
Length:

193.45m aph mafic dike with trace dissem py, contains xenolith of above/below unit

Sample 62586

194.82m light gray, fine-coarse grained, fragmental felsic volcanic to massive rhyolite, highly siliceous with many qtz veins brown/green chl alteration - black chl clasts, trace dissem vein-hosted py and po (<5%)

204m light-medium gray weak-mod welded ? volc. seds-lapilli tuff with whipsy elongate qtz/lapilli clasts reddish-brown wavy/irregular interbeds, possible cordierite spots, trace po, py, cpy (<5%)

211.32m dike with white lathy subhedral plag phenocrysts

213.31m light-dark gray volc. seds-tuff grading into lapilli tuff, whispy elongate beds gradationally disappear along with reddish interbeds, possible qtz-eye or gt porphyroblasts, ser and green chl alteration increases - could be mafic tuffs

Sample 62587, 62608

226.32m aph mafic dike

228.17m light-medium gray flow basalt strongly alt by chl (black) into irregular "clasts" or clotting somewhat predominantly light green color with plag/qtz veins, qtz-filled elongate amygdules

247.05m dark gray volcanic sediments (possible mafic tuffs) with localized dissem to semi-massive po in interbeds and veins, whispy elongate clasts, mod chl alteration

252.72m dike with lathy-irregular plag phenocrysts

Sample 62588, 62589

258.51m light-medium gray weak-mod alt welded volcanic sediments, strongly chloritized with coarse white/red interbeds - some interbeds seem more "clasty" as in lapilli or flows but beds are seen throughout ~273 shows flow-like characteristics with possible elongate amygdules but heavily alt, thinly laminated beds above and below, trace dissem po ininterbeds and veins

-could be gradational seds-flows-tuffs (?) - mafic flows and tuffs???

286.86m mafic aph dike

288.27m light gray, weak-mod welded and foliated, heavily alt by chl and mod by white chalky ser some pink k-feldspar alteration, large localized qtz veins, possible gt porphyroblasts

299.87m mafic aph dike

300.64m light gray highly siliceous, fine-grained bt spotted tuff mod alt by chl dissem vein-hosted py and po (<5%) increasing down unit, gt porphyroblasts, chunky feldspar crystals and sparse felsic lapilli, bluish qtz eyes, minor sil alteration

Sample 62592

307.9m mafic chloritized dike with fine white plag phenocrysts

310.38m dark rusty, fine-coarse grained semi-massive sulfide vein-hosted to bedded po (2-5%), py (20-25%), sp (8-10%), and cpy (<5%), buckshot textured, apple green epidote and qtz eyes

Sample 62594, 62597, 62599

311.04m mafic chloritized dike with fine white plag phenocrysts

311.53m same as above - dark rusty, fine-coarse grained semi-massive sulfide vein-hosted to bedded po (2-5%), py (20-25%), sp (8-10%), and cpy (<5%), buckshot textured, apple green epidote and qtz eyes

313.58m qtz-eye tuff with dissem sulfides (<5%)

319.21m dark rusty brown, semi-massive to massive sulfides hosted in qtz-eye tuff with reddish brown sp (35-50%), py (10-15%), po and cpy (<5%) with zoning and buckshot textures

324.70m light-medium gray, variably alt massive rhyolite to heavily altered tuff, highly siliceous with mod-strong chl and weak-mod ser, localized bright pink k-feldspar, zoned "ropey" siliceous veins, stringer sp-py

339.34m medium gray, porphyritic intermediate dike with plag phenocrysts and small bt and hornblende possibly k-feldspar

349.23m light-medium gray lapilli tuff - tuff mod alt by chl and weak-mod alt by ser, with reddish interbeds and white elongate irregular clasts, cordierite spots grading into bt spotted massive rhyolite ? , qtz eyes and gt porphyroblasts

Sample 62600

359.33m light gray, fine-medium grained variably alt tuff with dissem to semi-massive vein-hosted sp (2-8%), py (4-8%), cpy (<2%), bluish qtz-eyes, light green to black chl, weak-mod foliations, localized crenulations

364.33m mafic aph dike

367.32m sampled but relatively barren, variably alt rhyolite-tuff with black veins of chl and bt, presence of minor qtz eyes, trace sp (<5%), py (<5%), cpy (<2%) - grading into more tuffaceous, dusty gray-

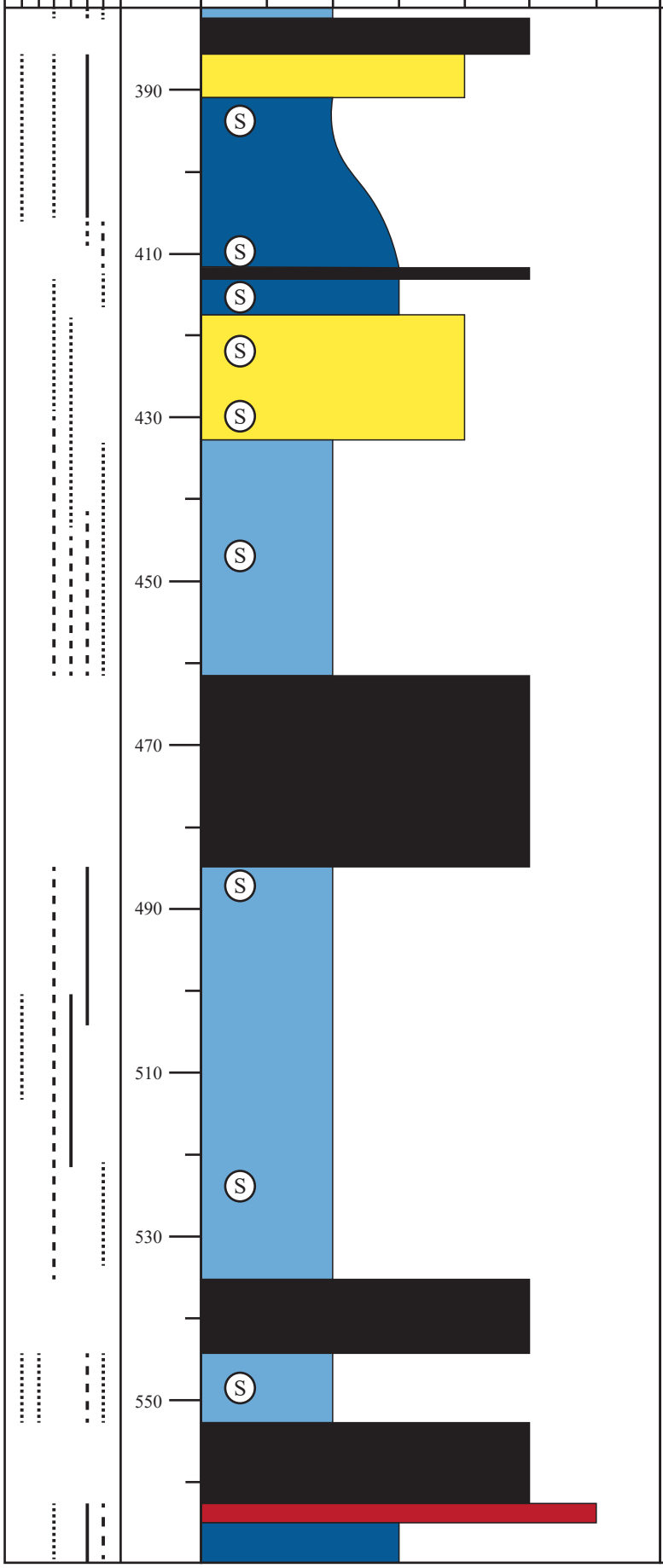

Project: Powderhorn Lake
Drill Hole: PH-18-34
Date:

UTM:
Azimuth, Dip:
Length:

bt-spotted with thin reddish interbeds, minor qtz eyes and veins, mod chl and ser alteration, crenulated
381.38m dike with fine-grained plag crystals
385.54m medium gray fine-coarse grained massive rhyolite mod-strongly alt by chl, irregular not as blue blue qtz eyes, pinkish gt porphyroblasts
391.10m light gray, siliceous qtz + feldspar crystal tuff with bt/chl blotches, bleached gradational contact to -
Sample 62603
406.2m light-medium gray fine-coarse grained qtz-crystal tuff with fine, local lapilli zones, moderate chl, po-py <5% and local sp, chl alt fades by ~409.5m - minor pick-up of po-py+/-cpy+/-sp in last 6cm of unit
Sample 62605
411.94m aph mafic dike
412.95m same as above, grainy, blue qtz eyes, very fine lapilli, less chl downhole, minor sp
Sample 62606, 62607
416.20m siliceous, qtz-phyric rhyolite with milky gray qtz eyes, minor ser alteration, trace sulfides that fade downhole
Sample 62609
433.57m light gray variably alt tuff with blotchy irregular red interbeds, high silica, fine local lapilli, trace sp, minor pinkish oxidation
437.8m dissem to semi-massive sulfide containing veins of po (~10%), sp (~10%), and py (<5%), more chl alt downhole
442m light green, highly siliceous, bt spotted tuff with minor qtz eyes, moderate chl alt in local beds/layers, becomes more pervasive ser alt downhole, gt porphyroblasts appear end of unit - more aphyric
Sample 62610
458.97m green/black chl clasts, somewhat pink (ksp?), possibly variably alt lapilli tuff with minor dissem py (5-15%), and cpy (2-4%)

461.94m porphyritic andesitic dike with plag, bt, and hornblende phenocrysts - variably alt by chl

484.35m medium gray tuff, grainy, siliceous and aphyric, mod to strongly alt by dark chl, with pink gt porphyroblasts, qtz veins bluish qtz eyes and clasts throughout, large 2cm bt-rhyolite xenolith
Sample 62611

~501.5m heavy ser alteration completely changes to tan color and grades back to gray zoned zoned qtz veins, slight orange oxidation

~524m minor sulfide occurrence with dissem sp (10%), cpy (<5%), po (<5%)
Sample 62613

535.70m dike with fine-grained plag phenocrysts and xenoliths of below unit (tuff)
544.20m light gray highly siliceous tuff with spotted bt, mod alt by chl, trace dissem sp, po, and py (<5%), gt porphyroblasts, minor sil alteration, minor qtz eyes, qtz-ep-gt zoned veins
Sample 62614
552.89m intermediate dike with fine plag and bt phenocrysts

562.22m qtz-phyric dissem to semi-massive sulfide with pinkish (ksp?) alt, mod-strongly alt by chl containing po (10-12%), sp and cpy (2-5%), minor qtz eyes

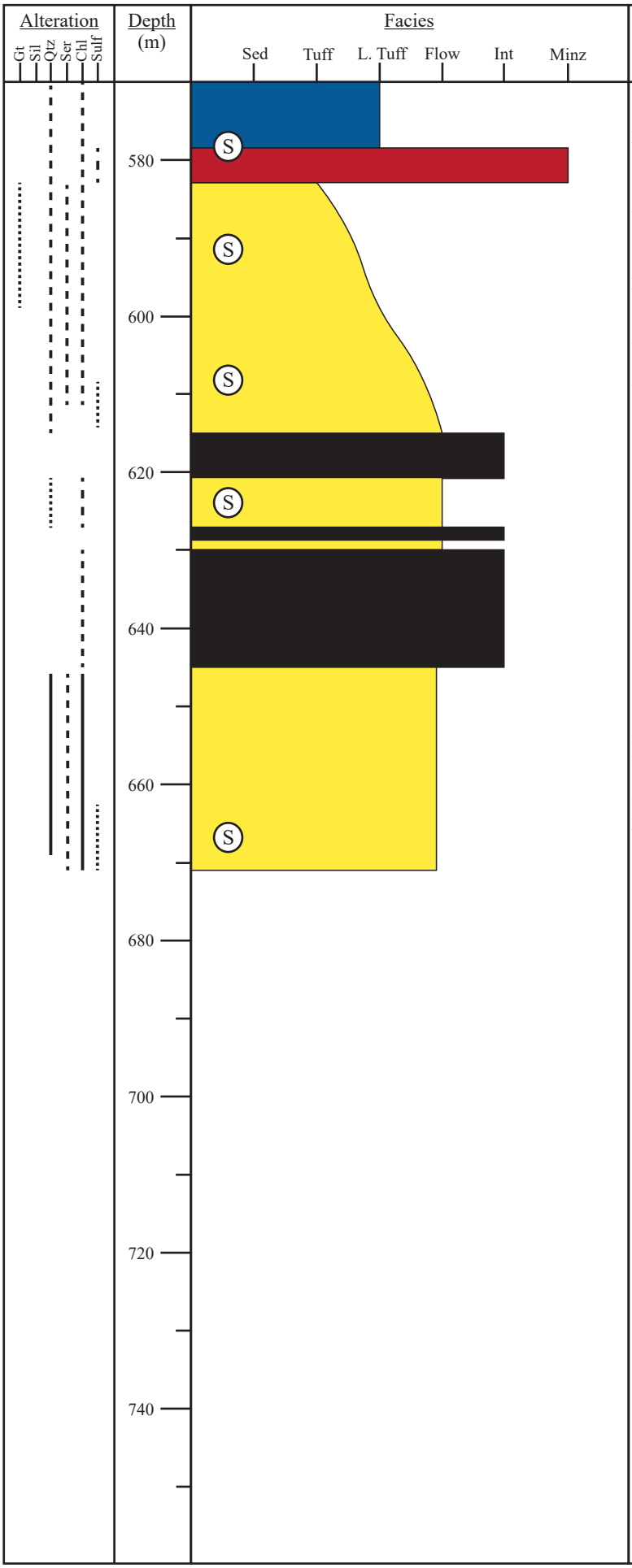

Project: Powderhorn Lake
Drill Hole: PH-18-34
Date:

UTM:
Azimuth, Dip:
Length:

565.10m light-medium gray tuff with minor spotted bt, weak-mod alt by ch, white lapilli, qtz phyric and slight pinkish brown ksp alteration, dissem po

Sample 62617

578.20m medium gray lapilli tuff containing dissem to semi-massive po (<10%), sp and cpy (5-12%), and py (10%), mod alt by chl, containing bluish qtz eyes, felsic lapilli

583m light gray, strongly foliated, mod-strongly alt tuff with pinkish gt porphyroblasts, bt follows foliation, qtz veins and clasts are localized

Sample 62619

~610m (sampled) trace dissem sp (<5%)

Sample 62620

~613m primary texture and banding appears with qtz eyes, seems more siliceous, possibly flow

615.52m mafic dike with fine, irregular spotted palgioclase phenocrysts

620.42m light gray, light-dark green and pink rhyolite variably alt by dark chl, mod foliated, minor qtz eyes

Sample 62620

627.54m aph mafic dike

628.66m same unit as above dike

630m dike with fine, white plag phenocrysts mod alt by chl

645.20m light gray-green and pink/red, variably alt rhyolite to massive rhyolite mod-strongly alt by chl (localized bands downhole), weak-mod alt by ser, highly siliceous with qtz veins throughout - some considerable qtz “beds” and dark elongate chl clasts, minor milky qtz eys, localized epidote (?) near end of hole along with more prominent bluish qtz eyes, minor felsic lapilli, and trace dissem py (<2%)

Sample 62622

671 EOH

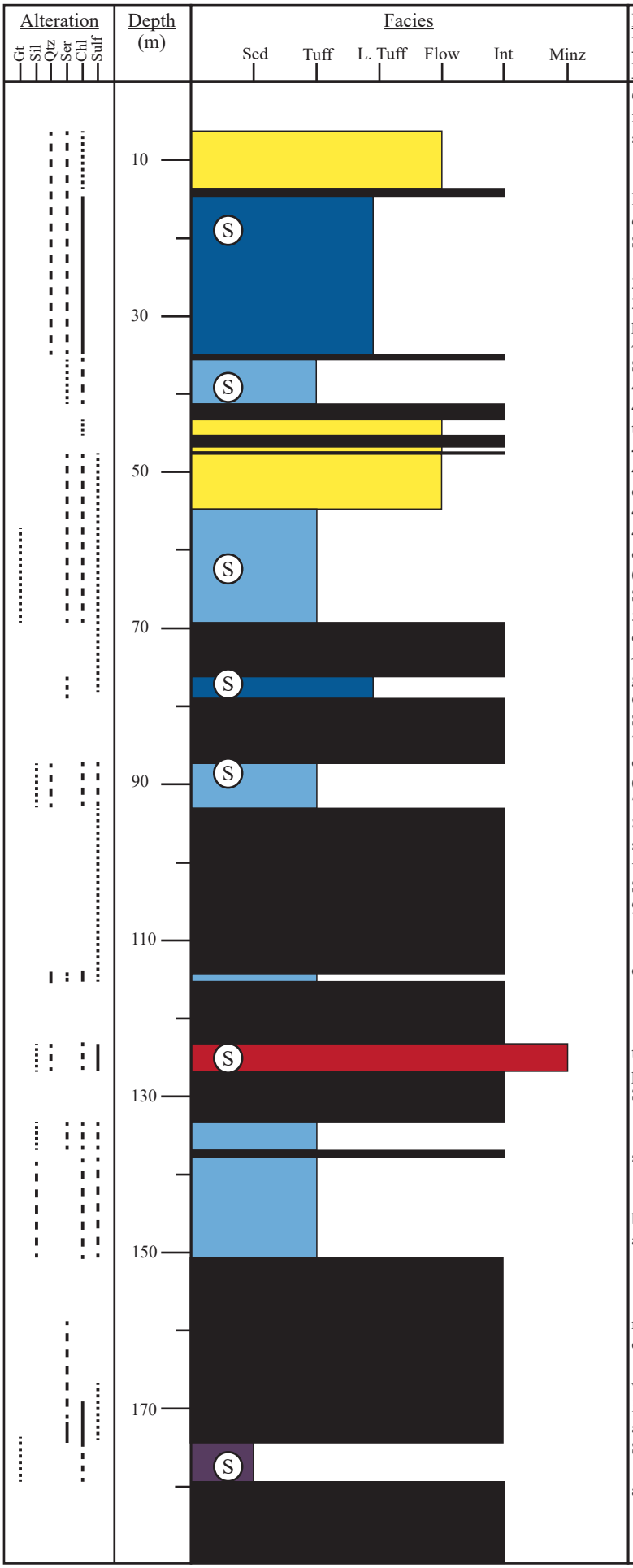

Project: Powderhorn Lake
Drill Hole: PH-18-40
Date: October 19, 2019

UTM: 564575E 5440438N (NAD83)
Azimuth, Dip: 360, -90
Length: 326.50m

6.22m light-medium gray massive rhy, mod ser and weak chl alt, weak-mod foliation, localized crenulations ~11m can see original flow banding, highly siliceous, milky qtz eyes, dissem py-po (<5%)
13.95m granitic dike
14.23m the unit becomes mod-strongly alt by chl and weak-mod ser (tan), light gray-green color with reddish brown mottling, oblong clasts/clots of dark chl -probable lapilli
Sample 62623

34.72m aph mafic dike
35.60m light gray, blue qtz-eye tuff with weak ser and mod chl alt, small gt porphyroblasts
~39m becomes more siliceous and less altered
Sample 62624
41.70m aph mafic dike
43.43m dark gray mass rhy, weakly chl alt, possible primary flow banding textures
45m aph mafic dike
46.38m light gray, green and pink mottled massive rhy with mod-strong chl+ser alt, blue qtz eyes
47.27m aph mafic dike
47.93m light gray, highly siliceous massive rhy, primarily alt by mod chl+ser, milky and blue qtz eyes, slight orangey oxidation, dissem py-po (<5%) throughout, gradational into next unit
Sample 62625
54.55m medium gray, fine-med grained, grainy tuff with reddish brown and dark green-black thinly laminated interbeds, weakly welded, blue qtz eyes
~58m light-medium gray, oxidized bt-spotted tuff, mod alt by chl+ser, minor gt porphyroblasts, trace dissem py (<5%)
69.68m aph mafic dike, slightly mag, trace dissem py (<5%)
Sample 62626
76.07m light gray-green, highly siliceous minz lapilli tuff with blue qtz eyes, darker oblong lapilli, dissem vein-stringer honey colored sp and py (<5-10%)
79.33m aph mafic dike with half+half core of minz tuff of prev unit
87.35m medium gray, dissem-semi-massive minz tuff with banded to stringer sp-py+/-cpy (10-15%; <5%; <2%), mod chl and minor sil alt, mod foliated, local qtz clasts (possible lapilli) and veins
Sample 62627
93.53m plag porphyritic dike with dissem py (<5%) throughout, slightly mag

114.02m strongly chl and mod ser alt, highly qtz-phyric end of unit with calcite veins, dissem py (<5%)
115.62m plag porphyritic dike

123.10m rusty brown massive sulfide containing banded to buckshot textured sp-po-cpy+/-gn (25-45%, 20-25%, <5%, <2%), blue qtz eyes present, mod chl and minor sil alt
Sample 62629
126.53m aph mafic dike with 10cm felsic volcanic raft
133.24m localized sp-cpy veins (5-10%; <2%) with mod chl+ser and minor sil alt
136.72m aph mafic dike
137.62m semi-massive to dissem bands of sp (10-15%) in first 3m of unit, blue qtz eyes, local semi-massive at 149.5m sp-py (15-20%; <10%), mod chl alt, highly siliceous with localized qtz veins

150.46m mafic dike that becomes lighter in color or bleached ~169m brick red QFP with lathy plag and greenish skarn-like intrusive - very alt, trace dissem py (<5%)
174.33m medium gray, pink gt-porphyroblast bt-rich volcaniclastic seds (?) with chocolate brown thinly laminated layers, qtz veins throughout with irregular whispy wavy shapes, few dark green chl bands, overall grainy appearance, trace dissem po-py (<5-10%)
Sample 62632
179.43m mafic dike with white lathy plag crystals/phenocrysts grading in and out

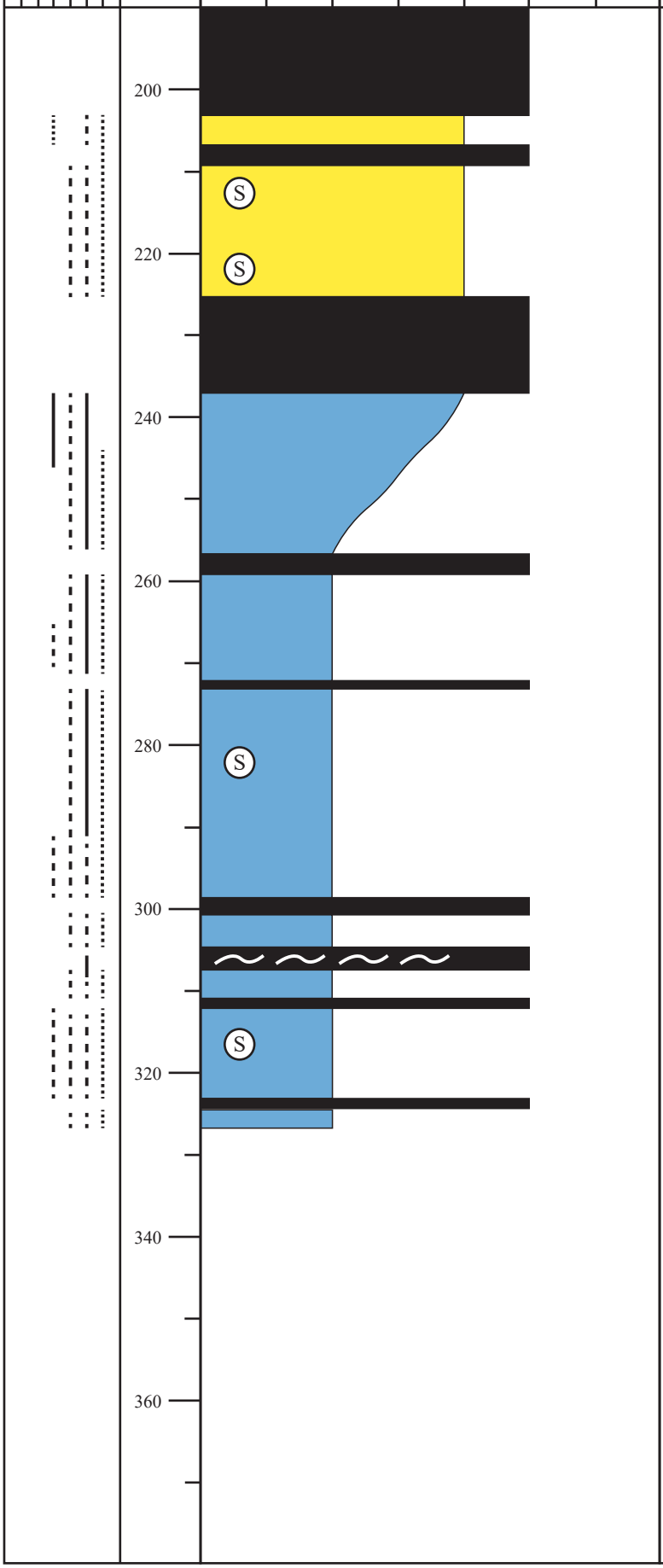

Project: Powderhorn Lake
Drill Hole: PH-18-40
Date:

UTM:
Azimuth, Dip:
Length:

203.96m light gray-pale green, highly siliceous bt-flow banded rhyolite with irregular dark wavy flow bands, mod alt by chl, mod foliated, minor milky qtz eyes

206.5m mafic dike with trace dissem py (<5%)

209.52m light-medium gray, fine-coarse grained massive rhy as above, mod alt by chl+ser with bluish qtz eyes, local sp-cpy (2-5%; <5%) with dissem py (<5%) throughout
Sample 62634, 62635

225.68m mafic dike with rafts of above unit

237m highly siliceous reddish brown, highly alt massive bt-spotted rhy with reddish elongate bands and dark green clasts - possible lapilli, micaceous minerals following moderate foliation, localized qtz veins to "layers"
~244m trace dissem cpy (<2%) appears along with po-py (<10%), bluish qtz eyes, end of unit is barren and looks fragmental - probable tuff

256.50m aph mafic dike

258.85m light gray-green, heavily alt bt-tuff strong chl, sparse blue qtz eyes, trace dissem py (<5%) throughout with minor trace sp (<5%) ~261.80m begin to see brownish red mottling 265-270m increase in qtz eyes, unit becomes more grainy

272.04m aph mafic dike

273.18m beginning of unit is dark and fine-grained rich in bt and chl (?) - heavily alt tuff, grades into characteristic siliceous pale green aphyric tuff, mod ser+chl alt, dissem trace py-sp (<5%)
Sample 62637

298.19m aph mafic dike

300.49m pale green, highly siliceous bt-tuff with localized 20-30cm qtz veins, tace dissem py (<5%)
304.31m bleached, crumbly, qtz-calcite veined mafic dike
307.48m same unit as above
310.49m aph mafic dike
312m highly siliceous, pale green tuff, mod foliated with trace dissem py (<5%)+/-po+/-sp following foliations - end of unit becomes grainy, minor qtz eyes
Sample 62639
323.02m aph mafic dike
324.27m disseminated py-sp-cpy (<5%) in qtz-eye tuff (would possibly continue minz)

326.50m EOH

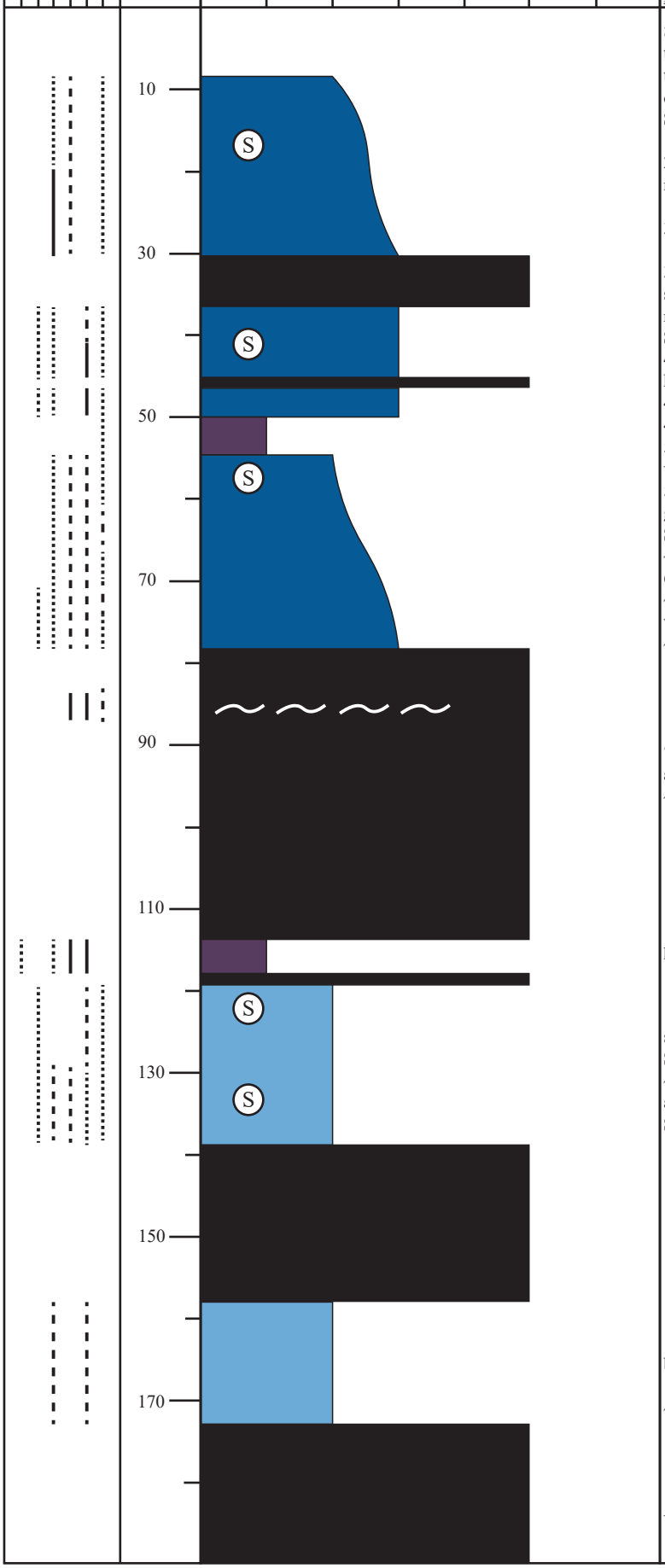

Project: Powderhorn Lake
Drill Hole: PH-18-42
Date: August 4, 2020

UTM: 564776E 5440218N (NAD83)
Azimuth, Dip: 360, -90
Length: 242m

8.57m first 40m very gradational, small sections of sediments, tuff, rhy hard to break-out units - light-medium gray, irregular banded-bedded bt-spotted tuff, moderately altered by ser, weakly foliated, minor qtz eyes, with trace disseminated py-po (<5%) - small sections of bt-metaseds
Sample 62697
19.82m light gray, highly siliceous qtz phyric rhyolite
25.44m dark gray, heavily altered volc. sediments to lapilli tuff with massive-thin reddish-brown beds, felsic white lapilli, py-po (5%)

30.21m medium gray, porphyritic plag dike, weakly mag

36.22m light-medium gray, bt-lapilli tuff with black chl, appearance of sillimanite and skarn-like veins, bands of chl, sparse qtz eyes, and disseminated po-py (<5%)
Sample 62698
42m half core of dissem bands and veinlets of po-py (up to 10-15% locally), heavy chl alteration, local sp and cpy (<2%)
45.62m medium gray dike as above, leucogranite ?
46.12m mineralization carries over, blue qtz eyes, felsic lapilli
50m dark massive sediemtns with disseminated py-po (<5%), localized qtz veins
55m light gray bt-spotted, qtz phyric tuff moderately alt by qtz+ser, with grainy bands of black chl repalced and filled with py+po, minor qtz eyes
Sample 62699
~58m clasty lapilli or chl being replaced by py+po
62m local matrix-fill sp band (20-25%), increase in dissem cpy for 30cm
~72m local massive banded py-po, gray qtz-phyric irregular chl banded tuff with minor sil alt, crenulations and small folds visible, minor qtz eyes
~73m increase in cpy and po in bands and streaks

78.04m dark gray, aph mafic dike, greenish buff cast ~84.25-87m heavily altered felsic volcanic, strong chl, py-po (<5%) +/- local sp (<5%)
~85.77-89m very broken core, rusty oxidation (fault/fracture zone)

113.97m dark, massive to strongly altered sediments with thin bt-bands, presence of zoned veins, barren in sulfides
118m black aph mafic dike

119.5m medium gray, bt-spotted tuff with whispy white sillimanite veins, sparse qtz eyes (milky), disseminated po-py trhougout (<5%)
Sample 62700
~130m lighter colored, qtz phyric bt-spotted tuff with increase in ser and qtz and less chl alteration, less prominent qtz eyes
Sample 62701

139.10m medium gray, porphyritic plag and pyroxene dike, non-mag

158.02m medium-dark gray, grainy qtz phyric tuff, moderate chl alteration, blue qtz eyes present

~170m increase in bt

173.38m mixed section of black aph mafic dikes with minor rafts of felsic volcanic and QFP rhyolite dikes

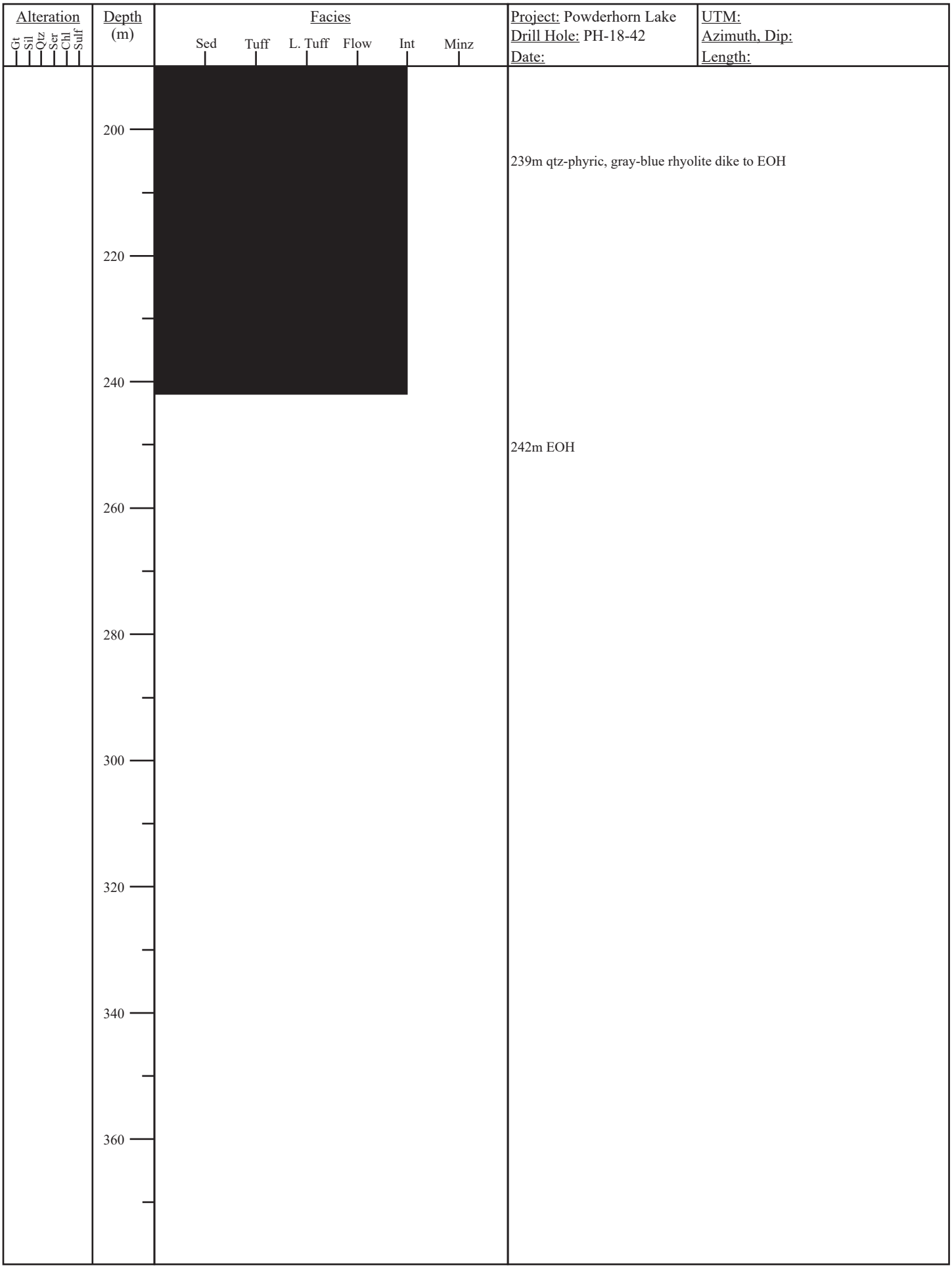
Alteration
Gt
Sil
Qtz
Ser
Chl
Sulf
Depth
(m)
Facies
Sed
Tuff
L. Tuff
Flow
Int
Minz
Project: Powderhorn Lake
Drill Hole: PH-18-42
Date:
UTM:
Azimuth, Dip:
Length:
200
220
240
260
280
300
320
340
360
239m qtz-phyric, gray-blue rhyolite dike to EOH
242m EOH

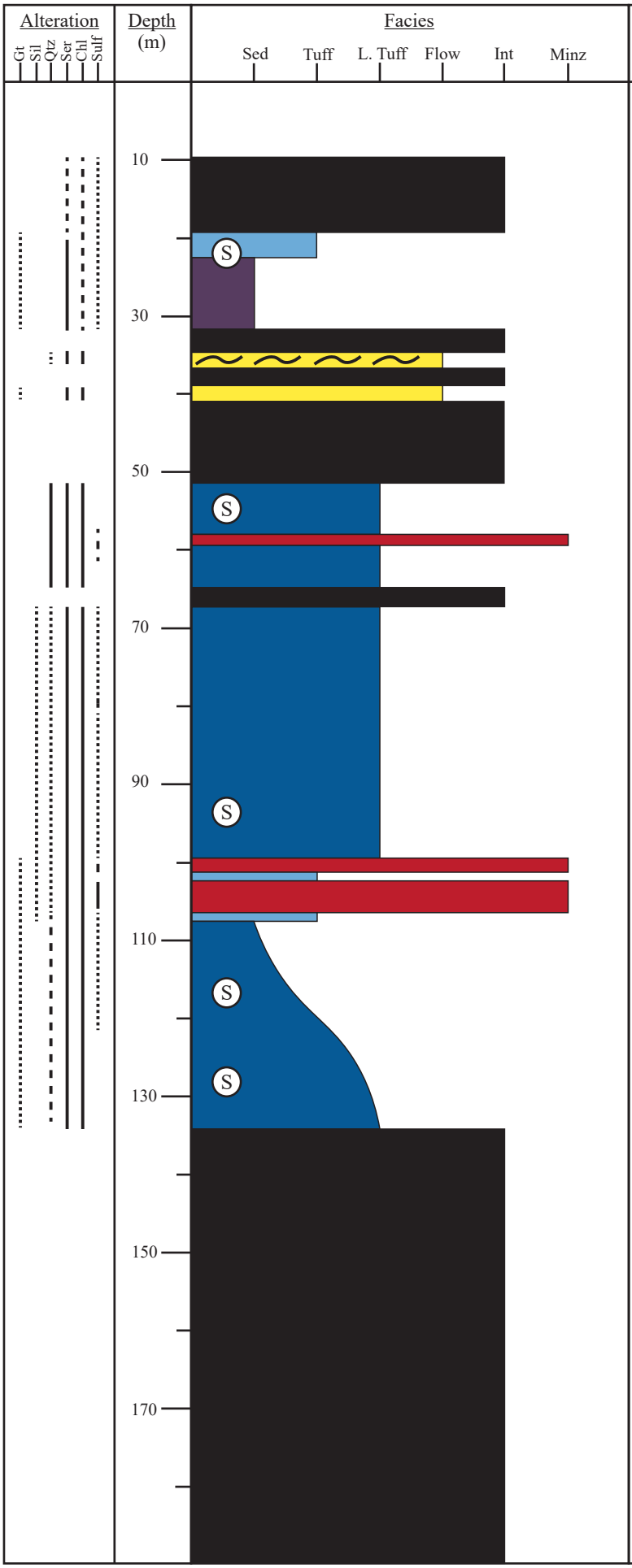

Project: Powderhorn Lake
Drill Hole: PH-18-44
Date: August 3, 2020

UTM: 564641E 5440368N (NAD83)
Azimuth, Dip: 360, -90
Length: 244.35m

9.90-13m fine-grained bt-plag porphyritic andesitic dike moderately altered by chl+ser, with euhedral py crystrals disseminated throughout (<5%)
13m medium gray QFP, weakly mag
19.79m light-medium gray, qtz phyric bt-spotted tuff with zoned veins
Sample 62692
22.47m darker gray than unit above, qtz-phyric sediments heavily alt by chl and moderately by ser+qtz, altered gts and opq white calcite, weak-moderately foliated, zoned veins, disseminated vein-fill po+/-trace sp (<5%)
32m black aph mafic dike, weakly mag
34.5m rusty, strong ser and chl altered fault zone, minor qtz eyes
36.4m black aph mafic dike, weakly mag
38.7m heavily altered massive rhyolite with zoned veins, minor albite ?

40.82m gray, aph to fine-grained dike, strongly mag
51.34m light gray lapilli tuff moderate-strongly altered by ser+chl+qtz, clasty black chl altered lapilli, presence of zoned veins, minor sparse qtz eyes (milky)
Sample 62693
57.5m vein-hosted red, orange, and honey sp (10%), localized veins - disseminated sp until 62m

64.9m black plag porphyritic dike

67.27m medium gray, grainy tuff with moderate-strong chl+ser alteration, weak-moderate foliation, not-prominent qtz eyes, crenulations, clasty black lapilli, chlorite zoned by sillimanite, trace veinlet-foliation hosted po+/-sp (<5%)
78-78.4m disseminated matrix-fill cpy (<10%) - returns to grainy, bedded bt-spotted tuff, strong ser, clasty lapilli altered by dark chl

Sample 62694
99.12m halved core, clasty, deformed/crenulations hosting semi-massive vein-matrix-fill po-py-sp-cpy in gt porphyroblast bt-tuff

101.52m bt-rich rhyolite tuff, minor qtz-crystals and gt porphyroblasts
102.13m best cpy-sp stringers, felsic lapilli +/- breccia frags
103.42m tuff unit as above - end of unit red, brown, honey colored sp-rich (10-15%)

107.58m dark gray, thinly bedded gt porphyroblast sediments with lots of altered zoned veins, trace disseminated po (<5%) - end of unit appears to be brecciated with trace veinlets of po+/-sp (<8%), grading into tuff

112.13m dark gray, grainy bt-spotted tuff with strong chl+ser alteration, with zoned veins, qtz eyes (milky) ~120m grades into red/green mottled, highly siliceous qtz-phyric tuff with dark clasty lapilli, qtz eyes decrease down unit
Sample 62695, 62696

134.05m black plag porphyritic dike, slightly mag

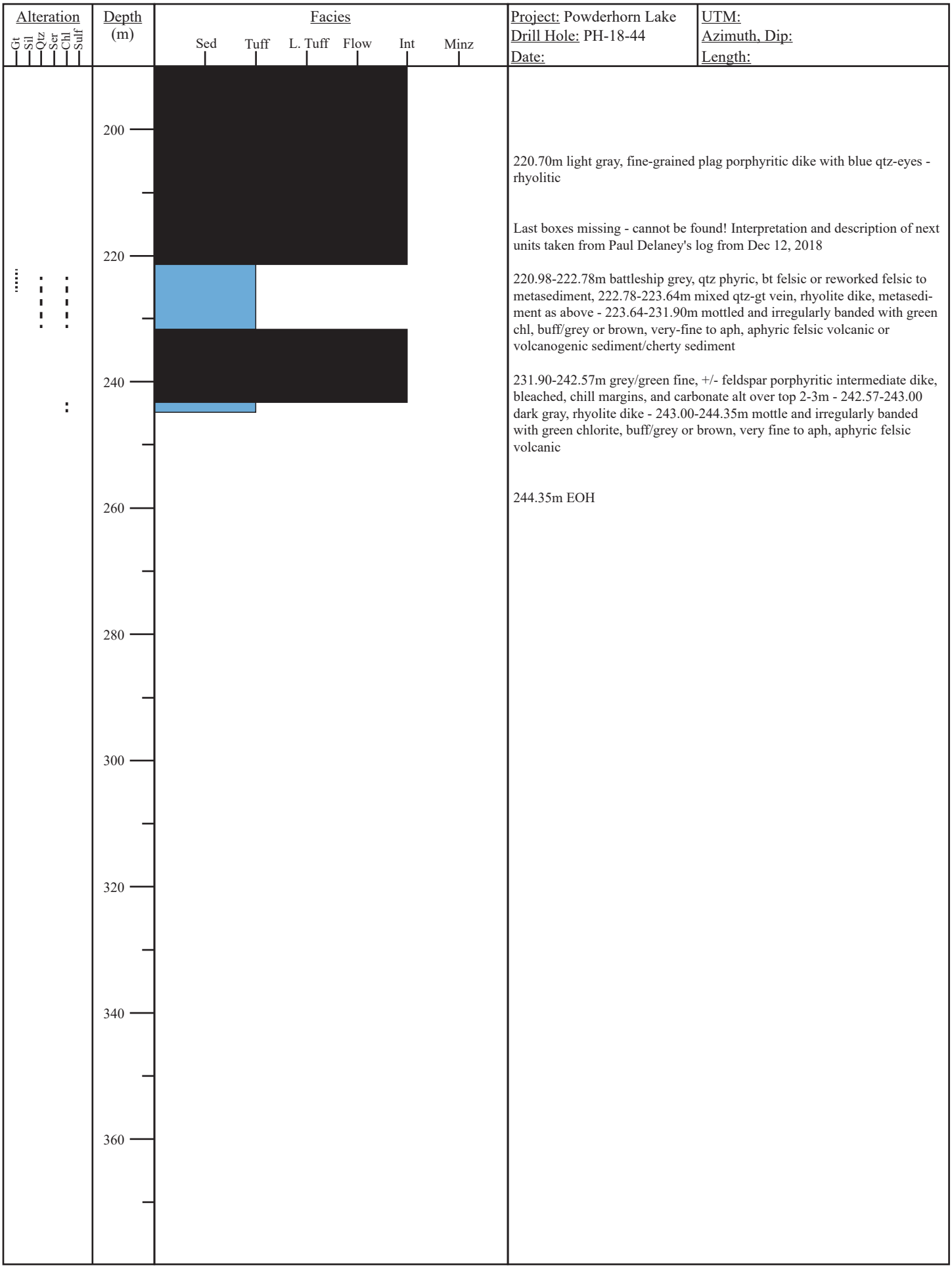

Project: Powderhorn Lake
Drill Hole: PH-18-44
Date:

UTM:
Azimuth, Dip:
Length:

220.70m light gray, fine-grained plag porphyritic dike with blue qtz-eyes - rhyolitic

Last boxes missing - cannot be found! Interpretation and description of next units taken from Paul Delaney's log from Dec 12, 2018

220.98-222.78m battleship grey, qtz phyric, bt felsic or reworked felsic to metasediment, 222.78-223.64m mixed qtz-gt vein, rhyolite dike, metasediment as above - 223.64-231.90m mottled and irregularly banded with green chl, buff/grey or brown, very-fine to aph, aphyric felsic volcanic or volcanogenic sediment/cherty sediment

231.90-242.57m grey/green fine, +/- feldspar porphyritic intermediate dike, bleached, chill margins, and carbonate alt over top 2-3m - 242.57-243.00 dark gray, rhyolite dike - 243.00-244.35m mottle and irregularly banded with green chlorite, buff/grey or brown, very fine to aph, aphyric felsic volcanic

244.35m EOH

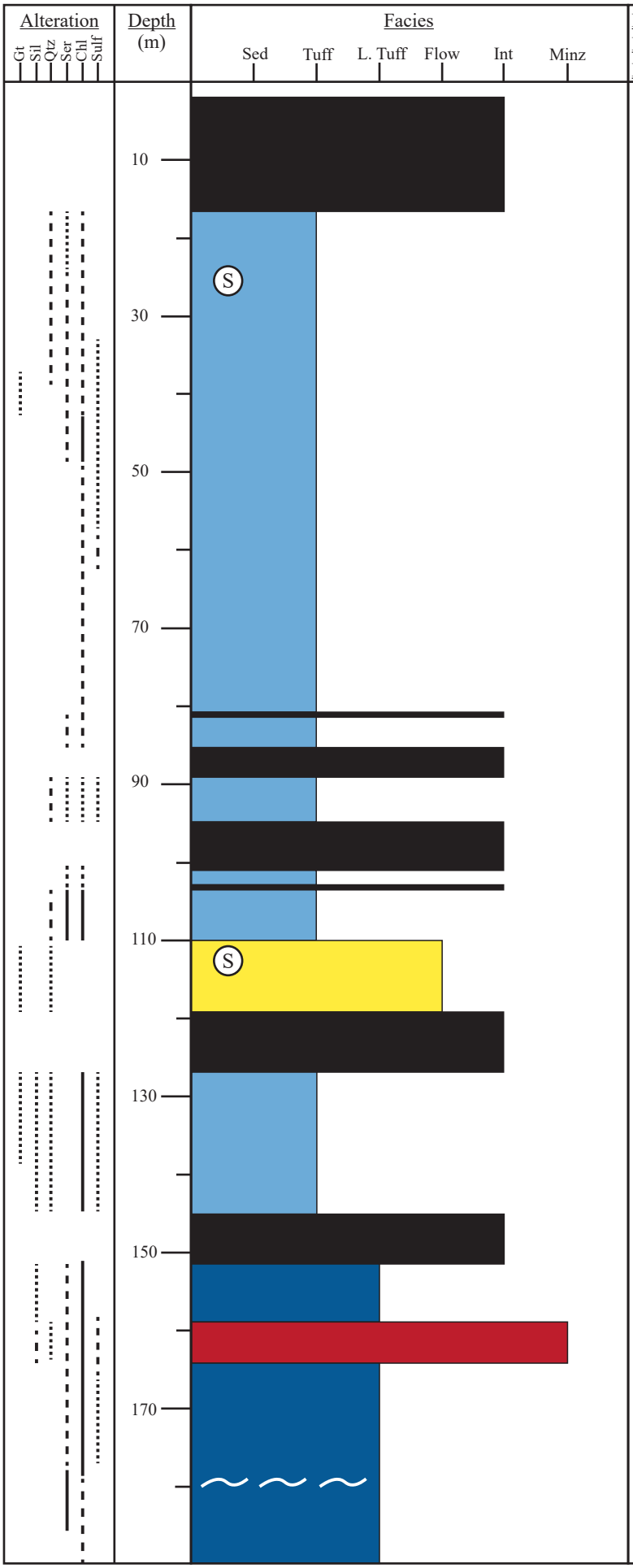

Project: Powderhorn Lake
Drill Hole: PH-19-09
Date: October 1, 2020

UTM: 564447E 5440732N (NAD83)
Azimuth, Dip: 135, -65
Length: 292m

2m medium-dark gray, plag and bt porphyritic andesitic dike with large (2-4mm) equigranular plag phenocrysts, and flakey-patchy anhedral bt phenocrysts - cut by aph mafic dike - both are slightly mag

16.38m medium-dark gray, fine-grained qtz phryic qtz-crystal tuff, qtz-crystals are ghosty white, minor bt, moderately chl and weakly ser altered, lighter siliceous bt-patches or beds in darker colored tuff
~24m looks to have flow-crenulated texture and boudinaged qtz veins, qtz phenocrysts begin to disappear
~25m increase qtz, decrease bt, increase apple green ser with red/pink mottling
Sample 62764
33m after <1m aph mafic dike - silicified pink mottled and patchy mineralized tuff with minor milky qtz eyes, black chl veinlets and qtz veins, minor disseminated blebs of po (<3%) +/- cpy (<2%), boundaries of qtz veins can see gn (<2%)
36m halved core with minor po stringers (<10%)

39m light gray with pale green cast tuff with network pattern black chl veinlets, large very altered gt-ser-ep-qtz-veins, minor disseminated blebs of po (<3-5%)
43m increase in bt, becomes darker in color but has same texture - larger olive green ser patches or fine-grained chl (stockwork alteration?) until 48.25m - returns to light gray siliceous tuff or aphric rhyolite with black chl veinlets, localized patch of po (30%) at 59m, bt roughly 10% that continues down unit

~78.5m rocks have red-brown cast

80.64m black aph mafic dike, slightly mag
81.45m siliceous tuff like above, becomes fine-grained and sericitic with zoned gt-veins near dike
85.68m black aph mafic dike, slightly mag
89.6m qtz-crystal tuff, minor ser+chl alteration, minor po blebs on fractures (<2%)
94.75m dark gray-black, aph mafic dike, slightly mag
101.06m darker-medium gray of unit above, moderate ser+chl
102.6m black aph mafic dike, slightly mag
103.54m beginning looks like characteristic qtz-crystal tuff but grades into very olive green sericitic/chl? cast - somewhat grainy and fine-grained

110m original texture is lost - massive rhyolite ? with zoned gt-ep-qtz-veins and minor presence of milky qtz eyes
Sample 62766
119.45m black aph mafic dike, slightly mag

126.53m light gray, siliceous bt-spotted tuff with dark brown/red mottling-bands, into dark fine-grained strongly chloritic possible sediments (?) in-and-out interbeds of bt-spotted tuff within darker "sed" sections - with zoned gt-ser-ep-qtz veins, minor disseminated blebs of po (<3%)
139.5m begins to look more like aphyric red/green mottled rhyolite or aphyric tuff with patchy bt-chl and whispy white sillimanite, sparse bluish qtz eyes
145.4m mixed dike section with <1m rhyolite/tuff sections, - black aph mafic dike, slightly mag
151.65m light-medium gray, fine-grained to aphyric siliceous and irregular whispy bands, local fine felsic lapilli, moderately altered by ser (white-light green fibrous - maybe amphibole?) and chl (dark green-black), few altered gts, sparse qtz eyes
159m half core into net-textured to whispy bands and veinlets sp+/-cpy stringer zone (up to 20-30% sp; <2% cpy), qtz eyes and sillimanite throughout minz

- past 165m primarily po-py+/-sp+/-cpy stringers, strong black chl alteration zone

~178m bleached and highly sericitic fault zone, breccia, calcite veins

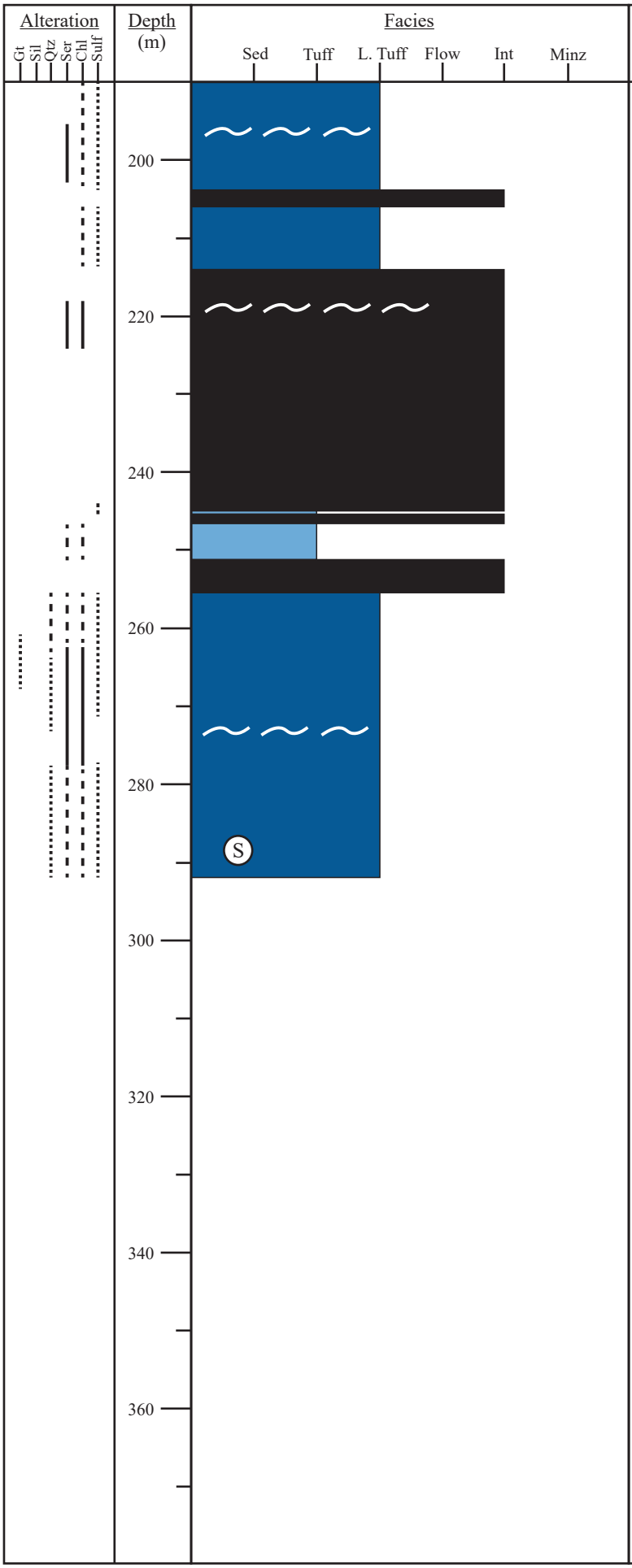

Project: Powderhorn Lake
Drill Hole: PH-19-09
Date:

UTM:
Azimuth, Dip:
Length:

~186m felsic lapilli, blue qtz eyes, dissem py-po, black chl still present
~191m lots of py-po patches and bads, increase in ser
~196m fault zone becomes extremely crumbly and clayey, bleached, highly altered by ser, disseminated patchy py-po throughout and trace sp (<2%)
204.8m mafic dike

206m as above, trace sp (<5%) associated with black chl, some dissem po-py

214m not faulted, black aph mafic dike with lots of calcite veins

219-224 highest damage, brecciated core - brownish green+yellow ser+chl+cal+ep, extremely crumbly, chalky, and clayey

244.9m tuff with local sp (10-15%) and disseminated py blebs (<5%)
245.82 black aph mafic dike
247.55m light gray siliceous tuff moderate chl+ser alteration

251.61m black aph mafic dike

255.65m mixed section of lapilli tuff, tuff, +/-flow
light gray, fine-grained qtz phyric bt-spotted lapilli tuff, fine felsic lapilli, weak-moderate ser+chl, sparse qtz eyes, disseminated blebs and veinlets of sp +/ gn (<2-5%)
~262.5m darker, fine-grained to aphyric tuff-rhyolite with olive green and fibrous ser/chl cast, overall rock has "camo" texture with disseminated patches to whispy bands of po-py or py-po (locally up to 20%), trace sp, sparse blue qtz eyes and zoned gt veins
~274.5m another crumbly fault zone until 278.5m with highly sericitic rhyolite? or silicified alt tuff - lots of crenulations before and after zone - rest of unit is dark-medium gray, fine-grained siliceous irregularly banded tuff to lapilli tuff, sparse milky qtz eyes, disseminated trace po-py stringers (<5%)
Sample 62767

292m EOH

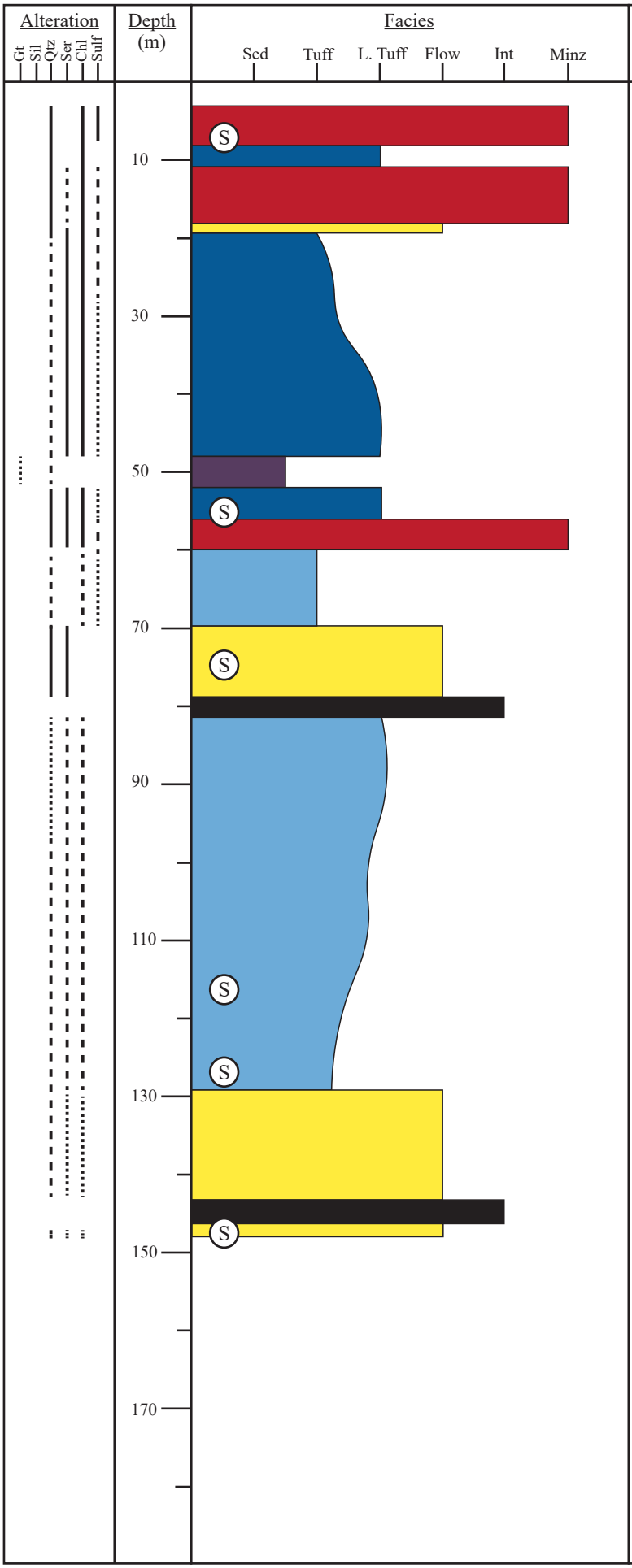

Project: Powderhorn Lake
Drill Hole: PH-19-10
Date: October 2, 2020

UTM: 565060E 5440204N (NAD83)
Azimuth, Dip: 360, -90
Length: 148m

2.63m light gray, qtz phyric siliceous tuff with sparse blue qtz eyes, felsic lapilli, hosting py-cpy and sp-cpy+/-po stringers beginning at 3.56m rusty semi-massive py-cpy (40-50% py; <2-3% cpy) into net-textured, crenulated/deformed sp-py+/-cpy (25-30% sp/py; <5% cpy), mineralization follows crenulation

Sample 62768

8m same as above, minus mineralization

10.3m unit becomes predominantly disseminated po-py to semi-massive stringers of sp-cpy, sparse qtz eyes still present, white whispy sillimanite

18m becomes slightly darker - overall still light gray with red/green mottling, possible flow with remnant flow banding and moderate-strong ser+chl alteration, bluish qtz eyes with disseminated to bleb py-po (<10% and locally to 20%; po <10-15%), sparse bt/chl, minor crenulations

19.68m more tuffaceous - light gray-pale green qtz-eye fine-grained altered tuff with moderate-strong ser+chl alteration, bluish qtz eyes with disseminated to bleb py-po (5-7%), sparse bt/chl, minor crenulations, felsic lapilli towards end of unit

48m very dark, fine-grained, thinly laminated sediments with small pink gt porphyroblast, qtz-phyric, and thin interbeds of bt-tuff

52.04m green, siliceous, irregular banded lapilli tuff, moderate-strongly altered by chl+ser, sparse qtz eyes, trace disseminated whispy bands of py (<5%)

Sample 62769

56m half core of light gray, siliceous, irregular wavy banded qtz phyric tuff with blue qtz eyes, po-py+/-sp-cpy (up to 10-15% locally and <10% disseminated throughout)

60m red/green mottled tuff with sparse qtz eyes, primarily po-py (<5%) stringers and local, trace cpy and sp (<3%) down unit

69.95m light beige-green, cherty and highly siliceous rhyolite moderate to strongly altered by ser

Sample 62770

78.4m medium gray plag and hornblende porphyritic dike

81.93m tan-pale green, fine-grained-aphyric highly siliceous lapilli tuff, moderate ser+chl alteration, sparse qtz eye and thin opq lapilli

~82.20 very dark, fine-grained 1-2cm black rounded clasts - selective alteration around lapilli

96.47m brown and grainy, fine-grained, qtz phyric tuff to lapilli tuff with blue qtz eyes, disseminated veinlets-whispy network of po-py+/-sp+/-cpy (<5-8%)

98.02m red and green mottled, qtz phyric bt-spotted tuff moderately altered by ser

Sample 62771

~126.73m dark, fine-grained and fibrous looking possible altered tuff or sediments with lots of white qtz-eyes - black fibrous veins possible altered glass?

Sample 62772

129.4m returns to light-medium gray, red/green mottled, irregular banded, siliceous and qtz phyric rhyolite with po (<5%) in whispy bands to patches/blebs

143.77m medium gray plag and hornblende porphyritic dike

146.08m less altered version of above unit, trace cpy (<1-2%)

Sample 62773

148m EOH

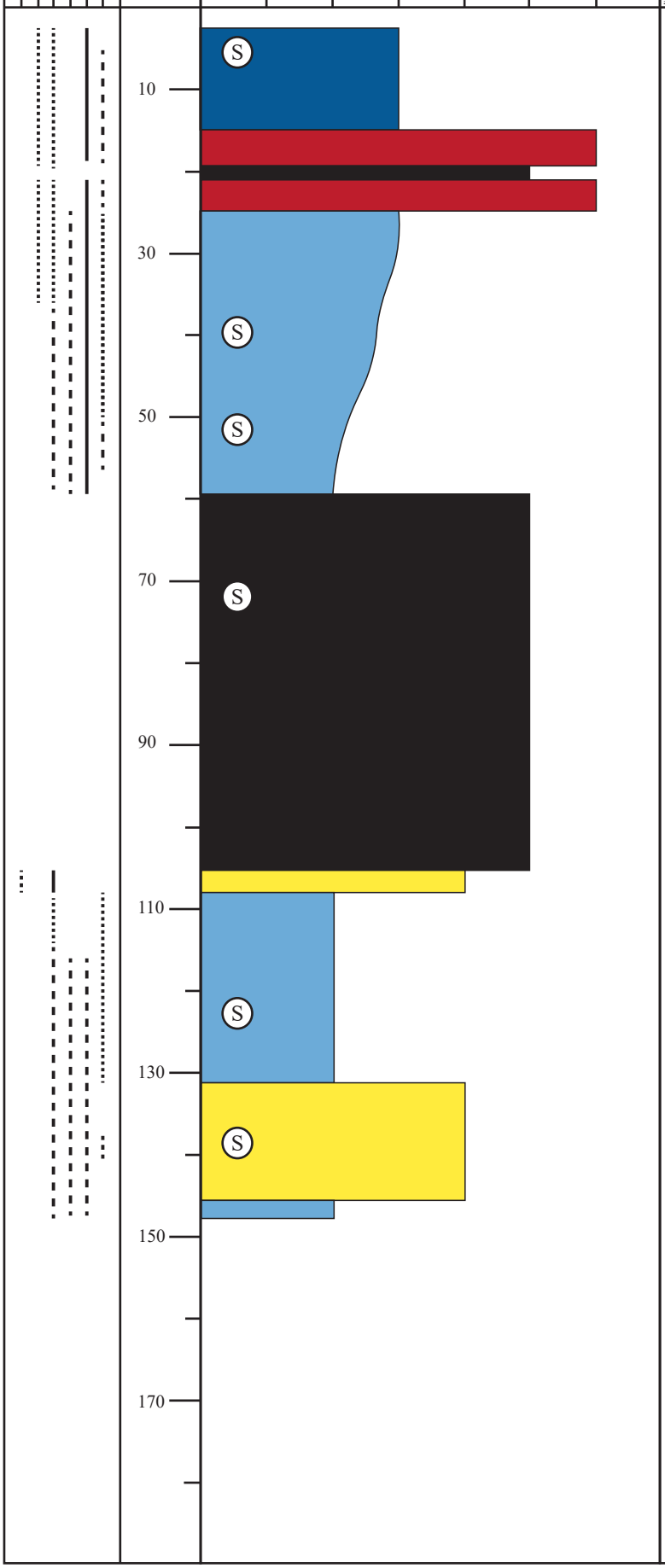

Project: Powderhorn Lake
Drill Hole: PH-19-11
Date: September 30, 2020

UTM: 564985E 5440137N (NAD83)
Azimuth, Dip: 360, -90
Length: 148m

2.46m light-medium gray, aphyric-fine-grained dark-banded lapilli tuff mod to strongly altered by chl and moderately by ser, whispy white silimanite and bluish qtz eyes present, predominantly sp-py+/-cpy (<5-8% sp; <5% py; <2% cpy) net-textured stringers

Sample 62753

11.72m very dark, fine-grained bt-spotted tuff, grainy, trace py

14.81m light gray, bt-spotted tuff/lapilli tuff with cpy-sp-py disseminated to semi-massive net-textured stringers (<15-20% cpy; <10% sp; <10% py), moderate-strong gray/green chl, sparse qtz eyes, whispy white sillimanite, and patchy bt

19.4m black aph mafic dike, non-mag

20.07m light gray, fine-grained-aphyric tuff stringer zone of po-cpy with local, moderate sp and grading into po-py-cpy, more po than py

24.64m sulfide stringers sporadic - po-py+/-cpy (<1-2%) whispy white sillimanite appears, sparse blue qtz eys, moderate-strongly altered by chl and moderate ser alteration

~28m better sulfide bands and zones

~36m darker, aphyric tuff with irregular to barely visible banding, fine lapilli, highly siliceous, sparse large qtz eyes, disseminated po-py-sp-cpy stringers fades downhole

~39m camo-textured qtz-phyric tuff, patchy moderate chl+ser altertaion, whispy white sillimanite

Sample 62755, 62756

53.64m po-py-cpy+/-sp stringers and semi-massive po-py-cpy-sp (<15% po; <10% py; <10% cpy; <5% sp), lots of qtz eyes, chl still present, no felsic lapilli - end of unit qtz-phyric with gt porphyroblasts

59.85m black aph mafic dike, slightly mag

Sample 62757

~80m plag porphyritic dike grades in and out by 83m, slightly mag

105.5m beginning of unit light-medium gray, red/green mottled massive to flow banded rhyolite or silicified tuff ?, localized pink gt porphyroblasts, sparse qtz eyes

108m halved core with minor sp (<5%) stringers and local cpy veinlets-bands (<5%) dark, fine-grained qtz phyric qtz-bt crystal stuff with prominent qtz eyes, localized patchy bt, predominantly altered by chl, disseminated blebs-whispy bands of py-po+/-cpy (<2%), crenulated in part - seeing silvery lusterous micaceous mineral on fractures - possible muscovite ? - brownish/green in overall color

Sample 62758

131.61m light-medium gray/pale green and red/green mottled, highly siliceous bt-spotted massive rhyolite, weakly foliated, moderate fibrous ser+chl alteration, bluish qtz eyes, large local qtz veins

Sample 62759

138.44-138.59m local semi-massive sp-cpy (up to 40% sp; <5% cpy)

145.55 dark, fine-grained qtz-phyric qtz-bt crystal stuff with prominent qtz eyes, localized patchy bt, predominantly moderately altered by chl

148m EOH

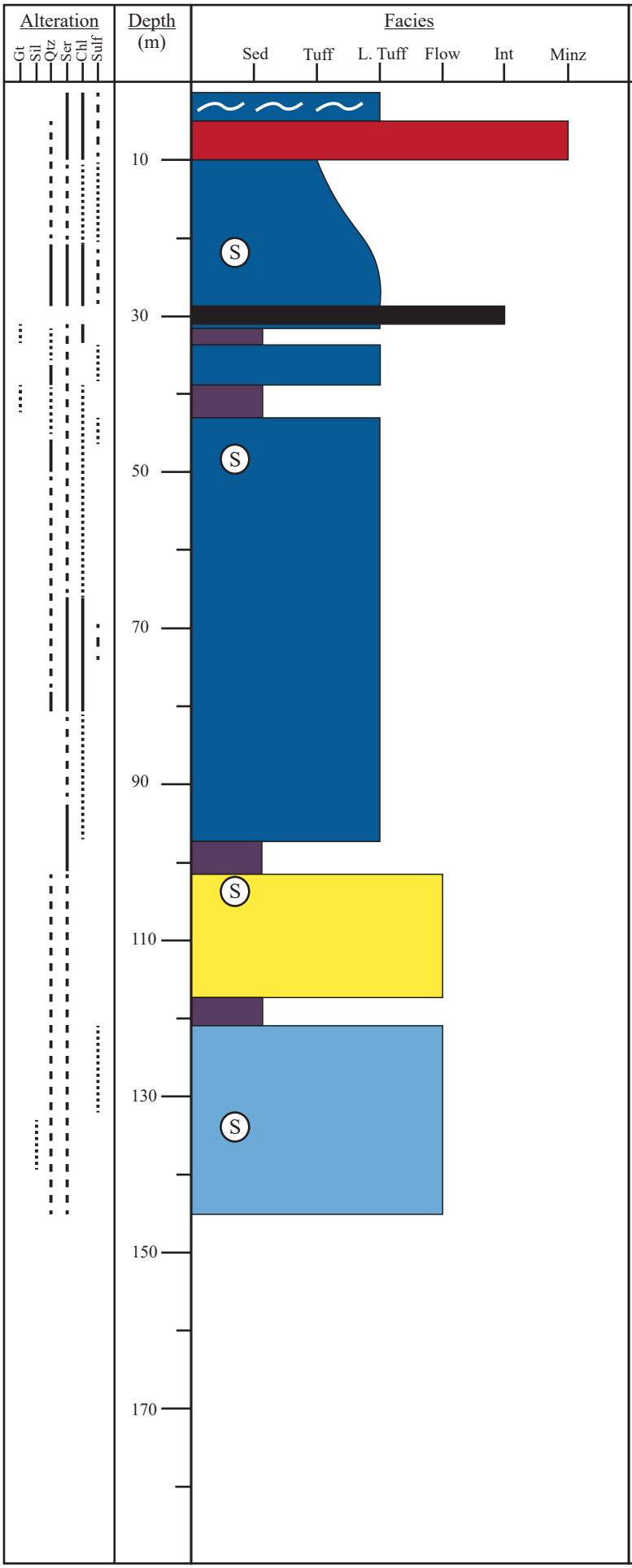

Project: Powderhorn Lake
Drill Hole: PH-19-12
Date: October 2, 2020

UTM: 565136E 5440271N (NAD83)
Azimuth, Dip: 360, -90
Length: 145.25m

1.86m gray and rusty orange, faulted unit of possible qtz phyric lapilli tuff with extreme ser alteration and minor sp-cpy and po-py stringers
5.5m dark gray, qtz phyric qtz-crystal tuff with blue qtz eyes and oxidized orange clay/ser-altered veins, broken/crumbly rock, local po-cpy (<5-8%) stringers
10m grades into pale green and red mottled, silicified bt-spotted tuff altered moderately by ser and weakly by chl, with crenulations and disseminated po-py (<10%)
20m sp-py+/-cpy (locally up to <10%) stringers hosted in irregular banded tuff to lapilli tuff with lots of qtz veining and fracutres, heavily altered by ser+chl, qtz eye rich, crenulations in part
Sample 62741
28.86m black aph mafic dike, magnetic
30.15m possible silicified unit of above
31.1m dark, fine-grained, thinly laminated gt-metasediments, layers look fibrous, ser veins and qtz eyes in part
33.76m medium gray, grainy bt lapilli tuff moderately altered by ser, local felsic lapilli and patches of coarse bt replace by minor sp+/-cpy (<5%), grading into aphyric, red/green mottled aphyric silica alt tuff ?
Sample 62742
38.83m same seds as unit above - less gt porphyroblasts, large qtz veins

42.94m dark gray-green qtz phyric lapilli tuff tuff with blue qtz eyes and po-py+/-sp-cpy (<5-8%) in thin beds to to veinlets, mod chl, ~45m 1.5m of orangey-brown oxidized stringers
46.3m red/green mottled highly siliceous qtz phyric tuff with coarse patchy bt, sometimes replaced by sp ~53m dark irregular banding/texture is lost - silicified, homogenous, cream colored, bt (returns at 54m)

~69m dark gray, clasty bt and chl-rich lapilli tuff, minor qtz eyes - difference in texture grades out by 71m

71m pale green highly siliceous, qtz eye phyric with disseminated oxidized po-py+/-sp+/-cpy (<10%) stringers, beginning of unit has local felsic lapilli and grades into gray, aphyric tuff to lapilli tuff, grainy with local lapilli zones, disseminated po-py and trace sp - end of unit is silified and strongly sericite alt
97.75m dark gray to splotchy green+yellow, highly altered metaseds with network veining ser
101.7m light gray with pale green cast and red mottled, qtz phyric massive bt-rhyolite - no real banding, bt (<15%), relatively barren but minor po stringers (<5%), lots of qtz veining
Sample 62743
117.64m dark, fine-grained, thin bedded bt-rich sediments with qtz eyes and green fibrous ser of fine-grained chl alteration

120.93m light gray and pale green, aphyric highly siliceous tuff moderately altered by ser, sparse blue qtz eyes and trace disseminated blebs-veinlets of po-sp-cpy (<2-4%) ~133m appearance of minor whispy white sillimanite ~137m becomes slightly grainier - start to see clasty banding, black glasses?, minor qtz eyes to end of unit
Sample 62744

145.25m EOH

Appendix B: Table B.1.1 Whole-rock Geochemistry and Terraspec™ Data

Sample ID	62667	62668	62669	62670	62671	62673	62674
Hole ID	PH-18-01	PH-18-01	PH-18-01	PH-18-01	PH-18-01	PH-18-01	PH-18-01
Depth (m)	22.61	73.95	142.64	181.61	205	270.87	331.72
Lithology	Tuff	Xtl-Tuff	Rhyolite	Rhyolite	Lap. Tuff	Rhyolite	Xtl-Tuff
Stratigraphy	HW	HW	MS	MS	FW	FW	MS
Alteration	QS	QS	QSC	QSC+Sil	QSC+Sil	QSC+Sil	QSCPy+Sil
SiO_2 (wt. %)	78.51	71.28	78.83	79.43	73.59	56.00	82.17
Al_2O_3	12.02	14.95	12.16	11.40	16.61	22.99	9.13
Fe_2O_3	1.47	3.03	1.55	2.87	3.47	7.63	3.96
CaO	1.38	1.98	2.08	0.271	0.357	0.387	0.296
MgO	0.677	0.712	2.16	1.22	2.80	7.24	3.54
Na_2O	3.87	4.83	2.07	3.95	1.23	2.80	0.245
K_2O	1.94	2.67	0.893	0.693	1.58	2.35	0.316
Cr_2O_3	0.002	0.002	0.003	0.002	0.002	0.001	0.002
TiO_2	0.101	0.376	0.133	0.090	0.200	0.293	0.122
MnO	0.010	0.051	0.072	0.050	0.084	0.24	0.18
P_2O_5	0.01	0.1	0.01	0.01	0.03	0.02	0.01
SrO	0.1	0.1	0.1	0.1	0.01	0.02	0.01
BaO	0.01	0.02	0.03	0.02	0.04	0.03	0.02
LOI	0.250	0.800	0.820	1.25	3.18	4.01	1.93
Total	99.22	99.14	98.24	100.8	98.30	99.72	100.0
C	0.40	0.070	0.030	0.030	0.060	0.040	0.040
S	0.13	0.74	0.16	0.70	1.1	1.9	0.94
Ba (ppm)	74.8	156	272	188	370	316	153
Ce	14.0	13.6	13.8	17.3	23.8	22.9	13.9
Cr	20	10	20	10	20	10	20
Cs	0.42	0.27	0.94	0.43	1.9	1.5	0.41
Dy	9.66	6.55	9.73	11.80	13.3	12.6	6.14
Er	6.78	4.84	6.73	8.39	9.43	9.56	4.41
Eu	1.2	1.3	1.1	1.1	2.0	2.2	1.1
Ga	10.9	15.2	13.0	14.9	17.7	23.2	12.2
Gd	7.4	5.6	6.6	8.2	9.7	10	5.4
Ge	<5	<5	<5	<5	<5	<5	<5
Hf	4.2	3.1	3.7	4.7	4.6	6.5	3.1
Ho	2.2	1.5	2.0	2.7	2.9	2.7	1.3
La	5.1	5.4	5.2	6.4	9.3	9.1	5.3
Lu	1.2	0.73	1.1	1.4	1.5	1.7	0.73
Nb	1.3	1.5	1.1	1.3	1.7	2.4	1.2
Nd	12.9	10.7	12.2	16.1	19.1	18.8	11.8
Pr	2.2	2.0	2.2	2.8	3.4	3.4	2.1
Rb	13.2	14.3	11.9	5.90	15.3	22.9	3.30
Sm	5.0	3.8	4.2	6.1	6.6	7.1	4.3
Sn	1.0	1.0	1.0	1.0	1.0	2.0	1.0
Sr	81.3	57.4	91.7	43.0	89.6	173.5	53.9
Ta	0.1	0.1	0.1	0.2	0.2	0.2	0.1
Tb	1.4	0.93	1.2	1.6	1.8	1.7	0.87

Sample ID	62667	62668	62669	62670	62671	62673	62674
Hole ID	PH-18-01	PH-18-01	PH-18-01	PH-18-01	PH-18-01	PH-18-01	PH-18-01
Depth (m)	22.61	73.95	142.64	181.61	205	270.87	331.72
Lithology	Tuff	Xtl-Tuff	Rhyolite	Rhyolite	Lap. Tuff	Rhyolite	Xtl-Tuff
Stratigraphy	HW	HW	MS	MS	FW	FW	MS
Alteration	QS	QS	QSC	QSC+Sil	QSC+Sil	QSC+Sil	QSCPy+Sil
Th	1.7	1.3	1.4	1.6	1.6	1.6	0.84
Tm	1.1	0.71	1.0	1.2	1.4	1.4	0.60
U	0.65	0.62	0.61	0.61	1.9	0.68	0.30
V	<5.00	8.00	5.00	6.00	18.0	17.0	6.00
W	<1.0	1	<1.0	<1.0	1	<1.0	<1.0
Y	60.9	39.5	57.8	74.7	80.6	77.9	37.9
Yb	7.62	5.14	7.32	8.99	10.1	10.6	4.19
Zr	112	88.0	99.0	118	128	181	85.0
As	1.0	5.4	0.60	1.3	1.8	1.2	1.8
Bi	0.03	0.1	0.1	0.6	0.2	0.8	0.3
Hg	<0.005	<0.005	<0.005	0.1	0.1	0.02	0.1
In	0.1	0.1	0.1	1	0.3	0.5	1.5
Re	<0.001	<0.001	0.002	0.001	0.002	0.01	0.001
Sb	0.1	0.1	0.1	0.1	0.1	0.1	0.1
Se	<0.2	<0.2	<0.2	0.3	0.2	0.2	<0.2
Te	0.02	0.1	0.02	0.4	0.1	0.1	0.1
Tl	0.04	0.03	0.4	0.1	0.1	0.4	0.1
Ag	<0.50	<0.50	<0.50	<0.50	1.5	1.1	<0.50
Cd	<0.50	<0.50	<0.50	12	3.1	<0.50	1.1
Co	1.0	<1.0	<1.0	<1.0	1.0	2.0	<1.0
Cu	7.000	7.000	15.00	82.00	76.00	61.00	624.0
Li	10	10	20	10	20	90	30
Mo	1.0	2.0	2.0	4.0	5.0	2.0	2.0
Ni	1.0	<1.0	2.0	1.0	2.0	1.0	1.0
Pb	10.0	2.00	41.0	8.00	231	49.0	10.0
Sc	19.0	18.0	13.0	23.0	9.00	20.0	7.00
Zn	58.000	119.00	80.000	1675.0	1005.0	689.00	530.00
AlOH WL (nm)	2198.5	2195.2	2204.9	2195.6	2197.7	2198.5	2195.2
AlOH Depth	0.1	0.05	0.2	0.2	0.4	0.1	0.05
FeOH WL (nm)	2248.4	2252.5	2247.3	2254.5	2247.5	2248.4	2252.5
FeOH Depth	0.1	0.1	0.1	0.1	0.2	0.1	0.1
AlOH depth/FeOH depth	1.3	0.66	1.5	1.8	1.9	1.3	0.66

Sample ID	62675	62676	62677	62678	62745	62746	62747
Hole ID	PH-18-01	PH-18-01	PH-18-01	PH-18-01	PH-18-04	PH-18-04	PH-18-04
Depth (m)	368	396.48	420.14	463	17.6	106	159.43
Lithology	Rhyolite	Lap. Tuff	Xtl-Tuff	Tuff	Tuff	Tuff	Rhyolite
Stratigraphy	MS	MS	FW	FW	HW	HW	HW
Alteration	QSC+Sil	QSC+Sil	QSC+Sil	QSC+Sil	QS	QSC+Sil	QS+Sil
SiO_2 (wt. %)	55.77	77.85	77.80	68.77	73.38	75.10	79.99
Al_2O_3	29.26	12.14	12.41	18.03	14.79	11.92	11.12
Fe_2O_3	7.31	3.56	3.01	2.58	2.05	3.15	1.58
CaO	0.359	0.492	0.184	1.12	0.962	0.900	0.975
MgO	2.14	2.79	2.33	1.38	2.03	0.940	0.700
Na_2O	2.94	1.69	3.45	4.39	1.58	2.64	2.93
K_2O	1.61	1.17	0.449	3.41	5.02	4.87	2.57
Cr_2O_3	0.001	0.002	0.002	0.001	0.002	0.002	0.003
TiO_2	0.338	0.133	0.255	0.163	0.130	0.336	0.102
MnO	0.16	0.12	0.061	0.071	0.030	0.049	0.020
P_2O_5	0.05	0.02	0.04	0.05	0.05	0.07	0.05
SrO	0.02	0.1	0.1	0.1	0.1	0.05	0.1
BaO	0.1	0.03	0.01	0.04	0.02	0.02	0.01
LOI	2.68	1.96	1.13	1.16	1.33	0.760	0.670
Total	97.36	99.58	99.07	99.61	101.1	101.8	99.18
C	0.020	0.060	0.030	0.040	0.020	0.040	0.020
S	2.3	0.21	0.77	0.35	0.070	0.66	0.31
Ba (ppm)	432	317	80.3	327	191	126	85.3
Ce	5.30	15.3	10.4	20.5	17.3	10.4	15.1
Cr	10	10	10	10	20	10	20
Cs	0.41	0.41	0.41	0.41	2.1	0.61	0.25
Dy	12.9	6.75	6.03	12.5	12.2	5.47	7.54
Er	10.8	5.52	4.45	9.19	9.05	3.55	4.91
Eu	1.1	0.74	0.65	1.8	1.4	0.85	1.0
Ga	25.3	13.6	12.7	20.0	16.8	14.0	10.8
Gd	6.1	5.0	4.5	9.2	8.4	4.0	5.3
Ge	<5	<5	<5	<5	<5	<5	<5
Hf	7.8	3.4	2.9	6.4	5.5	2.5	3.9
Ho	3.0	1.5	1.4	2.9	3.0	1.2	1.7
La	2.1	5.8	4.2	8.1	7.1	4.0	5.8
Lu	2.1	0.93	0.7	1.6	1.6	0.55	0.81
Nb	2.6	1.1	1.0	1.5	1.8	1.2	1.3
Nd	4.90	12.3	8.4	17.10	13.8	8.40	11.8
Pr	0.8	2.2	1.5	3.3	2.7	1.7	2.3
Rb	9.80	10.4	2.00	20.4	39.6	33.3	14.4
Sm	2.5	4.1	3.3	5.7	5.1	3.0	4.3
Sn	15	2.0	1.0	2.0	1.0	1.0	1.0
Sr	167.5	57.4	64.8	71.6	55.8	35.1	40.1
Ta	0.2	0.1	0.1	0.2	0.2	0.1	0.2
Tb	1.4	0.91	0.84	1.6	1.7	0.7	1.1

Sample ID	62675	62676	62677	62678	62745	62746	62747
Hole ID	PH-18-01	PH-18-01	PH-18-01	PH-18-01	PH-18-04	PH-18-04	PH-18-04
Depth (m)	368	396.48	420.14	463	17.6	106	159.43
Lithology	Rhyolite	Lap. Tuff	Xtl-Tuff	Tuff	Tuff	Tuff	Rhyolite
Stratigraphy	MS	MS	FW	FW	HW	HW	HW
Alteration	QSC+Sil	QSC+Sil	QSC+Sil	QSC+Sil	QS	QSC+Sil	QS+Sil
Th	1.9	1.3	0.70	2.1	1.5	1.0	0.88
Tm	1.7	0.84	0.74	1.3	1.5	0.56	0.77
U	0.87	0.54	0.38	0.66	0.79	0.68	0.47
V	6.00	<5.00	45.0	11.0	24.0	8.00	<5.00
W	6	<1.0	1	1	1	1	1
Y	90.9	42.2	38.6	78.8	83.1	30.0	44.8
Yb	12.4	6.07	5.04	10.1	10.8	3.76	5.44
Zr	226	106	77.0	166	147	74.0	100
As	1.0	0.60	0.50	1.0	1.0	3.4	0.60
Bi	3	0.2	0.3	0.1	0.1	0.1	0.04
Hg	0.1	0.006	0.04	<0.005	<0.005	<0.005	<0.005
In	0.8	0.1	0.1	0.1	0.1	0.1	0.03
Re	0.001	0.001	<0.001	0.001	0.004	<0.001	<0.001
Sb	0.1	0.1	<0.05	<0.05	0.1	0.1	0.1
Se	0.4	<0.2	0.2	0.2	<0.2	<0.2	<0.2
Te	0.4	0.1	0.3	0.1	0.03	0.1	0.01
Tl	0.03	0.04	<0.02	0.02	0.1	0.1	0.03
Ag	3.4	<0.50	<0.50	<0.50	<0.50	<0.50	<0.50
Cd	4.6	<0.50	<0.50	<0.50	<0.50	<0.50	<0.50
Co	<1.0	<1.0	1.0	<1.0	1.0	1.0	<1.0
Cu	718.0	37.00	17.00	6.000	16.00	10.00	4.000
Li	30	40	10	20	10	10	10
Mo	1.0	1.0	1.0	2.0	5.0	2.0	2.0
Ni	1.0	<1.0	2.0	1.0	<1.0	1.0	1.0
Pb	136	5.00	15.0	13.0	39.0	4.00	3.00
Sc	24.0	13.0	11.0	22.0	24.0	19.0	10.0
Zn	>10000.0	123.00	268.00	154.00	182.00	104.00	61.000
AlOH WL (nm)	2204.9	2195.6	2197.7	2201.5	2198.6	2203.0	2201.6
AlOH Depth	0.2	0.2	0.4	0.2	0.3	0.03	0.2
FeOH WL (nm)	2247.3	2254.5	2247.5	2249.1	2247.2	2250.9	2243.4
FeOH Depth	0.1	0.1	0.2	0.1	0.2	0.1	0.1
AlOH depth/FeOH depth	1.5	1.8	1.9	1.5	1.7	0.30	2.1

Sample ID	62748	62749	62750	62751	62752	62656	62657
Hole ID	PH-18-04	PH-18-04	PH-18-04	PH-18-04	PH-18-04	PH-18-06	PH-18-06
Depth (m)	169.64	70	231.85	290.28	319.33	10.37	75.1
Lithology	Tuff	Rhyolite	Tuff	Basalt	Basalt	Xtl-Tuff	Tuff
Stratigraphy	HW	HW	HW	HW	HW	HW	HW
Alteration	QSC+Sil	QSC+Sil	QSC+Sil	QSC	QSC	QS	QS+/-C
SiO_2 (wt. %)	72.36	83.37	73.88	50.86	59.59	74.51	73.98
Al_2O_3	12.08	11.37	15.17	18.92	19.10	13.44	12.75
Fe_2O_3	5.52	1.23	3.10	3.45	6.70	2.51	4.31
CaO	1.84	0.287	0.931	16.4	4.09	1.45	3.90
MgO	2.02	0.0307	2.02	0.974	1.00	1.51	1.52
Na_2O	2.70	0.707	1.19	5.21	7.32	4.00	2.26
K_2O	3.23	2.84	3.51	3.08	0.550	2.36	0.695
Cr_2O_3	0.002	0.003	0.004	0.002	0.001	0.001	0.003
TiO_2	0.112	0.123	0.140	0.809	1.160	0.151	0.343
MnO	0.10	0.010	0.020	0.20	0.090	0.050	0.14
P_2O_5	0.05	0.05	0.01	0.1	0.4	0.01	0.06
SrO	0.01	0.1	0.01	0.03	0.02	0.1	0.01
BaO	0.02	0.04	0.01	0.01	0.05	0.02	0.02
LOI	0.610	0.500	1.93	7.38	0.530	0.500	0.680
Total	98.73	98.14	101.8	98.80	100.6	99.82	99.89
C	0.040	0.030	0.040	2.4	0.040	0.030	0.050
S	0.10	0.25	0.77	0.67	0.64	0.38	0.33
Ba (ppm)	126	316	135	87.2	21.0	191	192
Ce	15.5	8.50	15.6	6.10	9.30	13.3	11.0
Cr	10	30	30	10	10	10	20
Cs	1.1	0.39	1.0	0.33	0.21	0.31	0.84
Dy	9.77	6.46	11.8	4.69	4.90	11.1	5.92
Er	7.47	4.91	8.60	3.13	3.62	7.67	4.12
Eu	0.89	0.63	1.4	0.79	1.0	1.1	1.2
Ga	15.7	5.70	17.3	15.6	16.9	15.2	14.8
Gd	6.2	4.3	7.9	3.1	3.8	8.0	4.6
Ge	<5	<5	<5	<5	<5	<5	<5
Hf	3.7	4.2	6.0	1.2	1.4	5.1	2.7
Ho	2.3	1.5	2.7	1.0	1.1	2.3	1.2
La	6.0	3.2	6.3	2.6	3.9	4.8	4.5
Lu	1.3	0.90	1.4	0.58	0.6	1.4	0.66
Nb	1.2	1.1	1.8	0.50	0.8	1.6	1.1
Nd	12.6	7.10	12.5	5.50	7.30	13.0	9.20
Pr	2.5	1.4	2.3	1.0	1.4	2.2	1.8
Rb	27.7	12.2	24.9	20.6	3.7	15.9	6.9
Sm	4.5	2.5	4.8	2.1	2.5	4.4	3.2
Sn	1.0	1.0	1.0	<1.0	<1.0	1.0	1.0
Sr	48.3	15.2	62.1	248.0	137.5	55.8	127.5
Ta	0.1	0.2	0.3	0.1	0.1	0.1	0.1
Tb	1.3	0.76	1.7	0.66	0.68	1.4	0.77

Sample ID	62748	62749	62750	62751	62752	62656	62657
Hole ID	PH-18-04	PH-18-04	PH-18-04	PH-18-04	PH-18-04	PH-18-06	PH-18-06
Depth (m)	169.64	70	231.85	290.28	319.33	10.37	75.1
Lithology	Tuff	Rhyolite	Tuff	Basalt	Basalt	Xtl-Tuff	Tuff
Stratigraphy	HW	HW	HW	HW	HW	HW	HW
Alteration	QSC+Sil	QSC+Sil	QSC+Sil	QSC	QSC	QS	QS+/-C
Th	1.4	1.2	1.1	0.24	0.52	1.7	0.92
Tm	1.2	0.79	1.4	0.49	0.58	1.2	0.62
U	0.58	0.76	1.2	3.2	1.6	0.77	0.25
V	<5.00	6.00	<5.00	389	246.00	11.0	15.0
W	<1.0	<1.0	1	2	1	1	1
Y	63.9	40.8	74.4	28.3	33.6	64.4	31.4
Yb	8.26	5.61	9.00	3.37	4.34	8.64	4.56
Zr	106.0	106	151	34.0	43.0	124	73.0
As	0.40	2.2	1.6	1.3	3.0	1.0	0.70
Bi	0.03	0.03	0.1	0.04	0.1	0.1	0.1
Hg	<0.005	<0.005	<0.005	<0.005	<0.005	<0.005	<0.005
In	0.1	0.01	0.02	0.03	0.02	0.2	0.1
Re	<0.001	<0.001	0.001	0.001	0.002	0.001	<0.001
Sb	<0.05	0.1	0.1	0.1	0.1	<0.05	0.1
Se	<0.2	<0.2	<0.2	0.4	<0.2	<0.2	<0.2
Te	0.04	0.02	0.1	0.1	0.1	0.2	0.2
Tl	0.2	<0.02	0.1	0.1	0.02	0.2	0.2
Ag	<0.50	<0.50	<0.50	<0.50	<0.50	<0.50	<0.50
Cd	<0.50	<0.50	<0.50	0.60	<0.50	0.50	<0.50
Co	1.0	1.0	<1.0	22	10.0	<1.0	1.0
Cu	3.000	4.000	3.000	42.00	14.00	12.00	42.00
Li	10	10	20	10	<10	10	10
Mo	1.0	3.0	9.0	1.0	1.0	2.0	1.0
Ni	<1.0	1.0	1.0	4.0	<1.0	<1.0	<1.0
Pb	<2.00	21.0	3.00	7.00	2.00	21.0	12.0
Sc	20.0	4.00	20.0	42.0	32.0	24.0	19.0
Zn	117.00	11.000	78.000	84.000	187.00	173.00	102.00
AlOH WL (nm)	2197.4	2196.5	2199.7	2199.2	-	2199.9	2200.0
AlOH Depth	0.03	0.2	0.3	0.02	-	0.2	0.1
FeOH WL (nm)	2251.5	2243.3	2245.9	2253.0	-	2250.3	2252.0
FeOH Depth	0.1	0.0	0.1	0.1	-	0.2	0.2
AlOH depth/FeOH depth	0.29	8.5	2.2	0.43	-	1.1	0.72

Sample ID	62658	62659	62661	62663	62664	62665	62666
Hole ID	PH-18-06	PH-18-06	PH-18-06	PH-18-06	PH-18-06	PH-18-06	PH-18-06
Depth (m)	127.54	164.2	205	263.35	301	310	321.69
Lithology	Xtl-Tuff	Xtl-Tuff	Xtl-Tuff	Tuff	Tuff	Tuff	Tuff
Stratigraphy	MS	FW	MS	FW	FW	FW	FW
Alteration	QSCPy	QSC+/-Py	QSCPy+Si	QSC+Sil	QSC+Sil	QS+/-C+Sil	QSC+Sil
SiO_2 (wt. %)	81.53	74.29	68.18	69.33	74.94	68.18	57.83
Al_2O_3	9.30	10.65	22.12	19.99	13.97	12.03	28.65
Fe_2O_3	4.97	4.76	3.76	2.52	1.75	3.72	5.13
CaO	0.702	0.800	0.201	0.372	2.08	11.4	0.429
MgO	0.609	8.06	0.543	3.60	2.75	1.90	1.48
Na_2O	0.495	0.540	2.98	2.00	3.40	1.85	2.58
K_2O	2.17	0.405	1.77	1.81	0.826	0.174	3.39
Cr_2O_3	0.003	0.002	0.002	0.002	0.002	0.002	0.002
TiO_2	0.155	0.218	0.362	0.227	0.153	0.235	0.314
MnO	0.031	0.24	0.010	0.062	0.082	0.40	0.042
P_2O_5	0.02	0.03	0.03	0.02	0.02	0.06	0.03
SrO	0.1	0.1	0.02	0.01	0.01	0.02	0.02
BaO	0.02	0.01	0.02	0.1	0.02	0.01	0.1
LOI	2.67	3.31	1.90	2.52	1.61	1.27	3.55
Total	99.57	99.56	101.3	99.31	99.69	98.95	99.18
C	0.18	0.030	0.020	0.030	0.030	0.13	0.020
S	2.2	1.3	1.6	0.67	0.45	0.57	2.9
Ba (ppm)	216	66.1	215	541	157	74.8	837
Ce	6.70	15.5	14.8	22.2	19.4	15.9	41.3
Cr	20	20	20	20	10	20	10
Cs	0.69	1.7	0.61	1.4	0.43	0.24	0.81
Dy	5.37	6.62	20.0	13.8	11.8	7.24	16.9
Er	4.48	4.40	14.7	9.52	8.39	5.06	12.0
Eu	0.9	1.3	2.1	1.4	1.0	1.6	1.6
Ga	15.9	13.3	38.9	20.8	14.2	13.8	29.1
Gd	3.8	5.1	12	9.8	8.3	6.1	13.1
Ge	<5	<5	<5	<5	<5	<5	<5
Hf	2.7	2.5	6.4	6.8	4.6	2.7	9.9
Ho	1.2	1.4	4.5	3.0	2.5	1.7	3.9
La	2.9	6.0	5.2	8.6	7.1	6.6	16
Lu	0.71	0.67	2.2	1.6	1.5	0.80	2.3
Nb	1.1	0.9	2.2	2.3	1.4	1.0	3.2
Nd	5.80	11.5	12.3	17.6	16.1	13.0	31.8
Pr	1.0	2.3	2.1	3.3	3.0	2.3	5.9
Rb	21.5	9.30	9.90	16.5	12.0	2.00	33.8
Sm	2.2	4.1	5.8	5.7	5.8	4.4	10.7
Sn	4.0	1.0	15	2.0	1.0	1.0	2.0
Sr	26.6	48.0	165.0	144.0	101.5	244.0	220
Ta	0.1	0.1	0.2	0.2	0.2	0.1	0.3
Tb	0.70	1.0	2.5	1.8	1.4	1.0	2.4

Sample ID	62658	62659	62661	62663	62664	62665	62666
Hole ID	PH-18-06	PH-18-06	PH-18-06	PH-18-06	PH-18-06	PH-18-06	PH-18-06
Depth (m)	127.54	164.2	205	263.35	301	310	321.69
Lithology	Xtl-Tuff	Xtl-Tuff	Xtl-Tuff	Tuff	Tuff	Tuff	Tuff
Stratigraphy	MS	FW	MS	FW	FW	FW	FW
Alteration	QSCPy	QSC+/-Py	QSCPy+Si	QSC+Sil	QSC+Sil	QS+/-C+Sil	QSC+Sil
Th	0.60	1.2	2.3	2.8	2.5	1.1	3.6
Tm	0.64	0.61	2.3	1.6	1.3	0.73	2.0
U	0.48	0.49	2.3	1.1	0.89	0.31	1.7
V	15.0	20.0	24.0	10.0	6.00	27.0	23.0
W	2	2	1	1	<1.0	2	2
Y	36.2	37.4	119.5	81.4	71.2	45.0	101
Yb	4.67	4.33	15.3	11.2	9.34	5.52	14.7
Zr	72.0	64.0	177	178	122	79.0	260
As	32.5	0.80	3.3	3.2	1.7	3.0	4.7
Bi	2.3	0.4	1.6	0.1	0.1	0.1	0.1
Hg	0.1	0.02	0.01	0.01	<0.005	0.01	<0.005
In	6	1.1	1.3	0.1	0.1	0.03	0.03
Re	0.001	0.003	0.002	0.001	0.001	0.001	0.004
Sb	0.7	0.1	0.4	0.2	0.1	0.1	0.2
Se	0.8	<0.2	0.4	<0.2	<0.2	<0.2	0.2
Te	1.2	0.3	0.7	0.02	0.01	0.1	0.04
Tl	0.1	0.1	0.2	0.6	0.3	0.1	0.5
Ag	6.0	0.60	2.0	<0.50	<0.50	<0.50	<0.50
Cd	51	1.1	1.2	<0.50	<0.50	1.0	<0.50
Co	1.0	2.0	2.0	2.0	<1.0	1.0	1.0
Cu	2000	347.000	328.0	5.000	4.000	9.000	15.00
Li	20	30	10	30	20	<10	10
Mo	18	7.0	4.0	3.0	2.0	2.0	8.0
Ni	2.0	2.0	<1.0	2.0	<1.0	<1.0	1.0
Pb	12.0	68.0	467	22.0	9.00	6.00	88.0
Sc	7.00	10.0	22.0	16.0	15.0	20.0	24.0
Zn	6900.0	666.00	251.00	79.000	52.000	427.00	77.000
AlOH WL (nm)	2197.6	2197.9	2197.8	2198.6	2200.3	2223.9	2200.6
AlOH Depth	0.3	0.1	0.3	0.3	0.2	0.0	0.3
FeOH WL (nm)	2244.1	2247.4	2241.8	2246.7	2248.1	2256.2	2245.3
FeOH Depth	0.1	0.1	0.1	0.2	0.2	0.1	0.1
AlOH depth/FeOH depth	4.9	0.95	4.6	1.8	1.3	0.36	2.8

Sample ID	62760	62761	62762	62763	62679	62680	62681
Hole ID	PH-18-08	PH-18-08	PH-18-08	PH-18-08	PH-18-10	PH-18-10	PH-18-10
Depth (m)	17.55	163.1	109	219.87	71.43	79.16	131
Lithology	Xtl-Tuff	Rhyolite	Xtl-Tuff	Xtl-Tuff	Rhyolite	Xtl-Tuff	Rhyolite
Stratigraphy	HW	HW	HW	HW	HW	MS	FW
Alteration	QS	QSC+Sil	QS	QS+Sil	QSC+Sil	QSCPy+Sil	QSC
SiO_2 (wt. %)	78.22	72.52	80.12	79.74	78.26	79.28	79.92
Al_2O_3	11.30	15.96	11.59	11.54	11.11	8.77	12.36
Fe_2O_3	1.77	2.46	0.99	1.16	5.26	8.17	2.80
CaO	0.490	0.665	0.388	1.91	0.351	0.594	0.176
MgO	0.330	1.73	0.0697	0.430	1.57	0.354	2.18
Na_2O	2.95	4.30	5.89	3.52	1.56	0.792	1.35
K_2O	4.77	2.07	0.806	1.53	1.70	1.82	0.941
Cr_2O_3	0.003	0.002	0.003	0.002	0.003	0.003	0.002
TiO_2	0.120	0.191	0.119	0.120	0.0827	0.146	0.134
MnO	0.020	0.030	0.010	0.040	0.062	0.021	0.093
P_2O_5	0.05	0.01	0.02	<0.01	0.01	0.02	0.01
SrO	0.1	0.01	<0.01	<0.01	0.1	0.1	0.01
BaO	0.02	0.04	0.00	0.01	0.03	0.03	0.02
LOI	0.520	1.64	0.0100	0.460	2.46	2.34	2.53
Total	100.5	100.9	100.5	100.5	99.19	98.33	99.25
C	0.020	0.030	0.020	0.030	0.080	0.12	0.020
S	0.69	0.42	0.13	0.20	1.4	3.2	0.60
Ba (ppm)	128	350	41.3	87.4	243	237	179
Ce	19.8	25.4	17.1	18.8	22.7	31.6	13.7
Cr	20	20	20	20	20	30	20
Cs	0.16	0.80	0.14	0.15	1.7	1.0	0.69
Dy	8.25	12.9	9.20	9.45	12.3	6.87	10.7
Er	5.77	9.82	7.26	6.79	8.57	4.29	7.21
Eu	0.70	1.2	0.85	0.77	0.88	1.9	1.0
Ga	14.3	16.7	8.80	11.3	15.7	14.5	11.9
Gd	5.9	8.9	7.3	7.1	10	7.7	7.3
Ge	<5	<5	<5	<5	<5	<5	<5
Hf	3.6	6.7	4.6	4.1	4.0	2.5	4.6
Ho	1.8	3.0	2.2	2.1	2.7	1.4	2.4
La	8.3	10	6.3	7.8	8.6	13	5.3
Lu	1.0	1.7	1.2	1.1	1.4	0.68	1.3
Nb	1.2	2.1	1.5	1.3	0.80	0.90	1.6
Nd	14.0	17.7	14.0	14.6	19.3	23.9	12.0
Pr	2.8	3.8	2.6	2.8	3.4	4.6	2.1
Rb	20.9	17.6	6.10	10.5	24.4	33.1	10.9
Sm	4.8	6.4	5.0	4.8	7.3	7.7	5.0
Sn	1.0	3.0	1.0	1.0	3.0	7.0	1.0
Sr	35.0	94.8	40.5	53.4	64.5	30.9	92.5
Ta	0.2	0.2	0.1	0.1	0.1	0.4	0.2
Tb	1.2	1.8	1.3	1.2	1.6	1.1	1.4

Sample ID	62760	62761	62762	62763	62679	62680	62681
Hole ID	PH-18-08	PH-18-08	PH-18-08	PH-18-08	PH-18-10	PH-18-10	PH-18-10
Depth (m)	17.55	163.1	109	219.87	71.43	79.16	131
Lithology	Xtl-Tuff	Rhyolite	Xtl-Tuff	Xtl-Tuff	Rhyolite	Xtl-Tuff	Rhyolite
Stratigraphy	HW	HW	HW	HW	HW	MS	FW
Alteration	QS	QSC+Sil	QS	QS+Sil	QSC+Sil	QSCPy+Sil	QSC
Th	1.5	1.2	1.6	1.8	2.0	1.3	1.7
Tm	0.93	1.6	1.1	1.0	1.3	0.58	1.2
U	6.2	3.6	1.3	1.0	0.49	0.77	0.56
V	<5.00	<5.00	<5.00	<5.00	<5.00	35.0	6.00
W	1	2	1	1	1	1	<1.0
Y	52.1	82.7	58.3	57.0	74.1	37.5	66.3
Yb	6.83	11.5	8.06	7.98	9.08	4.44	8.39
Zr	103	170	117	106	108	67.0	120
As	11.8	2.3	1.1	0.60	1.3	1.5	0.80
Bi	0.04	0.1	0.1	0.03	0.8	2	0.4
Hg	<0.005	<0.005	<0.005	<0.005	<0.005	0.02	0.01
In	0.02	0.02	0.02	0.01	0.02	7	0.1
Re	0.002	0.01	0.001	<0.001	<0.001	0.001	<0.001
Sb	0.3	<0.05	0.1	<0.05	0.3	0.2	0.1
Se	0.2	<0.2	<0.2	<0.2	0.5	1.1	<0.2
Te	0.02	0.03	0.02	0.02	0.8	1.1	0.1
Tl	0.03	0.1	<0.02	0.03	0.1	0.1	<0.02
Ag	<0.50	<0.50	<0.50	<0.50	<0.50	11	<0.50
Cd	<0.50	<0.50	<0.50	<0.50	<0.50	3.6	1.0
Co	<1.0	<1.0	<1.0	<1.0	<1.0	2.0	1.0
Cu	3.000	7.000	9.000	1.000	20.00	5710	66.00
Li	<10	10	<10	<10	20	10	20
Mo	6.0	19	4.0	3.0	5.0	7.0	2.0
Ni	2.0	1.0	2.0	<1.0	2.0	7.0	1.0
Pb	8.00	19.0	21.0	5.00	5.00	20.0	9.00
Sc	7.00	7.00	10.0	7.00	21.0	8.00	8.00
Zn	23.000	51.000	22.000	15.000	40.000	505.00	364.00
AlOH WL (nm)	2202.0	2196.0	2199.0	2197.7	2200.4	2196.3	2190.6
AlOH Depth	0.1	0.1	0.3	0.2	0.2	0.3	0.4
FeOH WL (nm)	2247.0	2244.0	2247.0	2245.5	2252.6	2247.1	2252.9
FeOH Depth	0.1	0.1	0.1	0.1	0.1	0.05	0.1
AlOH depth/FeOH depth	1.2	1.2	3.4	1.8	1.6	5.6	2.6

Sample ID	62683	62682	62684	62727	62728	62729
Hole ID	PH-18-10	PH-18-10	PH-18-10	PH-18-11	PH-18-11	PH-18-11
Depth (m)	170.04	203.17	239.71	119	136.54	157.71
Lithology	Lap. Tuff	Tuff	Lap. Tuff	Rhyolite	Lap. Tuff	Lap. Tuff
Stratigraphy	MS	MS	MS	FW	MS	MS
Alteration	QSC+Sil	QSC+/-Py	QSC	QS+/-C	QSC+/-Py+Sil	QSC+/-Py+Sil
SiO_2 (wt. %)	80.38	79.35	77.14	74.93	82.52	81.11
Al_2O_3	9.60	11.20	12.08	13.90	10.94	8.45
Fe_2O_3	5.39	3.92	3.62	2.13	1.83	6.54
CaO	0.155	0.114	0.247	1.35	0.429	0.644
MgO	2.60	2.66	3.59	1.42	0.951	0.765
Na_2O	0.808	0.705	1.77	5.21	2.02	1.89
K_2O	0.746	1.70	1.20	0.86	1.04	0.382
Cr_2O_3	0.003	0.003	0.002	0.003	0.004	0.003
TiO_2	0.155	0.145	0.144	0.143	0.164	0.0906
MnO	0.13	0.17	0.14	0.041	0.041	0.070
P_2O_5	0.02	0.01	0.04	0.01	0.02	0.04
SrO	0.1	0.1	0.1	0.01	0.01	0.01
BaO	0.01	0.03	0.02	0.01	0.02	0.01
LOI	2.61	2.31	2.34	0.810	0.920	1.16
Total	99.15	98.72	99.57	99.04	98.71	100.5
C	0.030	0.030	0.030	0.020	0.030	0.030
S	2.7	0.65	0.28	0.61	0.56	2.4
Ba (ppm)	146	321	166	128	197	81.0
Ce	10.9	13.8	17.7	21.2	13.6	12.6
Cr	20	20	20	20	30	20
Cs	0.59	1.1	0.79	0.49	0.53	0.60
Dy	5.57	7.06	8.42	10.5	7.82	8.61
Er	4.37	4.84	5.90	6.86	5.33	5.96
Eu	0.78	0.76	1.4	1.2	1.5	1.7
Ga	11.1	12.0	13.4	15.0	11.6	10.8
Gd	4.7	5.1	6.3	8.7	5.8	6.2
Ge	<5	<5	<5	<5	<5	<5
Hf	2.9	3.4	3.4	4.8	4.1	2.0
Ho	1.3	1.6	1.7	2.3	1.6	1.7
La	4.2	6.2	6.9	7.9	5.7	4.9
Lu	0.72	0.79	0.90	1.3	1.0	1.1
Nb	1.0	1.3	1.3	1.6	1.4	0.90
Nd	9.50	11.3	13.8	17.4	10.1	10.0
Pr	1.6	2.1	2.5	3.2	2.0	2.1
Rb	6.60	14.0	12.6	11.0	8.60	4.40
Sm	3.1	3.6	4.9	6.4	3.8	4.3
Sn	1.0	1.0	2.0	1.0	1.0	1.0
Sr	50.8	59.1	73.2	93.6	76.7	75.0
Ta	0.1	0.1	0.2	0.3	0.3	0.2
Tb	0.79	0.89	1.1	1.5	1.0	1.1

Sample ID	62683	62682	62684	62727	62728	62729
Hole ID	PH-18-10	PH-18-10	PH-18-10	PH-18-11	PH-18-11	PH-18-11
Depth (m)	170.04	203.17	239.71	119	136.54	157.71
Lithology	Lap. Tuff	Tuff	Lap. Tuff	Rhyolite	Lap. Tuff	Lap. Tuff
Stratigraphy	MS	MS	MS	FW	MS	MS
Alteration	QSC+Sil	QSC+/-Py	QSC	QS+/-C	QSC+/-Py+Sil	QSC+/-Py+Sil
Th	0.93	0.73	1.2	2.2	1.2	1.2
Tm	0.63	0.78	0.84	1.1	0.87	0.89
U	0.39	0.37	0.49	1.1	0.49	0.69
V	10.0	17.0	10.0	<5.00	8.00	<5.00
W	<1.0	2	1	1	1	1
Y	37.2	44.2	49.8	61.8	48.5	54.2
Yb	4.80	5.30	6.06	8.32	6.12	7.06
Zr	80.0	92.0	97.0	122	103	61.0
As	6.1	2.1	0.40	1.3	2.6	4.4
Bi	0.5	0.3	0.1	0.1	0.1	0.5
Hg	0.5	0.02	0.02	0.01	0.2	0.7
In	0.2	0.4	0.1	0.04	0.3	1.0
Re	0.004	0.001	0.002	0.001	0.001	0.002
Sb	<0.05	0.1	0.1	0.1	0.8	0.7
Se	0.7	0.2	<0.2	<0.2	<0.2	0.4
Te	2.3	0.2	0.03	0.04	0.03	0.2
Tl	0.04	0.02	0.03	0.1	0.3	0.2
Ag	0.70	<0.50	<0.50	<0.50	1.2	2.8
Cd	9.5	<0.50	0.80	<0.50	8.5	57
Co	4.0	1.0	1.0	1.0	1.0	1.0
Cu	288.0	148.0	52.00	10.00	82.00	210.0
Li	20	20	30	20	20	10
Mo	4.0	4.0	6.0	3.0	5.0	12
Ni	1.0	1.0	2.0	1.0	3.0	<1.0
Pb	11.0	5.00	20.0	38.0	333	482
Sc	6.00	10.0	10.0	12.0	7.00	6.00
Zn	1885.0	314.00	242.00	91.000	2490.0	7580.0
AlOH WL (nm)	2202.6	2196.9	2196.7	-	2197.0	2200.0
AlOH Depth	0.1	0.3	0.3	-	0.3	0.3
FeOH WL (nm)	2246.5	2252.2	2252.2	2247.9	2242.0	2266.0
FeOH Depth	0.05	0.2	0.3	0.1	0.1	0.2
AlOH depth/FeOH depth	2.0	1.3	1.2	-	2.4	1.3

Sample ID	62730	62702	62703	62704	62705	62706
Hole ID	PH-18-11	PH-18-13	PH-18-13	PH-18-13	PH-18-13	PH-18-13
Depth (m)	176.88	25	54.32	58.16	69.81	88.39
Lithology	Lap. Tuff	Dike	Xtl-Tuff	Lap. Tuff	Dike	Lap. Tuff
Stratigraphy	FW	HW	MS	MS	MS	MS
Alteration	QSC+Sil	SC	QSC+Sil	QSCPy+Sil	Unaltered	QSC+Sil
SiO_2 (wt. %)	78.39	67.22	62.47	75.37	47.55	85.84
Al_2O_3	12.85	15.06	21.06	9.40	17.15	7.45
Fe_2O_3	1.32	4.46	1.77	11.7	11.8	1.63
CaO	0.602	3.93	3.94	0.121	9.69	0.171
MgO	1.51	1.77	2.66	0.737	7.90	3.75
Na_2O	3.70	4.52	5.75	0.797	3.26	0.643
K_2O	1.40	2.04	1.90	1.77	0.359	0.352
Cr_2O_3	0.003	0.004	0.001	0.002	0.016	0.002
TiO_2	0.141	0.706	0.231	0.0908	1.864	0.0905
MnO	0.050	0.080	0.080	0.020	0.18	0.070
P_2O_5	0.01	0.1	0.03	0.01	0.2	0.01
SrO	0.01	0.03	0.01	0.01	0.03	0.01
BaO	0.03	0.04	0.1	0.04	0.01	0.01
LOI	1.19	1.22	1.24	2.80	1.14	1.76
Total	100.8	101.8	101.0	101.9	101.5	101.3
C	0.010	0.060	0.030	0.020	0.050	0.010
S	0.17	0.030	0.32	4.7	0.40	0.63
Ba (ppm)	291	354	875	367	83.7	36.9
Ce	16.8	38.5	31.3	10.3	21.8	8.70
Cr	20	30	10	20	110	20
Cs	0.78	0.67	1.0	0.62	0.80	0.72
Dy	10.2	3.58	14.8	7.37	5.36	5.34
Er	7.44	2.32	10.4	4.95	3.06	3.30
Eu	0.79	1.0	1.9	0.80	1.7	1.1
Ga	14.3	17.8	22.4	15.9	20.2	9.30
Gd	7.3	4.0	11	5.3	5.4	3.8
Ge	<5	<5	<5	<5	<5	<5
Hf	5.2	4.8	7.6	3.0	3.5	2.4
Ho	2.3	0.75	3.2	1.6	0.94	1.2
La	6.6	19	12	4.0	8.7	3.5
Lu	1.3	0.39	1.9	0.82	0.42	0.57
Nb	1.6	7.0	2.4	1.0	3.2	0.9
Nd	13.4	16.6	24.0	9.00	16.1	7.00
Pr	2.4	4.3	4.7	1.7	3.3	1.3
Rb	15.2	44.2	18.7	15.7	5.50	3.80
Sm	4.6	3.9	8.4	3.8	4.6	2.4
Sn	1.0	2.0	2.0	1.0	2.0	1.0
Sr	68.9	273	147	52.6	322	37.0
Ta	0.2	0.7	0.3	0.2	0.3	0.2
Tb	1.4	0.65	2.0	1.0	0.90	0.66

Sample ID	62730	62702	62703	62704	62705	62706
Hole ID	PH-18-11	PH-18-13	PH-18-13	PH-18-13	PH-18-13	PH-18-13
Depth (m)	176.88	25	54.32	58.16	69.81	88.39
Lithology	Lap. Tuff	Dike	Xtl-Tuff	Lap. Tuff	Dike	Lap. Tuff
Stratigraphy	FW	HW	MS	MS	MS	MS
Alteration	QSC+Sil	SC	QSC+Sil	QSCPy+Sil	Unaltered	QSC+Sil
Th	1.4	6.5	3.0	0.83	1.1	0.76
Tm	1.2	0.30	1.7	0.78	0.44	0.56
U	0.73	3.0	1.8	0.33	0.29	0.40
V	<5.00	70.0	<5.00	<5.00	229.0	<5.00
W	1	2	2	1	1	1
Y	61.1	22.4	91.5	46.8	29.2	32.1
Yb	8.60	2.70	12.65	5.91	2.82	3.71
Zr	128	187	193	91.0	136	64.0
As	2.4	0.50	1.0	0.80	3.2	0.70
Bi	0.1	0.1	0.4	1	0.2	0.2
Hg	0.01	<0.005	<0.005	0.01	<0.005	0.3
In	0.01	0.01	0.1	0.7	0.05	0.9
Re	0.002	<0.001	0.001	0.001	0.001	<0.001
Sb	0.1	0.2	0.2	0.2	0.2	<0.05
Se	<0.2	<0.2	<0.2	0.8	0.3	<0.2
Te	0.02	0.01	0.1	0.8	0.04	0.1
Tl	0.1	<0.02	0.7	0.1	0.1	0.1
Ag	<0.50	<0.50	1.0	2.5	0.60	<0.50
Cd	<0.50	<0.50	1.3	3.4	1.0	13
Co	<1.0	11	1.0	<1.0	48	<1.0
Cu	3.000	15.00	64.00	687.0	61.00	240.0
Li	20	10	20	10	10	20
Mo	2.0	2.0	16	2.0	1.0	3.0
Ni	1.0	8.0	1.0	3.0	107	<1.0
Pb	119	14.0	442	19.0	5.00	9.00
Sc	7.00	10.0	17.0	16.0	24.0	8.00
Zn	118.00	57.000	271.00	556.00	146.00	2910.0
AlOH WL (nm)	2200.2	2219.0	2218.9	2188.0	2220.0	-
AlOH Depth	0.4	0.05	0.1	0.3	0.4	-
FeOH WL (nm)	2247.7	2252.0	2249.4	2253.0	2252.0	-
FeOH Depth	0.2	0.1	0.2	0.3	0.5	-
AlOH depth/FeOH depth	2.1	0.48	0.61	1.0	1.0	-

Sample ID	62707	62708	62709	62710	62711	62712
Hole ID	PH-18-13	PH-18-13	PH-18-13	PH-18-13	PH-18-13	PH-18-13
Depth (m)	97.66	114.38	145	160.17	196.67	244.54
Lithology	Lap. Tuff	Lap. Tuff	Rhyolite	Lap. Tuff	Rhyolite	Sediment
Stratigraphy	MS	FW	FW	MS	FW	FW
Alteration	QSC+/-Py+Sil	QSC+/-Py+Sil	QS+/-Py	QSC+/-Py+Sil	QS	S+/-C
SiO_2 (wt. %)	70.38	76.30	79.21	75.10	79.07	74.74
Al_2O_3	16.57	11.24	10.92	12.67	12.57	13.42
Fe_2O_3	7.08	2.36	1.99	3.47	1.85	2.16
CaO	0.408	0.474	0.665	2.21	0.242	0.888
MgO	2.70	7.22	4.20	1.66	2.45	2.25
Na_2O	1.59	1.68	1.91	3.99	3.02	5.48
K_2O	0.949	0.312	0.804	0.384	0.545	0.848
Cr_2O_3	0.002	0.001	0.002	0.002	0.002	0.002
TiO_2	0.133	0.131	0.139	0.303	0.151	0.150
MnO	0.12	0.21	0.16	0.15	0.061	0.050
P_2O_5	0.01	0.08	0.01	0.05	0.01	0.01
SrO	0.01	0.01	<0.01	0.01	0.01	0.01
BaO	0.1	0.01	0.01	0.02	0.01	0.01
LOI	2.93	2.31	1.23	0.930	2.70	1.19
Total	101.0	101.5	102.0	100.0	101.7	101.4
C	0.030	0.010	0.010	0.010	<0.010	0.010
S	3.0	0.31	0.32	0.30	0.66	0.85
Ba (ppm)	442	20.7	72.1	140	129	113
Ce	24.8	10.0	14.4	12.2	12.1	19.7
Cr	10	10	20	10	20	20
Cs	1.0	1.1	0.58	0.55	0.86	0.31
Dy	17.5	8.02	7.72	6.64	8.28	9.18
Er	11.4	5.61	5.24	4.45	5.92	6.09
Eu	1.7	1.1	1.2	1.4	1.2	1.3
Ga	23.5	12.0	11.7	14.9	12.9	12.2
Gd	12	5.7	5.6	5.5	6.1	6.9
Ge	<5	<5	<5	<5	<5	<5
Hf	7.2	3.6	3.1	2.6	3.9	3.8
Ho	3.7	1.8	1.7	1.5	1.9	1.9
La	9.1	3.7	5.5	4.7	4.8	7.9
Lu	2.0	0.92	0.91	0.8	1.0	1.0
Nb	2.1	1.2	1.2	1.0	1.5	1.3
Nd	21.8	8.40	10.8	10.1	8.80	14.9
Pr	4.0	1.6	2.2	1.9	1.9	3.0
Rb	6.00	3.60	7.30	6.10	5.20	7.10
Sm	8.8	3.7	4.2	3.6	3.8	5.8
Sn	5.0	1.0	1.0	1.0	1.0	1.0
Sr	79.9	66.1	76.1	71.5	109	94.6
Ta	0.3	0.2	0.2	0.5	0.3	0.2
Tb	2.3	1.1	1.0	0.89	1.2	1.4

Sample ID	62707	62708	62709	62710	62711	62712
Hole ID	PH-18-13	PH-18-13	PH-18-13	PH-18-13	PH-18-13	PH-18-13
Depth (m)	97.66	114.38	145	160.17	196.67	244.54
Lithology	Lap. Tuff	Lap. Tuff	Rhyolite	Lap. Tuff	Rhyolite	Sediment
Stratigraphy	MS	FW	FW	MS	FW	FW
Alteration	QSC+/-Py+Sil	QSC+/-Py+Sil	QS+/-Py	QSC+/-Py+Sil	QS	S+/-C
Th	1.6	1.2	1.1	1.0	0.93	1.4
Tm	1.8	0.80	0.79	0.70	0.94	1.0
U	0.66	0.42	0.41	0.29	0.41	0.54
V	5.00	<5.00	<5.00	<5.00	5.00	<5.00
W	1	1	1	6	1	1
Y	99.5	50.4	48.1	40.7	54.5	56.9
Yb	13.1	6.15	5.79	4.53	6.71	6.70
Zr	190	96.0	84.0	82.0	104	107
As	1.9	0.50	0.50	0.60	1.1	2.6
Bi	1	0.1	0.04	0.6	0.04	0.2
Hg	0.1	0.01	0.04	<0.005	0.01	0.01
In	0.9	0.1	0.1	0.1	0.03	0.1
Re	<0.001	0.001	0.001	<0.001	0.001	0.002
Sb	0.1	0.1	<0.05	0.1	0.1	0.2
Se	0.4	<0.2	<0.2	<0.2	<0.2	<0.2
Te	0.5	0.02	0.02	0.04	0.02	0.1
Tl	0.1	0.1	0.2	0.1	0.02	0.3
Ag	2.2	<0.50	<0.50	<0.50	<0.50	1.1
Cd	3.6	<0.50	3.6	0.50	<0.50	<0.50
Co	<1.0	<1.0	<1.0	1.0	1.0	<1.0
Cu	1120	16.00	67.00	21.00	43.00	4.000
Li	50	40	30	10	20	20
Mo	2.0	3.0	4.0	1.0	3.0	4.0
Ni	1.0	<1.0	1.0	<1.0	1.0	<1.0
Pb	18.0	31.0	249	23.0	54.0	122
Sc	20.0	10.0	10.0	18.0	9.00	12.0
Zn	895.00	241.00	735.00	171.00	177.00	144.00
AlOH WL (nm)	2201.0	2200.0	2211.0	2187.2	-	2209.1
AlOH Depth	0.3	0.5	0.1	0.5	-	0.2
FeOH WL (nm)	2250.0	2255.0	2247.0	2247.5	2254.0	2247.9
FeOH Depth	0.3	0.3	0.2	0.4	0.2	0.3
AlOH depth/FeOH depth	0.83	1.5	0.64	1.4	-	0.81

Sample ID	62713	62714	62715	62552	62555
Hole ID	PH-18-13	PH-18-13	PH-18-13	PH-18-14	PH-18-14
Depth (m)	273.52	315.75	340.56	14.23	46
Lithology	Lap. Tuff	Rhyolite	Rhyolite	Lap. Tuff	Xtl-Tuff
Stratigraphy	FW	FW	FW	MS	MS
Alteration	QS	QSC+/-Py+Sil (Cd)	QSC+/-Py+Sil (Cd)	QSC+Sil	QSC+/-Py+Sil
SiO_2 (wt. %)	79.19	75.15	65.41	76.83	77.99
Al_2O_3	11.66	14.22	17.60	11.26	12.09
Fe_2O_3	1.53	2.55	6.44	1.59	4.44
CaO	1.35	1.33	1.35	5.34	0.277
MgO	0.367	3.64	5.22	0.948	3.84
Na_2O	5.11	1.25	1.33	3.46	0.77
K_2O	0.576	1.59	2.28	0.346	0.400
Cr_2O_3	0.003	0.002	0.002	0.003	0.004
TiO_2	0.129	0.122	0.153	0.102	0.113
MnO	0.040	0.11	0.16	0.11	0.051
P_2O_5	0.03	0.01	0.01	0.05	0.01
SrO	<0.01	0.01	0.01	0.1	0.1
BaO	0.02	0.03	0.03	0.01	0.02
LOI	0.680	2.81	3.48	0.650	2.81
Total	101.5	101.3	101.8	98.79	100.4
C	0.010	0.010	0.040	0.15	0.05
S	0.81	0.34	0.040	0.43	1.5
Ba (ppm)	194	301	292	70.4	221
Ce	18.3	19.6	19.7	19.2	17.5
Cr	20	20	10	20	30
Cs	0.16	1.1	2.0	0.11	0.40
Dy	10.3	12.2	17.0	10.4	12.3
Er	6.87	8.40	11.9	7.01	9.32
Eu	1.1	1.2	1.6	1.6	1.0
Ga	12.3	17.0	20.1	9.00	13.6
Gd	6.4	9.6	12	8.2	9.8
Ge	<5	<5	<5	<5	<5
Hf	3.8	4.6	6.0	3.6	5.7
Ho	2.1	2.8	3.8	2.2	2.8
La	6.8	7.5	6.7	8.0	7.0
Lu	1.2	1.4	2.0	1.2	1.4
Nb	4.0	1.5	1.7	1.2	1.6
Nd	13.6	16.0	18.1	16.5	15.7
Pr	2.7	3.1	3.3	2.9	2.8
Rb	6.20	19.6	28.8	2.70	2.90
Sm	5.2	6.6	7.3	5.8	5.9
Sn	1.0	2.0	2.0	1.0	3.0
Sr	56.0	105	155	84.3	42.6
Ta	0.2	0.2	0.3	0.1	0.1
Tb	1.2	1.8	2.4	1.4	1.7

Sample ID	62713	62714	62715	62552	62555
Hole ID	PH-18-13	PH-18-13	PH-18-13	PH-18-14	PH-18-14
Depth (m)	273.52	315.75	340.56	14.23	46
Lithology	Lap. Tuff	Rhyolite	Rhyolite	Lap. Tuff	Xtl-Tuff
Stratigraphy	FW	FW	FW	MS	MS
Alteration	QS	QSC+/-Py+Sil (Cd)	QSC+/-Py+Sil (Cd)	QSC+Sil	QSC+/-Py+Sil
Th	1.9	1.9	2.1	1.5	1.1
Tm	1.0	1.3	1.8	0.94	1.3
U	1.1	0.88	1.6	1.2	0.51
V	6.00	<5.00	49.0	5.00	<5.00
W	1	1	1	1	1
Y	62.9	77.0	105	56.7	72.5
Yb	7.53	9.84	13.4	8.07	9.00
Zr	101	128	156	97.0	140
As	3.2	1.2	0.30	1.6	0.50
Bi	0.1	0.1	0.01	0.2	0.2
Hg	0.01	0.04	0.01	<0.005	0.1
In	0.1	2	0.2	0.3	2
Re	0.001	0.001	0.02	0.001	0.001
Sb	0.2	0.1	<0.05	0.2	<0.05
Se	<0.2	<0.2	<0.2	<0.2	<0.2
Te	0.1	0.3	0.1	0.1	0.7
Tl	0.1	0.2	0.4	<0.02	0.03
Ag	0.50	0.80	<0.50	<0.50	0.60
Cd	0.90	6.6	<0.50	2.6	12.0
Co	<1.0	<1.0	3.0	<1.0	1.0
Cu	3.000	30.00	2.000	33.00	133.0
Li	10	40	50	<10	20
Mo	4.0	2.0	9.0	2.0	3.0
Ni	<1.0	1.0	<1.0	<1.0	1.0
Pb	31.0	46.0	10.0	12.0	2.00
Sc	9.00	30.0	29.0	15.0	13.0
Zn	211.00	1040.0	176.00	483.00	1925.0
AlOH WL (nm)	2197.9	2203.0	2208.0	2201.5	-
AlOH Depth	0.4	0.2	0.5	0.1	-
FeOH WL (nm)	2251.6	2253.0	2246.0	2261.0	-
FeOH Depth	0.4	0.2	0.5	0.04	-
AlOH depth/FeOH depth	1.2	1.2	1.0	2.2	-

Sample ID	62559	62563	62566	62569	62731	62733
Hole ID	PH-18-14	PH-18-14	PH-18-14	PH-18-14	PH-18-15	PH-18-15
Depth (m)	72.52	107.73	169.84	256.83	46.37	139.85
Lithology	Rhyolite	Rhyolite	Tuff	Tuff	Xtl-Tuff	Rhyolite
Stratigraphy	MS	FW	FW	FW	FW	FW
Alteration	QSC+Sil	QS	QSC+Sil	QSC+/-Py	QSC+/-Py	QSC+/-Py+Sil
SiO_2 (wt. %)	73.68	74.14	80.94	80.52	84.04	66.40
Al_2O_3	14.51	12.75	10.58	11.41	8.68	11.58
Fe_2O_3	2.94	4.34	1.41	2.49	2.55	7.61
CaO	0.634	2.49	1.85	0.123	0.321	0.319
MgO	3.69	1.04	0.672	2.92	0.361	12.30
Na_2O	3.27	3.70	3.02	1.36	3.30	0.865
K_2O	0.746	0.983	1.32	0.839	0.622	0.391
Cr_2O_3	0.001	0.001	0.003	0.004	0.004	0.002
TiO_2	0.245	0.298	0.0890	0.246	0.0602	0.124
MnO	0.20	0.16	0.089	0.061	0.030	0.38
P_2O_5	0.06	0.07	0.01	0.03	0.01	0.03
SrO	0.01	0.01	0.05	0.1	0.01	0.01
BaO	0.01	0.02	0.01	0.01	0.02	0.01
LOI	1.58	0.840	0.450	2.42	0.570	3.02
Total	99.44	101.6	101.6	100.2	100.2	100.2
C	0.020	0.09	0.06	0.020	0.010	0.020
S	0.60	0.21	0.19	0.49	0.52	1.4
Ba (ppm)	76.7	156	111	120	163	20.5
Ce	21.0	13.6	13.3	11.9	16.8	25.0
Cr	10	10	20	30	30	20
Cs	0.63	0.64	0.24	0.38	0.59	2.0
Dy	9.09	6.41	9.05	4.80	7.95	9.16
Er	6.03	4.34	6.45	3.52	5.88	5.79
Eu	1.6	1.3	0.89	0.77	0.76	1.5
Ga	13.5	13.7	11.7	13.1	8.1	15.0
Gd	6.2	5.0	7.1	3.9	6.1	8.7
Ge	<5	<5	<5	<5	<5	<5
Hf	4.3	2.9	3.7	2.7	3.1	3.3
Ho	2.1	1.5	2.0	1.1	1.8	1.8
La	8.7	5.1	5.2	4.7	6.8	11
Lu	1.2	0.69	1.1	0.61	0.86	1.0
Nb	1.5	0.90	1.2	0.90	1.1	1.1
Nd	15.7	11.2	12.6	9.20	13.9	19.8
Pr	3.1	2.1	2.2	1.8	2.6	3.8
Rb	9.70	11.80	10.3	4.20	12.7	6.00
Sm	5.1	3.9	4.3	3.0	4.4	6.4
Sn	1.0	1.0	1.0	1.0	<1.0	1.0
Sr	77.5	104	86.6	66.6	46.9	21.8
Ta	<0.1	<0.1	0.1	0.1	0.1	0.1
Tb	1.2	0.90	1.3	0.7	1.1	1.3

Sample ID	62559	62563	62566	62569	62731	62733
Hole ID	PH-18-14	PH-18-14	PH-18-14	PH-18-14	PH-18-15	PH-18-15
Depth (m)	72.52	107.73	169.84	256.83	46.37	139.85
Lithology	Rhyolite	Rhyolite	Tuff	Tuff	Xtl-Tuff	Rhyolite
Stratigraphy	MS	FW	FW	FW	FW	FW
Alteration	QSC+Sil	QS	QSC+Sil	QSC+/-Py	QSC+/-Py	QSC+/-Py+Sil
Th	1.7	1.0	1.3	1.0	1.5	1.4
Tm	1.0	0.64	1.0	0.54	0.83	0.85
U	1.7	0.26	0.49	0.24	0.41	0.42
V	23.0	<5.00	<5.00	24.0	<5.00	12.0
W	1	1	1	1	1	1
Y	57.7	36.9	52.5	30.0	47.4	50.0
Yb	7.10	4.63	7.26	4.33	5.91	6.46
Zr	123	83.0	94.0	71.0	85.0	88.0
As	0.90	0.90	0.60	1.2	3.1	0.70
Bi	0.2	0.2	0.03	0.2	0.3	0.4
Hg	0.05	<0.005	<0.005	0.01	<0.005	0.01
In	1.2	0.1	0.1	0.1	0.2	0.6
Re	0.002	<0.001	<0.001	0.001	<0.001	0.01
Sb	0.1	0.1	<0.05	0.1	<0.05	0.1
Se	<0.2	0.3	<0.2	<0.2	0.3	0.3
Te	0.1	0.1	0.04	0.1	0.2	0.2
Tl	0.1	0.1	0.02	<0.02	0.02	0.1
Ag	0.60	<0.50	<0.50	<0.50	<0.50	<0.50
Cd	8.2	<0.50	<0.50	<0.50	1.1	0.90
Co	3.0	2.0	<1.0	2.0	<1.0	1.0
Cu	121.0	18.00	2.000	191.0	79.00	469.0
Li	30	10	<10	10	10	80
Mo	2.0	1.0	2.0	2.0	3.0	13
Ni	1.0	2.0	1.0	1.0	1.0	<1.0
Pb	104	9.00	2.00	5.00	64.0	8.00
Sc	12.0	19.0	14.0	11.0	14.0	9.00
Zn	1635.0	114.00	53.000	238.00	210.00	928.00
AlOH WL (nm)	2204.0	2197.0	2205.3	2208.6	2201.0	2192.0
AlOH Depth	0.2	0.1	0.2	0.2	0.2	0.2
FeOH WL (nm)	2246.0	-	2246.0	2247.0	2248.3	2245.0
FeOH Depth	0.2	-	0.1	0.2	0.1	0.2
AlOH depth/FeOH depth	1.0	-	1.4	0.85	2.1	0.93

Sample ID	62734	62735	62736	62716	62717	62718
Hole ID	PH-18-15	PH-18-15	PH-18-15	PH-18-18	PH-18-18	PH-18-18
Depth (m)	166.73	223.33	251	9.78	23.83	33.63
Lithology	Tuff	Rhyolite	Tuff	Tuff	Lap. Tuff	Lap. Tuff
Stratigraphy	FW	FW	FW	HW	MS	FW
Alteration	QSC+/-Py+Sil	QS+Sil	QS	QS	QSC	QSC+/-Py+Sil
SiO_2 (wt. %)	78.16	77.77	79.54	80.98	62.22	82.23
Al_2O_3	11.32	11.78	11.31	9.94	17.96	9.49
Fe_2O_3	4.82	4.76	2.71	3.72	7.59	5.49
CaO	0.241	0.0717	0.193	0.261	1.64	0.111
MgO	2.13	2.80	2.61	2.18	7.61	0.403
Na_2O	0.842	0.902	2.58	0.492	1.27	0.584
K_2O	2.09	1.55	0.81	2.20	1.34	1.46
Cr_2O_3	0.003	0.003	0.003	0.002	0.002	0.003
TiO_2	0.130	0.164	0.132	0.100	0.194	0.161
MnO	0.17	0.14	0.091	0.080	0.10	0.020
P_2O_5	0.03	0.01	0.01	0.01	0.03	0.02
SrO	0.01	0.01	0.01	0.01	0.01	0.01
BaO	0.1	0.03	0.02	0.04	0.03	0.04
LOI	2.10	3.03	1.27	1.93	2.51	1.68
Total	101.9	100.6	99.84	101.6	100.2	101.0
C	0.06	0.020	0.020	0.020	0.040	0.030
S	0.29	1.3	0.09	1.4	1.5	2.6
Ba (ppm)	454	255	155	363	292	386
Ce	10.1	15.5	9.70	8.10	26.9	7.60
Cr	20	30	20	20	10	20
Cs	0.71	2.2	0.68	1.1	2.4	0.34
Dy	6.01	7.76	6.15	9.24	13.8	6.65
Er	4.23	5.86	4.42	5.99	10.0	4.72
Eu	0.60	1.1	0.88	0.69	3.0	1.2
Ga	13.9	13.9	11.7	13.5	35.1	19.1
Gd	4.4	6.2	4.1	5.8	10	4.3
Ge	<5	<5	<5	<5	<5	<5
Hf	2.7	3.5	3.5	3.8	6.8	3.1
Ho	1.3	1.7	1.3	2.0	3.1	1.4
La	4.3	6.5	4.2	3.2	10.2	3.3
Lu	0.73	0.88	0.79	1.1	1.7	0.86
Nb	0.70	1.4	1.2	1.1	2.2	1.1
Nd	8.1	12.9	7.70	7.10	21.8	6.60
Pr	1.5	2.5	1.5	1.2	4.2	1.2
Rb	18.6	17.7	8.40	19.1	13.9	10.0
Sm	2.9	4.1	2.3	3.1	7.6	2.7
Sn	3.0	2.0	2.0	4.0	2.0	1.0
Sr	32.3	65.2	53.7	37.0	57.3	44.3
Ta	0.1	0.1	0.1	0.2	0.3	0.2
Tb	0.72	1.1	0.82	1.2	1.9	0.84

Sample ID	62734	62735	62736	62716	62717	62718
Hole ID	PH-18-15	PH-18-15	PH-18-15	PH-18-18	PH-18-18	PH-18-18
Depth (m)	166.73	223.33	251	9.78	23.83	33.63
Lithology	Tuff	Rhyolite	Tuff	Tuff	Lap. Tuff	Lap. Tuff
Stratigraphy	FW	FW	FW	HW	MS	FW
Alteration	QSC+/-Py+Sil	QS+Sil	QS	QS	QSC	QSC+/-Py+Sil
Th	1.2	1.2	0.87	1.0	3.0	1.0
Tm	0.65	0.8	0.67	1.0	1.6	0.7
U	0.33	0.32	0.35	0.61	1.3	1.0
V	7.00	7.00	6.00	<5.00	10.0	10.0
W	1	1	1	1	1	2
Y	36.3	46.7	35.9	56.8	84.3	43.5
Yb	4.82	5.91	5.24	7.15	11.3	5.14
Zr	78.0	97.0	91.0	100	170	88.0
As	4.8	2.0	0.30	1.6	1.0	3.1
Bi	0.5	0.4	0.1	2	1	4
Hg	0.02	0.01	<0.005	0.01	0.02	0.01
In	0.5	0.03	0.05	0.2	0.7	0.1
Re	<0.001	0.004	0.001	<0.001	0.001	0.001
Sb	0.1	0.1	<0.05	0.1	0.1	0.1
Se	<0.2	0.5	<0.2	0.2	0.2	0.4
Te	0.1	0.3	0.04	1.5	2	4
Tl	0.02	0.02	0.03	0.1	1	0.3
Ag	0.60	<0.50	<0.50	0.5	0.5	<0.50
Cd	2.0	<0.50	<0.50	1.0	<0.50	<0.50
Co	<1.0	5.0	<1.0	<1.0	<1.0	1.0
Cu	247.0	16.00	6.000	86.0	447.0	194.0
Li	20	20	20	10	40	<10
Mo	1.0	3.0	2.0	2.0	4.0	9.0
Ni	1.0	1.0	<1.0	<1.0	<1.0	1.0
Pb	15.0	13.0	2.00	10.0	26.0	58.0
Sc	7.00	7.00	10.0	17.0	17.0	9.00
Zn	707.00	147.00	60.000	364.00	488.00	30.000
AlOH WL (nm)	2198.7	2195.9	2201.0	2198.4	-	2206.3
AlOH Depth	0.3	0.4	0.2	0.2	-	0.2
FeOH WL (nm)	2251.2	2249.3	2251.1	2244.5	2252.0	2242.3
FeOH Depth	0.2	0.2	0.2	0.1	0.2	0.1
AlOH depth/FeOH depth	1.8	1.6	0.83	2.6	-	2.7

Sample ID	62719	62720	62721	62722	62723	62685
Hole ID	PH-18-18	PH-18-18	PH-18-18	PH-18-18	PH-18-18	PH-18-21
Depth (m)	56.11	93.63	214.8	229.32	239	17
Lithology	Rhyolite	Rhyolite	Lap. Tuff	Lap. Tuff	Tuff	Sediment
Stratigraphy	MS	MS	FW	MS	FW	FW
Alteration	QS+/-C+/-Py	QS+/-Py	QS+Sil (Cd)	QSCPy+Sil	QSC+/-Py	QSC+/-Py
SiO_2 (wt. %)	80.33	81.46	78.14	78.03	76.45	73.89
Al_2O_3	9.35	9.28	12.29	9.72	13.13	13.08
Fe_2O_3	5.27	4.39	5.10	8.71	1.80	4.13
CaO	0.234	0.0510	0.0510	0.0517	1.05	3.58
MgO	1.92	2.47	1.30	1.36	0.977	1.37
Na_2O	1.43	0.653	0.745	0.611	2.11	1.84
K_2O	1.10	1.39	2.12	1.33	4.12	1.55
Cr_2O_3	0.003	0.004	0.002	0.003	0.002	0.001
TiO_2	0.173	0.122	0.153	0.135	0.224	0.338
MnO	0.14	0.14	0.020	0.031	0.071	0.12
P_2O_5	0.03	0.02	0.01	0.01	0.02	0.07
SrO	0.01	0.01	0.01	0.01	0.01	0.05
BaO	0.02	0.02	0.1	0.02	0.1	0.03
LOI	2.07	1.91	2.64	3.75	0.870	0.580
Total	100.4	99.87	100.7	100.4	99.11	101.1
C	0.030	0.020	0.020	0.030	0.020	0.030
S	2.0	0.67	2.7	5.2	0.090	0.29
Ba (ppm)	175	224	642	222	449	313
Ce	6.00	11.4	6.20	11.1	19.0	11.4
Cr	20	30	20	30	20	10
Cs	0.31	1.7	0.91	0.71	1.2	0.81
Dy	4.38	5.82	8.13	6.87	10.8	6.08
Er	3.15	3.89	5.83	4.73	7.33	3.95
Eu	0.83	0.78	0.73	0.70	1.0	1.0
Ga	11.9	10.3	21.7	13.4	14.5	16.7
Gd	2.8	4.6	5.2	5.1	7.5	4.8
Ge	<5	<5	<5	<5	<5	<5
Hf	2.5	2.8	3.7	2.7	6.2	2.4
Ho	1.0	1.2	1.8	1.5	2.3	1.3
La	2.5	4.4	2.6	4.3	7.4	4.3
Lu	0.57	0.68	0.89	0.82	1.2	0.65
Nb	1.0	1.0	1.3	1.0	2.2	1.1
Nd	4.60	8.90	5.30	8.90	15.1	9.30
Pr	0.9	1.7	0.9	1.7	2.8	1.7
Rb	7.20	22.0	17.7	8.80	31.3	17.2
Sm	1.9	3.6	2.5	3.7	5.3	3.1
Sn	1.0	2.0	9.0	5.0	1.0	1.0
Sr	47.2	49.2	43.3	55.5	59.3	87.0
Ta	0.2	0.2	0.2	0.2	0.3	0.1
Tb	0.60	0.80	1.1	0.90	1.4	0.86

Sample ID	62719	62720	62721	62722	62723	62685
Hole ID	PH-18-18	PH-18-18	PH-18-18	PH-18-18	PH-18-18	PH-18-21
Depth (m)	56.11	93.63	214.8	229.32	239	17
Lithology	Rhyolite	Rhyolite	Lap. Tuff	Lap. Tuff	Tuff	Sediment
Stratigraphy	MS	MS	FW	MS	FW	FW
Alteration	QS+/-C+/-Py	QS+/-Py	QS+Sil (Cd)	QSCPy+Sil	QSC+/-Py	QSC+/-Py
Th	0.68	1.0	1.0	0.89	1.9	1.1
Tm	0.50	0.64	0.93	0.67	1.2	0.60
U	0.44	0.36	0.37	0.34	0.62	0.33
V	21.0	5.00	5.00	<5.00	7.00	26.0
W	1	1	1	1	3	<1.0
Y	29.3	36.5	53.7	42.1	68.6	34.3
Yb	3.93	4.73	6.53	5.18	8.21	3.99
Zr	71.0	76.0	98.0	76.0	177	77.0
As	1.0	0.80	1.8	4.3	0.50	0.60
Bi	1	0.3	0.4	0.3	0.1	0.3
Hg	0.1	<0.005	<0.005	0.01	<0.005	<0.005
In	14	0.2	0.04	0.03	0.02	0.1
Re	0.002	0.002	0.001	0.001	0.001	<0.001
Sb	0.1	0.1	0.1	0.1	0.1	0.1
Se	0.5	0.2	2	0.7	<0.2	0.2
Te	0.3	0.3	0.1	0.2	0.02	0.2
Tl	0.03	0.04	0.03	0.02	0.04	0.4
Ag	2.0	<0.50	<0.50	<0.50	<0.50	<0.50
Cd	71	0.50	<0.50	<0.50	<0.50	<0.50
Co	2.0	<1.0	6.0	2.0	<1.0	2.0
Cu	1760	63.00	12.00	6.000	3.000	21.00
Li	10	20	10	10	10	10
Mo	15	3.0	4.0	5.0	5.0	1.0
Ni	1.0	1.0	1.0	3.0	1.0	2.0
Pb	18.0	6.00	3.00	2.00	10.0	3.00
Sc	6.00	10.0	11.0	9.00	11.0	18.0
Zn	>10000.0	137.00	28.000	20.000	47.000	94.000
AlOH WL (nm)	2196.1	2199.2	2198.5	2199.1	2197.8	2201.5
AlOH Depth	0.2	0.2	0.3	0.2	0.2	0.1
FeOH WL (nm)	2250.2	2250.1	2244.9	2247.5	2251.3	2254.0
FeOH Depth	0.1	0.2	0.1	0.1	0.2	0.2
AlOH depth/FeOH depth	1.6	1.4	3.4	3.3	1.1	0.52

Sample ID	62686	62688	62690	62691	62737	62738
Hole ID	PH-18-21	PH-18-21	PH-18-21	PH-18-21	PH-18-25	PH-18-25
Depth (m)	40.8	73.88	91.84	118.83	9.8	46
Lithology	Lap. Tuff	Lap. Tuff	Tuff	Rhyolite (sill)	Xtl-Tuff	Xtl-Tuff
Stratigraphy	MS	MS	FW	FW	HW	HW
Alteration	QSCPy	SQC+/-Py	SQC+/-Py	QS	QS+/-Py+/-Sil	QSC+Sil
SiO_2 (wt. %)	76.72	75.80	75.74	76.31	77.23	68.44
Al_2O_3	10.47	11.96	11.85	12.82	10.99	10.36
Fe_2O_3	5.72	2.02	3.71	1.92	2.19	1.14
CaO	0.32	0.509	0.252	0.971	2.88	13.2
MgO	4.36	6.70	5.44	0.250	0.353	0.770
Na_2O	0.143	2.27	2.19	4.90	2.98	0.690
K_2O	1.82	0.387	0.424	2.50	3.16	5.03
Cr_2O_3	0.002	0.001	0.001	0.003	0.002	0.002
TiO_2	0.184	0.132	0.151	0.210	0.121	0.110
MnO	0.21	0.20	0.21	0.020	0.030	0.22
P_2O_5	0.03	0.02	0.03	0.02	0.02	0.01
SrO	0.1	0.1	0.1	0.01	0.01	0.01
BaO	0.02	0.1	0.01	0.1	0.03	0.01
LOI	3.23	2.70	1.92	0.350	1.26	0.620
Total	101.1	101.0	101.1	100.2	100.4	100.6
C	0.090	0.050	0.040	0.040	0.21	0.21
S	0.82	0.12	1.0	0.46	0.37	0.030
Ba (ppm)	220	46.7	88.4	610	280	138
Ce	7.60	8.40	15.4	56.1	17.5	15.3
Cr	20	10	10	20	10	10
Cs	1.7	1.4	0.68	1.1	0.67	0.11
Dy	5.24	7.13	7.86	4.10	9.33	9.17
Er	3.69	5.32	5.46	2.58	6.64	7.29
Eu	0.56	0.80	1.1	0.75	0.94	0.69
Ga	13.7	11.9	12.5	16.5	13.0	10.0
Gd	3.5	5.0	6.0	3.9	6.7	6.7
Ge	<5	<5	<5	<5	<5	<5
Hf	3.1	3.6	3.2	5.5	3.7	3.7
Ho	1.2	1.6	1.6	0.80	2.0	2.2
La	2.9	3.5	5.9	29	7.1	6.3
Lu	0.67	0.86	0.93	0.46	1.1	1.3
Nb	1.4	1.2	1.2	6.2	1.3	1.3
Nd	5.60	6.80	13.3	22.8	14.1	12.7
Pr	1.1	1.3	2.2	5.9	2.6	2.4
Rb	31.5	6.60	3.90	43.2	33.9	26.1
Sm	2.2	3.1	4.5	4.3	4.6	4.4
Sn	1.0	1.0	1.0	1.0	1.0	1.0
Sr	10.1	50.6	45.3	92.2	121	97.6
Ta	0.2	0.1	0.2	0.6	0.1	0.2
Tb	0.66	1.0	1.0	0.62	1.3	1.3

Sample ID	62686	62688	62690	62691	62737	62738
Hole ID	PH-18-21	PH-18-21	PH-18-21	PH-18-21	PH-18-25	PH-18-25
Depth (m)	40.8	73.88	91.84	118.83	9.8	46
Lithology	Lap. Tuff	Lap. Tuff	Tuff	Rhyolite (sill)	Xtl-Tuff	Xtl-Tuff
Stratigraphy	MS	MS	FW	FW	HW	HW
Alteration	QSCPy	SQC+/-Py	SQC+/-Py	QS	QS+/-Py+/-Sil	QSC+Sil
Th	1.4	1.1	1.3	12.5	1.5	1.6
Tm	0.59	0.82	0.82	0.38	1.0	1.0
U	1.7	0.45	0.41	4.8	4.5	1.1
V	22.0	34.0	7.00	14.0	9.00	11.0
W	<1.0	5	<1.0	5	1	1
Y	33.6	43.5	47.6	24.3	55.4	58.6
Yb	4.37	5.48	5.64	2.85	7.37	7.58
Zr	78.0	96.0	92.0	180	95.0	99.0
As	72.1	0.30	0.60	1.0	1.3	1.2
Bi	0.4	0.1	0.5	1	0.5	0.03
Hg	0.01	0.01	0.01	<0.005	<0.005	<0.005
In	1	0.1	0.2	0.01	0.02	<0.005
Re	<0.001	<0.001	0.01	<0.001	0.001	0.001
Sb	0.3	0.1	<0.05	0.1	0.2	0.1
Se	0.2	<0.2	0.2	0.3	<0.2	<0.2
Te	0.4	0.01	0.1	0.4	0.1	0.02
Tl	0.1	0.02	0.02	0.02	0.02	<0.02
Ag	<0.50	<0.50	<0.50	<0.50	<0.50	<0.50
Cd	1.0	<0.50	<0.50	<0.50	<0.50	<0.50
Co	2.0	<1.0	2.0	1.0	1.0	<1.0
Cu	47.00	4.000	82.00	8.000	13.00	3.000
Li	20	20	30	<10	<10	<10
Mo	2.0	2.0	11	2.0	4.0	1.0
Ni	1.0	<1.0	<1.0	1.0	1.0	<1.0
Pb	2.00	57.0	6.00	17.0	14.0	14.0
Sc	10.0	11.0	11.0	3.00	10.0	10.0
Zn	594.00	100.00	422.00	24.000	44.000	21.000
AlOH WL (nm)	2201.4	2197.2	2202.0	2198.3	2193.2	-
AlOH Depth	0.3	0.2	0.1	0.1	0.1	-
FeOH WL (nm)	2252.1	2247.4	2248.0	2253.1	2254.7	2251.4
FeOH Depth	0.4	0.3	0.2	0.05	0.05	0.04
AlOH depth/FeOH depth	0.74	0.62	0.58	1.1	1.4	-

Sample ID	62739	62740	62641	62642	62644	62648
Hole ID	PH-18-25	PH-18-25	PH-18-26	PH-18-26	PH-18-26	PH-18-26
Depth (m)	122	148.75	11.16	26	63.56	39.34
Lithology	Lap. Tuff	Sediment	Sediment	Sediment	Tuff	Tuff
Stratigraphy	MS	FW	HW	HW	HW	HW
Alteration	QSC+/-Py+Sil	QS	QS+/-C (Cd+And)	QS+/-C+Bt	QS	QS
SiO_2 (wt. %)	84.42	74.77	80.54	76.23	70.13	67.38
Al_2O_3	10.28	12.41	10.02	10.83	15.98	11.72
Fe_2O_3	1.48	3.82	4.69	3.41	2.49	2.50
CaO	0.276	1.72	0.292	0.215	0.751	14.2
MgO	0.512	1.27	1.46	6.96	2.92	0.416
Na_2O	1.66	4.11	0.875	1.02	1.57	1.12
K_2O	1.20	1.24	1.79	0.899	5.92	1.97
Cr_2O_3	0.003	0.002	0.003	0.002	0.001	0.001
TiO_2	0.108	0.259	0.177	0.153	0.170	0.325
MnO	0.020	0.36	0.10	0.27	0.040	0.20
P_2O_5	0.01	0.04	0.03	0.01	0.01	0.1
SrO	<0.01	<0.01	0.01	0.01	<0.01	0.01
BaO	0.03	0.01	0.02	0.01	0.01	0.02
LOI	0.300	0.290	2.04	1.91	1.37	2.12
Total	101.9	100.6	98.02	99.77	101.2	100.7
C	0.020	0.030	0.040	0.030	0.010	0.48
S	0.14	<0.010	1.5	0.62	0.040	0.08
Ba (ppm)	295	76.0	236	92.4	103	186
Ce	12.7	13.5	11.7	13.9	17.5	13.8
Cr	30	10	30	20	10	10
Cs	0.47	0.27	1.0	1.6	1.9	0.42
Dy	9.03	7.04	7.70	7.67	12.8	6.17
Er	6.27	4.82	5.34	5.09	8.82	4.41
Eu	1.0	1.4	1.0	1.1	1.4	1.4
Ga	11.5	13.8	11.9	13.1	18.0	12.0
Gd	6.4	5.4	5.5	6.1	8.5	4.7
Ge	<5	<5	<5	<5	<5	<5
Hf	3.4	2.5	3.2	3.0	6.3	2.3
Ho	1.9	1.4	1.7	1.6	3.0	1.5
La	5.3	5.1	5.0	5.4	7.3	6.4
Lu	1.0	0.67	0.94	0.84	1.6	0.69
Nb	1.2	1.1	1.0	1.1	1.4	1.2
Nd	10.7	10.8	9.90	11.8	14.5	10.6
Pr	1.9	2.2	1.9	2.2	2.6	2.0
Rb	11.3	10.2	14.4	9.30	57.5	12.4
Sm	3.7	4.0	3.5	4.0	5.3	3.8
Sn	1.0	1.0	1.0	1.0	1.0	1.0
Sr	65.5	36.7	45.9	40.9	35.0	142
Ta	0.1	0.1	0.1	0.2	<0.1	<0.1
Tb	1.2	1.0	1.1	1.1	1.8	1.0

Sample ID	62739	62740	62641	62642	62644	62648
Hole ID	PH-18-25	PH-18-25	PH-18-26	PH-18-26	PH-18-26	PH-18-26
Depth (m)	122	148.75	11.16	26	63.56	39.34
Lithology	Lap. Tuff	Sediment	Sediment	Sediment	Tuff	Tuff
Stratigraphy	MS	FW	HW	HW	HW	HW
Alteration	QSC+/-Py+Sil	QS	QS+/-C (Cd+And)	QS+/-C+Bt	QS	QS
Th	1.5	0.93	1.4	1.2	1.6	1.0
Tm	1.0	0.7	0.82	0.79	1.5	0.7
U	0.57	0.28	0.45	0.38	1.5	1.1
V	<5.00	<5.00	14.0	7.00	<5.00	7.00
W	1	1	1	2	1	2
Y	52.6	38.0	47.5	43.9	80.0	39.5
Yb	7.03	5.05	5.85	5.59	9.17	4.64
Zr	84.0	81.0	83.0	80.0	168	73.0
As	1.6	0.20	1.3	0.30	0.50	1.0
Bi	0.1	0.01	0.7	0.3	0.02	0.1
Hg	0.03	<0.005	<0.005	0.01	<0.005	<0.005
In	0.04	0.1	0.1	0.2	0.1	0.1
Re	<0.001	<0.001	0.01	0.002	0.001	<0.001
Sb	0.2	<0.05	0.1	<0.05	0.1	0.1
Se	<0.2	<0.2	0.2	<0.2	0.2	0.5
Te	0.0	<0.01	0.4	0.1	0.01	0.04
Tl	0.3	0.1	0.1	0.1	0.2	<0.02
Ag	<0.50	<0.50	<0.50	<0.50	<0.50	<0.50
Cd	2.6	<0.50	<0.50	<0.50	<0.50	2.7
Co	<1.0	<1.0	1.0	1.0	1.0	1.0
Cu	36.00	1.000	80.00	24.00	2.000	4.000
Li	10	10	10	20	30	<10
Mo	7.0	1.0	4.0	18	<1.0	1.0
Ni	2.0	<1.0	1.0	1.0	2.0	1.0
Pb	332	<2.00	12.0	11.0	13.0	9.00
Sc	10.0	18.0	8.00	10.0	32.0	24.0
Zn	478.00	94.000	80.000	578.00	117.00	297.00
AlOH WL (nm)	2198.5	2185.8	-	2202.6	2204.0	-
AlOH Depth	0.3	0.02	-	0.4	0.2	-
FeOH WL (nm)	2244.0	2254.6	-	2247.2	-	-
FeOH Depth	0.1	0.1	-	0.3	-	-
AlOH depth/FeOH depth	3.8	0.18	-	1.3	-	-

Sample ID	62649	62653	62571	62573	62575	62579	62580
Hole ID	PH-18-26	PH-18-26	PH-18-34	PH-18-34	PH-18-34	PH-18-34	PH-18-34
Depth (m)	41	167	9.23	32.49	46.49	90.43	100.85
Lithology	Dike	Dike	Sediment	Sediment	Dike	Lap. Tuff	Lap. Tuff
Stratigraphy	HW	HW	HW	HW	HW	HW	HW
Alteration	Unaltered	Unaltered	GraQ	GraQ	Unaltered	QSC	QS
SiO_2 (wt. %)	75.48	79.78	63.24	62.93	50.11	67.44	73.84
Al_2O_3	12.55	11.05	17.36	17.91	17.01	13.76	10.58
Fe_2O_3	2.51	1.75	7.77	8.46	11.3	9.80	8.58
CaO	1.91	1.40	1.95	0.620	9.03	1.29	1.33
MgO	0.158	0.340	3.19	2.92	7.26	0.904	0.564
Na_2O	3.36	3.86	1.07	0.536	2.66	1.06	0.504
K_2O	3.56	1.62	4.12	5.29	0.505	4.18	3.13
Cr_2O_3	0.001	0.003	0.01	0.02	0.01	0.002	0.003
TiO_2	0.346	0.120	0.870	0.851	1.66	0.366	0.302
MnO	0.040	0.060	0.20	0.16	0.19	0.041	0.071
P_2O_5	0.08	0.01	0.1	0.2	0.2	0.8	0.1
SrO	<0.01	0.05	0.01	<0.01	0.0	<0.01	<0.01
BaO	0.02	0.02	0.1	0.1	0.01	0.4	1
LOI	0.180	0.0800	3.01	3.30	1.15	2.65	2.29
Total	101.4	100.1	98.36	98.49	98.14	101.1	101.6
C	0.020	0.040	1.2	0.050	0.010	0.010	0.010
S	0.55	0.19	0.67	3.2	0.53	4.2	3.4
Ba (ppm)	177	147	525	925	96.4	3440	8530
Ce	12.0	16.3	90.2	87.5	25.2	20.4	12.1
Cr	10	20	120	120	70	10	20
Cs	0.41	0.30	5.0	3.9	2.2	1.6	0.94
Dy	5.38	9.28	5.97	7.82	5.03	11.1	5.11
Er	3.85	6.52	3.57	4.64	3.37	7.50	3.36
Eu	1.0	0.85	1.6	1.7	1.6	1.6	1.0
Ga	12.4	9.60	24.1	26.7	19.0	17.4	15.0
Gd	3.9	6.7	6.4	8.4	5.5	10	4.3
Ge	<5	<5	<5	<5	<5	<5	<5
Hf	2.5	4.1	4.5	4.1	3.9	2.3	2.4
Ho	1.3	2.1	1.3	1.6	1.2	2.5	1.1
La	4.9	7.1	44	43	9.9	9.4	5.3
Lu	0.59	1.1	0.49	0.62	0.48	1.2	0.49
Nb	1.2	1.4	17.3	17.1	4.3	1.4	1.2
Nd	9.30	13.5	40.4	42.9	18.0	17.8	9.00
Pr	1.7	2.5	10.3	10.9	3.6	3.1	1.7
Rb	19.3	12.9	138	148	12.9	46.9	21.5
Sm	3.4	4.5	7.6	8.4	4.3	6.1	3.0
Sn	1.0	1.0	3.0	4.0	2.0	1.0	1.0
Sr	47.7	42.1	147.0	72.3	306.0	53.2	74.4
Ta	<0.1	0.2	1.0	1.2	0.2	0.1	0.1
Tb	0.87	1.3	1.1	1.3	0.89	1.6	0.7

Sample ID	62649	62653	62571	62573	62575	62579	62580
Hole ID	PH-18-26	PH-18-26	PH-18-34	PH-18-34	PH-18-34	PH-18-34	PH-18-34
Depth (m)	41	167	9.23	32.49	46.49	90.43	100.85
Lithology	Dike	Dike	Sediment	Sediment	Dike	Lap. Tuff	Lap. Tuff
Stratigraphy	HW	HW	HW	HW	HW	HW	HW
Alteration	Unaltered	Unaltered	GraQ	GraQ	Unaltered	QSC	QS
Th	1.0	1.7	13.5	16.1	1.1	1.0	1.1
Tm	0.56	1.0	0.53	0.64	0.48	1.1	0.49
U	0.43	0.64	6.5	19.2	0.51	10	2.4
V	5.00	35.0	252	626	241	8.00	24.0
W	1	2	2	6	1	1	2
Y	33.1	57.1	32.2	43.2	30.5	72.5	29.6
Yb	3.95	7.31	3.25	4.73	3.21	7.24	3.42
Zr	74.0	102	172	158	155	67.0	79.0
As	1.3	0.70	2.9	2.8	140	13	4.3
Bi	0.1	0.8	0.3	0.6	0.4	0.5	0.7
Hg	<0.005	<0.005	<0.005	0.01	<0.005	0.01	<0.005
In	0.04	0.02	0.04	0.1	0.01	0.03	0.03
Re	<0.001	<0.001	0.01	0.04	<0.001	0.01	0.004
Sb	0.1	0.1	0.2	0.3	0.3	0.3	0.2
Se	0.5	<0.2	1	4	0.3	0.7	0.7
Te	0.1	0.3	0.1	0.9	0.2	0.5	0.6
Tl	<0.02	0.02	0.6	0.6	0.1	0.2	0.1
Ag	<0.50	<0.50	<0.50	0.50	<0.50	1.3	0.80
Cd	<0.50	<0.50	0.50	0.90	0.60	0.50	0.50
Co	2.0	1.0	20	23	42	4.0	4.0
Cu	14.00	13.00	64.00	117.0	31.00	34.00	15.00
Li	<10	10	50	40	10	20	20
Mo	1.0	2.0	4.0	21	1.0	4.0	30
Ni	1.0	2.0	54	64	69	10	7.0
Pb	5.00	10.0	21.0	16.0	4.00	10.0	19.0
Sc	13.0	8.00	18.0	15.0	25.0	20.0	16.0
Zn	131.00	30.000	128.00	172.00	121.00	47.000	58.000
AlOH WL (nm)	2199.6	2208.6	-	2198.0	-	-	2196.0
AlOH Depth	0.3	0.2	-	0.2	-	-	0.2
FeOH WL (nm)	2253.0	2253.6	2251.0	-	-	-	-
FeOH Depth	0.2	0.1	0.3	-	-	-	-
AlOH depth/FeOH depth	1.3	1.4	-	-	-	-	-

Sample ID	62581	62582	62584	62585	62586	62587	62588
Hole ID	PH-18-34	PH-18-34	PH-18-34	PH-18-34	PH-18-34	PH-18-34	PH-18-34
Depth (m)	111	125.2	160.75	175.12	195	217.11	251
Lithology	Tuff	Lap. Tuff	Rhyolite	Lap. Tuff	Rhyolite	Basalt	Basalt
Stratigraphy	HW	HW	HW	HW	HW	HW	HW
Alteration	QS+/-C	QS+/-C	QS+/-C	QSC	QSC+Sil	CCal	CCal
SiO_2 (wt. %)	75.03	77.63	73.55	76.39	66.39	57.11	54.13
Al_2O_3	13.53	12.99	13.50	12.82	14.56	21.28	20.07
Fe_2O_3	1.89	2.53	2.45	1.22	6.49	6.65	9.90
CaO	2.04	0.637	2.20	2.18	1.64	4.13	4.40
MgO	0.374	0.189	0.231	0.283	0.102	2.76	4.20
Na_2O	3.95	2.16	4.17	3.88	0.540	1.00	1.59
K_2O	2.70	3.38	3.41	2.68	9.62	5.40	4.73
Cr_2O_3	0.002	0.003	0.002	0.002	0.002	0.002	0.008
TiO_2	0.364	0.358	0.361	0.333	0.428	1.425	0.849
MnO	0.040	0.020	0.020	0.020	0.010	0.041	0.060
P_2O_5	0.06	0.09	0.08	0.2	0.2	0.2	0.01
SrO	<0.01	<0.01	0.01	0.01	<0.01	<0.01	0.01
BaO	0.02	0.02	0.02	0.02	0.03	0.03	0.03
LOI	0.550	0.430	0.600	0.960	1.45	1.28	1.73
Total	99.57	100.9	100.3	100.1	99.66	99.51	101.9
C	0.040	<0.010	0.070	0.40	0.010	<0.010	0.010
S	0.22	0.81	0.90	0.23	2.3	0.17	2.0
Ba (ppm)	159	201	176	137	261	279	219
Ce	13.3	12.3	13.5	14.6	16.8	8.40	2.10
Cr	10	20	20	20	10	10	60
Cs	0.54	0.46	0.35	0.49	0.91	1.4	1.7
Dy	6.65	6.20	6.51	6.34	7.45	4.16	1.23
Er	4.74	4.14	4.30	4.24	4.98	2.55	0.78
Eu	1.5	1.1	1.2	1.5	1.5	1.1	0.53
Ga	15.9	13.7	14.7	13.2	14.4	25.6	20.6
Gd	5.2	4.6	5.3	5.0	5.8	3.5	1.0
Ge	<5	<5	<5	<5	<5	<5	<5
Hf	2.8	2.7	2.6	2.5	3.1	2.6	0.9
Ho	1.6	1.4	1.5	1.5	1.6	0.89	0.25
La	5.4	4.9	5.4	7.1	7.4	3.2	0.7
Lu	0.75	0.69	0.75	0.75	0.69	0.36	0.17
Nb	1.4	1.3	1.3	1.2	1.4	0.80	0.30
Nd	10.1	8.90	10.6	11.0	12.3	7.20	1.90
Pr	2.0	1.7	1.8	2.1	2.5	1.3	0.3
Rb	21.7	21.7	21.9	22.7	50.9	50.4	43.6
Sm	3.7	3.2	3.5	3.7	3.9	2.9	0.8
Sn	1.0	1.0	1.0	1.0	2.0	1.0	<1.0
Sr	60.9	32.8	67.6	102	85.0	78.0	100
Ta	<0.1	<0.1	<0.1	<0.1	0.1	<0.1	<0.1
Tb	1.0	0.91	0.94	0.87	1.1	0.67	0.19

Sample ID	62581	62582	62584	62585	62586	62587	62588
Hole ID	PH-18-34	PH-18-34	PH-18-34	PH-18-34	PH-18-34	PH-18-34	PH-18-34
Depth (m)	111	125.2	160.75	175.12	195	217.11	251
Lithology	Tuff	Lap. Tuff	Rhyolite	Lap. Tuff	Rhyolite	Basalt	Basalt
Stratigraphy	HW	HW	HW	HW	HW	HW	HW
Alteration	QS+/-C	QS+/-C	QS+/-C	QSC	QSC+Sil	CCal	CCal
Th	1.2	1.0	1.1	1.0	1.2	0.88	0.29
Tm	0.73	0.66	0.64	0.67	0.74	0.33	0.13
U	0.51	0.47	3.1	2.7	13	2.9	0.41
V	5.00	5.00	15.0	28.0	15.0	67.0	546
W	1	1	1	1	1	1	1
Y	40.7	37.2	39.5	41.4	44.7	22.1	5.8
Yb	4.92	4.41	4.57	4.85	4.75	2.36	1.02
Zr	87.0	82.0	83.0	77.0	85.0	85.0	26.0
As	5.1	1.3	3.1	1.7	2.9	2.4	0.50
Bi	0.1	0.1	0.1	0.02	0.3	0.04	0.1
Hg	<0.005	<0.005	<0.005	<0.005	<0.005	<0.005	0.01
In	0.1	0.04	0.04	0.1	0.03	0.1	0.1
Re	<0.001	<0.001	0.001	<0.001	0.02	<0.001	0.002
Sb	0.1	0.1	0.2	0.1	0.1	0.1	0.1
Se	0.2	<0.2	0.4	<0.2	0.5	<0.2	0.6
Te	0.1	0.04	0.1	0.02	0.4	0.01	0.04
Tl	<0.02	<0.02	<0.02	<0.02	<0.02	0.1	0.3
Ag	<0.50	<0.50	<0.50	<0.50	<0.50	<0.50	<0.50
Cd	<0.50	<0.50	<0.50	0.50	<0.50	<0.50	0.70
Co	<1.0	1.0	<1.0	<1.0	3.0	5.0	54
Cu	3.000	5.000	5.000	3.000	9.000	2.000	52.00
Li	10	10	<10	<10	<10	50	70
Mo	1.0	1.0	2.0	1.0	4.0	1.0	<1.0
Ni	3.0	1.0	4.0	3.0	11	2.0	13
Pb	4.00	3.00	2.00	2.00	13.0	3.00	3.00
Sc	17.0	14.0	14.0	14.0	20.0	46.0	59.0
Zn	185.00	43.000	68.000	71.000	70.000	59.000	110.00
AlOH WL (nm)	2210.0	2194.7	-	2208.0	2207.0	2203.0	2226.0
AlOH Depth	0.1	0.4	-	0.4	0.4	0.2	0.3
FeOH WL (nm)	2254.0	2257.6	-	-	2242.0	2251.0	2252.0
FeOH Depth	0.1	0.4	-	-	0.3	0.3	0.4
AlOH depth/FeOH depth	0.87	1.1	-	-	1.2	0.87	0.88

Sample ID	62589	62592	62594	62597	62599	62600
Hole ID	PH-18-34	PH-18-34	PH-18-34	PH-18-34	PH-18-34	PH-18-34
Depth (m)	269	304.74	315.2	319.77	337.5	356
Lithology	Basalt	Lap. Tuff	Tuff	Xtl-Tuff	Tuff	Tuff
Stratigraphy	HW	MS	MS	MS	FW	MS
Alteration	Ccal	QSC+Sil	QSCPy+/-Sil	QSCPy+/-Sil	QSC+/-Py	QSC (Cd)
SiO_2 (wt. %)	46.29	73.49	70.93	71.97	68.10	72.91
Al_2O_3	20.05	6.21	14.71	14.23	14.72	12.95
Fe_2O_3	13.5	16.3	5.43	5.43	3.16	4.00
CaO	9.17	1.65	1.93	1.64	1.51	3.88
MgO	5.18	0.563	0.991	2.31	10.4	0.704
Na_2O	3.59	1.21	5.18	3.24	1.01	4.01
K_2O	1.09	0.471	0.620	0.909	0.754	0.933
Cr_2O_3	0.009	0.004	0.002	0.003	0.002	0.004
TiO_2	0.934	0.0512	0.114	0.131	0.126	0.367
MnO	0.18	0.041	0.031	0.050	0.18	0.15
P_2O_5	0.01	0.01	0.01	0.01	0.03	0.09
SrO	0.03	<0.01	0.02	0.02	<0.01	<0.01
BaO	0.01	0.02	0.02	0.1	0.02	0.01
LOI	1.81	3.27	2.43	2.44	2.58	0.810
Total	100.3	101.0	99.28	101.5	98.03	101.6
C	0.10	0.020	0.010	0.020	0.010	0.13
S	1.2	7.7	3.3	3.1	0.40	0.32
Ba (ppm)	53.5	176	183	393	167	97.8
Ce	2.60	14.3	19.0	16.5	12.4	9.50
Cr	70	20	10	10	10	30
Cs	0.47	0.12	0.18	0.41	1.2	0.35
Dy	2.11	6.18	12.0	10.7	11.0	5.78
Er	1.33	3.99	7.52	6.64	7.51	3.86
Eu	0.50	5.0	2.2	2.6	1.7	0.94
Ga	26.2	11.1	18.2	21.4	16.4	14.7
Gd	1.6	5.0	9.0	7.3	7.8	4.3
Ge	<5	<5	<5	<5	<5	<5
Hf	1.1	1.8	4.5	4.7	4.9	2.2
Ho	0.46	1.2	2.6	2.3	2.6	1.2
La	1.0	6.7	7.8	6.4	4.4	4.2
Lu	0.22	0.67	1.2	1.02	1.4	0.63
Nb	0.40	0.60	1.4	1.7	1.5	1.1
Nd	2.50	11.9	16.4	13.4	12.7	8.30
Pr	0.4	2.2	2.9	2.5	2.1	1.4
Rb	13.1	5.00	8.10	13.0	8.90	11.6
Sm	0.8	3.9	5.7	5.1	5.1	2.8
Sn	2.0	2.0	1.0	1.0	1.0	1.0
Sr	280	78.7	182	158	65.6	89.5
Ta	0.1	<0.1	0.1	0.1	0.1	<0.1
Tb	0.31	0.84	1.6	1.4	1.6	0.75

Sample ID	62589	62592	62594	62597	62599	62600
Hole ID	PH-18-34	PH-18-34	PH-18-34	PH-18-34	PH-18-34	PH-18-34
Depth (m)	269	304.74	315.2	319.77	337.5	356
Lithology	Basalt	Lap. Tuff	Tuff	Xtl-Tuff	Tuff	Tuff
Stratigraphy	HW	MS	MS	MS	FW	MS
Alteration	Ccal	QSC+Sil	QSCPy+/-Sil	QSCPy+/-Sil	QSC+/-Py	QSC (Cd)
Th	0.26	0.74	1.6	1.8	1.8	0.90
Tm	0.25	0.58	1.2	1.0	1.4	0.53
U	0.25	2.0	5.6	7.7	1.1	0.36
V	523	7.00	14.0	8.00	<5.00	19.0
W	1	1	1	1	1	1
Y	10.7	38.0	68.4	55.0	69.4	32.3
Yb	1.47	4.18	7.86	6.95	8.80	3.94
Zr	29.0	52.0	123	120	131	70.0
As	1.0	16	32	89	1.4	1.2
Bi	0.2	6	0.1	0.5	0.1	0.1
Hg	<0.005	0.1	0.2	0.1	0.01	<0.005
In	0.04	0.9	0.1	0.1	0.1	0.04
Re	0.001	0.001	0.010	0.002	<0.001	<0.001
Sb	0.1	2	2	11	0.1	0.1
Se	0.3	1	1	0.3	<0.2	0.2
Te	0.4	15	1	3	0.02	0.2
Tl	0.1	0.9	4	6	0.9	0.1
Ag	<0.50	16	4.6	15	0.60	<0.50
Cd	<0.50	5.4	0.90	1.6	<0.50	<0.50
Co	65	4.0	1.0	1.0	2.0	2.0
Cu	47.00	2890	135.0	679.0	5.000	11.00
Li	40	10	20	40	70	10
Mo	1.0	42	41	8.0	2.0	1.0
Ni	16	6.0	28	5.0	1.0	2.0
Pb	8.00	276	133	638	48.0	20.0
Sc	71.0	10.0	25.0	20.0	24.0	17.0
Zn	143.00	1375.0	296.00	521.00	222.00	109.00
AlOH WL (nm)	-	-	-	-	2191.0	2190.0
AlOH Depth	-	-	-	-	0.2	0.1
FeOH WL (nm)	2251.0	2242.0	-	-	2243.0	-
FeOH Depth	0.3	0.4	-	-	0.3	-
AlOH depth/FeOH depth	-	-	-	-	0.73	-

Sample ID	62603	62605	62606	62607	62608	62609
Hole ID	PH-18-34	PH-18-34	PH-18-34	PH-18-34	PH-18-34	PH-18-34
Depth (m)	395	410.04	415.67	430.71	233.69	422.16
Lithology	Xtl-Tuff	Xtl-Tuff	Lap. Tuff	Rhyolite	Basalt	Rhyolite
Stratigraphy	FW	MS	FW	FW	HW	FW
Alteration	QS+/-C	QSCPy	QSC+/-Py+Sil	QS	C-Ep	Least-altered
SiO_2 (wt. %)	74.41	77.73	69.07	76.62	56.77	74.33
Al_2O_3	12.96	9.38	9.78	14.17	19.44	11.49
Fe_2O_3	3.67	7.06	4.25	1.51	7.88	1.16
CaO	1.89	0.702	9.54	1.26	5.72	6.63
MgO	0.676	3.49	6.15	2.45	0.657	0.702
Na_2O	5.16	0.621	0.633	0.891	7.25	4.85
K_2O	0.666	0.794	0.163	2.68	0.758	0.519
Cr_2O_3	0.002	0.002	0.003	0.003	0.003	0.003
TiO_2	0.288	0.102	0.112	0.200	1.16	0.132
MnO	0.18	0.081	0.28	0.14	0.12	0.15
P_2O_5	0.07	0.02	0.01	0.02	0.2	0.01
SrO	0.03	<0.01	0.01	0.01	0.01	0.01
BaO	0.01	0.02	<0.01	0.03	0.01	0.01
LOI	0.340	3.40	1.38	2.14	0.490	0.800
Total	101.0	101.7	99.25	102.0	99.49	99.14
C	0.030	<0.010	0.08	<0.010	0.14	0.17
S	0.030	2.8	0.74	0.070	0.24	0.26
Ba (ppm)	57.6	134	34.9	285	78.0	72.8
Ce	11.4	10.4	17.1	14.2	7.90	14.0
Cr	20	10	20	20	20	20
Cs	0.18	1.0	0.35	1.1	0.21	0.08
Dy	6.20	7.10	7.80	10.9	4.81	8.93
Er	3.90	4.86	5.33	7.07	3.14	5.98
Eu	1.4	0.94	0.82	1.1	0.91	0.90
Ga	15.0	15.9	11.7	15.0	20.4	12.9
Gd	4.9	5.2	5.9	7.4	3.8	6.4
Ge	<5	<5	<5	<5	<5	<5
Hf	2.4	2.6	2.8	4.6	1.4	3.3
Ho	1.3	1.5	1.7	2.4	1.1	2.0
La	4.0	3.7	7.2	5.4	3.1	5.6
Lu	0.61	0.77	0.88	1.2	0.42	1.1
Nb	0.80	0.80	1.2	1.8	0.6	1.1
Nd	10.2	9.10	13.4	11.8	7.10	11.6
Pr	1.9	1.6	2.6	2.3	1.2	2.2
Rb	5.50	9.60	2.50	23.6	4.60	3.70
Sm	3.5	3.3	4.3	4.4	2.5	4.1
Sn	1.0	2.0	2.0	1.0	1.0	1.0
Sr	240	62.0	103	108	133	105
Ta	<0.1	<0.1	<0.1	0.1	<0.1	<0.1
Tb	0.85	0.92	1.1	1.3	0.7	1.2

Sample ID	62603	62605	62606	62607	62608	62609
Hole ID	PH-18-34	PH-18-34	PH-18-34	PH-18-34	PH-18-34	PH-18-34
Depth (m)	395	410.04	415.67	430.71	233.69	422.16
Lithology	Xtl-Tuff	Xtl-Tuff	Lap. Tuff	Rhyolite	Basalt	Rhyolite
Stratigraphy	FW	MS	FW	FW	HW	FW
Alteration	QS+/-C	QSCPy	QSC+/-Py+Sil	QS	C-Ep	Least-altered
Th	1.0	1.0	1.9	1.4	0.61	1.2
Tm	0.56	0.69	0.72	1.1	0.43	0.93
U	0.61	0.57	0.39	0.73	0.51	1.3
V	7.00	<5.00	<5.00	5.00	341	10.0
W	1	5	<1.0	1	1	1
Y	34.6	40.4	44.9	63.3	25.2	55.9
Yb	4.01	5.13	5.25	7.49	3.05	7.22
Zr	73.0	74.0	78.0	130	44.0	90.0
As	0.80	2.5	2.6	2.5	15.7	2.7
Bi	0.02	1	0.1	0.1	0.1	0.1
Hg	<0.005	0.01	0.04	<0.005	<0.005	0.01
In	0.1	1	2	0.03	0.04	0.03
Re	<0.001	<0.001	<0.001	<0.001	0.001	<0.001
Sb	0.1	0.1	0.1	<0.05	0.1	0.1
Se	<0.2	<0.2	<0.2	<0.2	<0.2	<0.2
Te	0.01	2	0.6	0.01	0.1	0.01
Tl	0.04	0.1	0.02	0.1	0.04	0.04
Ag	<0.50	1.7	0.50	<0.50	<0.50	<0.50
Cd	<0.50	0.60	17	<0.50	<0.50	<0.50
Co	2.0	<1.0	<1.0	1.0	17	1.0
Cu	3.000	1360	111.0	3.000	27.00	4.000
Li	10	40	10	20	20	<10
Mo	1.0	1.0	2.0	2.0	1.0	1.0
Ni	3.0	2.0	2.0	3.0	3.0	2.0
Pb	7.00	33.0	16.0	9.00	3.00	12.0
Sc	19.0	12.0	11.0	10.0	44.0	15.0
Zn	122.00	390.00	3760.0	77.000	162.00	73.000
AlOH WL (nm)	2204.0	-	2225.0	2199.0	2204.0	-
AlOH Depth	0.3	-	0.3	0.5	0.2	-
FeOH WL (nm)	-	2247.0	2259.0	2248.0	2263.0	2260.0
FeOH Depth	-	0.2	0.3	0.4	0.2	0.2
AlOH depth/FeOH depth	-	-	0.83	1.6	0.86	-

Sample ID	62610	62611	62613	62614	62617	62618
Hole ID	PH-18-34	PH-18-34	PH-18-34	PH-18-34	PH-18-34	PH-18-34
Depth (m)	447.62	487.41	524.14	548	579.83	591.84
Lithology	Xtl-Tuff	Tuff	Tuff	Tuff	Lap. Tuff	Rhyolite
Stratigraphy	FW	FW	FW	FW	MS	MS
Alteration	QSC	QS+/-C	SQ+/-C+Sil	QSCPy+Sil	QSC+/-Py	QS+/-C+/-Py
SiO_2 (wt. %)	79.83	75.23	74.63	79.44	58.14	81.43
Al_2O_3	11.51	11.91	12.61	11.54	6.56	10.29
Fe_2O_3	0.80	2.79	4.18	1.77	31.78	1.49
CaO	0.703	4.96	2.19	1.23	0.136	2.30
MgO	0.642	1.32	0.65	0.554	1.47	0.482
Na_2O	4.83	2.61	4.42	3.07	0.283	3.34
K_2O	1.47	0.679	0.844	2.18	1.39	0.482
Cr_2O_3	0.003	0.001	0.001	0.003	0.002	0.002
TiO_2	0.122	0.233	0.251	0.101	0.102	0.0703
MnO	0.041	0.20	0.15	0.060	0.068	0.070
P_2O_5	0.02	0.05	0.06	0.03	0.03	0.03
SrO	<0.01	0.01	0.01	<0.01	<0.01	<0.01
BaO	0.03	0.01	0.01	0.02	0.03	0.01
LOI	0.400	0.630	0.650	1.05	9.41	0.580
Total	98.60	99.26	100.2	100.3	97.82	100.2
C	0.020	0.040	0.060	0.030	0.010	0.060
S	0.050	0.43	0.060	0.65	16.7	0.41
Ba (ppm)	263	87.6	76.9	159	267	87.6
Ce	11.8	14.9	12.8	15.5	10.2	15.1
Cr	20	20	10	20	10	20
Cs	0.16	0.40	0.28	0.44	0.51	0.23
Dy	8.26	6.76	6.58	9.64	4.44	7.66
Er	5.27	4.40	4.42	6.79	3.47	5.72
Eu	1.0	1.5	1.1	1.3	1.3	1.1
Ga	14.1	11.9	14.0	12.8	9.10	6.90
Gd	5.9	5.8	5.2	8.1	3.6	6.3
Ge	<5	<5	<5	<5	<5	<5
Hf	3.0	2.9	2.8	4.4	2.0	4.1
Ho	1.7	1.6	1.5	2.4	1.1	1.8
La	4.6	5.8	5.0	5.5	4.1	5.9
Lu	0.87	0.78	0.83	1.1	0.52	1.1
Nb	1.0	0.90	0.80	1.2	0.90	1.0
Nd	10.5	12.2	10.6	14.7	7.70	12.5
Pr	1.8	2.4	1.9	2.7	1.5	2.4
Rb	8.20	8.30	8.40	17.5	10.2	5.20
Sm	3.9	4.2	3.9	5.6	2.8	5.6
Sn	1.0	1.0	1.0	1.0	6.0	1.0
Sr	35.5	103	84.5	42.1	24.2	42.3
Ta	0.1	<0.1	<0.1	<0.1	<0.1	<0.1
Tb	1.0	1.0	1.1	1.5	0.68	1.2

Sample ID	62610	62611	62613	62614	62617	62618
Hole ID	PH-18-34	PH-18-34	PH-18-34	PH-18-34	PH-18-34	PH-18-34
Depth (m)	447.62	487.41	524.14	548	579.83	591.84
Lithology	Xtl-Tuff	Tuff	Tuff	Tuff	Lap. Tuff	Rhyolite
Stratigraphy	FW	FW	FW	FW	MS	MS
Alteration	QSC	QS+/-C	SQ+/-C+Sil	QSCPy+Sil	QSC+/-Py	QS+/-C+/-Py
Th	1.2	0.90	1.0	1.4	0.59	1.4
Tm	0.83	0.74	0.73	1.1	0.47	0.91
U	0.43	0.35	0.29	0.46	0.33	0.43
V	8.00	<5.00	<5.00	<5.00	<5.00	<5.00
W	1	1	1	1	2	<1.0
Y	46.2	42.4	38.4	63.2	28.6	49.6
Yb	6.08	4.78	5.03	7.55	3.46	6.38
Zr	86.0	82.0	86.0	106.0	58.0	106
As	2.2	2.3	1.3	6.0	16	4.2
Bi	0.01	0.1	0.04	0.1	4	0.2
Hg	<0.005	0.01	<0.005	<0.005	0.1	<0.005
In	0.1	0.04	0.1	0.1	61	0.1
Re	<0.001	0.001	<0.001	<0.001	0.001	<0.001
Sb	0.1	0.1	0.1	0.1	0.3	0.3
Se	<0.2	0.3	0.2	0.3	2	<0.2
Te	<0.01	0.1	0.01	0.03	1	0.1
Tl	0.1	0.1	0.04	0.1	0.2	0.1
Ag	<0.50	<0.50	<0.50	<0.50	6.8	0.70
Cd	<0.50	<0.50	<0.50	<0.50	10	0.70
Co	1.0	2.0	2.0	1.0	1.0	1.0
Cu	5.000	18.00	4.000	3.000	6880	48.00
Li	10	10	10	10	10	<10
Mo	1.0	2.0	1.0	2.0	52	2.0
Ni	3.0	2.0	1.0	2.0	<1.0	5.0
Pb	11.0	15.0	3.00	5.00	71.0	36.0
Sc	8.00	18.0	20.0	20.0	1.00	16.0
Zn	55.000	207.00	121.00	93.000	2200.0	240.00
AlOH WL (nm)	2216.7	2201.0	-	-	-	-
AlOH Depth	0.1	0.2	-	-	-	-
FeOH WL (nm)	2253.1	2254.0	2260.0	2253.0	-	2256.0
FeOH Depth	0.2	0.2	0.2	0.1	-	0.4
AlOH depth/FeOH depth	0.50	1.1	-	-	-	-

Sample ID	62619	62620	62622	62623	62624	62625	62626
Hole ID	PH-18-34	PH-18-34	PH-18-34	PH-18-40	PH-18-40	PH-18-40	PH-18-40
Depth (m)	608	625.2	667.18	19.65	39.85	64.2	78.75
Lithology	Rhyolite	Rhyolite	Tuff	Lap. Tuff	Tuff	Tuff	Lap. Tuff
Stratigraphy	FW	FW	FW	HW	HW	HW	MS
Alteration	QSC+Sil	QS+/-C+/-Py	QSC+/-Py	QS	QS+/-C	QS+/-C	QS+/-Py
SiO_2 (wt. %)	74.45	75.90	74.53	79.88	69.83	74.71	77.89
Al_2O_3	12.62	13.75	14.46	11.79	15.85	12.62	12.25
Fe_2O_3	4.15	1.83	2.11	1.84	2.60	3.32	1.96
CaO	2.23	3.33	0.703	2.08	0.843	1.53	0.635
MgO	0.822	1.30	2.37	2.10	0.171	0.740	2.80
Na_2O	4.13	1.60	2.86	1.62	5.34	4.58	2.03
K_2O	1.10	1.96	2.70	0.527	4.75	1.99	2.18
Cr_2O_3	0.001	0.001	0.001	0.002	0.001	0.001	0.001
TiO_2	0.257	0.160	0.161	0.0895	0.451	0.314	0.133
MnO	0.17	0.11	0.040	0.030	0.030	0.081	0.061
P_2O_5	0.06	0.02	0.03	0.01	0.1	0.08	0.03
SrO	0.01	0.02	0.02	0.03	0.01	<0.01	<0.01
BaO	0.01	0.02	0.01	0.01	0.03	0.03	0.03
LOI	0.500	1.12	1.23	1.45	0.340	0.740	2.23
Total	101.5	101.1	100.8	102.0	100.0	99.39	99.80
C	0.05	0.010	0.010	<0.01	0.030	0.10	0.090
S	0.20	0.17	0.47	0.080	0.44	0.090	0.32
Ba (ppm)	95.2	144	133	65.7	246	273	228
Ce	15.4	16.1	10.6	21.0	14.3	11.3	13.3
Cr	20	20	10	20	10	10	20
Cs	0.24	2.0	2.2	0.83	0.37	0.28	0.78
Dy	6.96	10.8	7.42	11.2	7.04	5.94	8.63
Er	5.03	7.76	5.56	7.81	4.58	4.27	6.48
Eu	1.4	1.3	1.3	1.1	1.1	1.1	1.1
Ga	15.0	14.8	12.1	13.4	17.3	15.1	14.6
Gd	5.9	7.5	5.5	8.9	5.4	4.9	6.4
Ge	<5	<5	<5	<5	<5	<5	<5
Hf	2.8	4.5	4.7	4.9	3.0	2.5	3.3
Ho	1.7	2.6	1.7	2.7	1.5	1.4	2.1
La	5.8	6.2	3.7	8.4	5.4	4.1	5.4
Lu	0.88	1.4	1.0	1.4	0.61	0.65	1.0
Nb	1.0	1.3	1.3	1.1	1.5	1.2	0.90
Nd	13.2	14.3	10.8	18.2	10.6	9.10	11.1
Pr	2.3	2.4	1.9	3.3	2.2	1.7	2.1
Rb	12.3	35.2	28.5	7.70	27.0	11.4	16.0
Sm	4.7	5.4	4.3	6.6	4.1	3.5	4.4
Sn	1.0	2.0	1.0	1.0	1.0	1.0	1.0
Sr	72.7	189	203	266	87.8	62.4	51.6
Ta	<0.1	0.2	<0.1	<0.1	<0.1	<0.1	<0.1
Tb	1.1	1.6	1.1	1.7	1.0	0.86	1.2

Sample ID	62619	62620	62622	62623	62624	62625	62626
Hole ID	PH-18-34	PH-18-34	PH-18-34	PH-18-40	PH-18-40	PH-18-40	PH-18-40
Depth (m)	608	625.2	667.18	19.65	39.85	64.2	78.75
Lithology	Rhyolite	Rhyolite	Tuff	Lap. Tuff	Tuff	Tuff	Lap. Tuff
Stratigraphy	FW	FW	FW	HW	HW	HW	MS
Alteration	QSC+Sil	QS+/-C+/-Py	QSC+/-Py	QS	QS+/-C	QS+/-C	QS+/-Py
Th	1.0	1.4	1.3	1.6	1.2	1.0	1.0
Tm	0.76	1.2	0.89	1.2	0.67	0.57	0.94
U	0.32	1.1	0.76	0.61	0.55	0.33	0.54
V	<5.00	<5.00	<5.00	<5.00	10.0	<5.00	7.00
W	1	1	<1.0	2	1	1	1
Y	43.9	72.2	42.9	72.6	38.3	35.0	54.9
Yb	5.00	8.47	6.58	8.33	4.34	4.05	6.57
Zr	88.0	119	118	128	99.0	81.0	96.0
As	1.3	1.1	2.1	0.30	17	1.7	1.6
Bi	0.04	0.1	0.2	0.03	0.2	0.03	0.1
Hg	<0.005	<0.005	<0.005	<0.005	<0.005	<0.005	0.1
In	0.1	0.1	0.1	0.1	0.1	0.1	0.2
Re	<0.001	0.001	<0.001	<0.001	<0.001	0.001	<0.001
Sb	0.1	0.1	0.1	<0.05	<0.05	0.1	0.2
Se	0.2	0.2	<0.2	0.3	<0.2	0.3	0.2
Te	0.04	0.01	0.03	0.01	0.1	0.03	0.03
Tl	0.1	0.2	0.2	<0.02	0.02	0.02	0.1
Ag	<0.50	<0.50	<0.50	<0.50	<0.50	<0.50	<0.50
Cd	<0.50	<0.50	<0.50	<0.50	<0.50	<0.50	8.0
Co	1.0	2.0	2.0	2.0	<1.0	1.0	1.0
Cu	4.000	3.000	4.000	1.000	13.00	2.00	123.0
Li	10	20	50	30	10	10	30
Mo	1.0	3.0	1.0	1.0	1.0	1.0	2.0
Ni	4.0	2.0	3.0	1.0	1.0	3.0	3.0
Pb	7.00	6.00	3.00	6.00	16.0	<2.00	20.0
Sc	19.0	18.0	17.0	23.0	21.0	17.0	15.0
Zn	267.00	131.00	100.00	89.000	141.00	89.000	1975.0
AlOH WL (nm)	2204.0	2198.9	-	2200.6	-	2194.0	2204.1
AlOH Depth	0.4	0.4	0.2	0.2	-	0.1	0.3
FeOH WL (nm)	2259.0	2248.2	2247.5	2250.4	-	2258.0	2247.0
FeOH Depth	0.3	0.3	-	0.2	-	0.1	0.1
AlOH depth/FeOH depth	1.1	1.6	-	1.2	-	0.51	1.8

Sample ID	62627	62629	62632	62634	62635	62637
Hole ID	PH-18-40	PH-18-40	PH-18-40	PH-18-40	PH-18-40	PH-18-40
Depth (m)	88	125.32	178	212.87	222.83	282.83
Lithology	Xtl-Tuff	Rhyolite	Sediment	Rhyolite	Rhyolite	Xtl-Tuff
Stratigraphy	MS	MS	FW	FW	FW	FW
Alteration	QS+/-C+/-Py+Sil	QSC+/-Sil	SC	QSC	QSC+/-Py	QS
SiO_2 (wt. %)	83.71	71.93	74.20	78.42	78.69	78.57
Al_2O_3	7.20	14.48	13.10	12.17	9.63	10.95
Fe_2O_3	5.33	5.78	3.76	2.17	3.10	2.80
CaO	0.253	0.463	1.74	0.160	1.45	1.51
MgO	0.557	3.09	1.51	1.84	4.22	1.25
Na_2O	1.56	2.25	3.98	3.99	2.27	4.15
K_2O	1.23	1.61	1.28	1.02	0.350	0.522
Cr_2O_3	0.002	0.001	0.001	0.001	0.001	0.001
TiO_2	0.0811	0.200	0.259	0.140	0.110	0.121
MnO	0.030	0.074	0.090	0.050	0.13	0.10
P_2O_5	0.02	0.09	0.05	0.03	0.02	0.02
SrO	<0.01	0.01	<0.01	<0.01	0.01	<0.01
BaO	0.03	0.02	0.02	0.01	0.01	0.01
LOI	2.10	3.07	0.690	1.57	1.70	1.07
Total	100.8	98.03	101.1	101.4	101.6	100.6
C	0.020	0.010	0.020	0.010	0.030	0.06
S	2.4	2.1	0.13	0.58	0.52	0.72
Ba (ppm)	241	223	132	132	48.1	103
Ce	5.80	13.7	11.5	20.6	10.9	14.9
Cr	20	10	20	20	10	10
Cs	0.45	1.2	1.1	0.88	0.57	0.26
Dy	5.46	5.71	6.56	8.07	5.08	6.68
Er	4.22	4.53	4.21	5.46	3.78	4.80
Eu	0.88	3.2	1.5	0.76	0.62	0.77
Ga	9.40	19.2	15.5	10.4	9.70	10.9
Gd	3.9	4.4	5.7	6.3	3.6	5.3
Ge	<5	<5	<5	<5	<5	<5
Hf	2.6	3.1	2.8	3.8	3.1	3.4
Ho	1.3	1.5	1.4	2.0	1.3	1.7
La	2.3	5.7	4.6	8.5	4.3	5.8
Lu	0.71	0.82	0.66	1.1	0.77	0.88
Nb	0.90	0.90	0.90	1.3	1.0	1.1
Nd	5.20	10.5	11.1	16.6	8.50	11.9
Pr	0.9	2.0	1.7	3.2	1.7	2.2
Rb	11.1	20.8	14.8	10.2	3.70	4.10
Sm	2.3	3.6	3.8	5.2	3.1	3.9
Sn	2.0	3.0	1.0	1.0	1.0	1.0
Sr	56.9	114	57.0	66.5	102	60.1
Ta	<0.1	<0.1	0.1	<0.1	<0.1	<0.1
Tb	0.78	0.89	1.0	1.4	0.76	1.0

Sample ID	62627	62629	62632	62634	62635	62637
Hole ID	PH-18-40	PH-18-40	PH-18-40	PH-18-40	PH-18-40	PH-18-40
Depth (m)	88	125.32	178	212.87	222.83	282.83
Lithology	Xtl-Tuff	Rhyolite	Sediment	Rhyolite	Rhyolite	Xtl-Tuff
Stratigraphy	MS	MS	FW	FW	FW	FW
Alteration	QS+/-C+/-Py+Sil	QSC+/-Sil	SC	QSC	QSC+/-Py	QS
Th	0.79	1.2	1.0	1.5	1.1	1.2
Tm	0.64	0.71	0.66	0.91	0.62	0.76
U	0.48	4.2	0.32	0.58	0.32	0.42
V	9.00	30.0	8.00	<5.00	<5.00	<5.00
W	1	2	1	1	<1.0	1
Y	32.2	39.5	38.8	49.7	33.6	44.2
Yb	4.68	4.88	4.61	6.22	4.21	5.54
Zr	75.0	86.0	85.0	98.0	78.0	93.0
As	15	2.3	0.20	3.1	0.60	4.5
Bi	1	8	0.2	0.7	1.0	0.6
Hg	0.2	0.1	<0.005	<0.005	0.01	<0.005
In	0.3	2	0.1	0.1	0.6	0.2
Re	0.001	0.01	<0.001	0.00	<0.001	<0.001
Sb	2	0.6	0.1	0.1	0.1	0.1
Se	0.4	0.9	<0.2	0.2	0.5	0.4
Te	1	0.6	0.1	0.2	0.6	0.5
Tl	0.1	0.3	0.1	0.02	0.02	<0.02
Ag	4.3	6.9	<0.50	<0.50	<0.50	<0.50
Cd	23	24	<0.50	<0.50	<0.50	<0.50
Co	5.0	2.0	2.0	2.0	1.0	2.0
Cu	184.0	901.0	6.000	36.00	184.0	8.000
Li	10	30	20	20	20	10
Mo	2.0	22	1.0	3.0	3.0	4.0
Ni	2.0	1.0	3.0	3.0	1.0	3.0
Pb	2480	1135	2.00	2.00	29.0	11.0
Sc	11.0	12.0	18.0	12.0	9.00	12.0
Zn	5830.0	3880.0	124.00	67.000	275.00	86.000
AlOH WL (nm)	-	-	2226.7	2197.8	-	-
AlOH Depth	-	-	0.05	0.2	-	-
FeOH WL (nm)	-	-	2253.9	2248.5	2246.0	2246.0
FeOH Depth	-	-	0.2	0.1	0.2	0.2
AlOH depth/FeOH depth	-	-	0.20	1.7	-	-

Sample ID	62639	62697	62698	62699	62700	62701	62692
Hole ID	PH-18-40	PH-18-42	PH-18-42	PH-18-42	PH-18-42	PH-18-42	PH-18-44
Depth (m)	315.83	17	42.44	56	121.7	133.82	22
Lithology	Xtl-Tuff	Xtl-Tuff	Lap. Tuff	Xtl-Tuff	Tuff	Tuff	Tuff
Stratigraphy	FW	HW	MS	FW	FW	FW	HW
Alteration	QSC	QSC	QSCPy	QS+/-Py	QSC+/-Py+Sil	QS+Sil	QS
SiO_2 (wt. %)	76.09	72.48	66.30	78.45	79.19	79.05	74.78
Al_2O_3	13.35	15.95	11.12	11.13	11.45	11.96	12.87
Fe_2O_3	2.84	3.92	13.21	4.84	4.31	1.46	1.74
CaO	0.23	0.67	1.51	0.151	0.0605	0.847	1.62
MgO	1.14	1.65	6.26	2.48	2.35	0.807	0.0807
Na_2O	5.26	2.17	0.397	1.27	0.585	4.53	3.32
K_2O	0.857	2.82	0.919	1.46	1.66	1.19	5.12
Cr_2O_3	0.002	0.002	0.001	0.002	0.007	0.002	0.002
TiO_2	0.151	0.196	0.115	0.111	0.192	0.110	0.353
MnO	0.060	0.041	0.14	0.060	0.15	0.050	0.020
P_2O_5	0.01	0.03	0.01	0.01	0.01	<0.01	0.08
SrO	0.1	0.01	0.01	0.01	0.01	<0.01	0.1
BaO	0.01	0.1	0.03	0.04	0.03	0.01	0.02
LOI	1.15	3.06	4.48	1.70	2.22	0.900	0.190
Total	100.4	99.91	100.3	101.0	101.4	101.2	99.28
C	0.030	0.010	0.020	0.010	0.020	0.020	0.040
S	0.63	2.2	4.3	1.3	1.0	0.38	0.42
Ba (ppm)	111	416	307	359	301	108	194
Ce	16.3	26.0	14.1	15.6	12.1	15.5	13.0
Cr	10	10	10	30	20	20	20
Cs	0.39	1.4	1.7	1.2	2.3	0.33	0.20
Dy	9.47	9.72	9.60	11.0	6.03	10.0	6.35
Er	6.86	6.06	6.00	7.48	4.21	6.84	4.56
Eu	1.0	1.1	0.77	1.0	0.70	1.2	1.1
Ga	15.2	17.3	18.7	15.6	13.5	12.5	12.6
Gd	6.5	8.6	6.6	8.0	4.3	7.2	4.8
Ge	<5	<5	<5	<5	<5	<5	<5
Hf	4.0	6.0	3.7	4.5	2.9	4.2	2.5
Ho	2.0	2.1	2.1	2.4	1.3	2.2	1.4
La	6.6	10	5.6	6.0	4.8	5.9	5.2
Lu	1.1	1.0	1.1	1.2	0.71	1.2	0.59
Nb	1.5	1.8	1.2	1.2	1.0	1.3	1.3
Nd	13.3	19.4	11.3	12.8	9.60	12.9	9.90
Pr	2.6	3.9	2.2	2.5	1.8	2.4	2.0
Rb	10.5	24.2	12.9	11.4	33.2	10.9	24.9
Sm	4.5	6.6	4.4	5.4	3.2	5.2	3.9
Sn	1.0	2.0	2.0	3.0	2.0	1.0	1.0
Sr	62.8	88.0	77.3	75.9	37.1	38.6	75.0
Ta	0.1	0.4	0.2	0.2	0.2	0.2	0.2
Tb	1.3	1.5	1.3	1.5	0.82	1.3	0.83

Sample ID	62639	62697	62698	62699	62700	62701	62692
Hole ID	PH-18-40	PH-18-42	PH-18-42	PH-18-42	PH-18-42	PH-18-42	PH-18-44
Depth (m)	315.83	17	42.44	56	121.7	133.82	22
Lithology	Xtl-Tuff	Xtl-Tuff	Lap. Tuff	Xtl-Tuff	Tuff	Tuff	Tuff
Stratigraphy	FW	HW	MS	FW	FW	FW	HW
Alteration	QSC	QSC	QSCPy	QS+/-Py	QSC+/-Py+Sil	QS+Sil	QS
Th	1.9	2.6	1.4	0.94	0.90	1.4	1.2
Tm	1.1	1.0	1.0	1.1	0.63	1.0	0.67
U	0.57	8.9	1.2	0.39	0.72	0.52	0.50
V	5.00	39.0	6.00	<5.00	9.00	<5.00	<5.00
W	1	1	1	1	1	1	<1.0
Y	56.2	54.3	55.7	68.7	37.5	61.8	37.5
Yb	7.37	6.96	6.94	8.55	4.72	8.07	4.68
Zr	107	145	103	116	79.0	108	75.0
As	3.5	4.6	1.0	0.90	1.1	1.1	3.2
Bi	0.4	0.4	2	0.9	0.8	0.1	0.1
Hg	<0.005	0.01	0.01	<0.005	0.01	<0.005	<0.005
In	0.04	4	0.5	0.1	0.2	0.03	0.1
Re	0.001	0.01	<0.001	<0.001	0.001	<0.001	0.001
Sb	0.1	0.1	0.1	0.1	0.1	<0.05	<0.05
Se	<0.2	1	3	0.3	0.2	<0.2	<0.2
Te	0.1	0.1	4	1.1	0.8	0.0	0.2
Tl	<0.02	0.1	0.2	0.1	0.04	<0.02	<0.02
Ag	<0.50	1.1	1.3	<0.50	<0.50	<0.50	<0.50
Cd	<0.50	0.90	2.8	<0.50	<0.50	<0.50	0.80
Co	1.0	<1.0	<1.0	<1.0	1.0	<1.0	<1.0
Cu	8.000	717.0	73.00	9.000	54.00	4.000	7.000
Li	10	10	10	20	40	10	<10
Mo	4.0	26	5.0	3.0	6.0	2.0	3.0
Ni	<1.0	8.0	6.0	2.0	2.0	<1.0	<1.0
Pb	<2.00	14.0	12.0	11.0	4.00	8.00	<2.00
Sc	14.0	12.0	18.0	20.0	12.0	18.0	11.0
Zn	38.000	186.00	550.00	102.00	60.000	55.000	332.00
AlOH WL (nm)	2202.5	2197.5	2217.6	2202.2	2201.4	2205.1	-
AlOH Depth	0.2	0.4	0.1	0.3	0.3	0.2	-
FeOH WL (nm)	2253.9	2240.9	2246.5	2248.5	2250.8	2249.0	-
FeOH Depth	0.1	0.1	0.1	0.2	0.2	0.1	-
AlOH depth/FeOH depth	1.3	4.2	0.5	1.6	1.6	1.6	-

Sample ID	62693	62694	62695	62696	62764	62766
Hole ID	PH-18-44	PH-18-44	PH-18-44	PH-18-44	PH-19-09	PH-19-09
Depth (m)	54.05	94.11	117.7	129.6	25.35	112.04
Lithology	Lap. Tuff	Lap. Tuff	Tuff	Lap. Tuff	Tuff	Rhyolite
Stratigraphy	HW	HW	MS	MS	HW	HW
Alteration	QSC	QSC+/-Py+Sil	QSCPy	QSCPy	QS+Sil	QS
SiO_2 (wt. %)	79.80	77.80	82.21	68.14	74.84	74.75
Al_2O_3	10.71	11.42	9.80	14.39	12.26	15.54
Fe_2O_3	1.77	4.93	1.82	1.91	3.67	2.01
CaO	0.837	1.41	0.281	1.14	0.610	2.09
MgO	2.23	1.15	2.63	10.85	0.0600	2.68
Na_2O	4.04	1.81	1.87	1.60	3.71	2.18
K_2O	0.398	1.24	1.06	1.49	4.37	0.578
Cr_2O_3	0.002	0.002	0.003	0.001	0.002	0.003
TiO_2	0.120	0.101	0.201	0.166	0.350	0.124
MnO	0.060	0.040	0.090	0.28	0.010	0.010
P_2O_5	0.02	0.02	0.02	0.02	0.09	0.01
SrO	0.05	0.01	0.01	0.01	0.1	0.03
BaO	0.01	0.1	0.01	0.01	0.02	0.1
LOI	1.06	2.18	1.55	5.10	0.80	2.11
Total	101.4	101.2	101.3	101.4	100.7	98.97
C	0.020	0.020	0.010	0.2	0.020	0.010
S	0.24	2.1	0.09	0.05	1.7	0.19
Ba (ppm)	76.7	590	134	96.3	192	45.7
Ce	14.5	16.9	9.40	9.30	12.4	29.0
Cr	10	20	20	10	20	20
Cs	0.62	1.4	1.0	3.3	0.21	0.82
Dy	8.99	9.36	5.62	8.52	5.87	14.4
Er	6.31	7.01	4.13	5.95	4.00	9.72
Eu	1.1	0.74	1.1	1.4	1.1	1.5
Ga	11.0	17.1	10.7	13.1	11.8	17.3
Gd	6.4	7.1	4.4	6.3	4.4	11
Ge	<5	<5	<5	<5	<5	<5
Hf	3.4	4.0	3.0	4.2	2.5	5.7
Ho	2.0	2.1	1.3	1.9	1.3	3.3
La	5.8	6.2	3.9	3.2	5.0	12
Lu	1.1	1.2	0.70	1.0	0.63	1.7
Nb	1.1	1.1	1.1	1.5	1.3	2.0
Nd	12.0	13.5	6.90	9.20	9.50	22.3
Pr	2.3	2.6	1.4	1.5	1.9	4.4
Rb	4.80	12.3	12.5	38.1	20.5	7.10
Sm	4.5	5.2	2.6	4.2	3.2	7.6
Sn	1.0	2.0	1.0	1.0	1.0	1.0
Sr	44.8	122	46.5	47.1	44.4	242
Ta	0.1	0.2	0.3	0.2	0.1	0.2
Tb	1.2	1.3	0.85	1.2	0.84	2.0

Sample ID	62693	62694	62695	62696	62764	62766
Hole ID	PH-18-44	PH-18-44	PH-18-44	PH-18-44	PH-19-09	PH-19-09
Depth (m)	54.05	94.11	117.7	129.6	25.35	112.04
Lithology	Lap. Tuff	Lap. Tuff	Tuff	Lap. Tuff	Tuff	Rhyolite
Stratigraphy	HW	HW	MS	MS	HW	HW
Alteration	QSC	QSC+/-Py+Sil	QSCPy	QSCPy	QS+Sil	QS
Th	1.2	1.4	0.94	1.4	0.91	2.0
Tm	0.93	1.1	0.58	0.89	0.57	1.6
U	0.51	0.52	0.93	0.54	2.5	0.71
V	14.0	6.00	29.0	<5.00	9.00	<5.00
W	<1.0	<1.0	1	4	1	1
Y	52.4	58.3	38.7	51.4	34.4	93.7
Yb	6.70	7.96	4.89	6.21	4.28	11.3
Zr	90.0	108	80.0	115	74.0	153
As	1.5	1.5	0.40	0.60	1.7	0.90
Bi	0.1	1	0.02	1	0.2	0.04
Hg	0.01	0.01	0.01	0.01	<0.005	<0.005
In	0.04	0.1	0.1	0.1	0.03	0.04
Re	0.001	0.001	0.001	0.001	0.003	<0.001
Sb	0.1	<0.05	0.1	0.1	0.1	0.1
Se	<0.2	1	<0.2	<0.2	0.3	<0.2
Te	0.1	1	0.02	0.04	0.1	0.01
Tl	0.03	0.1	0.1	0.2	<0.02	<0.02
Ag	<0.50	<0.50	<0.50	<0.50	<0.50	<0.50
Cd	1.5	<0.50	<0.50	<0.50	<0.50	<0.50
Co	<1.0	<1.0	1.0	<1.0	2.0	<1.0
Cu	29.00	15.00	10.00	9.000	5.000	1.000
Li	10	20	30	60	<10	30
Mo	2.0	5.0	5.0	3.0	1.0	1.0
Ni	<1.0	1.0	4.0	<1.0	3.0	1.0
Pb	5.00	5.00	21.0	80.0	7.00	6.00
Sc	12.0	19.0	9.00	11.0	15.0	26.0
Zn	340.00	71.000	326.00	308.00	57.000	73.000
AlOH WL (nm)	2209.8	2201.9	2198.2	2208.4	2202.8	2199.1
AlOH Depth	0.1	0.2	0.4	0.3	0.1	0.4
FeOH WL (nm)	2249.4	2249.6	2248.9	2248.5	2246.6	2251.7
FeOH Depth	0.2	0.1	0.3	0.3	0.1	0.3
AlOH depth/FeOH depth	0.65	2.0	1.5	0.75	1.3	1.5

Sample ID	62767	62768	62769	62770	62771	62772
Hole ID	PH-19-09	PH-19-10	PH-19-10	PH-19-10	PH-19-10	PH-19-10
Depth (m)	289	6.78	55.45	76.44	117.86	127.92
Lithology	Tuff	Lap. Tuff	Lap. Tuff	Rhyolite	Xtl-Tuff	Xtl-Tuff
Stratigraphy	FW	MS	MS	MS	FW	FW
Alteration	QS+/-C+/-Py	QSC+/-Py+Sil	QSC+/-Py+Sil	QSC	QSC	QSC
SiO_2 (wt. %)	77.09	81.56	73.27	78.86	75.39	76.28
Al_2O_3	11.91	9.50	13.41	11.24	12.40	12.38
Fe_2O_3	4.19	5.91	4.13	2.09	3.71	3.02
CaO	0.0821	0.0727	2.52	0.425	1.32	1.35
MgO	3.52	0.270	1.02	3.02	2.52	1.38
Na_2O	0.298	0.779	4.02	3.77	3.41	3.71
K_2O	2.63	1.68	1.02	0.294	0.853	1.55
Cr_2O_3	0.003	0.002	0.002	0.002	0.001	0.003
TiO_2	0.144	0.156	0.320	0.142	0.251	0.221
MnO	0.10	0.021	0.17	0.14	0.080	0.050
P_2O_5	0.02	0.02	0.07	0.01	0.05	0.04
SrO	0.01	0.1	0.01	0.01	0.01	0.01
BaO	0.02	0.03	0.02	0.01	0.01	0.01
LOI	2.57	1.83	0.250	1.48	1.24	0.470
Total	100.0	98.08	100.2	100.3	100.9	100.2
C	0.030	0.010	0.030	0.040	0.040	0.040
S	0.91	2.5	0.060	0.37	1.0	<0.01
Ba (ppm)	197	242	155	52.1	71.2	130
Ce	21.2	7.30	16.4	15.4	12.2	15.7
Cr	20	20	10	10	10	30
Cs	1.5	0.63	0.37	0.49	0.48	0.44
Dy	8.79	4.69	7.11	7.40	6.82	8.63
Er	6.01	3.35	5.34	5.23	4.86	5.86
Eu	1.1	1.0	1.3	0.88	0.91	1.2
Ga	15.4	14.0	15.5	9.70	12.5	14.6
Gd	7.2	3.0	5.4	5.4	5.2	6.6
Ge	<5	<5	<5	<5	<5	<5
Hf	3.1	2.9	2.9	3.4	2.8	3.4
Ho	1.9	1.1	1.7	1.7	1.5	1.8
La	8.6	3.0	6.3	6.1	4.7	5.8
Lu	0.93	0.67	0.79	0.90	0.8	0.88
Nb	1.1	1.0	1.1	1.3	1.0	1.0
Nd	17.4	5.60	13.0	11.9	10.3	13.3
Pr	3.3	1.1	2.5	2.3	1.9	2.5
Rb	33.7	12.6	11.1	3.20	7.30	12.3
Sm	5.6	2.1	4.1	4.2	3.9	4.7
Sn	2.0	3.0	1.0	<1.0	1.0	1.0
Sr	32.0	37.7	63.5	45.1	71.0	52.3
Ta	0.1	0.2	0.2	0.2	0.1	0.1
Tb	1.2	0.60	1.1	1.1	0.93	1.1

Sample ID	62767	62768	62769	62770	62771	62772
Hole ID	PH-19-09	PH-19-10	PH-19-10	PH-19-10	PH-19-10	PH-19-10
Depth (m)	289	6.78	55.45	76.44	117.86	127.92
Lithology	Tuff	Lap. Tuff	Lap. Tuff	Rhyolite	Xtl-Tuff	Xtl-Tuff
Stratigraphy	FW	MS	MS	MS	FW	FW
Alteration	QS+/-C+/-Py	QSC+/-Py+Sil	QSC+/-Py+Sil	QSC	QSC	QSC
Th	1.6	0.61	1.3	1.2	1.0	1.2
Tm	0.91	0.55	0.79	0.81	0.73	0.9
U	0.41	0.38	0.29	0.40	0.35	0.36
V	<5.00	6.00	<5.00	<5.00	28.0	14.0
W	1	2	1	1	2	1
Y	49.5	30.5	44.7	47.3	39.8	46.6
Yb	6.50	4.30	5.37	6.27	5.20	5.87
Zr	86.0	81.0	83.0	92.0	75.0	95.0
As	4.8	1.4	0.50	0.30	1.1	0.30
Bi	0.4	3	0.2	0.1	0.3	0.1
Hg	0.01	0.1	<0.005	0.01	<0.005	<0.005
In	1	11	0.1	0.03	0.1	0.1
Re	0.001	0.002	<0.001	0.001	0.001	<0.001
Sb	0.2	0.1	<0.05	0.1	<0.05	<0.05
Se	<0.2	0.7	<0.2	<0.2	0.6	<0.2
Te	0.1	0.4	0.03	0.1	0.1	<0.01
Tl	0.03	0.1	0.1	<0.02	0.04	0.04
Ag	<0.50	7.1	<0.50	<0.50	<0.50	<0.50
Cd	<0.50	25	<0.50	0.60	<0.50	<0.50
Co	<1.0	1.0	1.0	<1.0	4.0	2.0
Cu	268.0	5960	13.00	25.00	11.00	1.000
Li	20	<10	10	10	10	10
Mo	7.0	18	1.0	5.0	4.0	1.0
Ni	1.0	1.0	<1.0	2.0	1.0	2.0
Pb	<2.00	65.0	7.00	127	2.00	<2.00
Sc	15.0	8.00	20.0	10.0	13.0	15.0
Zn	224.00	4650.0	116.00	290.00	46.000	49.000
AlOH WL (nm)	2195.1	2198.1	2201.8	2201.3	2200.5	-
AlOH Depth	0.4	0.2	0.1	0.1	0.05	-
FeOH WL (nm)	2251.2	2249.7	2251.1	2247.5	2249.8	2253.0
FeOH Depth	0.2	0.04	0.2	0.2	0.1	0.2
AlOH depth/FeOH depth	1.6	4.5	0.54	0.70	0.38	-

Sample ID	62773	62753	62755	62756	62757	62758
Hole ID	PH-19-10	PH-19-11	PH-19-11	PH-19-11	PH-19-11	PH-19-11
Depth (m)	147.54	4.2	40	51.86	72.83	124.43
Lithology	Rhyolite	Lap. Tuff	Xtl-Tuff	Xtl-Tuff	Dike	Xtl-Tuff
Stratigraphy	FW	MS	MS	MS	MS	FW
Alteration	QS+/-C	QSC+Sil	QSCPy+/-Sil	QSCPy+Sil	Unaltered	QSC+/-Py
SiO_2 (wt. %)	75.99	77.87	78.60	78.33	54.21	72.07
Al_2O_3	13.12	12.93	9.83	10.60	14.15	12.91
Fe_2O_3	2.86	2.67	5.65	6.38	11.5	5.55
CaO	0.952	0.181	0.185	0.244	7.06	1.21
MgO	1.51	2.86	3.01	2.37	3.78	2.87
Na_2O	4.06	0.835	0.718	0.649	4.06	3.67
K_2O	1.11	2.40	1.75	1.18	1.11	1.04
Cr_2O_3	0.002	0.002	0.003	0.004	0.001	0.002
TiO_2	0.294	0.151	0.123	0.112	2.572	0.366
MnO	0.061	0.070	0.062	0.091	0.22	0.22
P_2O_5	0.02	0.05	0.03	0.01	1	0.07
SrO	0.01	0.01	0.01	0.01	0.05	0.01
BaO	0.02	0.03	0.03	0.03	0.05	0.01
LOI	1.19	2.30	2.81	2.35	0.280	1.88
Total	99.89	101.7	100.3	100.9	101.4	100.3
C	0.07	0.040	0.020	0.030	0.010	0.030
S	0.20	0.70	2.2	1.8	0.10	2.0
Ba (ppm)	185	301	252	241	563	99.1
Ce	10.5	18.1	7.40	15.0	80.2	13.7
Cr	20	20	20	20	20	10
Cs	0.46	1.5	1.0	1.6	1.5	0.59
Dy	7.11	7.64	4.51	8.48	11.6	6.23
Er	5.49	5.88	3.31	6.38	6.19	4.59
Eu	0.85	1.2	0.8	0.75	4.3	0.88
Ga	13.4	12.9	12.8	15.2	29.4	13.1
Gd	4.3	5.9	2.8	6.4	12	4.6
Ge	<5	<5	<5	<5	<5	<5
Hf	3.5	3.8	2.5	4.2	7.0	2.6
Ho	1.6	1.7	1.0	1.8	2.4	1.4
La	4.2	7.1	2.9	5.7	33.1	5.2
Lu	0.90	0.93	0.63	1.0	0.8	0.75
Nb	1.2	1.1	0.7	1.4	12	1.0
Nd	8.70	13.9	6.00	13.4	51.5	10.8
Pr	1.5	2.7	1.2	2.3	11.0	2.1
Rb	10.0	19.9	15.2	17.3	32.7	7.20
Sm	2.7	4.7	2.0	4.8	11.8	3.4
Sn	2.0	1.0	1.0	2.0	3.0	1.0
Sr	72.0	63.8	36.0	61.1	538	40.2
Ta	0.1	0.2	0.1	0.1	1.0	0.1
Tb	0.93	1.2	0.56	1.2	1.9	0.82

Sample ID	62773	62753	62755	62756	62757	62758
Hole ID	PH-19-10	PH-19-11	PH-19-11	PH-19-11	PH-19-11	PH-19-11
Depth (m)	147.54	4.2	40	51.86	72.83	124.43
Lithology	Rhyolite	Lap. Tuff	Xtl-Tuff	Xtl-Tuff	Dike	Xtl-Tuff
Stratigraphy	FW	MS	MS	MS	MS	FW
Alteration	QS+/-C	QSC+Sil	QSCPy+/-Sil	QSCPy+Sil	Unaltered	QSC+/-Py
Th	1.0	1.2	1.0	1.2	4.4	0.94
Tm	0.75	0.81	0.54	0.90	0.86	0.68
U	0.30	0.42	0.37	0.47	1.6	0.34
V	27.0	<5.00	5.00	5.00	279	57.0
W	1	1	1	1	2	2
Y	42.2	49.2	29.2	48.1	59.6	38.5
Yb	5.61	6.14	4.06	6.67	5.68	4.70
Zr	90.0	100	64.0	106	290	71.0
As	0.20	0.90	2.6	1.3	2.3	0.60
Bi	0.1	0.4	0.8	1	0.1	0.4
Hg	<0.005	0.02	<0.005	<0.005	<0.005	0.0
In	0.03	0.1	0.2	0.1	0.02	0.1
Re	0.001	0.001	0.001	0.001	0.001	0.001
Sb	<0.05	<0.05	0.1	0.1	0.2	<0.05
Se	<0.2	<0.2	0.4	0.6	<0.2	0.9
Te	0.04	0.2	0.5	0.8	0.01	0.3
Tl	<0.02	0.1	0.1	0.1	0.1	0.02
Ag	<0.50	<0.50	<0.50	<0.50	<0.50	<0.50
Cd	<0.50	0.70	<0.50	<0.50	<0.50	<0.50
Co	1.0	1.0	1.0	3.0	18	4.0
Cu	19.00	16.00	40.00	99.00	11.00	116.0
Li	10	20	20	20	10	10
Mo	1.0	6.0	6.0	2.0	1.0	3.0
Ni	1.0	2.0	<1.0	3.0	6.0	2.0
Pb	2.00	8.00	5.00	<2.00	6.00	10.0
Sc	13.0	12.0	9.00	18.0	28.0	16.0
Zn	71.000	311.00	73.000	82.000	120.00	112.00
AlOH WL (nm)	2199.9	2197.3	2200.9	2196.4	2198.0	-
AlOH Depth	0.3	0.3	0.2	0.2	0.2	-
FeOH WL (nm)	2252.8	2246.9	2249.9	2252.9	2252.0	2249.1
FeOH Depth	0.2	0.2	0.1	0.1	0.2	0.2
AlOH depth/FeOH depth	1.4	1.9	1.7	1.5	1.2	-

Sample ID	62759	62741	62742	62743	62744
Hole ID	PH-19-11	PH-19-12	PH-19-12	PH-19-12	PH-19-12
Depth (m)	138.47	22.55	49	103.39	135.81
Lithology	Rhyolite	Lap. Tuff	Lap. Tuff	Rhyolite	Tuff
Stratigraphy	FW	MS	MS	FW	FW
Alteration	QS+/-C+/Py	QSC+/-Py+Sil	QSC+/-Py	QSC+Sil	QSC
SiO_2 (wt. %)	75.25	80.54	76.23	75.93	79.57
Al_2O_3	13.29	10.02	10.83	13.27	12.30
Fe_2O_3	3.40	4.69	3.41	2.92	2.43
CaO	0.889	0.292	0.215	0.835	0.417
MgO	1.66	1.46	6.96	1.73	2.17
Na_2O	4.22	0.88	1.02	4.23	2.15
K_2O	0.87	1.79	0.899	0.694	0.681
Cr_2O_3	0.002	0.003	0.002	0.002	0.003
TiO_2	0.310	0.177	0.153	0.272	0.193
MnO	0.050	0.10	0.27	0.080	0.051
P_2O_5	0.04	0.03	0.01	0.03	0.01
SrO	0.01	0.01	0.01	0.01	0.1
BaO	0.01	0.02	0.01	0.01	0.02
LOI	1.28	2.04	1.91	0.820	2.02
Total	101.3	98.02	99.77	100.3	100.4
C	0.010	0.040	0.030	0.020	0.020
S	1.0	1.5	0.62	0.53	0.23
Ba (ppm)	121	236	92.4	92.4	194
Ce	11.6	11.7	13.9	12.9	4.50
Cr	20	30	20	20	30
Cs	0.57	1.0	1.6	0.37	0.53
Dy	5.73	7.70	7.67	6.74	4.62
Er	4.80	5.34	5.09	5.41	3.60
Eu	0.86	1.0	1.1	1.1	0.64
Ga	13.4	11.9	13.1	14.4	12.5
Gd	4.3	5.5	6.1	5.4	3.2
Ge	<5	<5	<5	<5	<5
Hf	3.2	3.2	3.0	3.0	3.3
Ho	1.5	1.7	1.6	1.6	1.0
La	4.5	5.0	5.4	5.2	1.8
Lu	0.76	0.94	0.84	0.77	0.68
Nb	1.2	1.0	1.1	1.1	1.3
Nd	9.00	9.90	11.8	11.4	4.00
Pr	1.7	1.9	2.2	2.0	0.7
Rb	9.00	14.4	9.30	6.10	6.20
Sm	3.2	3.5	4.0	3.9	1.7
Sn	1.0	1.0	1.0	<1.0	1.0
Sr	67.6	45.9	40.9	58.4	62.1
Ta	0.2	0.1	0.2	0.1	0.1
Tb	0.83	1.1	1.1	0.91	0.57

Sample ID	62759	62741	62742	62743	62744
Hole ID	PH-19-11	PH-19-12	PH-19-12	PH-19-12	PH-19-12
Depth (m)	138.47	22.55	49	103.39	135.81
Lithology	Rhyolite	Lap. Tuff	Lap. Tuff	Rhyolite	Tuff
Stratigraphy	FW	MS	MS	FW	FW
Alteration	QS+/-C+/Py	QSC+/-Py+Sil	QSC+/-Py	QSC+Sil	QSC
Th	0.92	1.4	1.2	1.1	0.75
Tm	0.73	0.82	0.79	0.74	0.53
U	0.35	0.45	0.38	0.46	0.36
V	24.0	14.0	7.00	23.0	21.0
W	1	1	2	2	<1.0
Y	40.1	47.5	43.9	40.6	29.8
Yb	5.12	5.85	5.59	5.33	4.17
Zr	84.0	83.0	80.0	80.0	90.0
As	0.80	1.3	0.30	0.60	0.50
Bi	0.4	0.7	0.3	0.3	0.2
Hg	0.01	<0.005	0.01	<0.005	0.3
In	0.02	0.1	0.2	0.1	0.2
Re	0.001	0.01	0.002	<0.001	0.02
Sb	0.1	0.1	<0.05	<0.05	<0.05
Se	0.3	0.2	<0.2	<0.2	0.2
Te	0.3	0.4	0.1	0.1	0.1
Tl	0.02	0.1	0.1	<0.02	<0.02
Ag	<0.50	<0.50	<0.50	<0.50	<0.50
Cd	1.0	<0.50	<0.50	<0.50	8.2
Co	2.0	1.0	1.0	2.0	2.0
Cu	52.00	80.00	24.00	84.00	114.0
Li	10	10	20	20	10
Mo	3.0	4.0	18	1.0	7.0
Ni	2.0	1.0	1.0	2.0	1.0
Pb	13.0	12.0	11.0	5.00	7.00
Sc	12.0	8.00	10.0	13.0	12.0
Zn	242.00	80.000	578.00	50.000	1875.0
AlOH WL (nm)	2200.1	2201.1	2197.0	2201.4	2194.7
AlOH Depth	0.2	0.3	0.1	0.2	0.3
FeOH WL (nm)	2249.8	2248.3	2247.7	2249.2	2252.0
FeOH Depth	0.1	0.1	0.2	0.1	0.2
AlOH depth/FeOH depth	2.3	2.0	0.43	1.2	1.8

Appendix C: Table C.1.1 Precision and accuracy data for internal reference (ORCA-1)

Analyte	LOD	Analysis Method	Accepted Values	ORCA-1-1	ORCA-1-2	62802	62803
SiO_2 (wt. %)	0.01	ME-ICP06	74.84	75.76	75.97	75.58	75.60
Al_2O_3	0.01	ME-ICP07	12.55	12.66	12.48	12.75	12.70
Fe_2O_3	0.01	ME-ICP08	2.91	2.87	2.89	2.87	2.88
CaO	0.01	ME-ICP09	1.14	1.15	1.13	1.11	1.13
MgO	0.01	ME-ICP10	0.47	0.47	0.48	0.48	0.48
Na_2O	0.01	ME-ICP11	4.59	4.58	4.49	4.62	4.62
K_2O	0.01	ME-ICP12	2.14	2.08	2.11	2.13	2.14
Cr_2O_3	0.01	ME-ICP13	-	0.01	0.01	0.01	0.01
TiO_2	0.01	ME-ICP14	0.30	0.28	0.29	0.29	0.29
MnO	0.01	ME-ICP15	0.06	0.06	0.06	0.06	0.06
P_2O_5	0.01	ME-ICP16	0.06	0.04	0.05	0.07	0.05
SrO	0.01	ME-ICP17	-	BDL	BDL	BDL	BDL
BaO	0.01	ME-ICP18	-	0.04	0.04	0.04	0.04
LOI	0.01	OA-GRA05	0.77	0.71	0.72	0.76	0.80
Total	0.01	TOT-ICP06	-	100.24	100.50	101.18	100.01
C	0.01	C-IRO7	0.01	0.01	0.02	0.02	0.02
S	0.01	S-IR08	0.05	0.02	0.01	BDL	BDL
Ba (ppm)	0.5	ME-MS81	374	347	377	410	407
Ce	0.1	ME-MS81	62.1	58.9	59.8	64.6	67.4
Cr	5	ME-MS81	65	80	70	70	80
Cs	0.01	ME-MS81	0.6	0.54	0.58	0.59	0.62
Dy	0.05	ME-MS81	11.7	12.35	11.15	11.95	12.3
Er	0.03	ME-MS81	7.6	7.51	7.73	8.16	7.58
Eu	0.02	ME-MS81	1.32	1.19	1.17	1.38	1.39
Ga	0.1	ME-MS81	16	17.6	17.1	18.4	17.8
Gd	0.05	ME-MS81	9.87	9.86	9.69	10.10	10.15
Ge	5	ME-MS81	-	BDL	BDL	BDL	BDL
Hf	0.05	ME-MS81	7.5	7.1	7.6	8.2	8.2
Ho	0.01	ME-MS81	2.53	2.45	2.34	2.49	2.48
La	0.1	ME-MS81	27	25.4	25.3	27.4	28.7
Lu	0.01	ME-MS81	1.21	1.15	1.13	1.26	1.25
Nb	0.05	ME-MS81	11.6	11.4	11.1	11.5	13
Nd	0.1	ME-MS81	34.8	35.1	33.6	38.2	38.4
Pr	0.02	ME-MS81	8.2	7.77	7.75	8.39	8.54
Rb	0.2	ME-MS81	52.1	49.4	48.6	53.8	53.1
Sm	0.03	ME-MS81	8.95	8.78	8.93	9.38	9.48
Sn	0.5	ME-MS81	-	4	4	4	4
Sr	0.1	ME-MS81	71.6	72.4	70.6	74.9	74.0
Ta	0.1	ME-MS81	0.99	0.9	0.9	0.9	1.0
Tb	0.01	ME-MS81	1.8	1.77	1.80	1.71	1.66
Th	0.05	ME-MS81	4.91	4.79	4.67	5.21	5.45

Analyte	LOD	Analysis Method	Accepted Values	ORCA-1-1	ORCA-1-2	62802	62803
Tm	0.01	ME-MS81	1.19	1.14	1.09	1.27	1.17
U	0.05	ME-MS81	1.29	1.23	1.24	1.31	1.34
V	5	ME-MS81	10.2	15	12	13	24
W	0.5	ME-MS81	-	1	1	1	1
Y	0.1	ME-MS81	70.8	68.9	66.4	72.2	72.2
Yb	0.03	ME-MS81	7.85	8.00	7.46	8.54	8.02
Zr	1	ME-MS81	246	250	255	267	264
As	0.1	ME-MS42	-	0.6	0.6	0.7	0.6
Bi	0.01	ME-MS42	-	0.05	0.06	0.05	0.05
Hg	0.005	ME-MS42	-	BDL	BDL	BDL	BDL
In	0.005	ME-MS42	-	0.021	0.028	0.024	0.025
Re	0.001	ME-MS42	-	0.001	0.001	0.001	0.001
Sb	0.05	ME-MS42	-	0.1	0.1	0.1	0.1
Se	0.2	ME-MS42	-	BDL	0.3	BDL	BDL
Te	0.01	ME-MS42	-	BDL	0.01	BDL	BDL
Tl	0.02	ME-MS42	0.2	0.02	BDL	0.02	BDL
Ag	0.5	ME-4ACD81	-	BDL	BDL	BDL	BDL
Cd	0.5	ME-4ACD81	-	BDL	BDL	BDL	BDL
Co	1	ME-4ACD81	3	3	5	3	2
Cu	1	ME-4ACD81	12	12	12	12	12
Li	10	ME-4ACD81	6.1	10	10	10	10
Mo	1	ME-4ACD81	4.4	4	5	5	4
Ni	1	ME-4ACD81	6	5	7	6	4
Pb	2	ME-4ACD81	5	5	6	4	BDL
Sc	1	ME-4ACD81	7.3	7	7	7	7
Zn	2	ME-4ACD81	51.2	58	60	55	55

Analyte	62804	62805	62806	Mean	σ	% RSD	% RD
SiO_2 (wt. %)	75.80	75.55	75.39	75.66	0.19	0.3	1.10
Al_2O_3	12.55	12.61	12.80	12.65	0.11	0.9	0.79
Fe_2O_3	2.90	2.91	2.91	2.89	0.02	0.6	-0.70
CaO	1.15	1.17	1.14	1.14	0.02	1.9	-0.11
MgO	0.48	0.49	0.49	0.48	0.01	1.3	2.53
Na_2O	4.50	4.62	4.61	4.58	0.06	1.3	-0.27
K_2O	2.14	2.17	2.20	2.14	0.04	1.8	-0.01
Cr_2O_3	0.01	0.01	0.01	0.01	0.00	7.4	-
TiO_2	0.30	0.30	0.30	0.29	0.01	2.2	-1.83
MnO	0.06	0.06	0.06	0.06	0.00	0.9	5.68
P_2O_5	0.07	0.06	0.05	0.06	0.01	20.2	-1.89
SrO	0.01	0.01	0.01	0.01	0.00	42.4	-
BaO	0.04	0.04	0.04	0.04	0.00	0.9	-
LOI	0.66	0.70	0.79	0.73	0.05	6.9	-4.64
Total	100.66	98.65	101.20	100.35	0.87	0.9	-
C	0.03	0.03	0.02	0.02	0.01	32.2	114.29
S	BDL	BDL	0.01	0.01	0.01	43.3	-72.22
Ba (ppm)	380	375	396	385	21.8	5.7	2.83
Ce	62.3	61.6	66.8	63.1	3.31	5.3	1.54
Cr	80	70	80	76	5.35	7.1	16.48
Cs	0.54	0.58	0.67	0.59	0.05	7.8	-1.90
Dy	12.65	12.75	11.45	12.09	0.60	5.0	3.30
Er	8.93	8.31	7.68	7.99	0.51	6.4	5.08
Eu	1.36	1.15	1.34	1.28	0.11	8.4	-2.81
Ga	17.2	16.9	17.7	17.5	0.51	2.9	9.55
Gd	10.45	10.70	9.94	10.13	0.35	3.4	2.61
Ge	BDL	BDL	BDL	-	-	-	-
Hf	8.1	8.1	8.4	8.0	0.45	5.7	6.10
Ho	2.76	2.50	2.65	2.52	0.14	5.5	-0.23
La	27.3	28.0	28.6	27.2	1.40	5.1	0.90
Lu	1.24	1.14	1.30	1.21	0.07	5.6	0.00
Nb	11.9	11.8	12.2	11.8	0.62	5.3	2.09
Nd	36.4	37.2	38.0	36.7	1.80	4.9	5.46
Pr	8.36	8.23	8.86	8.27	0.40	4.8	0.87
Rb	53.8	51.8	55.2	52.2	2.45	4.7	0.27
Sm	9.02	8.63	9.63	9.12	0.38	4.1	1.92
Sn	4	4	4	4	0.00	0.0	-
Sr	74.5	73.2	77.1	73.8	2.05	2.8	3.09
Ta	1.0	1.0	1.1	1.0	0.08	7.8	-1.88
Tb	1.89	1.72	1.82	1.77	0.08	4.4	-1.83
Th	4.97	4.84	4.91	4.98	0.27	5.4	1.37

Analyte	62804	62805	62806	Mean	σ	% RSD	% RD
Tm	1.18	1.24	1.24	1.19	0.06	5.4	0.00
U	1.31	1.26	1.29	1.28	0.04	3.2	-0.55
V	13	37	11	18	9.49	53.2	75.07
W	1	2	1	1	0.38	33.1	-
Y	70.1	69.2	74.7	70.5	2.73	3.9	-0.38
Yb	8.73	8.42	8.86	8.29	0.49	5.9	5.61
Zr	262	254	271	260	7.63	2.9	5.87
As	0.9	0.6	0.6	0.7	0.11	17.3	-
Bi	0.05	0.05	0.05	0.05	0.00	7.3	-
Hg	BDL	BDL	BDL	-	-	-	-
In	0.022	0.023	0.026	0.024	0.00	10.0	-
Re	0.001	0.001	0.001	0.00	0.00	0.0	-
Sb	0.1	0.1	0.1	0.1	0.01	12.2	-
Se	BDL	BDL	BDL	0.3	-	-	-
Te	BDL	BDL	BDL	0.01	-	-	-
Tl	0.02	0.02	0.02	0.02	0.00	0.0	-89.9
Ag	BDL	BDL	BDL	-	-	-	-
Cd	BDL	BDL	BDL	-	-	-	-
Co	2	3	2	3	1.07	37.4	-4.76
Cu	12	11	12	12	0.38	3.2	-1.19
Li	10	10	10	10	0.00	0.00	63.93
Mo	5	4	4	4	0.53	12.1	0.65
Ni	5	4	6	5	1.11	21.1	-11.90
Pb	5	BDL	8	6	1.52	27.1	12.00
Sc	7	7	7	7	0.00	0.0	-4.11
Zn	56	53	55	56	2.31	4.1	9.37

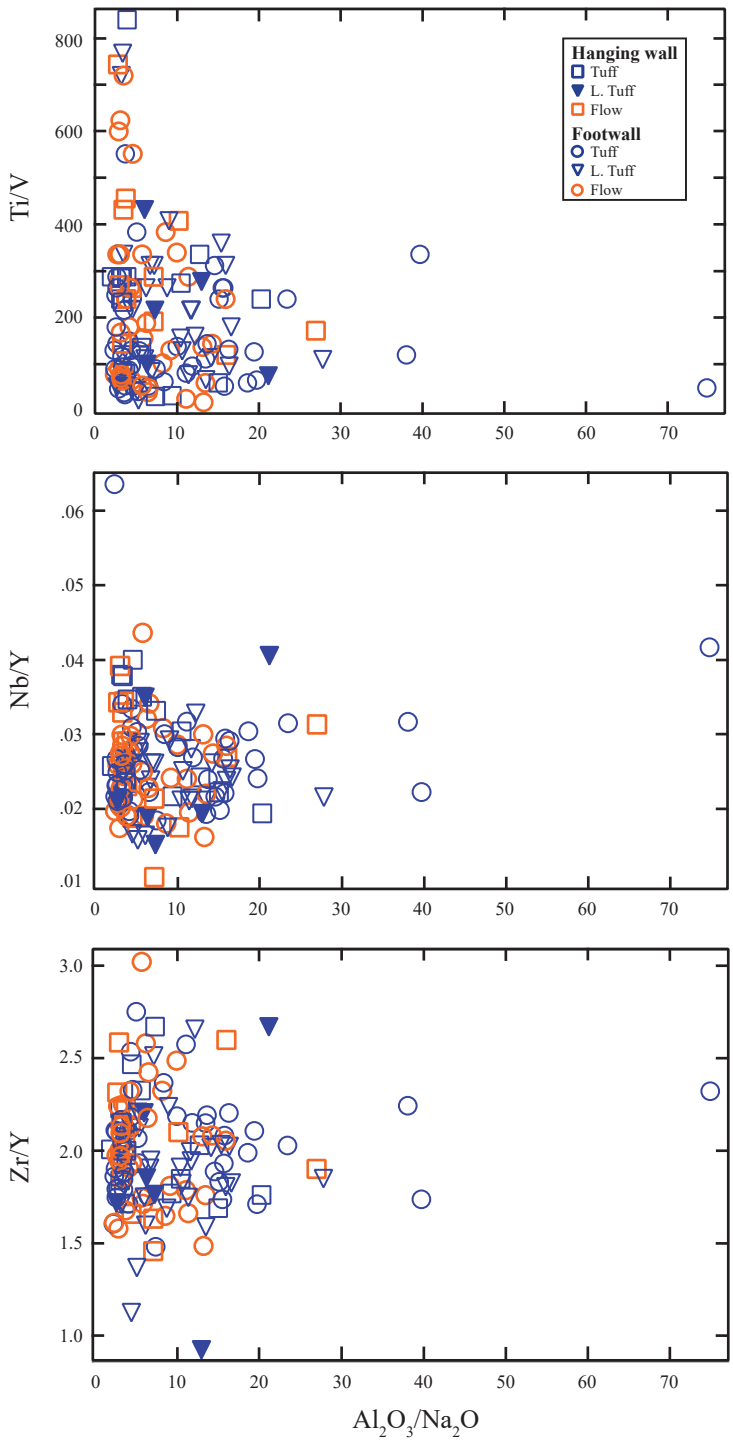

Appendix D. Element ratio plots testing mobility of select elements versus the alteration index (Al2O3/Na2O; Spitz and Darling, 1978). A) Ti/V element ratio; B) Nb/Y element ratio; and C) Zr/Y element ratio.

Appendix E: Table E.1.1 Mass Change Calculation Results

Sample ID	62571	62581	62582	62584	62585	62586	62587	62575
Hole ID	PH-18-34	PH-18-34	PH-18-34	PH-18-34	PH-18-34	PH-18-34	PH-18-34	PH-18-34
Depth (m)	9.23	111	125.2	160.75	175.12	195	217.11	46.49
Lithology	Sediment	Tuff	Lap. Tuff	Rhyolite	Lap. Tuff	Rhyolite	Basalt	Dike
Stratigraphy	HW	HW	HW	HW	HW	HW	HW	HW
Alteration	GraQ	QS+/-C	QS+/-C	QS+/-C	QSC	QSC+Sil	CCal	Unaltered
SiO_2	-32.47	-10.62	-5.65	-11.71	-5.84	-21.94	-43.49	-40.49
Al_2O_3	0.00	0.00	0.00	0.00	0.00	0.00	0.00	0.00
Fe_2O_3	3.99	0.44	1.08	0.93	-0.060	3.96	2.43	6.47
CaO	-5.34	-4.90	-6.07	-4.76	-4.68	-5.34	-4.40	-0.53
MgO	1.41	-0.38	-0.53	-0.51	-0.45	-0.62	0.79	4.20
Na_2O	-4.14	-1.5	-2.94	-1.30	-1.38	-4.42	-4.31	-3.05
K_2O	2.21	1.77	2.48	2.39	1.89	7.07	2.40	-0.18
Cr_2O_3	0.01	0.00	0.00	0.00	0.00	0.00	0.00	0.00
TiO_2	0.44	0.18	0.18	0.18	0.17	0.21	0.64	0.99
MnO	-0.02	-0.12	-0.13	-0.14	-0.13	-0.14	-0.13	-0.03
P_2O_5	0.09	0.04	0.07	0.06	0.13	0.14	0.09	0.15
SrO	0.00	-0.01	-0.01	0.00	0.00	-0.01	-0.01	0.01
BaO	0.03	0.01	0.01	0.01	0.01	0.01	0.01	0.00
LOI	1.19	-0.33	-0.42	-0.29	0.06	0.34	-0.11	-0.02
Total	-34.02	-14.59	-9.86	-13.78	-9.44	-20.49	-45.4	-32.85
C	0.60	-0.14	-0.17	-0.11	0.19	-0.16	-0.17	-0.16
S	0.18	-0.07	0.46	0.51	-0.05	1.57	-0.17	0.10
Ba	274.76	62.21	105.03	76.62	50.03	133.17	77.88	-7.69
Ce	45.71	-2.71	-3.12	-2.51	-0.91	-0.74	-9.46	3.02
Cr	59.44	-11.51	-2.31	-2.97	-2.07	-12.11	-14.6	27.28
Cs	3.25	0.38	0.33	0.22	0.36	0.64	0.65	1.41
Dy	-4.98	-3.28	-3.44	-3.39	-3.25	-3.05	-6.68	-5.53
Er	-3.62	-1.96	-2.32	-2.32	-2.18	-2.05	-4.60	-3.70
Eu	0.13	0.37	0.05	0.16	0.40	0.29	-0.32	0.18
Ga	3.05	0.60	-0.78	-0.38	-1.07	-1.54	0.93	-0.07
Gd	-2.11	-1.97	-2.25	-1.89	-1.88	-1.81	-4.46	-2.67
Ge	-0.84	-0.38	-0.29	-0.37	-0.26	-0.53	-1.15	-0.81
Hf	-0.32	-0.92	-0.91	-1.09	-1.06	-0.85	-1.9	-0.67
Ho	-1.12	-0.63	-0.71	-0.66	-0.62	-0.66	-1.47	-1.13
La	23.33	-1.01	-1.26	-1.00	0.77	0.24	-3.87	1.09
Lu	-0.76	-0.44	-0.47	-0.44	-0.41	-0.54	-0.89	-0.76
Nb	10.35	0.09	0.05	0.01	-0.02	0.00	-0.67	1.80
Nd	15.15	-3.02	-3.73	-2.57	-1.74	-1.89	-7.71	0.56
Pr	4.61	-0.55	-0.74	-0.66	-0.33	-0.26	-1.51	0.23
Rb	87.33	14.73	15.5	14.95	16.65	36.47	23.52	5.01
Sm	0.89	-1.00	-1.29	-1.10	-0.80	-1.06	-2.54	-1.22
Sn	0.99	-0.15	-0.12	-0.15	-0.1	0.58	-0.46	0.35
Sr	-7.18	-52.79	-75.48	-46.94	-13.50	-37.42	-62.38	102.18
Ta	0.61	0.37	0.39	0.38	0.40	0.03	0.22	0.09

Sample ID	62571	62581	62582	62584	62585	62586	62587	62575
Hole ID	PH-18-34	PH-18-34	PH-18-34	PH-18-34	PH-18-34	PH-18-34	PH-18-34	PH-18-34
Depth (m)	9.23	111	125.2	160.75	175.12	195	217.11	46.49
Lithology	Sediment	Tuff	Lap. Tuff	Rhyolite	Lap. Tuff	Rhyolite	Basalt	Dike
Stratigraphy	HW	HW	HW	HW	HW	HW	HW	HW
Alteration	GraQ	QS+/-C	QS+/-C	QS+/-C	QSC	QSC+Sil	CCal	Unaltered
Tb	-0.45	-0.34	-0.35	-0.36	-0.38	-0.33	-0.80	-0.56
Th	7.78	-0.18	-0.26	-0.21	-0.23	-0.18	-0.68	-0.43
Tm	-0.58	-0.31	-0.35	-0.39	-0.33	-0.35	-0.75	-0.61
U	2.98	-0.89	-0.90	1.29	1.06	8.86	0.24	-0.98
V	156.83	-5.75	-5.58	2.77	15.1	1.84	26.18	152.78
W	0.32	-0.15	-0.12	-0.15	-0.10	-0.21	-0.46	-0.32
Y	-34.58	-21.34	-22.99	-22.27	-18.78	-20.62	-43.96	-35.3
Yb	-5.07	-3.04	-3.32	-3.33	-2.87	-3.47	-5.95	-5.05
Zr	23.87	-16.13	-17.45	-19.33	-20.97	-22.92	-44.09	14.69
As	-0.78	1.63	-1.55	-0.06	-1.18	-0.41	-1.40	94.56
Bi	0.11	-0.03	-0.02	0.02	-0.05	0.13	-0.05	0.17
Hg	0.00	0.00	0.00	0.00	0.00	0.00	0.00	0.00
In	-0.01	0.03	0.01	0.00	0.02	-0.01	0.01	-0.02
Re	0.01	0.00	0.00	0.00	0.00	0.01	0.00	0.00
Sb	0.02	-0.03	-0.05	0.04	-0.05	-0.03	-0.06	0.09
Se	0.69	0.07	-0.01	0.24	-0.01	0.29	-0.05	0.10
Te	0.06	0.03	0.03	0.08	0.01	0.31	0.00	0.10
Tl	0.38	-0.03	-0.03	-0.03	-0.03	-0.03	0.04	0.05
Ag	-0.08	-0.04	-0.03	-0.04	-0.03	-0.05	-0.11	-0.08
Cd	0.08	-0.04	-0.03	-0.04	0.20	-0.05	-0.11	0.16
Co	12.24	-0.58	-0.12	-0.57	-0.55	1.37	1.70	27.37
Cu	38.37	-1.45	0.42	0.26	-1.31	3.10	-2.92	16.94
Li	28.10	3.49	3.85	-4.57	-4.55	-4.61	22.00	1.75
Mo	1.65	-0.15	-0.12	0.70	-0.10	2.16	-0.46	-0.32
Ni	33.75	0.55	-1.12	1.41	0.69	6.68	-0.92	44.60
Pb	1.90	-8.60	-9.35	-10.3	-10.21	-1.74	-10.38	-9.30
Sc	-3.08	-0.57	-2.61	-3.08	-2.45	0.78	9.84	1.89
Zn	11.74	84.08	-34.96	-15.1	-9.35	-17.76	-41.14	8.73

Sample ID	62599	62603	62605	62606	62607	62608	62610
Hole ID	PH-18-34	PH-18-34	PH-18-34	PH-18-34	PH-18-34	PH-18-34	PH-18-34
Depth (m)	337.5	395	410.04	415.67	430.71	233.69	447.62
Lithology	Tuff	Xtl-Tuff	Xtl-Tuff	Lap. Tuff	Rhyolite	Basalt	Xtl-Tuff
Stratigraphy	FW	FW	MS	FW	FW	HW	FW
Alteration	QSC+/-Py	QS+/-C	QSCPy	QSC+/-Py+Sil	QS	C-Ep	QSC
SiO_2	-21.17	-8.38	20.88	6.83	-12.21	-40.79	5.39
Al_2O_3	0.00	0.00	0.00	0.00	0.00	0.00	0.00
Fe_2O_3	1.31	2.09	7.49	3.84	0.07	3.50	-0.36
CaO	-5.45	-4.96	-5.77	4.58	-5.61	-3.25	-5.93
MgO	7.41	-0.10	3.57	6.53	1.29	-0.31	-0.06
Na_2O	-4.07	-0.28	-4.09	-4.11	-4.13	-0.56	-0.03
K_2O	0.07	0.07	0.45	-0.33	1.66	-0.07	0.95
Cr_2O_3	0.00	0.00	0.00	0.00	0.00	0.00	0.00
TiO_2	-0.03	0.12	-0.01	0.00	0.03	0.55	-0.01
MnO	-0.01	0.01	-0.05	0.17	-0.04	-0.08	-0.11
P_2O_5	0.01	0.05	0.01	0.00	0.01	0.12	0.01
SrO	-0.01	0.02	0.00	0.00	0.00	0.00	-0.01
BaO	0.01	0.00	0.01	0.00	0.01	0.00	0.02
LOI	1.21	-0.50	3.36	0.82	0.94	-0.51	-0.4
Total	-22.62	-9.62	25.43	17.49	-16.46	-40.35	-0.68
C	-0.16	-0.14	-0.16	-0.08	-0.17	-0.09	-0.15
S	0.05	-0.23	3.16	0.61	-0.20	-0.12	-0.21
Ba	57.56	-21.75	90.73	-31.79	158.27	-26.71	189.83
Ce	-4.32	-3.90	-1.26	6.09	-2.49	-9.33	-2.22
Cr	-12.19	-2.27	-7.75	3.50	-3.78	-8.18	-0.03
Cs	0.83	0.08	1.08	0.33	0.78	0.04	0.08
Dy	-0.38	-3.43	-0.23	0.24	-0.09	-6.09	-0.68
Er	-0.12	-2.52	-0.03	0.28	-0.25	-4.12	-0.72
Eu	0.44	0.31	0.25	0.06	0.00	-0.36	0.05
Ga	-0.10	0.39	6.58	0.85	-0.74	-0.84	1.18
Gd	-0.28	-2.03	-0.05	0.61	-0.36	-4.13	-0.43
Ge	-0.55	-0.28	0.56	0.44	-0.47	-1.02	0.00
Hf	0.53	-1.17	-0.12	-0.01	0.43	-2.47	-0.30
Ho	0.08	-0.80	-0.06	-0.01	-0.02	-1.33	-0.25
La	-2.17	-2.05	-1.07	2.86	-1.22	-3.77	-1.01
Lu	0.04	-0.54	-0.14	-0.05	-0.12	-0.83	-0.21
Nb	0.07	-0.39	-0.12	0.31	0.36	-0.75	-0.10
Nd	-1.69	-2.56	-0.45	4.15	-2.03	-7.40	-1.11
Pr	-0.61	-0.54	-0.26	0.79	-0.37	-1.49	-0.44
Rb	3.25	1.17	8.06	-0.76	15.43	-0.98	4.49
Sm	-0.12	-1.04	-0.12	0.92	-0.54	-2.62	-0.18
Sn	-0.22	-0.11	1.45	1.35	-0.19	-0.41	0.00
Sr	-53.29	108.22	-28.55	16.54	-16.94	-26.2	-69.05
Ta	0.03	0.39	0.56	0.54	0.03	0.25	0.05

Sample ID	62599	62603	62605	62606	62607	62608	62610
Hole ID	PH-18-34	PH-18-34	PH-18-34	PH-18-34	PH-18-34	PH-18-34	PH-18-34
Depth (m)	337.5	395	410.04	415.67	430.71	233.69	447.62
Lithology	Tuff	Xtl-Tuff	Xtl-Tuff	Lap. Tuff	Rhyolite	Basalt	Xtl-Tuff
Stratigraphy	FW	FW	MS	FW	FW	HW	FW
Alteration	QSC+/-Py	QS+/-C	QSCPy	QSC+/-Py+Sil	QS	C-Ep	QSC
Tb	0.06	-0.41	-0.03	0.09	-0.11	-0.75	-0.13
Th	0.24	-0.31	0.08	1.10	-0.05	-0.80	0.00
Tm	0.13	-0.43	-0.08	-0.08	-0.02	-0.68	-0.10
U	-0.46	-0.78	-0.62	-0.86	-0.73	-1.02	-0.89
V	-8.05	-3.80	-6.94	-7.06	-5.95	191.51	-2.01
W	-0.22	-0.11	5.12	-0.41	-0.19	-0.41	0.00
Y	-1.72	-25.23	-6.41	-3.14	-4.58	-41.01	-9.77
Yb	-0.35	-3.67	-0.94	-1.05	-1.15	-5.42	-1.15
Zr	12.26	-25.3	0.65	1.66	15.40	-64.00	-4.12
As	-1.61	-1.99	0.36	0.36	-0.67	6.58	-0.5
Bi	-0.02	-0.05	1.18	0.07	-0.03	-0.03	-0.06
Hg	0.00	0.00	0.00	0.04	0.00	0.00	0.00
In	0.02	0.04	1.73	2.78	-0.01	-0.01	0.02
Re	0.00	0.00	0.00	0.00	0.00	0.00	0.00
Sb	0.00	-0.06	0.06	0.00	-0.09	-0.06	-0.02
Se	-0.02	-0.01	0.02	0.02	-0.02	-0.04	0.00
Te	0.01	0.00	1.93	0.67	0.00	0.03	-0.01
Tl	0.66	0.00	0.07	-0.02	0.07	-0.02	0.06
Ag	0.22	-0.03	1.83	0.34	-0.05	-0.10	0.00
Cd	-0.05	-0.03	0.48	19.49	-0.05	-0.10	0.00
Co	0.56	0.77	-0.39	-0.41	-0.19	9.05	0.00
Cu	-0.10	-1.34	1661.95	126.44	-1.57	11.96	0.99
Li	49.64	3.86	44.00	6.75	11.22	6.82	4.99
Mo	0.56	-0.11	0.22	1.35	0.62	-0.41	0.00
Ni	-1.22	0.66	0.45	0.35	0.43	-0.23	1.00
Pb	25.47	-5.80	28.42	6.80	-4.70	-10.23	-1.02
Sc	3.74	1.84	-0.30	-2.07	-6.89	11.00	-7.01
Zn	100.30	35.13	404.73	4345.49	-10.57	22.73	-18.08

Sample ID	62597	62594	62573	62600	62580	62579	62592
Hole ID	PH-18-34	PH-18-34	PH-18-34	PH-18-34	PH-18-34	PH-18-34	PH-18-34
Depth (m)	319.77	315.2	32.49	356	100.85	90.43	304.74
Lithology	Xtl-Tuff	Tuff	Sediment	Tuff	Lap. Tuff	Lap. Tuff	Lap. Tuff
Stratigraphy	MS	MS	HW	MS	HW	HW	MS
Alteration	QSCPy+/-Sil	QSCPy+/-Sil	GraQ	QSC (Cd)	QS	QSC	QSC+Sil
SiO_2	-16.23	-18.94	-33.96	-9.62	5.88	-18.02	61.58
Al_2O_3	0.00	0.00	0.00	0.00	0.00	0.00	0.00
Fe_2O_3	3.23	3.08	4.27	2.39	8.16	7.02	28.94
CaO	-5.31	-5.12	-6.23	-3.19	-5.19	-5.55	-3.58
MgO	1.16	0.07	1.17	-0.08	-0.09	0.05	0.34
Na_2O	-2.23	-0.80	-4.51	-1.29	-4.30	-3.97	-2.62
K_2O	0.21	-0.03	2.88	0.31	2.88	2.98	0.35
Cr_2O_3	0.00	0.00	0.01	0.00	0.00	0.00	0.00
TiO_2	-0.03	-0.04	0.41	0.19	0.20	0.17	-0.04
MnO	-0.11	-0.13	-0.05	-0.02	-0.08	-0.12	-0.08
P_2O_5	0.00	0.00	0.11	0.07	0.10	0.62	0.01
SrO	0.01	0.01	-0.01	-0.01	0.00	-0.01	0.00
BaO	0.03	0.01	0.06	0.00	1.06	0.33	0.03
LOI	1.17	1.10	1.32	-0.08	1.69	1.41	5.25
Total	-17.2	-21.61	-35.96	-8.95	11.17	-14.72	87.57
C	-0.15	-0.16	-0.14	-0.05	-0.16	-0.16	-0.13
S	2.25	2.30	1.76	0.02	3.48	3.26	14.02
Ba	244.46	69.73	520.57	14.00	9192.98	2799.45	251.76
Ce	-0.68	0.84	42.13	-5.57	-0.86	3.03	12.45
Cr	-11.93	-12.19	56.98	6.63	1.73	-11.65	16.99
Cs	0.25	0.06	2.43	0.23	0.94	1.28	0.14
Dy	-0.33	0.40	-3.91	-3.80	-3.38	0.34	2.50
Er	-0.62	-0.11	-3.00	-2.55	-2.33	0.28	1.40
Eu	1.22	0.83	0.22	-0.07	0.14	0.44	8.40
Ga	4.38	1.31	4.23	0.15	3.39	1.63	7.63
Gd	-0.45	0.68	-0.98	-2.51	-1.69	1.97	2.79
Ge	-0.48	-0.55	-0.90	-0.28	0.22	-0.41	2.12
Hf	0.49	0.21	-0.67	-1.35	-0.69	-1.38	0.03
Ho	-0.13	0.04	-0.94	-0.86	-0.76	0.12	0.32
La	-0.43	0.49	22.18	-1.87	0.16	2.25	6.79
Lu	-0.26	-0.14	-0.68	-0.52	-0.55	-0.12	0.16
Nb	0.27	-0.01	9.87	-0.12	0.20	0.07	0.01
Nd	-0.78	1.21	15.92	-4.23	-1.82	3.26	10.41
Pr	-0.19	0.06	4.75	-0.96	-0.36	0.39	1.82
Rb	6.79	2.63	91.24	6.60	19.65	35.46	5.55
Sm	0.04	0.36	1.30	-1.62	-0.87	1.02	3.14
Sn	-0.19	-0.22	1.57	-0.11	0.09	-0.17	2.70
Sr	22.65	37.63	-58.12	-25.06	-23.68	-60.08	41.04
Ta	0.03	0.03	0.72	0.39	0.06	0.03	0.87

Sample ID	62597	62594	62573	62600	62580	62579	62592
Hole ID	PH-18-34	PH-18-34	PH-18-34	PH-18-34	PH-18-34	PH-18-34	PH-18-34
Depth (m)	319.77	315.2	32.49	356	100.85	90.43	304.74
Lithology	Xtl-Tuff	Tuff	Sediment	Tuff	Lap. Tuff	Lap. Tuff	Lap. Tuff
Stratigraphy	MS	MS	HW	MS	HW	HW	MS
Alteration	QSCPy+/-Sil	QSCPy+/-Sil	GraQ	QSC (Cd)	QS	QSC	QSC+Sil
Tb	-0.07	0.09	-0.35	-0.49	-0.41	0.14	0.39
Th	0.26	0.06	9.14	-0.36	-0.02	-0.33	0.21
Tm	-0.16	-0.02	-0.52	-0.46	-0.40	0.01	0.14
U	4.91	3.02	11.00	-1.00	1.24	7.32	2.36
V	-3.54	0.93	391.57	6.86	16.07	-3.32	2.95
W	-0.19	-0.22	2.85	-0.11	1.17	-0.17	0.85
Y	-11.5	-2.48	-28.19	-27.23	-23.75	4.63	14.37
Yb	-1.61	-1.08	-4.19	-3.72	-3.50	-1.17	0.51
Zr	6.87	6.06	11.35	-27.87	-4.19	-34.06	6.17
As	68.91	21.98	-0.90	-1.63	1.97	7.90	27.26
Bi	0.32	0.03	0.29	-0.03	0.66	0.32	11.28
Hg	0.06	0.18	0.00	0.00	0.00	0.00	0.19
In	0.06	0.04	0.01	0.00	0.00	-0.01	1.62
Re	0.00	0.01	0.02	0.00	0.00	0.01	0.00
Sb	9.05	1.29	0.11	-0.03	0.13	0.10	3.63
Se	0.14	0.84	2.21	0.08	0.66	0.48	1.93
Te	2.73	0.74	0.56	0.16	0.64	0.42	28.10
Tl	4.45	2.94	0.34	0.05	0.01	0.13	1.57
Ag	11.94	3.34	0.07	-0.03	0.62	0.84	30.08
Cd	1.04	0.45	0.33	-0.03	0.29	0.17	9.74
Co	-0.19	-0.22	13.75	0.78	3.35	2.34	6.40
Cu	544.15	101.43	71.05	5.76	12.29	24.39	5340.56
Li	27.29	10.62	20.66	3.88	16.73	11.70	13.49
Mo	5.46	31.02	12.47	-0.11	31.59	2.34	76.67
Ni	2.04	19.87	39.05	-0.22	5.60	6.35	9.10
Pb	503.05	91.87	-1.74	5.75	8.64	-3.65	498.41
Sc	1.15	4.52	-5.38	0.09	2.38	1.70	3.49
Zn	347.60	158.16	37.33	23.75	-10.00	-33.76	2469.83

Sample ID	62588	62611	62613	62614	62618	62619	62623
Hole ID	PH-18-34	PH-18-34	PH-18-34	PH-18-34	PH-18-34	PH-18-34	PH-18-40
Depth (m)	251	487.41	524.14	548	591.84	608	19.65
Lithology	Basalt	Tuff	Tuff	Tuff	Rhyolite	Rhyolite	Lap. Tuff
Stratigraphy	HW	FW	FW	FW	MS	FW	HW
Alteration	CCal	QS+/-C	SQ+/-C+Sil	QSCPy+Sil	QS+/-C+/-Py	QSC+Sil	QS
SiO_2	-43.35	-1.77	-6.30	4.75	16.58	-6.56	3.53
Al_2O_3	0.00	0.00	0.00	0.00	0.00	0.00	0.00
Fe_2O_3	4.51	1.53	2.65	0.61	0.50	2.62	0.63
CaO	-4.11	-1.85	-4.63	-5.41	-4.06	-4.6	-4.6
MgO	1.71	0.57	-0.11	-0.15	-0.16	0.05	1.34
Na_2O	-3.94	-2.34	-0.82	-1.79	-1.12	-1.09	-3.27
K_2O	2.19	0.14	0.25	1.65	0.02	0.48	0.00
Cr_2O_3	0.00	0.00	0.00	0.00	0.00	0.00	0.00
TiO_2	0.35	0.09	0.10	-0.03	-0.05	0.10	-0.04
MnO	-0.12	0.04	-0.02	-0.09	-0.07	0.00	-0.12
P_2O_5	0.00	0.04	0.04	0.02	0.02	0.04	0.00
SrO	0.00	0.00	0.00	-0.01	0.00	0.00	0.02
BaO	0.01	0.00	0.00	0.01	0.00	0.00	0.00
LOI	0.19	-0.19	-0.21	0.25	-0.15	-0.34	0.61
Total	-40.84	-3.40	-7.79	0.66	12.69	-6.73	0.27
C	-0.16	-0.13	-0.12	-0.14	-0.1	-0.12	-0.17
S	0.86	0.15	-0.21	0.39	0.20	-0.08	-0.18
Ba	52.55	11.69	-2.70	84.99	25.00	13.86	-8.76
Ce	-12.80	0.37	-2.33	1.43	2.86	0.02	6.47
Cr	14.34	-0.71	-10.88	-0.09	2.33	-1.79	-0.5
Cs	0.87	0.31	0.18	0.36	0.18	0.14	0.73
Dy	-8.23	-2.41	-2.93	0.67	-0.38	-2.59	1.99
Er	-5.53	-1.74	-1.95	0.78	0.41	-1.4	1.63
Eu	-0.6	0.57	0.12	0.35	0.32	0.37	0.20
Ga	-1.11	-1.42	-0.14	-0.16	-5.20	0.75	0.16
Gd	-5.8	-0.79	-1.6	1.72	0.64	-0.98	2.28
Ge	-1.07	-0.09	-0.22	-0.01	0.29	-0.22	-0.06
Hf	-2.78	-0.50	-0.75	1.08	1.28	-0.75	1.48
Ho	-1.81	-0.46	-0.61	0.41	0.03	-0.39	0.64
La	-5.20	-0.01	-1.04	-0.12	0.99	-0.32	2.59
Lu	-0.98	-0.33	-0.32	0.03	0.10	-0.28	0.28
Nb	-0.93	-0.23	-0.37	0.09	0.02	-0.19	-0.03
Nd	-10.51	0.17	-1.94	3.03	2.36	0.42	6.14
Pr	-2.03	0.09	-0.44	0.45	0.46	-0.08	1.01
Rb	21.26	4.31	3.96	13.72	2.11	7.5	3.81
Sm	-3.64	-0.03	-0.57	1.43	2.15	0.20	2.27
Sn	-0.71	-0.04	-0.09	0.00	0.12	-0.09	-0.03
Sr	-47.26	-5.16	-27.47	-62.59	-57.28	-38.32	154.79
Ta	0.24	0.43	0.41	0.45	0.51	0.41	0.44

Sample ID	62588	62611	62613	62614	62618	62619	62623
Hole ID	PH-18-34	PH-18-34	PH-18-34	PH-18-34	PH-18-34	PH-18-34	PH-18-40
Depth (m)	251	487.41	524.14	548	591.84	608	19.65
Lithology	Basalt	Tuff	Tuff	Tuff	Rhyolite	Rhyolite	Lap. Tuff
Stratigraphy	HW	FW	FW	FW	MS	FW	HW
Alteration	CCal	QS+/-C	SQ+/-C+Sil	QSCPy+Sil	QS+/-C+/-Py	QSC+Sil	QS
Tb	-1.05	-0.16	-0.20	0.31	0.15	-0.14	0.47
Th	-0.99	-0.29	-0.21	0.24	0.36	-0.25	0.43
Tm	-0.86	-0.22	-0.26	0.18	0.09	-0.24	0.28
U	-1.09	-0.98	-1.06	-0.86	-0.84	-1.03	-0.73
V	302.53	-7.59	-7.72	-7.51	-7.21	-7.72	-7.56
W	-0.43	-0.04	-0.09	0.00	-0.44	-0.09	0.95
Y	-52.58	-15.00	-20.9	7.02	-0.53	-15.94	14.87
Yb	-6.64	-2.61	-2.63	0.30	-0.10	-2.67	0.90
Zr	-75.12	-10.91	-11.61	15.52	28.34	-9.89	34.77
As	-2.41	-0.48	-1.51	3.27	1.99	-1.52	-2.41
Bi	-0.04	0.03	-0.03	-0.02	0.14	-0.03	-0.04
Hg	0.00	0.00	0.00	0.00	0.00	0.00	0.00
In	0.00	0.00	0.03	0.02	0.05	0.06	0.04
Re	0.00	0.00	0.00	0.00	0.00	0.00	0.00
Sb	-0.08	-0.05	-0.06	-0.04	0.19	-0.03	-0.09
Se	0.24	0.19	0.08	0.20	0.01	0.08	0.19
Te	0.01	0.06	0.00	0.02	0.06	0.03	0.00
Tl	0.11	0.06	0.00	0.01	0.08	0.04	-0.03
Ag	-0.11	-0.01	-0.02	0.00	0.53	-0.02	-0.01
Cd	0.15	-0.01	-0.02	0.00	0.53	-0.02	-0.01
Co	29.91	0.93	0.82	0.00	0.12	-0.09	0.95
Cu	25.76	13.36	-0.35	-1.01	49.59	-0.36	-3.03
Li	35.07	4.65	4.12	4.95	-4.44	4.1	24.24
Mo	-0.71	0.93	-0.09	0.99	1.23	-0.09	-0.03
Ni	5.44	-0.07	-1.09	-0.01	3.58	1.64	-1.03
Pb	-10.28	2.47	-9.27	-7.02	28.19	-5.63	-6.15
Sc	18.77	2.36	3.23	4.91	2.86	2.30	7.42
Zn	-10.04	126.65	37.3	19.58	194.94	170.05	13.76

Sample ID	62624	62625	62626	62632	62634	62635	62637	62642
Hole ID	PH-18-40	PH-18-40	PH-18-40	PH-18-40	PH-18-40	PH-18-40	PH-18-40	PH-18-26
Depth (m)	39.85	64.2	78.75	178	212.87	222.83	282.83	26
Lithology	Tuff	Tuff	Lap. Tuff	Sediment	Rhyolite	Rhyolite	Xtl-Tuff	Sediment
Stratigraphy	HW	HW	MS	FW	FW	FW	FW	HW
Alteration	QS+/-C	QS+/-C	QS	SC	QSC	QSC+/-Py	QS	QS+/-C+Bt
SiO_2	-23.72	-6.31	-1.25	-9.23	-0.28	19.55	8.10	-46.12
Al_2O_3	0.00	0.00	0.00	0.00	0.00	0.00	0.00	0.00
Fe_2O_3	0.72	1.87	0.68	2.14	0.89	2.54	1.78	5.25
CaO	-6.02	-5.24	-6.03	-5.1	-6.48	-4.9	-5.05	-1.49
MgO	-0.58	-0.03	1.92	0.63	1.04	4.34	0.61	2.58
Na_2O	-0.98	-0.68	-2.95	-1.36	-1.09	-2.14	-0.50	-3.16
K_2O	2.92	1.29	1.53	0.61	0.45	-0.10	0.03	0.77
Cr_2O_3	0.00	0.00	0.00	0.00	0.00	0.00	0.00	0.00
TiO_2	0.20	0.15	-0.01	0.09	0.00	0.00	-0.01	0.26
MnO	-0.13	-0.08	-0.09	-0.07	-0.11	0.00	-0.05	-0.05
P_2O_5	0.06	0.06	0.02	0.03	0.02	0.01	0.01	0.09
SrO	0.00	-0.01	-0.01	-0.01	-0.01	0.00	0.00	0.00
BaO	0.01	0.02	0.02	0.01	0.00	0.00	0.00	0.00
LOI	-0.55	-0.13	1.29	-0.19	0.68	1.23	0.32	0.94
Total	-26.65	-8.65	-5.51	-10.44	-3.37	22.07	6.41	-41.24
C	-0.15	-0.08	-0.09	-0.15	-0.16	-0.13	-0.11	-0.15
S	0.06	-0.18	0.04	-0.15	0.29	0.36	0.50	0.71
Ba	105.51	175.76	141.10	43.01	51.85	-15.41	35.27	51.01
Ce	-3.63	-3.71	-1.52	-3.91	5.45	-1.00	1.63	-11.91
Cr	-12.75	-10.9	-1.24	-2.45	-1.11	-8.07	-9.51	-8.37
Cs	0.19	0.17	0.65	0.89	0.75	0.60	0.19	1.37
Dy	-3.83	-3.52	-0.83	-3.17	-1.31	-2.87	-1.92	-7.48
Er	-2.66	-2.09	0.10	-2.29	-0.82	-1.47	-0.94	-5.03
Eu	-0.08	0.09	0.13	0.41	-0.18	-0.16	-0.09	-0.54
Ga	-0.36	0.85	0.80	0.70	-3.08	-1.33	-1.46	-2.15
Gd	-2.42	-1.94	-0.37	-1.33	-0.40	-2.02	-0.81	-5.31
Ge	-0.69	-0.22	-0.15	-0.31	-0.14	0.48	0.12	-1.05
Hf	-1.13	-1.02	-0.20	-0.84	0.29	0.40	0.27	-2.95
Ho	-0.89	-0.68	-0.03	-0.75	-0.10	-0.42	-0.17	-1.64
La	-1.69	-1.87	-0.53	-1.56	2.43	-0.47	0.49	-4.73
Lu	-0.64	-0.49	-0.14	-0.50	-0.05	-0.16	-0.16	-0.92
Nb	-0.01	-0.01	-0.26	-0.31	0.13	0.09	0.05	-0.93
Nd	-3.92	-3.31	-1.19	-1.86	4.08	-1.46	0.89	-9.74
Pr	-0.65	-0.66	-0.29	-0.71	0.84	-0.24	0.13	-1.89
Rb	15.87	6.68	11.31	9.29	5.93	0.71	0.60	9.79
Sm	-1.17	-0.90	-0.01	-0.78	0.75	-0.40	-0.07	-3.42
Sn	-0.28	-0.09	-0.06	-0.12	-0.06	0.19	0.05	-0.42
Sr	-40.86	-47.69	-56.09	-54.49	-41.7	17.20	-41.44	-22.83
Ta	0.31	0.41	0.42	0.04	0.42	0.55	0.47	0.24

Sample ID	62624	62625	62626	62632	62634	62635	62637	62642
Hole ID	PH-18-40	PH-18-40	PH-18-40	PH-18-40	PH-18-40	PH-18-40	PH-18-40	PH-18-26
Depth (m)	39.85	64.2	78.75	178	212.87	222.83	282.83	26
Lithology	Tuff	Tuff	Lap. Tuff	Sediment	Rhyolite	Rhyolite	Xtl-Tuff	Sediment
Stratigraphy	HW	HW	MS	FW	FW	FW	FW	HW
Alteration	QS+/-C	QS+/-C	QS	SC	QSC	QSC+/-Py	QS	QS+/-C+Bt
Tb	-0.43	-0.38	-0.03	-0.33	0.13	-0.25	-0.12	-0.95
Th	-0.30	-0.24	-0.22	-0.29	0.28	0.09	0.07	-1.08
Tm	-0.44	-0.41	-0.05	-0.35	-0.07	-0.19	-0.13	-0.78
U	-0.92	-1.02	-0.81	-1.04	-0.77	-0.94	-0.88	-1.19
V	-2.75	-7.72	-3.43	-2.98	-7.64	-7.02	-7.38	183.56
W	-0.28	-0.09	-0.06	-0.12	-0.06	-0.40	0.05	14.11
Y	-28.14	-24.03	-4.39	-21.86	-8.97	-15.81	-9.52	-47.59
Yb	-4.07	-3.53	-1.06	-3.18	-1.35	-2.20	-1.41	-6.23
Zr	-18.24	-16.25	0.06	-15.42	2.54	3.06	7.58	-80.12
As	9.62	-1.15	-1.20	-2.52	0.23	-1.98	2.02	-1.71
Bi	0.07	-0.04	0.01	0.10	0.58	1.10	0.55	0.08
Hg	0.00	0.00	0.04	0.00	0.00	0.00	0.00	0.00
In	0.02	0.05	0.12	0.07	0.09	0.69	0.16	-0.01
Re	0.00	0.00	0.00	0.00	0.00	0.00	0.00	0.00
Sb	-0.09	-0.04	0.06	-0.06	-0.04	-0.04	-0.05	-0.10
Se	-0.03	0.17	0.09	-0.01	0.09	0.50	0.32	0.42
Te	0.08	0.02	0.02	0.09	0.20	0.68	0.51	0.86
Tl	-0.03	-0.02	0.08	0.07	-0.02	-0.02	-0.03	0.15
Ag	-0.07	-0.02	-0.02	-0.03	-0.01	0.05	0.01	-0.10
Cd	-0.07	-0.02	7.26	-0.03	-0.01	0.05	0.01	0.22
Co	-0.64	-0.09	-0.06	0.75	0.89	0.19	1.10	27.48
Cu	5.42	-2.18	111.4	1.26	29.99	215.53	4.39	39.01
Li	2.25	4.10	23.15	12.55	13.89	18.86	5.49	12.44
Mo	-0.28	-0.09	0.88	-0.12	1.83	2.58	3.20	0.16
Ni	-1.28	0.73	0.81	0.63	0.83	-0.81	1.15	16.02
Pb	-0.40	-11.09	6.76	-10.25	-10.11	22.60	-0.46	-6.19
Sc	0.22	0.48	-0.93	0.79	-3.67	-4.26	-2.41	9.41
Zn	29.20	8.03	1779.89	35.79	-9.73	255.11	17.23	10.12

Sample ID	62648	62649	62563	62620	62622	62627
Hole ID	PH-18-26	PH-18-26	PH-18-14	PH-18-34	PH-18-34	PH-18-40
Depth (m)	39.34	41	107.73	625.2	667.18	88
Lithology	Tuff	Dike	Rhyolite	Rhyolite	Tuff	Xtl-Tuff
Stratigraphy	HW	HW	FW	FW	FW	MS
Alteration	QS	Unaltered	QS	QS+/-C+/-Py	QSC+/-Py	QS+/-C+/-Py+Sil
SiO_2	-8.27	-5.21	-7.54	-10.90	-15.12	49.96
Al_2O_3	0.00	0.00	0.00	0.00	0.00	4.29
Fe_2O_3	1.29	1.14	2.75	0.37	0.52	3.18
CaO	7.30	-4.88	-4.39	-3.85	-6.07	0.15
MgO	-0.29	-0.56	0.24	0.38	1.18	0.33
Na_2O	-3.76	-1.77	-1.52	-3.51	-2.58	0.93
K_2O	1.41	2.74	0.37	1.12	1.63	0.73
Cr_2O_3	0.00	0.00	0.00	0.00	0.00	0.00
TiO_2	0.19	0.18	0.14	0.00	0.00	0.05
MnO	0.05	-0.12	-0.01	-0.06	-0.12	0.02
P_2O_5	0.12	0.06	0.05	0.01	0.01	0.01
SrO	0.00	-0.01	0.00	0.01	0.01	0.00
BaO	0.01	0.01	0.01	0.01	0.00	0.02
LOI	1.28	-0.64	-0.04	0.14	0.18	1.25
Total	-0.46	-6.28	-7.6	-14.64	-19.07	60.14
C	0.30	-0.15	-0.09	-0.16	-0.16	0.01
S	-0.18	0.24	-0.07	-0.12	0.11	1.42
Ba	109.54	89.3	67.30	47.54	32.86	143.84
Ce	-0.47	-3.01	-1.75	-0.55	-5.58	3.46
Cr	-10.2	-10.84	-10.99	-3.29	-12.06	11.94
Cs	0.33	0.30	0.50	1.61	1.70	0.27
Dy	-2.88	-4.00	-3.15	0.10	-3.04	3.26
Er	-1.66	-2.45	-2.07	0.50	-1.56	2.52
Eu	0.42	0.03	0.23	0.16	0.11	0.53
Ga	-1.14	-1.54	-0.56	-0.53	-3.29	5.61
Gd	-1.72	-2.80	-1.82	-0.09	-2.01	2.30
Ge	-0.05	-0.21	-0.25	-0.41	-0.51	1.49
Hf	-1.05	-1.01	-0.69	0.46	0.43	1.55
Ho	-0.48	-0.76	-0.64	0.20	-0.62	0.77
La	0.67	-1.11	-1.00	-0.42	-2.66	1.37
Lu	-0.40	-0.54	-0.46	0.08	-0.27	0.42
Nb	0.08	0.00	-0.29	-0.01	-0.07	0.54
Nd	-1.21	-3.08	-1.51	0.35	-3.02	3.10
Pr	-0.21	-0.66	-0.36	-0.19	-0.72	0.56
Rb	8.46	13.97	6.93	25.72	18.94	6.62
Sm	-0.40	-0.96	-0.56	0.39	-0.69	1.35
Sn	-0.02	-0.08	-0.10	0.67	-0.21	1.19
Sr	34.21	-60.82	-11.25	53.02	56.77	33.96
Ta	0.44	0.41	0.40	0.12	0.35	0.30

Sample ID	62648	62649	62563	62620	62622	62627
Hole ID	PH-18-26	PH-18-26	PH-18-14	PH-18-34	PH-18-34	PH-18-40
Depth (m)	39.34	41	107.73	625.2	667.18	88
Lithology	Tuff	Dike	Rhyolite	Rhyolite	Tuff	Xtl-Tuff
Stratigraphy	HW	HW	FW	FW	FW	MS
Alteration	QS	Unaltered	QS	QS+/-C+/-Py	QSC+/-Py	QS+/-C+/-Py+Sil
Tb	-0.22	-0.36	-0.35	0.15	-0.32	0.47
Th	-0.18	-0.25	-0.28	0.04	-0.11	0.47
Tm	-0.26	-0.42	-0.35	0.06	-0.22	0.38
U	-0.25	-0.93	-1.09	-0.44	-0.72	0.29
V	-3.14	-5.42	-7.75	-7.91	-8.01	5.37
W	0.96	-0.08	-0.10	-0.16	-0.60	0.60
Y	-17.18	-25.59	-22.65	4.44	-21.82	19.22
Yb	-2.67	-3.60	-3.05	-0.14	-1.99	2.79
Zr	-18.44	-22.23	-15.22	9.44	3.74	44.76
As	-1.72	-1.51	-1.89	-1.78	-1.03	8.83
Bi	-0.02	0.02	0.07	-0.02	0.07	0.66
Hg	0.00	0.00	0.00	0.00	0.00	0.10
In	0.05	0.01	0.07	0.03	0.02	0.20
Re	0.00	0.00	0.00	0.00	0.00	0.00
Sb	-0.06	-0.06	-0.05	-0.04	-0.04	0.90
Se	0.39	0.36	0.17	0.07	-0.02	0.24
Te	0.03	0.09	0.05	0.00	0.01	0.78
Tl	-0.03	-0.03	0.02	0.13	0.12	0.07
Ag	0.00	-0.02	-0.02	-0.04	-0.05	2.57
Cd	2.40	-0.02	-0.02	-0.04	-0.05	13.43
Co	-0.02	0.83	0.80	0.67	0.59	2.98
Cu	-0.08	8.82	12.22	-1.49	-0.82	109.82
Li	-4.51	-4.54	4.01	11.71	34.72	5.97
Mo	-0.02	-0.08	-0.10	1.51	-0.21	1.19
Ni	-1.02	-1.08	-0.20	-0.33	0.38	1.19
Pb	-3.18	-7.42	-3.89	-6.99	-9.62	1480.17
Sc	8.53	-3.09	2.12	0.04	-1.49	6.57
Zn	218.15	46.97	29.71	36.47	6.44	3479.59

Sample ID	62641	62644	62629	62559	62617	62695	62696
Hole ID	PH-18-26	PH-18-26	PH-18-40	PH-18-14	PH-18-34	PH-18-44	PH-18-44
Depth (m)	11.16	63.56	125.32	72.52	579.83	117.7	129.6
Lithology	Sediment	Tuff	Rhyolite	Rhyolite	Lap. Tuff	Tuff	Lap. Tuff
Stratigraphy	HW	HW	MS	MS	MS	MS	MS
Alteration	QS+/-C (Cd+And)	QS	QSC+/-Sil	QSC+Sil	QSC+/-Py	QSCPy	QSCPy
SiO_2	-32.65	-23.90	-17.26	-15.99	27.50	22.11	-19.91
Al_2O_3	0.00	0.00	0.00	0.00	0.00	0.00	0.00
Fe_2O_3	4.13	0.63	3.43	1.17	54.51	0.98	0.37
CaO	-5.97	-6.09	-6.26	-6.13	-6.39	-6.30	-5.72
MgO	1.19	1.39	1.75	2.22	1.88	2.38	7.97
Na_2O	-4.29	-3.72	-3.06	-2.26	-4.35	-2.65	-3.57
K_2O	2.82	3.74	0.76	0.07	1.92	0.73	0.67
Cr_2O_3	0.01	0.00	0.00	0.00	0.00	0.00	0.00
TiO_2	0.47	-0.01	0.03	0.06	0.05	0.11	0.00
MnO	-0.03	-0.12	-0.09	0.01	-0.03	-0.04	0.07
P_2O_5	0.06	0.00	0.07	0.04	0.05	0.01	0.01
SrO	0.00	-0.01	0.00	0.00	0.00	0.00	-0.01
BaO	0.03	0.00	0.01	0.00	0.05	0.00	0.00
LOI	1.67	0.19	1.64	0.45	15.68	1.02	3.27
Total	-33.06	-26.39	-21.35	-20.4	72.19	19.67	-18.18
C	0.47	-0.16	-0.16	-0.15	-0.15	-0.16	-0.04
S	0.50	-0.23	1.42	0.22	28.90	-0.15	-0.22
Ba	289.54	0.90	104.16	-12.06	394.83	83.79	4.11
Ce	42.88	-1.42	-3.13	2.63	3.86	-2.97	-6.57
Cr	39.18	-12.81	-12.06	-12.08	-2.49	3.46	-12.01
Cs	3.27	1.28	0.90	0.42	0.81	1.14	2.58
Dy	-5.33	0.24	-4.40	-1.73	-1.15	-2.34	-2.13
Er	-3.69	0.36	-2.39	-1.21	0.10	-1.14	-1.23
Eu	-0.06	0.14	1.65	0.37	1.34	0.39	0.23
Ga	4.00	0.04	2.34	-2.21	3.04	-0.35	-2.44
Gd	-2.29	-0.23	-2.89	-1.42	-0.07	-1.15	-1.32
Ge	-0.86	-0.70	-0.52	-0.52	1.88	0.43	-0.50
Hf	-0.54	1.23	-0.84	0.11	0.20	0.22	0.05
Ho	-1.25	0.21	-0.75	-0.26	-0.04	-0.43	-0.47
La	21.82	-0.35	-1.08	1.29	1.58	-1.03	-3.04
Lu	-0.79	0.06	-0.43	-0.15	-0.17	-0.26	-0.27
Nb	9.68	-0.09	-0.39	0.09	0.48	0.19	0.10
Nd	12.93	-1.17	-3.27	0.83	1.89	-3.51	-4.25
Pr	4.31	-0.31	-0.62	0.22	0.42	-0.61	-1.01
Rb	86.06	37.64	12.81	3.98	14.16	10.96	26.73
Sm	0.72	-0.32	-1.29	-0.06	0.86	-1.11	-0.73
Sn	0.97	-0.28	1.38	-0.21	9.51	0.17	-0.20
Sr	-44.2	-79.33	-14.43	-43.13	-62.12	-49.96	-66.88
Ta	0.74	0.31	0.35	0.35	0.83	0.30	0.11

Sample ID	62641	62644	62629	62559	62617	62695	62696
Hole ID	PH-18-26	PH-18-26	PH-18-40	PH-18-14	PH-18-34	PH-18-44	PH-18-44
Depth (m)	11.16	63.56	125.32	72.52	579.83	117.7	129.6
Lithology	Sediment	Tuff	Rhyolite	Rhyolite	Lap. Tuff	Tuff	Lap. Tuff
Stratigraphy	HW	HW	MS	MS	MS	MS	MS
Alteration	QS+/-C (Cd+And)	QS	QSC+/-Sil	QSC+Sil	QSC+/-Py	QSCPy	QSCPy
Tb	-0.56	0.14	-0.45	-0.18	0.03	-0.16	-0.19
Th	7.88	-0.05	-0.20	0.19	-0.13	-0.06	-0.02
Tm	-0.63	0.11	-0.37	-0.15	-0.11	-0.25	-0.22
U	2.41	-0.26	1.99	0.02	-0.74	-0.23	-0.89
V	109.68	-8.20	13.81	8.21	-5.62	24.02	-8.00
W	0.32	-0.28	0.59	-0.21	2.50	0.17	2.19
Y	-36.7	1.62	-24.55	-10.21	-5.81	-10.51	-14.85
Yb	-5.16	-0.63	-3.35	-1.6	-1.16	-1.48	-2.26
Zr	15.22	30.8	-21.75	7.40	11.58	3.84	1.85
As	3.02	-2.34	-0.87	-1.99	25.67	-2.23	-2.22
Bi	0.38	-0.06	6.04	0.10	6.18	-0.05	0.83
Hg	0.00	0.00	0.09	0.03	0.19	0.01	0.00
In	-0.01	0.03	1.65	0.92	106.63	0.04	0.03
Re	0.01	0.00	0.00	0.00	0.00	0.00	0.00
Sb	-0.08	-0.05	0.37	-0.03	0.45	-0.04	-0.03
Se	1.08	0.04	0.61	-0.02	2.70	0.02	-0.02
Te	0.35	0.00	0.48	0.05	1.74	0.01	0.02
Tl	0.31	0.08	0.17	0.07	0.36	0.11	0.11
Ag	-0.09	-0.07	5.23	0.23	11.66	0.04	-0.05
Cd	0.14	-0.07	18.64	6.24	17.44	0.04	-0.05
Co	16.10	-0.28	0.59	1.38	0.75	0.17	-0.60
Cu	48.61	-2.56	710.99	91.82	12045.86	7.73	3.19
Li	14.73	16.57	18.81	18.76	12.51	30.19	42.92
Mo	1.63	-0.64	16.46	0.58	90.07	4.86	1.40
Ni	32.85	-0.56	-1.21	-1.21	-1.12	2.69	-1.60
Pb	9.70	-2.65	888.68	70.35	112.35	12.63	51.89
Sc	-2.51	8.01	-5.48	-5.50	-13.25	-4.44	-6.21
Zn	28.93	11.13	3005.96	1221.7	3780.15	309.40	172.99

Sample ID	62697	62698	62699	62700	62701	62702	62703
Hole ID	PH-18-42	PH-18-42	PH-18-42	PH-18-42	PH-18-42	PH-18-13	PH-18-13
Depth (m)	17	42.44	56	121.7	133.82	25	54.32
Lithology	Xtl-Tuff	Lap. Tuff	Xtl-Tuff	Tuff	Tuff	Dike	Xtl-Tuff
Stratigraphy	HW	MS	FW	FW	FW	HW	MS
Alteration	QSC	QSCPy	QS+/-Py	QSC+/-Py+Sil	QS+Sil	SC	QSC+Sil
SiO_2	-5.82	-22.12	6.67	5.14	1.60	-23.06	-40.24
Al_2O_3	0.00	0.00	0.00	0.00	0.00	0.00	0.00
Fe_2O_3	12.49	1.67	3.84	3.16	0.24	2.25	-0.19
CaO	-5.07	-6.15	-6.47	-6.57	-5.82	-3.63	-4.48
MgO	5.77	0.49	1.86	1.66	0.08	0.65	0.75
Na_2O	-4.44	-3.29	-3.54	-4.26	-0.50	-1.40	-1.71
K_2O	0.43	1.51	0.99	1.15	0.62	1.03	0.51
Cr_2O_3	0.00	0.00	0.00	0.01	0.00	0.00	0.00
TiO_2	-0.01	0.01	-0.02	0.06	-0.02	0.41	0.00
MnO	-0.01	-0.12	-0.09	0.00	-0.10	-0.09	-0.11
P_2O_5	0.00	0.01	0.00	0.00	-0.01	0.10	0.01
SrO	0.00	0.00	0.00	0.00	-0.01	0.01	0.00
BaO	0.02	0.03	0.03	0.02	0.00	0.02	0.04
LOI	3.83	1.40	0.96	1.43	0.06	0.13	-0.12
Total	4.46	-27.18	5.15	2.57	-1.91	-21.50	-44.06
C	-0.15	-0.16	-0.16	-0.15	-0.15	-0.12	-0.15
S	4.22	1.30	1.06	0.78	0.11	-0.24	-0.09
Ba	244.44	226.83	297.88	229.26	30.46	197.21	404.61
Ce	0.57	4.73	2.11	-1.86	0.89	15.37	3.08
Cr	-9.67	-12.80	10.98	0.07	-0.79	2.88	-14.54
Cs	1.65	0.90	1.11	2.24	0.24	0.43	0.47
Dy	0.99	-1.93	2.43	-2.88	0.68	-6.20	-0.85
Er	0.22	-1.62	1.74	-1.76	0.59	-4.21	-0.33
Eu	-0.10	-0.12	0.13	-0.20	0.25	-0.11	0.15
Ga	6.42	-0.44	3.21	0.65	-0.89	0.68	-0.68
Gd	0.42	-0.20	1.86	-2.10	0.59	-3.28	-0.47
Ge	0.08	-0.70	0.08	0.01	-0.10	-0.59	-1.14
Hf	0.52	1.02	1.35	-0.39	0.73	0.36	0.85
Ho	0.23	-0.47	0.55	-0.62	0.14	-1.38	-0.20
La	0.19	1.60	0.60	-0.78	0.07	9.04	1.11
Lu	0.01	-0.35	0.16	-0.37	0.04	-0.78	-0.05
Nb	0.14	0.20	0.14	-0.10	0.15	4.24	0.21
Nd	0.08	2.37	1.62	-1.97	0.79	1.06	1.49
Pr	0.01	0.62	0.35	-0.40	0.11	1.06	0.33
Rb	9.63	13.73	8.07	29.62	6.77	30.01	6.50
Sm	0.40	0.61	1.41	-0.93	0.88	-1.16	0.49
Sn	1.07	0.44	2.10	1.01	-0.04	0.53	0.09
Sr	-24.62	-41.12	-26.13	-67.27	-67.42	103.73	-24.30
Ta	0.16	0.24	0.16	0.15	0.14	0.48	0.11

Sample ID	62697	62698	62699	62700	62701	62702	62703
Hole ID	PH-18-42	PH-18-42	PH-18-42	PH-18-42	PH-18-42	PH-18-13	PH-18-13
Depth (m)	17	42.44	56	121.7	133.82	25	54.32
Lithology	Xtl-Tuff	Lap. Tuff	Xtl-Tuff	Tuff	Tuff	Dike	Xtl-Tuff
Stratigraphy	HW	MS	FW	FW	FW	HW	MS
Alteration	QSC	QSCPy	QS+/-Py	QSC+/-Py+Sil	QS+Sil	SC	QSC+Sil
Tb	0.13	-0.10	0.39	-0.34	0.11	-0.66	-0.06
Th	0.30	0.70	-0.19	-0.26	0.22	3.80	0.48
Tm	0.09	-0.21	0.22	-0.30	0.03	-0.70	-0.01
U	-0.06	5.10	-0.92	-0.60	-0.82	0.97	-0.32
V	-3.80	18.09	-7.42	-0.97	-7.60	43.39	-8.64
W	0.03	-0.28	0.03	0.00	-0.04	0.53	0.09
Y	1.66	-16.79	15.04	-18.27	3.46	-38.81	-5.98
Yb	-0.05	-2.21	1.61	-2.48	0.53	-5.16	-0.32
Zr	16.43	14.44	29.77	-10.72	13.74	52.63	15.30
As	-1.67	0.61	-1.77	-1.60	-1.64	-2.32	-2.15
Bi	2.21	0.23	0.81	0.70	0.03	-0.01	0.13
Hg	0.00	0.00	0.00	0.00	0.00	0.00	0.00
In	0.44	2.76	0.03	0.20	0.00	-0.03	0.02
Re	0.00	0.00	0.00	0.00	0.00	0.00	0.00
Sb	-0.03	-0.05	-0.06	-0.05	-0.09	0.01	0.01
Se	3.41	0.76	0.21	0.10	0.00	-0.02	-0.05
Te	4.02	0.04	1.14	0.80	0.03	0.00	0.02
Tl	0.14	0.05	0.07	0.00	-0.03	-0.03	0.35
Ag	1.09	0.54	0.01	0.00	-0.01	-0.06	0.30
Cd	2.64	0.40	0.01	0.00	-0.01	-0.06	0.46
Co	-0.48	-0.64	-0.48	0.00	-0.52	7.39	-0.45
Cu	71.43	512.43	5.29	50.19	-0.16	7.44	30.92
Li	5.33	2.20	15.65	35.14	4.61	2.63	5.91
Mo	4.17	17.73	2.10	5.02	0.92	0.53	7.73
Ni	4.20	3.76	0.07	0.01	-1.52	4.10	-1.45
Pb	0.40	-1.92	-0.64	-7.99	-4.32	-1.32	229.16
Sc	3.60	-6.36	5.65	-2.96	2.29	-7.37	-5.72
Zn	495.34	60.97	32.32	-12.79	-20.17	-29.52	74.86

Sample ID	62704	62705	62706	62707	62708	62709	62710
Hole ID	PH-18-13	PH-18-13	PH-18-13	PH-18-13	PH-18-13	PH-18-13	PH-18-13
Depth (m)	58.16	69.81	88.39	97.66	114.38	145	160.17
Lithology	Lap. Tuff	Dike	Lap. Tuff	Lap. Tuff	Lap. Tuff	Rhyolite	Lap. Tuff
Stratigraphy	MS	MS	MS	MS	FW	FW	MS
Alteration	QSCPy+Sil	Unaltered	QSC+Sil	QSC+/-Py+Sil	QSC+/-Py+Sil	QS+/-Py	QSC+/-Py+Sil
SiO_2	17.76	-42.47	58.09	-25.54	3.68	9.02	-6.21
Al_2O_3	0.00	0.00	0.00	0.00	0.00	0.00	0.00
Fe_2O_3	13.08	6.72	1.35	3.75	1.25	0.93	1.99
CaO	-6.48	-0.14	-6.37	-6.35	-6.15	-5.93	-4.62
MgO	0.20	4.60	5.08	1.17	6.68	3.72	0.80
Na_2O	-3.88	-2.67	-3.86	-3.75	-3.13	-2.84	-1.23
K_2O	1.64	-0.28	0.02	0.14	-0.20	0.33	-0.17
Cr_2O_3	0.00	0.01	0.00	0.00	0.00	0.00	0.00
TiO_2	-0.02	1.12	0.01	-0.04	0.00	0.02	0.14
MnO	-0.13	-0.03	-0.04	-0.07	0.07	0.02	-0.01
P_2O_5	0.00	0.14	0.01	-0.01	0.07	0.00	0.04
SrO	0.00	0.01	0.00	0.00	0.00	0.00	-0.01
BaO	0.04	0.00	0.00	0.03	0.00	0.00	0.01
LOI	2.62	-0.04	1.92	1.23	1.56	0.49	0.04
Total	25.38	-31.15	57.06	-29.15	4.67	8.18	-8.44
C	-0.15	-0.14	-0.15	-0.15	-0.16	-0.16	-0.16
S	5.51	0.01	0.71	1.83	0.06	0.08	0.01
Ba	375.62	-16.71	-15.87	233.60	-51.64	3.08	53.73
Ce	-1.41	0.61	-0.58	3.19	-3.78	1.15	-2.93
Cr	4.44	53.72	10.85	-13.07	-9.78	1.05	-10.93
Cs	0.68	0.46	1.03	0.59	1.09	0.53	0.42
Dy	0.08	-5.34	-0.69	3.20	-0.73	-0.81	-2.91
Er	0.07	-3.93	-0.89	1.89	-0.24	-0.47	-1.94
Eu	0.08	0.22	0.72	0.25	0.22	0.40	0.37
Ga	6.53	0.64	1.45	3.39	-0.63	-0.59	0.61
Gd	0.13	-2.73	-0.53	2.10	-0.55	-0.49	-1.39
Ge	0.55	-0.82	1.36	-0.77	0.06	0.13	-0.23
Hf	0.37	-0.95	0.40	1.69	0.38	-0.04	-0.94
Ho	0.04	-1.32	-0.16	0.58	-0.13	-0.16	-0.63
La	-0.71	0.23	-0.20	0.71	-1.82	0.19	-1.34
Lu	-0.08	-0.80	-0.20	0.28	-0.14	-0.12	-0.35
Nb	0.12	1.04	0.29	0.36	0.13	0.16	-0.19
Nd	-0.60	-0.81	-0.80	3.51	-3.01	-0.23	-2.44
Pr	-0.12	0.01	-0.16	0.54	-0.63	0.12	-0.45
Rb	15.48	-0.01	2.16	0.46	-0.02	3.98	1.83
Sm	0.57	-1.03	-0.42	1.96	-0.33	0.31	-0.81
Sn	0.22	0.34	0.54	2.47	0.02	0.05	-0.09
Sr	-40.23	111.29	-47.42	-49.11	-36.92	-24.41	-39.65
Ta	0.19	0.15	0.26	0.16	0.15	0.16	0.40

Sample ID	62704	62705	62706	62707	62708	62709	62710
Hole ID	PH-18-13	PH-18-13	PH-18-13	PH-18-13	PH-18-13	PH-18-13	PH-18-13
Depth (m)	58.16	69.81	88.39	97.66	114.38	145	160.17
Lithology	Lap. Tuff	Dike	Lap. Tuff	Lap. Tuff	Lap. Tuff	Rhyolite	Lap. Tuff
Stratigraphy	MS	MS	MS	MS	FW	FW	MS
Alteration	QSCPy+Sil	Unaltered	QSC+Sil	QSC+/-Py+Sil	QSC+/-Py+Sil	QS+/-Py	QSC+/-Py+Sil
Tb	0.10	-0.56	-0.14	0.46	-0.05	-0.08	-0.35
Th	-0.15	-0.43	0.01	-0.07	0.03	0.04	-0.27
Tm	0.02	-0.64	-0.07	0.31	-0.11	-0.10	-0.30
U	-0.92	-1.13	-0.70	-0.86	-0.89	-0.89	-1.06
V	-6.95	143.47	-6.14	-6.53	-7.44	-7.37	-7.73
W	0.22	-0.33	0.54	-0.31	0.02	0.05	4.44
Y	1.28	-36.33	-6.38	13.08	-4.37	-5.28	-18.98
Yb	0.00	-5.33	-1.50	1.83	-0.93	-1.13	-3.11
Zr	21.19	1.14	8.73	41.71	8.16	-1.60	-15.62
As	-1.72	-0.56	-1.62	-1.38	-2.19	-2.17	-2.16
Bi	1.53	0.03	0.16	0.82	0.01	-0.03	0.47
Hg	0.00	0.00	0.46	0.03	0.00	0.03	0.00
In	0.80	0.00	1.29	0.63	0.04	0.07	0.02
Re	0.00	0.00	0.00	0.00	0.00	0.00	0.00
Sb	0.11	0.02	-0.07	-0.08	-0.05	-0.08	-0.06
Se	0.88	0.10	0.05	0.18	0.00	0.01	-0.01
Te	1.02	0.02	0.19	0.32	0.01	0.01	0.03
Tl	0.06	0.01	0.07	0.05	0.01	0.15	0.06
Ag	2.80	0.15	0.14	1.28	0.01	0.01	-0.02
Cd	3.90	0.42	19.96	2.25	0.01	3.54	0.20
Co	-0.39	31.17	-0.23	-0.65	-0.49	-0.47	-0.09
Cu	835.42	36.88	366.25	772.40	12.36	66.51	15.05
Li	7.22	1.70	25.85	29.66	35.90	26.57	4.07
Mo	1.44	-0.33	3.63	0.39	2.07	3.21	-0.09
Ni	1.67	69.71	-1.23	-1.31	-1.49	-0.95	-1.55
Pb	11.22	-8.65	1.88	0.48	19.70	250.04	8.86
Sc	4.55	1.08	-2.66	-1.14	-4.78	-4.48	1.33
Zn	606.35	24.84	4416.25	547.43	173.41	700.50	82.10

Sample ID	62711	62712	62713	62714	62715	62716
Hole ID	PH-18-13	PH-18-13	PH-18-13	PH-18-13	PH-18-13	PH-18-18
Depth (m)	196.67	244.54	273.52	315.75	340.56	9.78
Lithology	Rhyolite	Sediment	Lap. Tuff	Rhyolite	Rhyolite	Tuff
Stratigraphy	FW	FW	FW	FW	FW	HW
Alteration	QS	S+/-C	QS	QSC+/-Py+Sil (Cd)	QSC+/-Py+Sil (Cd)	QS
SiO_2	-2.07	-10.34	3.70	-13.60	-31.62	19.24
Al_2O_3	0.00	0.00	0.00	0.00	0.00	0.00
Fe_2O_3	0.53	0.69	0.35	0.90	3.04	3.14
CaO	-6.41	-5.87	-5.30	-5.55	-5.75	-6.33
MgO	1.54	1.22	-0.34	2.24	2.71	1.82
Na_2O	-2.09	-0.16	0.19	-3.84	-3.98	-4.28
K_2O	-0.02	0.21	0.05	0.77	0.97	2.02
Cr_2O_3	0.00	0.00	0.00	0.00	0.00	0.00
TiO_2	0.01	0.00	0.00	-0.03	-0.03	-0.01
MnO	-0.09	-0.11	-0.11	-0.06	-0.04	-0.06
P_2O_5	0.00	0.00	0.02	-0.01	0.00	0.00
SrO	0.00	0.00	-0.01	0.00	0.00	0.00
BaO	0.00	0.00	0.01	0.01	0.01	0.04
LOI	1.67	0.22	-0.13	1.47	1.47	1.43
Total	-6.18	-12.32	0.83	-17.29	-32.69	18.25
C	-0.17	-0.16	-0.16	-0.16	-0.14	-0.15
S	0.34	0.47	0.54	0.01	-0.24	1.33
Ba	44.63	23.95	118.37	170.46	117.84	346.64
Ce	-2.94	2.87	4.03	1.84	-1.14	-4.64
Cr	-1.72	-2.88	-0.29	-3.84	-13.47	3.11
Cs	0.71	0.19	0.08	0.77	1.21	1.19
Dy	-1.36	-1.07	1.17	0.89	2.17	1.75
Er	-0.57	-0.77	0.79	0.81	1.76	0.94
Eu	0.21	0.17	0.15	0.03	0.11	-0.10
Ga	-1.11	-2.45	-0.78	0.84	0.22	2.70
Gd	-0.77	-0.45	-0.05	1.38	1.74	0.35
Ge	-0.22	-0.36	-0.04	-0.48	-0.87	0.39
Hf	0.26	-0.05	0.44	0.42	0.62	1.09
Ho	-0.20	-0.29	0.16	0.30	0.50	0.34
La	-1.21	1.16	1.10	0.46	-1.23	-1.90
Lu	-0.13	-0.23	0.07	0.02	0.23	0.16
Nb	0.27	0.01	2.84	0.11	0.01	0.17
Nd	-3.56	1.16	1.80	1.33	0.22	-3.40
Pr	-0.52	0.32	0.49	0.29	-0.08	-0.78
Rb	1.05	2.38	2.41	12.14	15.10	18.37
Sm	-0.63	0.89	1.04	1.23	0.66	-0.49
Sn	-0.09	-0.14	-0.01	0.62	0.31	3.62
Sr	-4.89	-23.51	-49.32	-19.64	-3.30	-61.75
Ta	0.22	0.12	0.15	0.11	0.15	0.18

Sample ID	62711	62712	62713	62714	62715	62716
Hole ID	PH-18-13	PH-18-13	PH-18-13	PH-18-13	PH-18-13	PH-18-18
Depth (m)	196.67	244.54	273.52	315.75	340.56	9.78
Lithology	Rhyolite	Sediment	Lap. Tuff	Rhyolite	Rhyolite	Tuff
Stratigraphy	FW	FW	FW	FW	FW	HW
Alteration	QS	S+/-C	QS	QSC+/-Py+Sil (Cd)	QSC+/-Py+Sil (Cd)	QS
Tb	-0.09	0.01	0.06	0.32	0.38	0.20
Th	-0.31	0.03	0.75	0.35	0.20	-0.03
Tm	-0.07	-0.12	0.09	0.10	0.23	0.17
U	-0.95	-0.86	-0.26	-0.61	-0.29	-0.62
V	-5.43	-7.86	-4.09	-7.98	21.99	-7.11
W	-0.09	-0.14	-0.01	-0.19	-0.35	0.16
Y	-6.10	-7.18	6.08	6.33	12.65	9.73
Yb	-1.09	-1.48	0.20	0.73	1.53	1.04
Zr	5.04	1.61	9.53	13.44	11.85	25.55
As	-1.69	-0.47	0.45	-1.73	-2.50	-0.85
Bi	-0.03	0.12	0.06	-0.03	-0.06	2.07
Hg	0.00	0.00	0.00	0.03	0.00	0.01
In	0.00	0.02	0.10	1.45	0.09	0.14
Re	0.00	0.00	0.00	0.00	0.02	0.00
Sb	-0.03	0.08	0.04	-0.03	-0.09	0.01
Se	-0.01	-0.01	0.00	-0.02	-0.03	0.13
Te	0.01	0.03	0.10	0.22	0.04	1.68
Tl	-0.02	0.19	0.07	0.10	0.21	0.11
Ag	-0.02	0.69	0.24	0.40	-0.09	0.33
Cd	-0.02	-0.04	0.64	5.08	-0.09	0.91
Co	-0.09	-0.57	-0.51	-0.60	0.96	-0.42
Cu	35.30	-0.58	-1.04	20.24	-2.69	95.37
Li	13.28	12.12	4.85	27.33	27.64	6.55
Mo	1.74	2.42	2.94	0.62	4.88	1.31
Ni	-1.09	-1.57	-1.51	-1.19	-1.67	-1.42
Pb	37.35	92.45	18.55	25.18	-5.47	-0.45
Sc	-6.78	-4.73	-6.13	9.24	3.93	4.64
Zn	88.75	50.29	134.92	767.48	41.91	347.60

Sample ID	62717	62718	62719	62720	62721	62722	62723
Hole ID	PH-18-18	PH-18-18	PH-18-18	PH-18-18	PH-18-18	PH-18-18	PH-18-18
Depth (m)	23.83	33.63	56.11	93.63	214.8	229.32	239
Lithology	Lap. Tuff	Lap. Tuff	Rhyolite	Rhyolite	Lap. Tuff	Lap. Tuff	Tuff
Stratigraphy	MS	FW	MS	MS	FW	MS	FW
Alteration	QSC	QSC+/-Py+Sil	QS+/-C+/-Py	QS+/-Py	QS+Sil (Cd)	QSCPy+Sil	QSC+/-Py
SiO_2	-34.52	25.22	24.44	26.54	-1.29	17.93	-7.44
Al_2O_3	0.00	0.00	0.00	0.00	0.00	0.00	0.00
Fe_2O_3	3.70	5.48	5.32	4.28	3.61	9.14	0.42
CaO	-5.58	-6.50	-6.34	-6.57	-6.58	-6.57	-5.71
MgO	4.17	-0.21	1.66	2.36	0.51	0.90	0.16
Na_2O	-4.04	-4.14	-3.09	-4.04	-4.15	-4.13	-3.01
K_2O	0.34	1.25	0.83	1.20	1.46	1.06	3.09
Cr_2O_3	0.00	0.00	0.00	0.01	0.00	0.00	0.00
TiO_2	-0.01	0.06	0.08	0.02	0.01	0.03	0.07
MnO	-0.08	-0.13	0.03	0.03	-0.13	-0.11	-0.09
P_2O_5	0.01	0.01	0.03	0.02	0.00	0.00	0.01
SrO	-0.01	0.00	0.00	0.00	-0.01	0.00	-0.01
BaO	0.01	0.04	0.02	0.02	0.06	0.01	0.03
LOI	0.81	1.23	1.75	1.57	1.67	3.63	-0.04
Total	-35.03	23.18	24.32	24.52	-5.04	19.55	-12.42
C	-0.14	-0.13	-0.13	-0.15	-0.15	-0.13	-0.15
S	0.67	2.85	2.25	0.57	2.30	5.86	-0.18
Ba	113.99	394.51	141.75	204.57	527.30	189.69	320.08
Ce	3.21	-4.80	-6.62	0.12	-8.20	-0.88	2.63
Cr	-13.60	4.21	4.59	17.15	-1.31	15.47	-2.50
Cs	1.44	0.33	0.30	2.05	0.77	0.76	1.00
Dy	-0.10	-0.88	-3.54	-1.72	-1.33	-0.81	0.48
Er	0.42	-0.27	-2.11	-1.16	-0.53	-0.39	0.43
Eu	1.03	0.56	0.12	0.07	-0.22	-0.07	-0.05
Ga	9.55	10.22	1.73	-0.15	7.38	2.94	-0.21
Gd	0.29	-1.20	-2.87	-0.69	-1.46	-0.37	0.24
Ge	-0.90	0.53	0.57	0.60	-0.16	0.46	-0.31
Hf	1.05	0.45	-0.23	0.17	0.16	-0.11	2.13
Ho	0.04	-0.30	-0.76	-0.41	-0.23	-0.22	0.03
La	0.93	-1.60	-2.53	-0.15	-3.17	-0.52	0.88
Lu	-0.02	-0.04	-0.38	-0.24	-0.25	-0.11	-0.03
Nb	0.31	0.23	0.13	0.14	0.12	0.08	0.83
Nd	2.35	-3.61	-5.94	-0.58	-6.65	-1.08	1.61
Pr	0.48	-0.72	-1.16	-0.09	-1.35	-0.22	0.21
Rb	5.19	8.41	5.15	23.54	12.84	6.71	23.69
Sm	0.76	-0.88	-1.72	0.37	-1.82	0.23	0.55
Sn	0.28	0.21	0.23	1.48	7.41	4.91	-0.12
Sr	-67.84	-50.87	-46.47	-43.58	-64.03	-38.88	-52.61
Ta	0.14	0.19	0.20	0.20	0.14	0.19	0.21

Sample ID	62717	62718	62719	62720	62721	62722	62723
Hole ID	PH-18-18	PH-18-18	PH-18-18	PH-18-18	PH-18-18	PH-18-18	PH-18-18
Depth (m)	23.83	33.63	56.11	93.63	214.8	229.32	239
Lithology	Lap. Tuff	Lap. Tuff	Rhyolite	Rhyolite	Lap. Tuff	Lap. Tuff	Tuff
Stratigraphy	MS	FW	MS	MS	FW	MS	FW
Alteration	QSC	QSC+/-Py+Sil	QS+/-C+/-Py	QS+/-Py	QS+Sil (Cd)	QSCPy+Sil	QSC+/-Py
Tb	0.08	-0.14	-0.42	-0.17	-0.16	-0.10	0.10
Th	0.78	0.04	-0.32	0.05	-0.26	-0.11	0.47
Tm	0.06	-0.14	-0.32	-0.14	-0.06	-0.14	0.11
U	-0.50	-0.15	-0.78	-0.87	-0.97	-0.92	-0.78
V	-3.60	2.11	15.82	-3.81	-5.33	-7.04	-3.87
W	-0.36	1.42	0.23	0.24	-0.07	0.18	1.63
Y	-1.97	-3.24	-19.88	-10.70	-5.70	-6.12	4.13
Yb	0.01	-1.00	-2.39	-1.36	-1.12	-1.10	-0.04
Zr	18.75	16.54	-2.70	4.11	1.60	-0.14	64.88
As	-2.06	1.05	-1.47	-1.71	-1.02	2.38	-2.26
Bi	0.58	4.17	1.45	0.35	0.26	0.32	0.04
Hg	0.01	0.01	0.08	0.00	0.00	0.00	0.00
In	0.44	0.13	16.75	0.22	0.01	0.00	-0.01
Re	0.00	0.00	0.00	0.00	0.00	0.00	0.00
Sb	-0.05	0.02	0.03	-0.02	-0.04	-0.02	-0.05
Se	0.03	0.38	0.51	0.15	1.40	0.73	-0.01
Te	1.14	4.49	0.32	0.32	0.12	0.17	0.01
Tl	0.68	0.32	0.00	0.01	-0.01	-0.02	0.00
Ag	0.07	0.05	2.21	0.06	-0.02	0.05	-0.03
Cd	-0.09	0.05	86.55	0.37	-0.02	0.05	-0.03
Co	-0.68	0.21	1.46	-0.38	4.61	1.36	-0.56
Cu	281.95	230.87	2159.95	74.01	7.22	3.09	-1.37
Li	20.59	-4.39	7.30	19.76	4.35	6.82	3.75
Mo	1.56	9.90	17.44	2.71	2.74	4.91	3.38
Ni	-1.68	-0.79	-0.77	-0.76	-1.07	1.55	-1.12
Pb	4.63	58.22	10.13	-4.57	-9.20	-9.64	-3.25
Sc	-4.12	-4.10	-7.62	-2.62	-4.72	-4.36	-5.37
Zn	239.18	-36.68	#VALUE!	96.64	-46.83	-49.35	-31.87

Sample ID	62727	62728	62734	62735	62736	62737	62738
Hole ID	PH-18-11	PH-18-11	PH-18-15	PH-18-15	PH-18-15	PH-18-25	PH-18-25
Depth (m)	119	136.54	166.73	223.33	251	9.8	46
Lithology	Rhyolite	Lap. Tuff	Tuff	Rhyolite	Tuff	Xtl-Tuff	Xtl-Tuff
Stratigraphy	FW	MS	FW	FW	FW	HW	HW
Alteration	QS+/-C	QSC+/-Py+Sil	QSC+/-Py+Sil	QS+Sil	QS	QS+/-Py+/-Sil	QSC+Sil
SiO_2	-12.38	12.33	4.98	1.50	6.46	6.42	1.60
Al_2O_3	0.00	0.00	0.00	0.00	0.00	0.00	0.00
Fe_2O_3	0.60	0.76	3.73	3.49	1.59	1.13	0.11
CaO	-5.51	-6.18	-6.39	-6.56	-6.43	-3.61	8.02
MgO	0.47	0.30	1.47	2.03	1.95	-0.33	0.15
Na_2O	-0.54	-2.72	-4.00	-3.97	-2.23	-1.73	-4.08
K_2O	0.19	0.58	1.61	0.99	0.31	2.78	5.07
Cr_2O_3	0.00	0.00	0.00	0.00	0.00	0.00	0.00
TiO_2	-0.01	0.04	0.00	0.03	0.00	-0.01	-0.01
MnO	-0.12	-0.11	0.02	-0.01	-0.06	-0.12	0.09
P_2O_5	0.00	0.01	0.02	0.00	-0.01	0.01	0.00
SrO	0.00	0.00	0.00	0.00	0.00	0.00	0.00
BaO	0.00	0.01	0.04	0.02	0.01	0.02	0.00
LOI	-0.13	0.17	1.33	2.15	0.49	0.52	-0.11
Total	-17.25	4.52	4.25	-1.03	2.28	5.87	12.43
C	-0.15	-0.14	-0.11	-0.15	-0.15	0.05	0.06
S	0.24	0.33	0.03	1.02	-0.17	0.13	-0.23
Ba	33.04	133.54	387.86	175.84	84.65	219.95	79.76
Ce	3.53	0.28	-3.75	1.11	-4.15	4.30	2.98
Cr	-3.46	11.50	0.29	9.25	0.32	-9.54	-8.9
Cs	0.33	0.48	0.64	2.09	0.61	0.62	0.04
Dy	-0.25	-0.72	-2.83	-1.36	-2.68	0.82	1.24
Er	-0.31	-0.38	-1.69	-0.27	-1.49	0.96	2.11
Eu	0.08	0.62	-0.29	0.17	-0.01	0.08	-0.13
Ga	-0.50	-0.72	1.20	0.65	-1.02	0.69	-1.8
Gd	0.83	-0.29	-1.93	-0.29	-2.17	0.68	1.10
Ge	-0.43	0.13	0.04	-0.06	0.04	0.11	0.27
Hf	0.67	1.01	-0.56	0.11	0.26	0.57	0.81
Ho	-0.08	-0.26	-0.60	-0.26	-0.60	0.15	0.45
La	0.93	0.39	-1.24	0.74	-1.33	1.82	1.39
Lu	-0.05	-0.04	-0.34	-0.22	-0.28	0.10	0.32
Nb	0.22	0.37	-0.39	0.27	0.12	0.26	0.34
Nd	2.79	-0.99	-3.38	0.98	-3.78	3.14	2.49
Pr	0.47	-0.07	-0.70	0.19	-0.72	0.53	0.45
Rb	5.40	5.33	15.17	13.56	4.83	31.74	25.26
Sm	1.20	-0.10	-1.22	-0.15	-1.76	0.70	0.76
Sn	-0.17	0.05	2.04	0.95	1.03	0.05	0.11
Sr	-27.11	-23.96	-71.73	-40.93	-49.95	21.49	3.79
Ta	0.20	0.27	0.05	0.05	0.05	0.05	0.17

Sample ID	62727	62728	62734	62735	62736	62737	62738
Hole ID	PH-18-11	PH-18-11	PH-18-15	PH-18-15	PH-18-15	PH-18-25	PH-18-25
Depth (m)	119	136.54	166.73	223.33	251	9.8	46
Lithology	Rhyolite	Lap. Tuff	Tuff	Rhyolite	Tuff	Xtl-Tuff	Xtl-Tuff
Stratigraphy	FW	MS	FW	FW	FW	HW	HW
Alteration	QS+/-C	QSC+/-Py+Sil	QSC+/-Py+Sil	QS+Sil	QS	QS+/-Py+/-Sil	QSC+Sil
Tb	0.09	-0.13	-0.43	-0.12	-0.33	0.15	0.25
Th	0.66	0.12	0.07	0.02	-0.28	0.43	0.63
Tm	-0.01	-0.02	-0.27	-0.13	-0.25	0.08	0.20
U	-0.41	-0.81	-0.99	-1.01	-0.96	3.34	-0.11
V	-7.93	-1.60	-2.90	-3.17	-3.91	-0.59	2.20
W	-0.17	0.05	0.01	-0.02	0.02	0.05	0.11
Y	-4.80	-4.97	-19.07	-10.37	-19.43	2.02	9.12
Yb	-0.34	-0.79	-2.33	-1.46	-1.90	0.49	1.19
Zr	10.88	18.16	-10.86	4.58	2.44	9.32	19.84
As	-1.63	0.03	2.17	-0.75	-2.40	-1.34	-1.37
Bi	-0.01	-0.01	0.42	0.35	-0.01	0.46	-0.04
Hg	0.00	0.23	0.01	0.00	0.00	0.00	0.00
In	0.01	0.26	0.47	0.00	0.02	-0.01	-0.03
Re	0.00	0.00	0.00	0.00	0.00	0.00	0.00
Sb	-0.01	0.71	-0.06	-0.06	-0.08	0.10	-0.04
Se	-0.02	0.01	0.00	0.39	0.00	0.00	0.01
Te	0.02	0.02	0.13	0.25	0.03	0.05	0.01
Tl	0.08	0.28	-0.02	-0.02	-0.01	-0.02	-0.03
Ag	-0.04	1.01	0.36	-0.01	0.00	0.01	0.03
Cd	-0.04	8.68	1.78	-0.01	0.00	0.01	0.03
Co	-0.17	0.05	-0.49	3.88	-0.49	0.05	-0.45
Cu	4.27	82.11	246.63	11.60	2.09	9.59	-0.67
Li	11.54	16.00	15.29	14.50	15.32	-4.48	-4.45
Mo	1.48	4.25	0.01	1.93	1.03	3.18	0.11
Ni	-1.17	1.15	-0.99	-1.02	-1.49	-0.95	-1.45
Pb	19.42	337.68	3.22	0.68	-9.97	2.64	3.53
Sc	-5.08	-7.65	-7.90	-8.17	-4.84	-4.54	-3.90
Zn	2.24	2541.75	644.38	70.33	-12.05	-27.00	-49.7

Sample ID	62739	62740	62741	62742	62743	62763	62762
Hole ID	PH-18-25	PH-18-25	PH-19-12	PH-19-12	PH-19-12	PH-18-08	PH-18-08
Depth (m)	122	148.75	22.55	49	103.39	219.87	109
Lithology	Lap. Tuff	Sediment	Lap. Tuff	Lap. Tuff	Rhyolite	Xtl-Tuff	Xtl-Tuff
Stratigraphy	MS	FW	MS	MS	FW	HW	HW
Alteration	QSC+/-Py+Sil	QS	QSC+/-Py+Sil	QSC+/-Py	QSC+Sil	QS+Sil	QS
SiO_2	20.01	-5.11	18.00	6.53	-8.61	10.55	5.07
Al_2O_3	0.00	0.00	0.00	0.00	0.00	0.00	0.00
Fe_2O_3	0.49	2.38	4.22	2.46	1.37	5.76	-0.18
CaO	-6.32	-5.03	-6.30	-6.40	-5.91	-6.37	-6.25
MgO	-0.13	0.47	0.97	6.68	0.80	1.87	-0.63
Na_2O	-2.99	-1.05	-3.85	-3.77	-1.19	-4.15	0.99
K_2O	0.82	0.63	1.54	0.44	0.08	0.76	0.28
Cr_2O_3	0.00	0.00	0.00	0.00	0.00	0.00	0.00
TiO_2	-0.01	0.11	0.07	0.03	0.10	-0.01	-0.01
MnO	-0.13	0.18	-0.03	0.13	-0.08	-0.05	-0.14
P_2O_5	0.00	0.03	0.03	0.00	0.02	0.00	0.01
SrO	0.00	-0.01	0.00	0.00	-0.01	0.00	-0.01
BaO	0.02	0.00	0.01	0.00	0.00	0.02	-0.01
LOI	-0.46	-0.53	1.54	1.23	-0.09	1.75	-0.79
Total	14.76	-6.01	13.23	6.70	-12.35	10.22	0.45
C	-0.15	-0.14	-0.12	-0.14	-0.15	-0.14	-0.15
S	-0.1	-0.26	1.45	0.40	0.20	1.65	-0.13
Ba	256.86	-2.44	197.75	25.22	7.18	188.38	-31.87
Ce	0.19	-1.50	-0.59	0.75	-2.83	2.26	2.95
Cr	13.52	-10.74	14.39	1.22	-2.69	1.67	-0.18
Cs	0.45	0.17	1.10	1.61	0.24	1.63	0.06
Dy	1.16	-2.41	-0.1	-0.79	-3.1	0.26	0.19
Er	1.03	-1.52	0.14	-0.58	-1.3	0.93	1.21
Eu	0.20	0.41	0.21	0.24	0.01	-0.09	-0.06
Ga	-0.05	-0.12	0.74	1.00	-0.44	3.57	-4.18
Gd	0.80	-1.41	-0.10	0.10	-1.65	0.54	0.90
Ge	0.29	-0.19	0.37	0.15	-0.34	0.21	-0.02
Hf	0.50	-0.99	0.37	-0.12	-0.70	1.25	1.26
Ho	0.15	-0.63	-0.05	-0.23	-0.59	0.01	0.25
La	0.32	-0.88	0.13	0.13	-1.10	0.58	0.64
Lu	0.00	-0.46	0.00	-0.19	-0.41	0.01	0.08
Nb	0.24	-0.08	0.05	0.07	-0.15	0.42	0.39
Nd	0.36	-1.60	-0.25	0.92	-1.73	2.92	2.27
Pr	-0.05	-0.21	-0.08	0.12	-0.47	0.26	0.40
Rb	8.93	5.74	12.81	6.17	1.58	15.05	2.35
Sm	0.02	-0.40	-0.11	0.17	-0.73	1.04	0.86
Sn	0.12	-0.07	0.15	0.06	-0.57	1.17	-0.01
Sr	-31.3	-70.52	-51.88	-61.11	-53.95	-38.28	-64.36
Ta	0.06	0.04	0.06	0.16	0.04	0.06	0.05

Sample ID	62739	62740	62741	62742	62743	62763	62762
Hole ID	PH-18-25	PH-18-25	PH-19-12	PH-19-12	PH-19-12	PH-18-08	PH-18-08
Depth (m)	122	148.75	22.55	49	103.39	219.87	109
Lithology	Lap. Tuff	Sediment	Lap. Tuff	Lap. Tuff	Rhyolite	Xtl-Tuff	Xtl-Tuff
Stratigraphy	MS	FW	MS	MS	FW	HW	HW
Alteration	QSC+/-Py+Sil	QS	QSC+/-Py+Sil	QSC+/-Py	QSC+Sil	QS+Sil	QS
Tb	0.14	-0.22	0.06	-0.04	-0.37	0.12	0.11
Th	0.52	-0.30	0.40	0.14	-0.20	0.15	0.45
Tm	0.19	-0.29	0.01	-0.09	-0.29	0.05	0.20
U	-0.68	-1.06	-0.80	-0.92	-0.92	-0.81	-0.04
V	-7.21	-7.69	6.05	-2.57	9.91	-4.58	-7.52
W	0.12	-0.07	0.15	1.12	0.73	0.08	-0.01
Y	2.88	-20.72	-1.45	-9.33	-20.76	-3.77	1.88
Yb	0.64	-2.54	-0.51	-1.29	-2.61	0.01	0.77
Zr	3.87	-15.01	5.15	-5.14	-20.75	24.87	25.95
As	-0.91	-2.51	-1.21	-2.38	-2.18	-1.29	-1.61
Bi	0.01	-0.06	0.76	0.21	0.15	1.19	0.00
Hg	0.03	0.00	0.00	0.00	0.00	0.00	0.00
In	0.01	0.05	0.09	0.22	0.02	0.10	-0.01
Re	0.00	0.00	0.01	0.00	0.00	0.00	0.00
Sb	0.11	-0.09	-0.04	-0.08	-0.09	-0.02	-0.04
Se	0.01	-0.01	0.13	0.01	-0.01	0.55	0.00
Te	0.00	-0.01	0.44	0.04	0.03	0.84	0.01
Tl	0.30	0.08	0.03	0.06	-0.03	0.04	-0.03
Ag	0.03	-0.02	0.04	0.02	-0.03	0.02	0.00
Cd	2.66	-0.02	0.04	0.02	-0.03	0.02	0.00
Co	-0.44	-0.54	0.15	0.06	0.73	2.25	-0.5
Cu	36.23	-3.07	87.71	21.46	68.71	103.29	4.92
Li	6.17	4.26	6.46	16.22	12.31	16.67	-4.50
Mo	6.82	-0.07	3.59	18.09	-0.13	1.17	2.96
Ni	0.23	-1.54	-0.85	-0.94	-0.27	1.25	-0.02
Pb	359.00	-11.07	1.76	-0.33	-7.67	-10.92	8.81
Sc	-3.83	1.66	-5.83	-4.39	-3.75	4.51	-5.09
Zn	461.16	14.02	18.71	540.14	-29.72	15.87	-51.2

Sample ID	62767	62771	62772	62773	62744	62745	62746	62747
Hole ID	PH-19-09	PH-19-10	PH-19-10	PH-19-10	PH-19-12	PH-18-04	PH-18-04	PH-18-04
Depth (m)	289	117.86	127.92	147.54	135.81	17.6	106	159.43
Lithology	Tuff	Xtl-Tuff	Xtl-Tuff	Rhyolite	Tuff	Tuff	Tuff	Rhyolite
Stratigraphy	FW	FW	FW	FW	FW	HW	HW	HW
Alteration	QS+/-C+/-Py	QSC	QSC	QS+/-C	QSC	QS	QSC+Sil	QS+Sil
SiO_2	0.06	-4.46	-3.53	-7.78	0.02	-17.31	-1.96	8.36
Al_2O_3	0.00	0.00	0.00	0.00	0.00	0.00	0.00	0.00
Fe_2O_3	2.88	2.28	1.64	1.34	1.11	0.44	1.87	0.48
CaO	-6.55	-5.41	-5.37	-5.8	-6.24	-5.88	-5.76	-5.62
MgO	2.70	1.63	0.58	0.62	1.33	0.88	0.20	0.02
Na_2O	-4.56	-1.69	-1.41	-1.29	-2.84	-3.62	-2.30	-1.82
K_2O	2.02	0.27	0.92	0.46	0.12	3.38	4.17	2.14
Cr_2O_3	0.00	0.00	0.00	0.00	0.00	0.00	0.00	0.00
TiO_2	0.01	0.10	0.07	0.13	0.05	-0.03	0.19	-0.03
MnO	-0.05	-0.08	-0.11	-0.10	-0.11	-0.13	-0.10	-0.13
P_2O_5	0.01	0.04	0.03	0.01	0.00	0.03	0.06	0.04
SrO	-0.01	-0.01	-0.01	-0.01	0.04	0.03	0.04	0.04
BaO	0.01	0.00	0.00	0.01	0.01	0.01	0.01	0.00
LOI	1.68	0.35	-0.36	0.24	1.09	0.23	-0.07	-0.11
Total	-2.65	-5.68	-6.11	-11.66	-5.3	-20.58	-1.02	3.38
C	-0.14	-0.13	-0.13	-0.11	-0.15	-0.15	-0.13	-0.15
S	0.62	0.66	-0.26	-0.08	-0.05	-0.21	0.38	0.06
Ba	117.30	-6.81	47.86	88.78	108.48	75.63	48.14	15.38
Ce	6.46	-2.69	0.57	-4.8	-9.80	-0.56	-3.98	1.61
Cr	-0.7	-10.73	7.84	-2.48	8.03	-4.46	-10.36	0.67
Cs	1.35	0.36	0.33	0.32	0.42	1.51	0.51	0.18
Dy	-0.45	-2.61	-0.92	-2.70	-4.61	0.55	-3.66	-1.14
Er	-0.18	-1.48	-0.54	-1.17	-2.62	1.05	-2.56	-0.9
Eu	0.17	-0.06	0.25	-0.16	-0.30	0.17	-0.08	0.18
Ga	1.96	-1.32	0.65	-1.16	-1.22	0.16	0.59	-1.74
Gd	0.55	-1.59	-0.20	-2.57	-3.40	0.14	-2.51	-0.88
Ge	-0.09	-0.18	-0.18	-0.31	-0.16	-0.56	-0.09	0.08
Hf	-0.31	-0.71	-0.14	-0.23	-0.22	0.97	-0.89	0.73
Ho	-0.11	-0.60	-0.32	-0.59	-1.02	0.37	-0.83	-0.23
La	2.70	-1.24	-0.22	-1.92	-3.92	-0.08	-1.75	0.40
Lu	-0.18	-0.38	-0.26	-0.29	-0.44	0.19	-0.55	-0.24
Nb	-0.04	-0.17	-0.17	-0.05	0.11	0.30	0.06	0.24
Nd	5.19	-2.05	0.74	-3.98	-7.86	-0.88	-3.51	0.60
Pr	0.95	-0.43	0.09	-0.88	-1.56	-0.12	-0.55	0.18
Rb	28.82	3.07	7.72	5.06	2.09	27.07	28.39	11.19
Sm	1.27	-0.47	0.27	-1.71	-2.52	-0.15	-1.24	0.33
Sn	0.93	-0.07	-0.07	0.75	-0.07	-0.22	-0.04	0.03
Sr	-73.62	-38.7	-55.96	-41.45	-46.47	-61.14	-70.68	-63.05
Ta	0.05	0.04	0.04	0.04	0.04	0.11	0.05	0.16

Sample ID	62767	62771	62772	62773	62744	62745	62746	62747
Hole ID	PH-19-09	PH-19-10	PH-19-10	PH-19-10	PH-19-12	PH-18-04	PH-18-04	PH-18-04
Depth (m)	289	117.86	127.92	147.54	135.81	17.6	106	159.43
Lithology	Tuff	Xtl-Tuff	Xtl-Tuff	Rhyolite	Tuff	Tuff	Tuff	Rhyolite
Stratigraphy	FW	FW	FW	FW	FW	HW	HW	HW
Alteration	QS+/-C+/-Py	QSC	QSC	QS+/-C	QSC	QS	QSC+Sil	QS+Sil
Tb	-0.02	-0.30	-0.16	-0.35	-0.63	0.17	-0.46	-0.07
Th	0.34	-0.21	-0.04	-0.31	-0.46	-0.03	-0.24	-0.25
Tm	-0.05	-0.25	-0.13	-0.27	-0.43	0.24	-0.39	-0.13
U	-0.92	-1.00	-0.99	-1.06	-0.98	-0.71	-0.66	-0.83
V	-7.59	15.95	2.99	13.65	9.62	8.65	-2.29	-7.42
W	-0.04	0.85	-0.07	-0.12	-0.53	-0.22	-0.04	0.03
Y	-8.13	-19.01	-12.65	-18.94	-28.05	8.68	-26.99	-9.59
Yb	-0.95	-2.4	-1.77	-2.31	-3.32	1.17	-3.60	-1.60
Zr	-7.01	-20.49	-1.82	-11.18	-5.90	24.24	-18.69	13.37
As	1.93	-1.68	-2.42	-2.52	-2.23	-1.92	0.58	-2.08
Bi	0.29	0.20	-0.01	-0.01	0.12	-0.03	0.01	-0.03
Hg	0.00	0.00	0.00	0.00	0.25	0.00	0.00	0.00
In	0.93	0.06	0.06	0.00	0.13	0.02	0.04	0.00
Re	0.00	0.00	0.00	0.00	0.02	0.00	0.00	0.00
Sb	0.06	-0.09	-0.09	-0.09	-0.09	-0.06	-0.05	-0.06
Se	0.00	0.46	-0.01	-0.01	0.09	-0.02	0.00	0.00
Te	0.10	0.11	-0.01	0.03	0.06	0.01	0.04	0.00
Tl	-0.01	0.00	0.00	-0.03	-0.03	0.05	0.04	-0.01
Ag	-0.01	-0.02	-0.02	-0.03	-0.02	-0.06	-0.01	0.01
Cd	-0.01	-0.02	-0.02	-0.03	7.41	-0.06	-0.01	0.01
Co	-0.52	2.71	0.86	-0.12	0.87	-0.22	-0.04	-0.48
Cu	254.62	6.19	-3.07	12.64	102.52	8.43	5.64	0.13
Li	14.3	4.27	4.28	3.76	4.34	2.77	4.64	5.34
Mo	5.75	2.71	-0.07	-0.12	5.54	2.89	0.93	1.07
Ni	-1.04	-1.07	-0.14	-1.12	-1.07	-1.61	-1.04	-0.97
Pb	-11.04	-10.15	-11.07	-10.25	-5.46	18.31	-8.15	-8.90
Sc	-0.53	-2.95	-1.08	-3.62	-3.79	3.65	3.31	-4.66
Zn	143.16	-30.37	-27.52	-10.82	1679.05	68.44	27.22	-9.94

Sample ID	62748	62749	62750	62751	62752	62753	62755	62757
Hole ID	PH-18-04	PH-18-04	PH-18-04	PH-18-04	PH-18-04	PH-19-11	PH-19-11	PH-19-11
Depth (m)	169.64	70	231.85	290.28	319.33	4.2	40	72.83
Lithology	Tuff	Rhyolite	Tuff	Basalt	Basalt	Lap. Tuff	Xtl-Tuff	Dike
Stratigraphy	HW	HW	HW	HW	HW	MS	MS	MS
Alteration	QSC+Sil	QS+Sil	QSC+Sil	QSC	QSC	QSC+Sil	QSCPy+/-Sil	Unaltered
SiO_2	-5.49	9.93	-18.36	-43.45	-38.48	-5.12	17.54	-30.3
Al_2O_3	0.00	0.00	0.00	0.00	0.00	0.00	0.00	0.00
Fe_2O_3	4.1	0.08	1.19	0.93	2.87	1.21	5.45	8.16
CaO	-4.87	-6.34	-5.92	3.30	-4.17	-6.47	-6.41	-0.89
MgO	1.22	-0.67	0.83	-0.11	-0.10	1.84	2.81	2.37
Na_2O	-2.28	-4.14	-3.95	-1.69	-0.45	-4.11	-4.01	-1.56
K_2O	2.56	2.35	2.14	1.35	-0.19	1.62	1.53	0.38
Cr_2O_3	0.00	0.00	0.00	0.00	0.00	0.00	0.00	0.00
TiO_2	-0.03	-0.01	-0.03	0.36	0.57	0.00	0.01	1.96
MnO	-0.06	-0.14	-0.14	-0.03	-0.10	-0.09	-0.08	0.02
P_2O_5	0.04	0.04	0.00	0.05	0.22	0.03	0.03	1.03
SrO	0.00	0.04	0.00	0.01	0.00	0.00	0.00	0.03
BaO	0.01	0.03	0.00	0.00	0.02	0.02	0.03	0.03
LOI	-0.22	-0.29	0.66	3.68	-0.48	1.24	2.48	-0.57
Total	-5.21	0.05	-22.00	-39.15	-38.64	-8.75	18.07	-16.8
C	-0.13	-0.14	-0.14	1.30	-0.15	-0.13	-0.15	-0.16
S	-0.16	-0.01	0.32	0.15	0.13	0.36	2.36	-0.18
Ba	46.6	246.59	29.10	-19.85	-60.16	194.74	221.78	384.52
Ce	0.75	-5.41	-2.18	-10.30	-8.40	2.09	-5.35	51.15
Cr	-10.49	10.32	2.73	-13.93	-13.98	-2.22	3.38	-3.75
Cs	0.95	0.31	0.69	0.12	0.05	1.24	1.11	1.13
Dy	0.37	-2.4	-0.03	-6.08	-5.98	-2.14	-3.66	0.45
Er	1.13	-1.02	0.54	-4.08	-3.80	-0.75	-2.11	-0.95
Eu	-0.05	-0.26	0.15	-0.42	-0.31	0.20	0.01	2.58
Ga	2.04	-7.14	0.21	-3.43	-2.73	-1.43	2.06	10.98
Gd	-0.49	-1.98	-0.37	-4.45	-4.1	-1.12	-3.12	3.75
Ge	-0.12	0.03	-0.61	-0.98	-1.00	-0.28	0.42	-0.47
Hf	0.22	0.95	1.25	-2.57	-2.46	0.08	-0.38	2.39
Ho	0.25	-0.44	0.12	-1.32	-1.27	-0.42	-0.73	-0.04
La	0.11	-2.37	-0.83	-4.02	-3.25	0.71	-2.21	21.29
Lu	0.13	-0.17	0.00	-0.73	-0.71	-0.25	-0.34	-0.40
Nb	0.04	0.01	0.26	-0.80	-0.62	-0.12	-0.28	8.97
Nd	0.39	-4.42	-2.13	-8.26	-7.21	0.75	-4.59	30.23
Pr	0.12	-0.82	-0.44	-1.61	-1.40	0.21	-0.84	6.68
Rb	22.65	8.63	15.16	8.81	-1.47	13.99	14.07	22.86
Sm	0.13	-1.55	-0.47	-2.82	-2.61	0.02	-1.77	5.47
Sn	-0.05	0.01	-0.24	-0.70	-0.70	-0.11	0.17	1.44
Sr	-58.55	-89.14	-57.45	46.09	-21.76	-47.79	-62.42	332.51
Ta	0.05	0.15	0.18	0.01	0.01	0.13	0.07	0.76

Sample ID	62748	62749	62750	62751	62752	62753	62755	62757
Hole ID	PH-18-04	PH-18-04	PH-18-04	PH-18-04	PH-18-04	PH-19-11	PH-19-11	PH-19-11
Depth (m)	169.64	70	231.85	290.28	319.33	4.2	40	72.83
Lithology	Tuff	Rhyolite	Tuff	Basalt	Basalt	Lap. Tuff	Xtl-Tuff	Dike
Stratigraphy	HW	HW	HW	HW	HW	MS	MS	MS
Alteration	QSC+Sil	QS+Sil	QSC+Sil	QSC	QSC	QSC+Sil	QSCPy+/-Sil	Unaltered
Tb	0.11	-0.39	0.1	-0.76	-0.75	-0.14	-0.51	0.36
Th	0.12	0.03	-0.36	-1.01	-0.85	-0.1	0.03	2.41
Tm	0.16	-0.13	0.10	-0.63	-0.58	-0.21	-0.30	-0.23
U	-0.77	-0.55	-0.38	0.62	-0.36	-0.95	-0.89	-0.02
V	-7.62	-3.94	-8.11	226.2	138.02	-7.78	-4.16	216.63
W	-0.52	-0.49	-0.24	0.21	-0.40	-0.11	0.17	0.62
Y	4.90	-14.66	0.47	-38.72	-35.68	-12.17	-21.77	-7.49
Yb	0.64	-1.55	-0.40	-5.17	-4.61	-1.76	-2.47	-2.61
Zr	10.85	17.14	24.40	-69.36	-64.13	-1.12	-15.19	145.56
As	-2.32	-0.48	-1.49	-1.91	-0.89	-1.9	0.34	-0.83
Bi	-0.04	-0.04	0.03	-0.05	-0.02	0.28	0.87	0.00
Hg	0.00	0.00	0.00	0.00	0.00	0.01	0.00	0.00
In	0.06	-0.02	-0.01	-0.01	-0.02	0.10	0.19	-0.01
Re	0.00	0.00	0.00	0.00	0.00	0.00	0.00	0.00
Sb	-0.09	-0.06	-0.03	-0.07	-0.08	-0.09	0.00	0.06
Se	0.00	0.00	-0.02	0.14	-0.04	-0.01	0.37	-0.02
Te	0.03	0.01	0.07	0.03	0.03	0.12	0.52	0.00
Tl	0.13	-0.03	0.00	0.00	-0.03	0.07	0.09	0.07
Ag	-0.01	0.00	-0.06	-0.1	-0.10	-0.03	0.04	-0.05
Cd	-0.01	0.00	-0.06	0.11	-0.10	0.37	0.04	-0.05
Co	-0.05	0.01	-0.62	12.36	5.02	-0.11	0.17	13.62
Cu	-1.15	0.04	-1.73	21.5	4.42	10.22	42.76	4.94
Li	4.51	5.11	10.15	1.07	-4.70	12.78	18.38	3.12
Mo	-0.05	2.03	5.82	-0.39	-0.4	4.33	6.01	-0.19
Ni	-1.52	-0.99	-1.24	0.43	-1.70	-0.22	-1.42	2.87
Pb	-11.05	9.23	-9.73	-7.75	-10.80	-4.89	-6.16	-7.13
Sc	4.03	-10.96	0.15	10.50	4.25	-4.33	-4.48	7.74
Zn	38.32	-61.88	-13.91	-22.00	39.52	203.43	12.33	24.47

Sample ID	62758	62759	62760	62761	62764	62766	62768
Hole ID	PH-19-11	PH-19-11	PH-18-08	PH-18-08	PH-19-09	PH-19-09	PH-19-10
Depth (m)	124.43	138.47	17.55	163.1	25.35	112.04	6.78
Lithology	Xtl-Tuff	Rhyolite	Xtl-Tuff	Rhyolite	Tuff	Rhyolite	Lap. Tuff
Stratigraphy	FW	FW	HW	HW	HW	HW	MS
Alteration	QSC+/-Py	QS+/-C+/Py	QS	QSC+Sil	QS+Sil	QS	QSC+/-Py+Sil
SiO_2	-10.18	-9.28	5.19	-22.14	-4.17	-19.06	24.35
Al_2O_3	0.00	0.00	0.00	0.00	0.00	0.00	0.00
Fe_2O_3	3.78	1.78	0.64	0.61	2.28	0.33	5.99
CaO	-5.55	-5.86	-6.13	-6.15	-6.06	-5.09	-6.54
MgO	1.85	0.73	-0.37	0.55	-0.65	1.28	-0.37
Na_2O	-1.58	-1.20	-1.85	-1.75	-1.37	-3.24	-3.91
K_2O	0.40	0.23	4.33	0.97	3.58	-0.09	1.52
Cr_2O_3	0.00	0.00	0.00	0.00	0.00	0.00	0.00
TiO_2	0.19	0.14	-0.01	0.01	0.20	-0.04	0.06
MnO	0.05	-0.11	-0.13	-0.13	-0.14	-0.14	-0.13
P_2O_5	0.05	0.02	0.04	0.00	0.07	0.00	0.01
SrO	0.00	0.00	0.04	0.00	0.04	0.01	0.05
BaO	0.00	0.00	0.01	0.02	0.01	0.03	0.03
LOI	0.87	0.31	-0.27	0.38	-0.05	0.76	1.41
Total	-9.92	-11.54	3.01	-26.51	-4.70	-25.95	19.54
C	-0.14	-0.16	-0.15	-0.15	-0.15	-0.16	-0.16
S	1.48	0.60	0.44	0.04	1.30	-0.12	2.81
Ba	15.4	31.80	57.32	179.1	107.19	-39.00	220.02
Ce	-1.81	-3.97	6.13	4.28	-2.38	7.45	-5.17
Cr	-11.1	-2.71	0.33	-5.61	-1.25	-5.21	4.2
Cs	0.45	0.41	0.08	0.50	0.12	0.53	0.68
Dy	-3.39	-3.98	-0.54	0.35	-3.43	1.68	-3.26
Er	-1.89	-1.83	-0.11	1.09	-2.23	1.21	-1.93
Eu	-0.12	-0.16	-0.19	-0.06	0.15	0.17	0.25
Ga	-1.24	-1.32	1.64	-0.88	-1.84	-0.11	4.04
Gd	-2.28	-2.68	-0.32	0.06	-2.24	1.48	-2.73
Ge	-0.27	-0.34	0.04	-0.70	-0.16	-0.65	0.53
Hf	-0.99	-0.53	0.36	1.52	-0.96	0.92	0.21
Ho	-0.70	-0.70	-0.13	0.23	-0.75	0.48	-0.61
La	-0.97	-1.71	2.84	1.89	-0.91	2.90	-1.97
Lu	-0.41	-0.42	-0.07	0.17	-0.49	0.18	-0.27
Nb	-0.21	-0.06	0.12	0.41	0.12	0.38	0.11
Nd	-1.99	-3.82	2.63	1.14	-2.69	4.89	-4.82
Pr	-0.34	-0.71	0.64	0.54	-0.43	1.03	-0.89
Rb	2.71	4.08	17.55	8.97	15.52	1.55	11.55
Sm	-1.10	-1.34	0.77	0.51	-1.16	1.54	-1.52
Sn	-0.11	-0.14	0.02	1.16	-0.06	-0.26	2.63
Sr	-68.72	-46.06	-68.92	-36.27	-62.88	74.46	-58.88
Ta	0.04	0.12	0.15	0.09	0.04	0.10	0.19

Sample ID	62758	62759	62760	62761	62764	62766	62768
Hole ID	PH-19-11	PH-19-11	PH-18-08	PH-18-08	PH-19-09	PH-19-09	PH-19-10
Depth (m)	124.43	138.47	17.55	163.1	25.35	112.04	6.78
Lithology	Xtl-Tuff	Rhyolite	Xtl-Tuff	Rhyolite	Tuff	Rhyolite	Lap. Tuff
Stratigraphy	FW	FW	HW	HW	HW	HW	MS
Alteration	QSC+/-Py	QS+/-C+/Py	QS	QSC+Sil	QS+Sil	QS	QSC+/-Py+Sil
Tb	-0.43	-0.44	0.03	0.13	-0.37	0.33	-0.43
Th	-0.32	-0.36	0.34	-0.27	-0.31	0.29	-0.42
Tm	-0.32	-0.30	0.02	0.20	-0.40	0.22	-0.26
U	-1.02	-1.02	4.98	1.30	0.99	-0.79	-0.86
V	40.73	10.75	-7.46	-8.2	-1.56	-8.15	-2.74
W	0.78	-0.14	0.02	0.44	-0.06	-0.26	1.42
Y	-21.63	-21.24	-2.94	3.62	-23.65	13.39	-18.99
Yb	-3.04	-2.79	-0.28	1.06	-3.21	1.14	-2.02
Zr	-26.81	-17.39	14.70	32.35	-20.63	23.14	8.01
As	-2.17	-2.01	9.30	-1.04	-1.11	-2.03	-1.01
Bi	0.32	0.27	-0.03	-0.02	0.12	-0.04	3.22
Hg	0.00	0.00	0.00	0.00	0.00	0.00	0.13
In	0.03	-0.01	-0.01	-0.02	0.00	0.00	12.80
Re	0.00	0.00	0.00	0.01	0.00	0.00	0.00
Sb	-0.09	-0.07	0.17	-0.09	-0.03	-0.06	0.06
Se	0.70	0.16	0.10	-0.03	0.18	-0.03	0.75
Te	0.21	0.21	0.01	0.01	0.07	0.00	0.51
Tl	-0.02	-0.02	-0.01	0.03	-0.03	-0.03	0.02
Ag	-0.03	-0.03	0.00	-0.07	-0.02	-0.07	8.34
Cd	-0.03	0.61	0.00	-0.07	-0.02	-0.07	29.40
Co	2.56	0.73	-0.49	-0.64	0.87	-0.63	0.21
Cu	99.24	40.95	-0.95	1.04	0.69	-3.26	7207.67
Li	3.90	3.64	-4.49	2.20	-4.53	17.19	-4.39
Mo	1.67	1.59	5.10	12.67	-0.06	-0.26	20.78
Ni	-0.22	-0.27	0.03	-1.28	0.81	-1.26	-0.79
Pb	-3.10	-0.76	-3.87	1.67	-5.44	-7.56	66.65
Sc	-0.76	-4.63	-7.88	-9.96	-0.94	4.23	-5.32
Zn	26.68	136.20	-49.62	-36.29	-19.57	-19.02	5553.55

Sample ID	62769	62770	62552	62555	62566	62569	62579
Hole ID	PH-19-10	PH-19-10	PH-18-14	PH-18-14	PH-18-14	PH-18-14	PH-18-34
Depth (m)	55.45	76.44	14.23	46	169.84	256.83	90.43
Lithology	Lap. Tuff	Rhyolite	Lap. Tuff	Xtl-Tuff	Tuff	Tuff	Lap. Tuff
Stratigraphy	MS	MS	MS	MS	FW	FW	HW
Alteration	QSC+/-Py+Sil	QSC	QSC+Sil	QSC+/-Py+Sil	QSC+Sil	QSC+/-Py	QSC
SiO_2	-11.56	6.31	4.07	-0.23	13.62	6.77	-18.04
Al_2O_3	0.00	0.00	0.00	0.00	0.00	0.00	0.00
Fe_2O_3	2.38	0.97	0.46	3.06	0.38	1.34	6.81
CaO	-4.47	-6.2	-1.18	-6.37	-4.62	-6.51	-5.12
MgO	0.17	2.38	0.27	2.95	0.03	2.24	0.06
Na_2O	-1.40	-1.00	-1.31	-4.12	-1.56	-3.48	-3.95
K_2O	0.36	-0.22	-0.17	-0.14	0.92	0.33	3.04
Cr_2O_3	0.00	0.00	0.00	0.00	0.00	0.00	0.00
TiO_2	0.14	0.01	-0.03	-0.03	-0.04	0.12	0.20
MnO	-0.01	-0.01	-0.04	-0.10	-0.06	-0.09	-0.12
P_2O_5	0.05	0.00	0.04	0.00	0.00	0.02	1.00
SrO	0.00	0.00	0.04	0.04	0.04	0.04	0.03
BaO	0.01	0.00	0.00	0.01	0.00	0.00	0.33
LOI	-0.59	0.71	-0.14	1.87	-0.31	1.64	1.15
Total	-13.35	3.38	1.68	-3.75	11.29	1.75	-14.79
C	-0.14	-0.13	-0.02	-0.12	-0.10	-0.15	-0.14
S	-0.21	0.12	0.18	1.15	-0.05	0.23	3.08
Ba	59.98	-19.53	-0.96	137.19	47.81	47.57	2941.96
Ce	0.05	1.75	5.59	2.63	0.45	-2.01	6.72
Cr	-11.43	-9.77	0.41	8.51	1.73	10.22	-11.58
Cs	0.24	0.42	0.03	0.30	0.18	0.30	1.23
Dy	-2.84	-1.36	1.68	2.76	0.90	-4.10	2.82
Er	-1.41	-0.63	1.17	2.88	1.03	-2.43	2.00
Eu	0.23	0.00	0.70	0.05	0.07	-0.12	1.10
Ga	0.38	-2.98	-3.72	0.02	-0.19	0.29	2.43
Gd	-1.72	-0.84	1.96	2.94	1.37	-2.44	3.75
Ge	-0.36	0.06	0.05	-0.12	0.22	0.02	-0.39
Hf	-0.82	0.18	0.37	2.12	0.72	-0.58	-0.94
Ho	-0.52	-0.24	0.33	0.66	0.20	-0.83	0.65
La	-0.20	0.64	2.56	1.05	0.05	-0.87	4.25
Lu	-0.40	-0.16	0.10	0.21	0.09	-0.47	0.11
Nb	-0.16	0.23	0.12	0.42	0.20	-0.19	0.25
Nd	-0.46	0.57	5.24	3.32	2.09	-2.33	7.43
Pr	-0.04	0.17	0.79	0.44	0.16	-0.38	1.02
Rb	5.81	-0.43	-0.94	-0.94	7.49	0.53	38.07
Sm	-0.57	0.13	1.84	1.49	0.59	-1.10	2.60
Sn	-0.14	-0.49	0.02	1.85	0.09	0.01	-0.16
Sr	-50.10	-58.38	-18.47	-64.02	-10.41	-37.42	-53.72
Ta	0.12	0.15	0.05	0.05	0.06	0.05	0.03

Sample ID	62769	62770	62552	62555	62566	62569	62579
Hole ID	PH-19-10	PH-19-10	PH-18-14	PH-18-14	PH-18-14	PH-18-14	PH-18-34
Depth (m)	55.45	76.44	14.23	46	169.84	256.83	90.43
Lithology	Lap. Tuff	Rhyolite	Lap. Tuff	Xtl-Tuff	Tuff	Tuff	Lap. Tuff
Stratigraphy	MS	MS	MS	MS	FW	FW	HW
Alteration	QSC+/-Py+Sil	QSC	QSC+Sil	QSC+/-Py+Sil	QSC+Sil	QSC+/-Py	QSC
Tb	-0.24	-0.05	0.23	0.42	0.20	-0.47	0.58
Th	-0.04	0.11	0.33	-0.14	0.25	-0.18	-0.22
Tm	-0.25	-0.10	0.03	0.31	0.13	-0.39	0.22
U	-1.07	-0.91	-0.13	-0.84	-0.79	-1.08	10.51
V	-7.86	-7.44	-4.90	-7.62	-7.28	14.17	-3.26
W	-0.14	0.02	0.02	-0.05	0.09	0.01	0.68
Y	-17.61	-7.53	1.96	12.99	1.14	-25.68	20.9
Yb	-2.62	-0.81	1.02	1.33	0.67	-2.86	0.66
Zr	-18.90	4.07	8.99	43.03	12.13	-18.49	-27.68
As	-2.27	-2.39	-1.07	-2.22	-2.05	-1.49	4.63
Bi	0.07	0.05	0.13	0.15	-0.04	0.17	0.28
Hg	0.00	0.00	0.00	0.05	0.00	0.01	0.00
In	0.05	0.00	0.26	1.97	0.03	0.09	-0.01
Re	0.00	0.00	0.00	0.00	0.00	0.00	0.01
Sb	-0.09	-0.04	0.07	-0.09	-0.08	-0.02	0.08
Se	-0.01	0.00	0.00	0.00	0.01	0.00	0.15
Te	0.02	0.04	0.05	0.68	0.03	0.07	0.36
Tl	0.00	-0.03	-0.03	-0.01	-0.02	-0.03	0.15
Ag	-0.04	0.01	0.01	0.32	0.02	0.00	0.42
Cd	-0.04	0.36	2.40	11.15	0.02	0.00	-0.04
Co	-0.14	-0.49	-0.49	-0.05	-0.46	1.01	0.68
Cu	7.14	21.56	29.68	122.38	-1.83	188.38	17.05
Li	3.57	5.23	-4.49	14.00	-4.46	5.07	11.84
Mo	-0.14	4.11	1.04	1.85	1.17	1.01	2.37
Ni	-1.57	0.05	-1.49	-1.05	-0.91	-0.99	3.05
Pb	-6.00	117.86	0.25	-10.10	-9.83	-6.96	-4.42
Sc	2.13	-4.77	0.31	-2.65	0.21	-3.92	1.84
Zn	26.37	223.54	419.91	1756.13	-15.41	166.72	-42.68

Sample ID	62589	62639	62653	62656	62657	62658	62659	62661
Hole ID	PH-18-34	PH-18-40	PH-18-26	PH-18-06	PH-18-06	PH-18-06	PH-18-06	PH-18-06
Depth (m)	269	315.83	167	10.37	75.1	127.54	164.2	205
Lithology	Basalt	Xtl-Tuff	Dike	Xtl-Tuff	Tuff	Xtl-Tuff	Xtl-Tuff	Xtl-Tuff
Stratigraphy	HW	FW	HW	HW	HW	MS	FW	MS
Alteration	Ccal	QSC+/-Py	Unaltered	QS	QS+/-C	QSCPy	QSC+/-Py	QSCPy+Si
SiO_2	-47.8	-8.86	8.65	-10.64	-7.66	26.42	5.82	-38.92
Al_2O_3	0.00	0.00	0.00	0.00	0.00	0.00	0.00	0.00
Fe_2O_3	6.55	1.29	0.66	0.98	2.73	4.99	3.98	0.79
CaO	-1.38	-6.43	-5.17	-5.39	-3.11	-5.76	-5.77	-6.53
MgO	2.27	0.28	-0.35	0.59	0.67	0.05	8.00	-0.42
Na_2O	-2.79	-0.32	-0.84	-1.43	-2.82	-4.24	-4.27	-3.30
K_2O	0.10	0.22	1.17	1.50	0.11	2.16	-0.08	0.40
Cr_2O_3	0.00	0.00	0.00	0.00	0.00	0.00	0.00	0.00
TiO_2	0.40	0.00	-0.01	0.00	0.18	0.06	0.10	0.06
MnO	-0.05	-0.1	-0.09	-0.11	-0.03	-0.11	0.11	-0.15
P_2O_5	0.00	0.00	0.00	0.00	0.04	0.02	0.02	0.01
SrO	0.01	0.03	0.04	0.03	0.00	0.05	0.05	0.00
BaO	0.00	0.00	0.01	0.01	0.01	0.02	0.00	0.00
LOI	0.24	0.19	-0.72	-0.37	-0.19	2.50	2.77	0.19
Total	-41.66	-12.76	4.99	-13.81	-9.12	23.9	8.28	-46.51
C	-0.11	-0.14	-0.13	-0.14	-0.12	0.05	-0.14	-0.16
S	0.42	0.28	-0.06	0.06	0.04	2.46	1.12	0.55
Ba	-42.14	22.29	80.1	90.48	100.22	194.12	-1.48	38.86
Ce	-12.51	0.03	2.95	-2.63	-4.09	-5.72	2.72	-6.31
Cr	20.11	-11.39	0.80	-11.45	-1.98	4.72	1.58	-9.61
Cs	0.19	0.26	0.23	0.19	0.68	0.77	1.79	0.24
Dy	-7.72	-0.78	0.72	0.56	-3.6	-2.29	-1.79	1.46
Er	-5.22	-0.08	0.80	0.58	-2.27	-0.44	-1.23	1.65
Eu	-0.61	-0.07	-0.02	0.07	0.15	0.22	0.52	0.19
Ga	2.11	0.18	-2.91	0.09	0.44	6.75	1.45	7.30
Gd	-5.44	-0.74	0.60	0.51	-2.22	-1.63	-0.81	0.08
Ge	-1.07	-0.35	0.10	-0.36	-0.25	0.59	0.20	-1.2
Hf	-2.67	0.14	0.96	1.06	-0.87	0.04	-0.60	0.02
Ho	-1.69	-0.22	0.23	0.01	-0.83	-0.45	-0.48	0.40
La	-5.03	0.08	1.79	-1.50	-1.54	-2.02	0.87	-2.9
Lu	-0.95	-0.12	0.06	0.10	-0.49	-0.20	-0.36	0.05
Nb	-0.87	0.19	0.36	0.27	-0.11	0.26	-0.13	0.04
Nd	-10.17	-0.16	2.44	-0.49	-3.31	-4.43	0.81	-5.21
Pr	-1.99	0.04	0.42	-0.30	-0.59	-0.95	0.30	-1.10
Rb	3.81	5.34	9.72	9.89	2.52	22.87	6.33	1.44
Sm	-3.65	-0.21	0.52	-0.34	-1.24	-1.38	0.36	-1.12
Sn	0.15	-0.14	0.04	-0.15	-0.10	3.94	0.08	6.79
Sr	55.96	-50.46	-60.71	-56.8	10.4	-71.63	-52.71	-18.8
Ta	0.01	0.04	0.16	0.04	0.04	0.07	0.06	0.05

Sample ID	62589	62639	62653	62656	62657	62658	62659	62661
Hole ID	PH-18-34	PH-18-40	PH-18-26	PH-18-06	PH-18-06	PH-18-06	PH-18-06	PH-18-06
Depth (m)	269	315.83	167	10.37	75.1	127.54	164.2	205
Lithology	Basalt	Xtl-Tuff	Dike	Xtl-Tuff	Tuff	Xtl-Tuff	Xtl-Tuff	Xtl-Tuff
Stratigraphy	HW	FW	HW	HW	HW	MS	FW	MS
Alteration	Ccal	QSC+/-Py	Unaltered	QS	QS+/-C	QSCPy	QSC+/-Py	QSCPy+Si
Tb	-0.98	-0.07	0.18	0.03	-0.47	-0.29	-0.09	0.16
Th	-1.01	0.47	0.62	0.27	-0.33	-0.42	0.08	0.05
Tm	-0.79	-0.03	0.15	0.06	-0.37	-0.14	-0.27	0.24
U	-1.18	-0.83	-0.65	-0.66	-1.09	-0.73	-0.79	-0.15
V	289.71	-5.70	26.41	-0.60	3.52	8.54	11.58	2.46
W	-0.43	-0.14	1.08	-0.15	-0.10	1.47	1.16	-0.48
Y	-49.77	-7.54	3.49	-0.85	-27.6	-11.17	-15.55	6.16
Yb	-6.38	-0.88	0.38	0.17	-3.11	-1.45	-2.55	0.70
Zr	-73.38	2.08	16.10	16.00	-24.22	-1.03	-20.95	1.93
As	-2.13	0.31	-1.97	-1.85	-2.07	37.46	-1.84	-0.99
Bi	0.07	0.24	0.75	0.02	0.06	2.74	0.31	0.77
Hg	0.00	0.00	0.00	0.00	0.00	0.17	0.02	0.00
In	0.00	0.00	-0.01	0.12	0.03	7.61	1.21	0.63
Re	0.00	0.00	0.00	0.00	0.00	0.00	0.00	0.00
Sb	-0.06	-0.06	-0.06	-0.09	-0.06	0.79	0.01	0.12
Se	0.07	-0.01	0.00	-0.01	-0.01	0.89	0.01	0.11
Te	0.20	0.11	0.25	0.12	0.13	1.44	0.27	0.36
Tl	0.02	-0.03	-0.02	0.12	0.15	0.06	0.06	0.04
Ag	-0.11	-0.03	0.01	-0.04	-0.02	7.16	0.40	0.79
Cd	-0.11	-0.03	0.01	0.18	-0.02	62.77	0.94	0.37
Co	36.25	-0.14	0.04	-0.57	-0.10	0.24	1.16	0.04
Cu	22.93	2.88	9.52	6.26	33.85	2467.52	370.4	166.35
Li	17.92	3.61	5.40	3.55	4.01	19.72	27.37	0.19
Mo	-0.43	2.44	1.08	0.71	-0.10	21.24	6.55	1.08
Ni	7.17	-1.57	0.08	-1.57	-1.55	0.47	0.16	-1.74
Pb	-7.42	-11.14	-1.60	5.95	-1.19	2.83	61.37	230.54
Sc	25.69	-2.95	-6.68	5.52	2.12	-6.35	-4.21	-3.57
Zn	8.95	-40.3	-41.79	74.89	18.92	8453.74	645.60	57.36

Sample ID	62663	62664	62665	62666	62667	62668	62669	62670
Hole ID	PH-18-06	PH-18-06	PH-18-06	PH-18-06	PH-18-01	PH-18-01	PH-18-01	PH-18-01
Depth (m)	263.35	301	310	321.69	22.61	73.95	142.64	180.61
Lithology	Tuff	Tuff	Tuff	Tuff	Tuff	Xtl-Tuff	Rhyolite	Rhyolite
Stratigraphy	FW	FW	FW	FW	HW	HW	MS	MS
Alteration	QSC+Sil	QSC+Sil	QS+/-C+Sil	QSC+Sil	QS	QS	QSC	QSC+Sil
SiO_2	-34.49	-12.69	-9.20	-51.14	0.69	-19.54	0.14	5.75
Al_2O_3	0.00	0.00	0.00	0.00	0.00	0.00	0.00	0.00
Fe_2O_3	0.29	0.28	2.39	0.90	0.24	1.17	0.30	1.74
CaO	-6.42	-4.92	4.27	-6.46	-5.31	-5.11	-4.66	-6.36
MgO	1.36	1.56	1.12	-0.11	-0.05	-0.15	1.33	0.52
Na_2O	-3.70	-2.06	-3.08	-3.81	-1.15	-1.14	-2.89	-0.87
K_2O	0.52	0.16	-0.35	0.84	1.34	1.54	0.33	0.18
Cr_2O_3	0.00	0.00	0.00	0.00	0.00	0.00	0.00	0.00
TiO_2	0.00	-0.01	0.09	-0.01	-0.04	0.16	-0.01	-0.04
MnO	-0.12	-0.09	0.23	-0.14	-0.14	-0.11	-0.08	-0.10
P_2O_5	0.00	0.01	0.05	0.00	0.00	0.06	0.00	0.00
SrO	0.00	0.00	0.01	0.00	0.04	0.03	0.04	0.04
BaO	0.03	0.01	0.00	0.03	0.00	0.01	0.02	0.01
LOI	0.65	0.52	0.41	0.62	-0.56	-0.19	-0.03	0.46
Total	-42.06	-17.13	-4.62	-59.37	-4.32	-22.93	-6.34	2.51
C	-0.15	-0.15	-0.05	-0.16	-0.13	-0.12	-0.14	-0.14
S	0.13	0.11	0.28	0.91	-0.14	0.31	-0.11	0.45
Ba	238.14	55.94	-1.35	262.86	-1.32	47.11	184.14	116.22
Ce	-1.24	1.96	1.19	2.56	-0.62	-3.55	-0.96	3.44
Cr	-8.50	-11.77	-0.90	-15.99	-0.89	-12.31	-1.11	-9.92
Cs	0.71	0.27	0.15	0.24	0.32	0.13	0.81	0.35
Dy	-1.03	0.78	-2.01	-2.17	0.30	-3.9	0.26	2.97
Er	-0.51	0.92	-1.15	-1.19	0.50	-2.26	0.38	2.48
Eu	-0.11	-0.09	0.60	-0.25	0.20	0.12	0.09	0.17
Ga	-0.95	-1.22	0.28	-1.23	-2.48	-1.22	-0.62	2.12
Gd	-0.74	0.43	-0.56	-1.13	0.72	-2.03	-0.09	1.92
Ge	-1.06	-0.44	-0.11	-1.50	-0.11	-0.58	-0.14	0.02
Hf	0.61	0.48	-0.72	0.67	0.71	-0.92	0.20	1.44
Ho	-0.24	0.11	-0.32	-0.41	0.19	-0.80	-0.07	0.75
La	-0.66	0.24	0.70	0.86	-0.73	-1.45	-0.69	0.85
Lu	-0.19	0.13	-0.32	-0.14	0.03	-0.52	-0.03	0.29
Nb	0.22	0.05	-0.14	0.18	0.14	0.05	-0.06	0.21
Nd	-1.48	1.64	0.82	1.15	0.73	-3.38	-0.08	4.63
Pr	-0.29	0.26	0.00	0.17	-0.08	-0.67	-0.13	0.57
Rb	5.78	6.17	-1.79	9.85	8.91	7.29	7.54	2.25
Sm	-0.81	0.64	0.09	0.18	0.62	-1.23	-0.15	2.03
Sn	0.15	-0.18	-0.04	-0.20	-0.04	-0.23	-0.06	0.01
Sr	-21.73	-21.00	128.57	-16.27	-26.81	-60.38	-17.88	-61.15
Ta	0.06	0.11	0.05	0.07	0.05	0.03	0.04	0.15

Sample ID	62663	62664	62665	62666	62667	62668	62669	62670
Hole ID	PH-18-06	PH-18-06	PH-18-06	PH-18-06	PH-18-01	PH-18-01	PH-18-01	PH-18-01
Depth (m)	263.35	301	310	321.69	22.61	73.95	142.64	180.61
Lithology	Tuff	Tuff	Tuff	Tuff	Tuff	Xtl-Tuff	Rhyolite	Rhyolite
Stratigraphy	FW	FW	FW	FW	HW	HW	MS	MS
Alteration	QSC+Sil	QSC+Sil	QS+/-C+Sil	QSC+Sil	QS	QS	QSC	QSC+Sil
Tb	-0.11	0.02	-0.18	-0.21	0.13	-0.45	0.00	0.49
Th	0.43	0.86	-0.14	0.30	0.43	-0.18	0.18	0.41
Tm	-0.03	0.16	-0.23	-0.14	0.11	-0.38	0.00	0.32
U	-0.68	-0.59	-1.02	-0.66	-0.70	-0.84	-0.74	-0.71
V	-4.25	-5.06	15.79	-0.78	-7.61	-3.85	-5.28	-3.95
W	-0.43	-0.59	0.91	-0.20	-0.52	-0.23	-0.53	-0.50
Y	-9.11	2.67	-12.92	-15.4	2.30	-25.54	-1.30	19.41
Yb	-0.81	0.46	-1.95	-1.34	0.06	-3.27	-0.31	1.84
Zr	12.31	10.36	-14.54	14.27	17.03	-22.36	3.52	28.96
As	-0.86	-1.30	0.17	-0.82	-1.74	1.45	-2.13	-1.39
Bi	-0.02	-0.01	0.03	-0.01	-0.04	0.00	-0.02	0.49
Hg	0.00	0.00	0.00	0.00	0.00	0.00	0.00	0.05
In	0.00	0.03	0.00	-0.02	0.03	0.04	0.02	0.99
Re	0.00	0.00	0.00	0.00	0.00	0.00	0.00	0.00
Sb	-0.02	-0.07	-0.01	-0.01	-0.06	-0.05	-0.03	-0.03
Se	-0.04	-0.02	0.00	-0.02	0.00	-0.02	-0.01	0.20
Te	0.00	0.00	0.08	0.01	0.01	0.07	0.01	0.38
Tl	0.32	0.19	0.02	0.15	0.00	-0.02	0.38	0.07
Ag	-0.11	-0.04	-0.01	-0.15	-0.01	-0.06	-0.01	0.00
Cd	-0.11	-0.04	0.71	-0.15	-0.01	-0.06	-0.01	11.75
Co	0.15	-0.59	-0.04	-0.60	-0.04	-0.62	-0.53	-0.50
Cu	-1.13	-0.71	4.60	2.02	2.69	1.38	10.17	78.67
Li	12.24	11.45	-4.52	-0.99	4.56	2.69	13.89	5.08
Mo	0.72	0.65	0.91	2.21	-0.04	0.54	0.89	3.03
Ni	-0.85	-1.59	-1.52	-1.60	-1.04	-1.62	-0.11	-0.99
Pb	0.64	-4.60	-6.27	23.29	-2.44	-10.46	26.73	-3.94
Sc	-5.80	-2.66	4.10	-5.38	3.16	-1.16	-2.72	8.19
Zn	-27.59	-30.22	334.88	-42.12	-17.57	18.47	2.57	1615.6

Sample ID	62671	62673	62674	62675	62676	62677	62678	62679
Hole ID	PH-18-01	PH-18-01	PH-18-01	PH-18-01	PH-18-01	PH-18-01	PH-18-01	PH-18-10
Depth (m)	205	270.87	331.72	368	396.48	420.14	463	71.43
Lithology	Lap. Tuff	Rhyolite	Xtl-Tuff	Rhyolite	Lap. Tuff	Xtl-Tuff	Tuff	Rhyolite
Stratigraphy	FW	FW	MS	MS	MS	FW	FW	HW
Alteration	QSC+Sil	QSC+Sil	QSCPy+Sil	QSC+Sil	QSC+Sil	QSC	QSC+Sil	QSC+Sil
SiO_2	-23.42	-46.34	29.03	-52.43	-0.64	-2.27	-30.51	6.58
Al_2O_3	0.00	0.00	0.00	0.00	0.00	0.00	0.00	0.00
Fe_2O_3	1.24	2.65	3.82	1.71	2.22	1.63	0.49	4.28
CaO	-6.38	-6.44	-6.26	-6.49	-6.16	-6.46	-5.92	-6.27
MgO	1.23	2.92	3.75	0.14	1.94	1.45	0.18	0.92
Na_2O	-4.00	-3.45	-4.54	-3.70	-3.25	-1.65	-2.05	-3.24
K_2O	0.57	0.66	-0.12	0.11	0.59	-0.10	1.66	1.23
Cr_2O_3	0.00	0.00	0.00	0.00	0.00	0.00	0.00	0.00
TiO_2	0.01	0.01	0.02	0.00	-0.01	0.1	-0.03	-0.05
MnO	-0.09	-0.03	0.08	-0.09	-0.04	-0.10	-0.11	-0.09
P_2O_5	0.01	0.00	0.00	0.01	0.01	0.03	0.02	0.00
SrO	0.00	0.00	0.00	0.00	0.04	0.04	0.02	0.04
BaO	0.02	0.01	0.02	0.01	0.02	0.00	0.02	0.02
LOI	1.40	1.20	1.63	0.25	1.06	0.25	-0.06	1.74
Total	-31.14	-49.29	26.68	-60.9	-4.88	-7.38	-35.66	3.41
C	-0.13	-0.15	-0.12	-0.16	-0.11	-0.14	-0.14	-0.09
S	0.49	0.67	0.92	0.63	-0.06	0.45	-0.04	1.16
Ba	183.15	85.16	119.66	96.87	227.26	1.58	135.6	178.44
Ce	2.46	-2.55	3.49	-11.92	0.48	-4.37	-0.94	9.47
Cr	-6.16	-15.00	5.16	-16.07	-10.53	-10.74	-13.63	0.68
Cs	1.25	0.65	0.44	0.27	0.53	0.06	0.39	1.63
Dy	0.24	-2.66	-1.21	-3.86	-2.54	-3.34	-0.96	3.79
Er	0.54	-1.2	-0.43	-1.76	-0.75	-1.86	-0.12	2.88
Eu	0.50	0.18	0.48	-0.47	-0.20	-0.30	0.23	0.01
Ga	-0.66	-1.30	2.45	-2.96	-0.03	-1.14	-0.15	3.33
Gd	0.32	-1.31	0.48	-3.98	-1.67	-2.20	-0.48	3.95
Ge	-0.77	-1.25	0.64	-1.52	-0.13	-0.18	-0.91	0.08
Hf	-0.12	-0.05	0.60	-0.24	-0.08	-0.61	0.78	0.84
Ho	0.08	-0.60	-0.30	-0.76	-0.55	-0.66	-0.10	0.82
La	0.83	-1.05	1.07	-4.78	-0.11	-1.71	-0.44	3.29
Lu	-0.04	-0.26	-0.16	-0.27	-0.20	-0.42	-0.07	0.40
Nb	0.08	0.10	0.41	-0.08	-0.06	-0.17	-0.14	-0.27
Nd	1.61	-2.20	3.24	-9.68	0.04	-3.82	-0.70	8.35
Pr	0.17	-0.52	0.39	-1.90	-0.13	-0.83	-0.10	1.35
Rb	6.88	7.75	0.45	0.15	6.14	-1.85	9.30	21.53
Sm	0.48	-0.58	1.27	-3.15	-0.24	-1.09	-0.47	3.48
Sn	-0.31	0.00	0.26	4.89	0.89	-0.07	0.27	2.10
Sr	-42.52	-17.77	-36.70	-38.71	-50.17	-44.48	-58.87	-37.81
Ta	0.09	0.05	0.08	0.03	0.04	0.04	0.08	0.05

Sample ID	62671	62673	62674	62675	62676	62677	62678	62679
Hole ID	PH-18-01	PH-18-01	PH-18-01	PH-18-01	PH-18-01	PH-18-01	PH-18-01	PH-18-10
Depth (m)	205	270.87	331.72	368	396.48	420.14	463	71.43
Lithology	Lap. Tuff	Rhyolite	Xtl-Tuff	Rhyolite	Lap. Tuff	Xtl-Tuff	Tuff	Rhyolite
Stratigraphy	FW	FW	MS	MS	MS	FW	FW	HW
Alteration	QSC+Sil	QSC+Sil	QSCPy+Sil	QSC+Sil	QSC+Sil	QSC	QSC+Sil	QSC+Sil
Tb	0.06	-0.32	-0.07	-0.61	-0.30	-0.38	-0.12	0.51
Th	-0.06	-0.37	-0.1	-0.41	0.08	-0.51	0.19	0.87
Tm	0.02	-0.21	-0.18	-0.25	-0.13	-0.24	-0.08	0.37
U	-0.01	-0.98	-0.94	-0.98	-0.81	-0.97	-0.90	-0.81
V	2.45	-1.50	-2.45	-7.64	-7.63	31.68	-2.99	-7.42
W	-0.31	-0.75	-0.37	1.36	-0.53	-0.07	-0.36	0.03
Y	-0.14	-16.96	-8.22	-20.20	-15.95	-20.15	-5.68	20.71
Yb	-0.23	-1.95	-1.95	-2.35	-1.47	-2.55	-0.82	2.17
Zr	-1.46	0.48	16.92	-1.24	10.34	-18.68	15.79	21.66
As	-1.45	-2.10	-0.44	-2.31	-2.13	-2.24	-2.06	-1.36
Bi	0.05	0.31	0.27	1.07	0.07	0.17	0.02	0.79
Hg	0.04	0.00	0.06	0.04	0.00	0.03	0.00	0.00
In	0.16	0.20	1.84	0.27	0.06	0.05	0.00	-0.01
Re	0.00	0.00	0.00	0.00	0.00	0.00	0.00	0.00
Sb	-0.03	-0.07	0.03	-0.08	-0.03	-0.09	-0.09	0.24
Se	0.04	0.00	0.03	0.06	-0.01	0.09	0.03	0.42
Te	0.08	0.05	0.08	0.14	0.09	0.22	0.03	0.86
Tl	0.05	0.14	0.10	-0.03	0.00	-0.03	-0.03	0.04
Ag	0.79	0.30	0.06	1.09	-0.01	-0.02	-0.09	0.01
Cd	1.89	-0.13	1.13	1.56	-0.01	-0.02	-0.09	0.01
Co	-0.31	0.00	-0.37	-0.80	-0.53	-0.07	-0.68	-0.48
Cu	48.57	26.49	780.94	277.99	31.02	11.75	-0.18	16.68
Li	8.84	39.99	32.74	6.78	32.86	4.26	7.75	15.68
Mo	2.46	0.00	1.52	-0.61	-0.05	-0.07	0.27	4.17
Ni	-0.62	-1.50	-0.74	-1.61	-1.53	-0.15	-1.36	0.07
Pb	147.79	12.49	0.58	41.41	-7.27	1.89	-3.71	-6.83
Sc	-8.77	-5.00	-6.19	-5.57	-2.69	-4.81	-0.98	6.71
Zn	622.21	271.42	593.7	>10000	43.43	175.23	25.15	-31.64

Sample ID	62680	62681	62682	62683	62684	62685	62686	62688
Hole ID	PH-18-10	PH-18-10	PH-18-10	PH-18-10	PH-18-10	PH-18-21	PH-18-21	PH-18-21
Depth (m)	79.16	131	203.17	170.04	239.71	17	40.8	73.88
Lithology	Xtl-Tuff	Rhyolite	Tuff	Lap. Tuff	Lap. Tuff	Sediment	Lap. Tuff	Lap. Tuff
Stratigraphy	MS	FW	MS	MS	MS	FW	MS	MS
Alteration	QSCPy+Sil	QSC	QSC+/-Py	QSC+Sil	QSC	QSC+/-Py	QSCPy	SQC+/-Py
SiO_2	29.52	0.00	7.06	21.86	-0.99	-9.41	9.86	-1.48
Al_2O_3	0.00	0.00	0.00	0.00	0.00	0.00	0.00	0.00
Fe_2O_3	9.54	1.45	2.86	5.29	2.28	2.47	5.12	0.79
CaO	-5.85	-6.47	-6.51	-6.44	-6.4	-3.48	-6.28	-6.14
MgO	-0.24	1.33	2.02	2.41	2.71	0.50	4.09	5.73
Na_2O	-3.81	-3.59	-4.13	-3.88	-3.17	-3.23	-4.69	-2.67
K_2O	1.87	0.36	1.23	0.37	0.63	0.84	1.48	-0.15
Cr_2O_3	0.00	0.00	0.00	0.00	0.00	0.00	0.00	0.00
TiO_2	0.06	-0.01	0.02	0.05	0.00	0.16	0.07	-0.01
MnO	-0.13	-0.07	0.02	0.01	-0.02	-0.05	0.08	0.04
P_2O_5	0.02	0.00	0.00	0.01	0.03	0.05	0.02	0.01
SrO	0.06	0.00	0.04	0.05	0.04	0.03	0.05	0.04
BaO	0.03	0.01	0.02	0.00	0.01	0.02	0.01	0.04
LOI	2.27	1.55	1.57	2.32	1.42	-0.29	2.74	1.79
Total	29.67	-6.84	2.12	19.51	-4.47	-10.29	11.83	-2.09
C	-0.01	-0.15	-0.14	-0.13	-0.14	-0.14	-0.07	-0.12
S	3.97	0.30	0.41	2.91	0.01	-0.01	0.64	-0.14
Ba	237.65	93.67	256.46	101.31	84.56	202.2	168.62	-27.92
Ce	27.39	-1.26	0.16	-0.96	2.83	-3.98	-5.66	-5.93
Cr	19.3	-1.40	0.51	3.93	-0.98	-11.21	1.95	-10.39
Cs	1.18	0.56	1.07	0.63	0.67	0.63	1.76	1.25
Dy	0.07	0.97	-1.69	-2.26	-0.92	-3.59	-3.18	-2.08
Er	-0.36	0.73	-1.02	-0.75	-0.37	-2.51	-1.93	-0.87
Eu	1.62	-0.01	-0.12	0.03	0.41	-0.03	-0.29	-0.13
Ga	6.09	-1.83	-0.59	0.38	-0.16	1.77	2.13	-1.46
Gd	3.75	0.40	-1.18	-0.69	-0.37	-2.11	-2.50	-1.52
Ge	0.77	-0.17	0.06	0.49	-0.12	-0.30	0.24	-0.10
Hf	-0.03	0.98	0.19	0.17	-0.07	-1.19	0.10	0.16
Ho	-0.18	0.25	-0.31	-0.38	-0.31	-0.85	-0.66	-0.44
La	11.43	-0.67	0.76	-0.57	0.96	-1.82	-2.42	-2.24
Lu	-0.19	0.14	-0.27	-0.22	-0.22	-0.51	-0.34	-0.25
Nb	0.08	0.39	0.23	0.10	0.14	-0.13	0.44	0.05
Nd	19.71	-0.44	-0.01	-0.23	1.52	-3.43	-5.45	-5.06
Pr	3.78	-0.29	-0.06	-0.32	0.16	-0.74	-1.06	-0.98
Rb	39.66	6.44	10.66	4.20	8.28	11.41	30.87	2.64
Sm	6.03	0.53	-0.38	-0.39	0.54	-1.41	-1.71	-1.10
Sn	8.17	-0.07	0.03	0.20	0.90	-0.12	0.10	-0.04
Sr	-64.02	-18.47	-43.88	-43.71	-34.90	-28.06	-93.42	-55.87
Ta	0.47	0.14	0.05	0.07	0.14	0.04	0.17	0.05

Sample ID	62680	62681	62682	62683	62684	62685	62686	62688
Hole ID	PH-18-10	PH-18-10	PH-18-10	PH-18-10	PH-18-10	PH-18-21	PH-18-21	PH-18-21
Depth (m)	79.16	131	203.17	170.04	239.71	17	40.8	73.88
Lithology	Xtl-Tuff	Rhyolite	Tuff	Lap. Tuff	Lap. Tuff	Sediment	Lap. Tuff	Lap. Tuff
Stratigraphy	MS	FW	MS	MS	MS	FW	MS	MS
Alteration	QSCPy+Sil	QSC	QSC+/-Py	QSC+Sil	QSC	QSC+/-Py	QSCPy	SQC+/-Py
Tb	0.31	0.14	-0.25	-0.21	-0.14	-0.40	-0.44	-0.23
Th	0.60	0.44	-0.41	-0.05	-0.07	-0.22	0.35	-0.06
Tm	-0.17	0.20	-0.13	-0.18	-0.13	-0.40	-0.28	-0.14
U	-0.31	-0.80	-0.94	-0.85	-0.85	-1.03	0.49	-0.89
V	35.85	-4.42	7.44	1.97	-0.49	12.84	14.14	22.68
W	0.31	-0.53	1.05	-0.40	-0.05	-0.56	-0.45	3.81
Y	-6.78	5.76	-10.56	-11.39	-8.55	-25.76	-19.03	-14.09
Yb	-1.40	0.58	-1.78	-1.48	-1.46	-3.71	-2.42	-1.95
Zr	-2.23	21.60	4.37	5.73	2.23	-22.35	-4.41	2.26
As	-0.74	-1.96	-0.55	4.60	-2.32	-2.17	76.42	-2.41
Bi	2.22	0.31	0.19	0.53	-0.02	0.23	0.34	0.00
Hg	0.02	0.00	0.01	0.64	0.01	0.00	0.00	0.00
In	9.48	0.05	0.36	0.15	0.09	0.05	1.27	0.04
Re	0.00	0.00	0.00	0.00	0.00	0.00	0.00	0.00
Sb	0.15	-0.04	0.03	-0.08	-0.03	-0.07	0.19	-0.05
Se	1.34	-0.01	0.11	0.74	0.00	0.08	0.12	0.00
Te	1.37	0.1	0.22	2.68	0.02	0.14	0.40	0.00
Tl	0.06	-0.03	-0.02	0.01	-0.01	0.30	0.03	-0.02
Ag	14.42	-0.02	0.01	0.59	-0.01	-0.03	0.02	-0.01
Cd	4.47	0.68	0.01	11.12	0.51	-0.03	0.85	-0.01
Co	1.62	-0.07	0.03	3.79	-0.05	0.76	1.19	-0.52
Cu	7475.71	57.38	147.81	340.63	45.44	14.45	47.58	-0.16
Li	8.10	13.60	15.51	18.93	23.52	3.79	16.95	14.22
Mo	8.17	0.86	3.10	3.79	4.70	-0.12	1.19	0.92
Ni	7.17	-1.07	-0.97	-0.80	-0.10	-0.24	-0.90	-1.52
Pb	14.2	-3.63	-6.87	1.16	7.02	-9.36	-9.81	42.78
Sc	-4.52	-7.56	-4.74	-7.82	-5.49	0.81	-4.03	-4.43
Zn	588.52	265.52	249.08	2182.66	157.1	9.59	578.83	23.11

Sample ID	62690	62691	62692	62693	62694
Hole ID	PH-18-21	PH-18-21	PH-18-44	PH-18-44	PH-18-44
Depth (m)	91.84	118.83	22	54.05	94.11
Lithology	Tuff	Rhyolite (sill)	Tuff	Lap. Tuff	Lap. Tuff
Stratigraphy	FW	FW	HW	HW	HW
Alteration	SQC+/-Py	QS	QS	QSC	QSC+/-Py+Sil
SiO_2	-0.89	-5.93	-7.55	11.29	3.97
Al_2O_3	0.00	0.00	0.00	0.00	0.00
Fe_2O_3	2.44	0.56	0.39	0.74	3.80
CaO	-6.39	-5.76	-5.18	-5.73	-5.21
MgO	4.57	-0.48	-0.63	1.69	0.46
Na_2O	-2.73	-0.46	-1.89	-0.51	-3.03
K_2O	-0.11	1.73	4.05	-0.09	0.73
Cr_2O_3	0.00	0.00	0.00	0.00	0.00
TiO_2	0.01	0.06	0.18	0.00	-0.03
MnO	0.05	-0.13	-0.13	-0.09	-0.11
P_2O_5	0.02	0.01	0.06	0.01	0.01
SrO	0.04	0.00	0.03	0.04	0.00
BaO	0.00	0.05	0.01	0.00	0.05
LOI	1.06	-0.49	-0.63	0.34	1.39
Total	-1.12	-9.31	-10.48	9.70	2.65
C	-0.13	-0.13	-0.13	-0.15	-0.15
S	0.73	0.15	0.12	0.00	1.89
Ba	12.92	474.02	100.00	9.49	520.96
Ce	0.93	36.29	-2.39	1.56	3.01
Cr	-10.3	-2.07	-2.14	-9.27	0.13
Cs	0.58	0.94	0.10	0.59	1.34
Dy	-1.31	-5.25	-3.26	0.72	0.49
Er	-0.69	-3.67	-1.91	0.79	1.07
Eu	0.20	-0.23	0.05	0.32	-0.16
Ga	-0.78	1.89	-1.65	-1.10	4.31
Gd	-0.57	-2.89	-2.06	0.50	0.77
Ge	-0.08	-0.26	-0.27	0.18	0.02
Hf	-0.20	1.63	-1.07	0.35	0.73
Ho	-0.37	-1.23	-0.68	0.17	0.12
La	0.12	19.95	-0.96	0.62	0.64
Lu	-0.18	-0.67	-0.55	0.07	0.12
Nb	0.06	4.46	0.06	0.08	0.01
Nd	1.30	8.84	-2.76	1.28	1.99
Pr	-0.08	3.11	-0.42	0.21	0.42
Rb	0.08	35.03	18.54	1.45	8.68
Sm	0.21	-0.30	-0.59	0.70	1.12
Sn	-0.03	-0.1	-0.11	0.07	1.01
Sr	-60.57	-21.85	-37.52	-56.43	18.28
Ta	0.14	0.49	0.13	0.06	0.15

Sample ID	62690	62691	62692	62693	62694
Hole ID	PH-18-21	PH-18-21	PH-18-44	PH-18-44	PH-18-44
Depth (m)	91.84	118.83	22	54.05	94.11
Lithology	Tuff	Rhyolite (sill)	Tuff	Lap. Tuff	Lap. Tuff
Stratigraphy	FW	FW	HW	HW	HW
Alteration	SQC+/-Py	QS	QS	QSC	QSC+/-Py+Sil
Tb	-0.16	-0.60	-0.42	0.10	0.12
Th	0.13	10.05	-0.13	0.14	0.22
Tm	-0.13	-0.59	-0.33	0.07	0.13
U	-0.92	2.94	-0.87	-0.77	-0.80
V	-3.21	2.55	-7.77	5.02	-3.96
W	-0.52	3.48	-0.55	-0.46	-0.50
Y	-9.74	-34.12	-22.41	0.32	2.77
Yb	-1.75	-4.67	-3.04	-0.03	0.79
Zr	-0.79	71.36	-23.02	6.56	18.69
As	-2.12	-1.80	0.16	-1.09	-1.19
Bi	0.42	0.89	0.06	0.02	1.00
Hg	0.01	0.00	0.00	0.00	0.00
In	0.13	-0.02	0.02	0.02	0.03
Re	0.00	0.00	0.00	0.00	0.00
Sb	-0.09	-0.03	-0.09	0.00	-0.08
Se	0.09	0.17	-0.01	0.01	1.21
Te	0.10	0.38	0.12	0.04	1.15
Tl	-0.02	-0.02	-0.03	-0.01	0.02
Ag	-0.01	-0.03	-0.03	0.02	0.00
Cd	-0.01	-0.03	0.46	1.36	0.00
Co	0.94	-0.10	-0.55	-0.46	-0.50
Cu	75.51	3.17	2.25	27.12	11.10
Li	24.09	-4.55	-4.55	5.73	15.13
Mo	9.67	0.79	1.68	1.15	4.03
Ni	-1.52	-1.10	-1.55	-1.46	-0.99
Pb	-6.18	3.24	-11.11	-6.64	-6.97
Sc	-4.33	-12.31	-5.18	-2.12	4.12
Zn	336.21	-51.49	223.48	291.80	-1.55

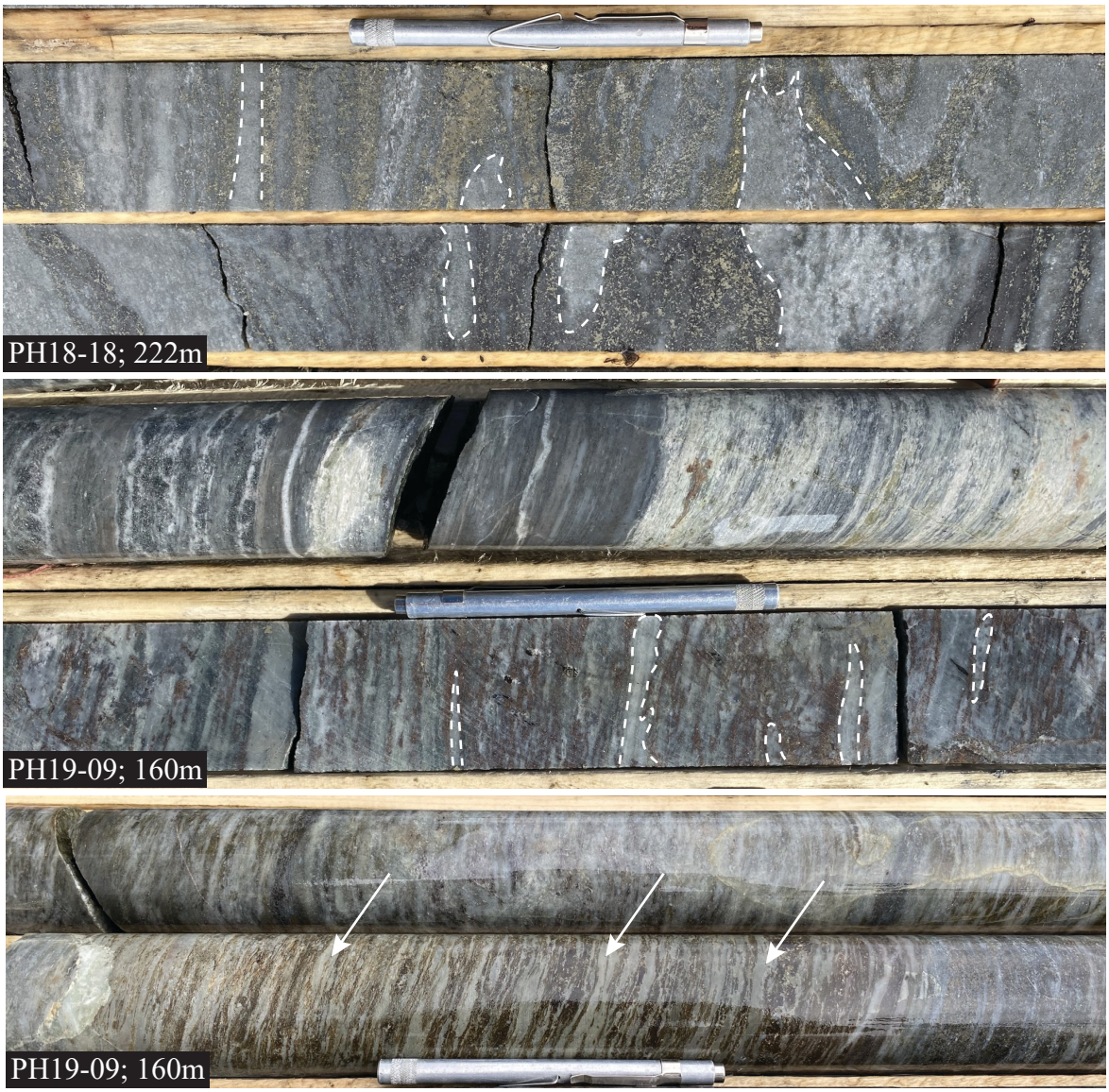

Appendix F. Additional photographs depicting evidence for replacement style mineralization at the Powderhorn Lake deposit. A) Cpy-po stringers with relict host rock clasts. Clasts are outlined in white and altered by white mica, chlorite, and sillimanite. B) Sp stringers in moderate to strongly chlorite altered lapilli tuff. Relict lapilli outlined in white. C) Sp+/-cpy stringers with visible relict bedding identified with arrows.